Universidade de Aveiro Departamento de Química
2018

Ana Francisca Osório de Almeida Coelho e Silva

Extração e separação de fármacos utilizando solventes alternativos

Extraction and separation of drugs using alternative solvents

Universidade de Aveiro Departamento de Química
2018

Ana Francisca Osório de Almeida Coelho e Silva

Extração e separação de fármacos utilizando solventes alternativos

Extraction and separation of drugs using alternative solvents

Tese apresentada à Universidade de Aveiro para cumprimento dos requisitos necessários à obtenção do grau de Doutor em Engenharia Química, realizada sob a orientação científica do Doutor João Manuel Costa Araújo Pereira Coutinho, Professor Catedrático do Departamento de Química da Universidade de Aveiro e da Doutora Sónia Patrícia Marques Ventura, Equiparada a Investigadora Auxiliar do Departamento de Química da Universidade de Aveiro.

Apoio financeiro através da FCT/MEC, no âmbito dos projetos POCI-01-0145-FEDER-016403 e POCI-01-0145-FEDER-030750.

Apoio financeiro do POCTI no âmbito do III Quadro Comunitário de Apoio.

O doutorando agradece o apoio financeiro da FCT no âmbito do III Quadro Comunitário de Apoio (SFRH/BD/94901/2013).

o júri

presidente

Doutora Silvina Maria Vagos Santana
Professora Catedrática, Universidade de Aveiro
Doutora Isabel Maria Jana Marrucho Ferreira
Professora Associada com Agregação, Instituto Superior Técnico da Universidade de Lisboa
Doutor Óscar Rodríguez Figueiras
Investigador "Ramón y Cajal", Universidade de Santiago de Compostela
Doutor José António Couto Teixeira
Professor Catedrático, Universidade do Minho
Doutora Tânia Ereira Sintra
Estagiária de Pós-Doutoramento, Universidade de Aveiro
Doutora Sónia Patrícia Marques Ventura
Equiparada a Investigadora Auxiliar, Universidade de Aveiro

agradecimentos

Quatro anos que passaram e apesar da *long and winding road* atravessada, está nas nossas mãos agarrar numa *sad song and make it better*. Na verdade, *there's nothing we can do that can't be done* e, no fundo, *all we need is love*.

Ao Path pela companhia e inspiração ao percorrer este longo caminho – porque acompanhados é sempre mais fácil. A todos os alunos que colaboraram comigo, pelo esforço. Ao meu orietandor, Professor João Coutinho, por tantas vezes me mostrar que menos é mais. À minha orientadora, Sónia Ventura, por me fazer acreditar que posso ir mais além.

Ao Rogers' group pela integração e entreajuda demonstrada durante a minha estadia em Montreal. Em especial ao Steven, por partilhar comigo a sua visão especial da ciência. Ao Professor Robin Rogers, por todas as perguntas que me deixaram sem resposta.

Aos meus amigos, os de sempre e os de agora para sempre, por todas as conversas e convívios.

Ao Guilherme pelo amor e apoio incondicional nesta etapa ultrapassada a dois.

Aos meus pais, aos meus avós, aos meus irmãos, à minha sobrinha, às minhas tias, aos meus primos, pelos olhos com que sempre me viram e todo o incentivo.

palavras-chave

Economia Circular, Química Verde, Fármacos, Resíduos farmacêuticos, Líquidos Iónicos, Sistemas Aquosos Bifásicos, Separação enantiomérica, Solventes Eutéticos Profundos

resumo

Os processos de produção da indústria química e relacionadas baseiam-se no uso de solventes orgânicos voláteis, gerando quantidades elevadas de resíduos perigosos. Durante as últimas décadas, têm sido realizados inúmeros esforços para modificar os processos químicos tendo em conta os princípios da Química Verde, Sustentabilidade e, mais recentemente, da Economia Circular. Esta tese pretende solucionar dois importantes desafios da indústria farmacêutica, a valorização de resíduos farmacêuticos e a separação de enantiómeros, utilizando duas classes de solventes alternativos, em particular, os Líquidos Iónicos (LIs) e os Solventes Eutéticos Profundos.

No âmbito do conceito da Economia Circular e na procura de uma alternativa à estratégia atualmente utilizada (i.e., incineração), novas estratégias para a valorização de resíduos farmacêuticos domésticos (medicamentos não usados e/ou fora da validade) são apresentadas. Dado que cerca de 90 % dos princípios ativos num medicamento fora do prazo permanecem no seu estado ativo, é aqui sugerida a recuperação de fármacos a partir de resíduos farmacêuticos utilizando processos de extração com LIs. Os processos de separação dos princípios ativos de fármacos a partir destes resíduos requerem uma etapa inicial de extração sólido-líquido, desenvolvida neste trabalho pelo uso de diferentes LIs, reconhecidos pelo seu elevado poder solvente para uma larga gama de compostos/biomoléculas. A etapa de separação dos princípios ativos após a sua recuperação dos resíduos foi estudada pela aplicação de sistemas aquosos bifásicos (SABs) e sistemas de partição de três fases aquosas igualmente constituídos por LIs. Por sua vez, a etapa de isolamento dos princípios ativos após a sua separação foi desenvolvida pela adição de anti-solventes devidamente selecionados.

O desafio de lidar com misturas racémicas e com as atividades biológicas diferenciadas que os enantiómeros geralmente apresentam foi investigado nesta tese. As duas práticas mais comuns na obtenção de enantiómeros puros são a síntese assimétrica e a separação de racematos. Apesar da síntese assimétrica ser considerada a abordagem mais poderosa, esta é limitada pelos elevados custos e complexidade tecnológica. A separação de racematos, por sua vez, representa uma alternativa mais flexível e simples do ponto de vista operacional e de custos. Neste contexto, o uso de SABs formados por LIs quirais foi considerado neste trabalho como uma alternativa na separação de misturas recémicas. Dois conjuntos distintos de LIs quirais, um com quiralidade no catião e o segundo com quiralidade no anião foram sintetizados e aplicados na separação de enantiómeros. Assim, e após caracterização dos diagramas de fase para os diferentes SABs (LI quiral + sal, LI quiral + polímero), foi possível avaliar a sua enantioseletividade na separação dos enantiómeros do ácido mandélico, aplicado neste trabalho como mistura racémica modelo. Numa segunda abordagem, a possibilidade de implementação de solventes eutécticos profundos como solventes quirais foi investigada pelo estudo do impacto da quiralidade no diagrama de equilíbrio sólido-líquido.

keywords

Circular Economy, Green chemistry, Pharmaceuticals, Pharmaceutical wastes, Ionic liquids, Aqueous biphasic systems, Enantioseparation, Deep Eutectic Solvents

abstract

The processes of production in chemical-related industries often rely on the use of volatile organic solvents, normally generating large amounts of hazardous wastes. During the past decades, major efforts have been done to transform chemical processes included in the principles of Green Chemistry, Sustainability and, more recently, Circular Economy. This thesis intends to work on two important challenges of pharmaceutical industry, namely the valorization of pharmaceutical wastes and the separation of enantiomers resorting on the application of alternative solvents, in particular, ionic liquids (ILs) and deep eutectic solvents (DES).

Motivated by circular economy and searching for a new strategy to the currently proposed (i.e., incineration), novel aproaches to valorize wastes of domestic origin (unspent and/or outdated medicines) are proposed. Since circa 90 % of the active ingredients in an outdated medicine are still in their active form, in this work, the recovery of valuable active drugs from pharmaceutical wastes using IL-mediated extraction processes is proposed. The processes of extraction and separation of drugs from pharmaceutical wastes require an initial step of solid-liquid extraction, which was designed in this work by the use of different ILs, well-recognized by their solvency power of ILs for a large plethora of compounds/biomolecules. The separation stage of the extracted active ingredients was also investigated by the application of IL-based aqueous biphasic systems (ABS) or IL-based three-phase partitioning (TPP). In the end, the isolation of the active ingredients was accomplished by the addition of anti-solvents properly selected. The wide applicability of the proposed ABS-based technology was evidenced by the recovery of several model active pharmaceutical ingredients (three non-steroidal anti-inflammatory drugs and one antidepressant).

The challenge of dealing with racemic mixtures and the differentiated biological activities that enantiomers generally present is investigated in this thesis. The most common two approaches to obtain pure enantiomers are the asymmetric synthesis and the separation of racemates. Although being considered the most powerful approach, the asymmetric synthesis is limited by the high costs and complexity of the processes. In turn, the separation of racemates is more flexible, cheaper and simpler. Under this scenario, it is here proposed the use of ABS composed of chiral ILs (CILs) as an alternative to enantioseparation. Two groups of CILs, i.e., those bearing chiral cations and those containing chiral anions were synthesized and applied to enantioseparation. After the characterization of the ABS phase diagrams (CIL + salt, CIL + polymer) it was possible to evaluate their enantioselectivity on the separation of racemic mandelic acid, here used as model racemic compound. In a second approach, deep eutectic solvents (DES) were envisaged as potential chiral solvents by the study of chirality impact on the solid-liquid equilibrium diagram.

Contents

List of Figures

List of Tables

Nomenclature

Abbreviations

ABS	Aqueous Biphasic systems
Ami	Amitriptyline
API	Active Pharmaceutical Ingredient
Asp	Aspartic acid
ATR	Attenuated Total Reflection
CIL	Chiral Ionic Liquid
COSMO-RS	COnductor-like Screening MOdel
DAD	Diode Array Detector
DES	Deep Eutectic Solvent
DFT	Density Functional Theory
D-MalA	D-Malic Acid
D-Phe	D-Phenylalanine
D-Pro	D-Pro
DSC	Differential Scanning Calorimetry
e.e.	Enantiomeric Excess
EE	Extraction Efficiency
ELLE	Enantioselective Liquid-Liquid Extraction
FTIR	Fourier-transform infrared spectroscopy
HBA	Hydrogen bond acceptor
HBD	Hydrogen bond donor
His	Histidine
HPLC	High Performance Liquid Chromatography
IBU	Ibuprofen
IE	Isolation Efficiency
Ile	Isoleucine
IL	Ionic Liquid
KET	Ketoprofen
LLE	Liquid-Liquid Extraction
L-MalA	L-Malic acid
L-Phe	L-Phenylalanine
L-Pro	L-Proline
L-Val	L-Valine
MD	Molecular Dynamics
NAP	Naproxen
NMR	Nuclear Magnetic Resonance
NSAID	Non-Steroidal Anti-Inflammatory Drug
PEG	Polyethylene glycol
Phe	Phenylalanine
PL35	Pluronic L-35
PPG	Polypropylene glycol

PXRD	Powder X-ray diffraction
RE	Recovery Efficiency
R-MA	R-Mandelic acid
R_T	Recovery
Ser	Serine
S-MA	S-Mandelic acid
SPE	Solid-Phase Extraction
St	Relative Stability
TGA	Thermogravimetric analysis
Thr	Threonine
TL	Tie-line
TLL	Tie-line length
TPP	Three-Phase Partitioning
Trp	Tryptophan
Tyr	Tyrosine
UV	Ultraviolet
UV-Vis	Ultraviolet-visible

Chemicals

$(CH_3)_2SO_4$	Dimethyl sulfate
$(NH_4)_2SO_4$	Ammonium sulfate
$C_2H_4O_2$	Acetic acid
C_2H_3N, ACN	Acetonitrile
$Al_2(SO_4)_3$	Aluminium sulphate
$Al_2(SO_4)_3 \bullet 16H_2O$	Aluminium sulphate hexadecahydrate
CH_3CH_2Br	Bromoethane
C_2H_5OH	Ethanol
C_3H_6O	Acetone
C_4H_8O	Tetrahydrofuran
$C_4H_8O_2$	Ethyl acetate
$C_6H_5K_3O_7$	Potassium citrate tribasic
$C_6H_5K_3O_7 \bullet H_2O$	Potassium citrate tribasic monohydrate
$C_6H_8O_7$	Citric acid
$C_6H_8O_7 \bullet H_2O$	Citric acid monohydrate
CH_2Cl_2	Dichloromethane
CH_2O	Formaldehyde
CH_3I	Iodomethane
CH_3OH	Methanol
$CHCl_3$	Chloroform
CO_2	Carbon Dioxide
$Cu(CH_3CO_2)_2$	Copper (II) acetate
$Cu(NO_3)_2$	Copper (II) nitrate
$CuSO_4$	Copper (II) sulphate

$CuSO_4 \cdot 5H_2O$	Copper (II) sulphate pentahydrate
H_2SO_4	Sulfuric acid
HCl	Hydrochloric acid
HCOOH	Formic acid
$K_2C_4H_4O_6$	Potassium tartrate
K_2CO_3	Potassium carbonate
K_2HPO_4	Potassium phosphate dibasic
K_3PO_4	Potassium phosphate tribasic
KCH_3CO_2	Potassium acetate
KCl	Potassium chloride
KH_2PO_4	Potassium phosphate monobasic
$KNaC_4H_4O_6$	Potassium sodium tartrate
$KNaC_4H_4O_6 \cdot 4H_2O$	Potassium sodium tartrate tetrahydrate
KOH	Potassium hydroxide
$Na_2C_4H_4O_4 \cdot 6H_2O$	Sodium succinate dibasic hexahydrate
Na_2CO_3	Sodium carbonate
Na_2HPO_4	Sodium phosphate dibasic
Na_2SO_4	Sodium sulfate
$NaBH_4$	Sodium borohydride
NaH_2PO_4	Sodium phosphate monobasic
NaOH	Sodium hydroxide
$NH_4C_2H_3O_2$	Ammonium acetate
$ZnSO_4$	Zinc sulfate

Ionic Liquids Anions

$[BF_4]^-$	Tetrafluoroborate
$[Bic]^-$	Bicarbonate
$[CF_3SO_3]^-$	Trifluoromethanesulfonate
$[C_nCO_2]^-$	Carboxylate
$[C_nPO_3]^-$	Alkylphosphonate
$[C_nSO_4]^-$	Alkylsulphate
$[DHCit]^-$	Dihydrogencitrate
$[D\text{-}Phe]^-$	D-Phenylalaninate
$[Glut]^-$	Glutarate
$[H_2PO_4]^-$	Dihydrogenophosphate
$[L\text{-}Ala]^-$	L-Alaninate
$[Lev]^-$	Levulinate
$[L\text{-}Glu]^{2-}$	L-Glutamate
$[L\text{-}Phe]^-$	L-Phenylalaninate
$[L\text{-}Pro]^-$	L-Prolinate
$[L\text{-}Tar]^{2-}$	L-Tartrate
$[L\text{-}Val]^-$	L-valinate
$[N(CN)_2]^-$	Dicyanamide
$[NTf_2]^-$	Bis(trifluoromethylsulfonyl)imide

$[PF_6]^-$	Hexafluorophosphate
$[Suc]^-$	Succinate
$[Tos]^-$	Tosylate
Br^-	Bromide
Cl^-	Chloride
I^-	Iodide
OH^-	Hydroxide

Ionic Liquids Cations

$[(C_6H_{13}OCH_2)_2im]^+$	1,3-dihexyloxymethylimidazolium
$[(C_6H_{13}OCH_2)C_1im]^+$	1-hexyloxymethyl-3-methylimidazolium
$[(OH)C_nC_1im]^+$	1-hydroxyalkyl-3-methylimidazolium
$[aaim]^+$	1,3-diallylimidazolium
$[aC_nim]^+$	1-allyl-3-alkylimidazolium
$[BzCh]^+$	Benzyldimethyl(2-hydroxyethyl)ammonium
$[C_{10}H_{18}N_3O_2]^+$	(*R*)-3-(2-((1-hydroxybutan-2-yl)amino)-2-oxoethyl)-1-methyl-imidazolium
$[C_{11}H_{21}N_4O_2]^+$	*(R)*-3-(2-(3-(1-hydroxybutan-2-yl)ureido)ethyl)-1-methyl-imidazolium
$[C_1C_1C_1Pro]^+$	*N,N*-dimethyl-L-proline methyl ester
$[C_1C_1C_1Val]^+$	*N,N,N*-trimethyl-L-valinolium iodide
$[C_1im\text{-}C_n\text{-}imC_1]^+$	3,3´-(1,6-alkanedyl)bis(1-methylimidazolium)
$[C_1Qui]^+$	1-methyl quininium
$[C_2(L\text{-}Phe)]^+$	Ethyl L-phenylalaninium
$[C_2C_2C_2Pro]^+$	*N,N*-diethyl-L-proline ethyl ester
$[C_7H_7C_1im]^+$	1-benzyl-3-methylimidazolium
$[Ch]^+$	Cholinium *N,N,N*-trimethyl-*N*-(2-hydroxyethyl)ammonium
$[C_nC_1C_1im]^+$	1-alkyl-2,3-dimethylimidazolium
$[C_nC_1im]^+$	1-alkyl-3-methylimidazolium
$[C_nC_1pyrr]^+$	1-alkyl-1-methylpyrrolidinium
$[C_npyr]^+$	1-alkylpyridinium
$[C_ntro]^+$	Alkyltropinium
$[C_ntro\text{-}C_n\text{-}troC_n]^+$	Bis(alkyl)-alkaneditropinium
$[N_{11n(2OH)}]^+$	*N*-Alkyl-*N,N*-dimethyl-*N*-(2-hydroxyethyl)ammonium
$[N_{1888}]^+$	*N*-methyl-*N,N,N*-trioctylammonium
$[N_{nnnn}]^+$	Tetraalkylammonium
$[P_{4441}]^+$	Tributylmethylphosphonium
$[P_{i(444)1}]^+$	Triisobutyl(methyl)phosphonium
$[Pip]^+$	Pipecoloxylididinium
$[P_{nnnn}]^+$	Tetraalkylphosphonium

Symbols

$K_{o/w}$	Octanol-water partition coefficient
K	Partition coefficient
pKa	Acid dissociation constant
T	Temperature
T_m	Melting temperature
σ	Standard deviation
T_d, $T_{5\%dec}$	Decomposition temperature
$[\alpha]_D^{25}$	Optical rotation
α	Enantioselectivity
T_{Eut}	Eutectic temperature
x	Mole fraction
wt%	Weight fraction percentage
w	Weight fraction
m	Mass
β	Hydrogen-bond accepting ability

CHAPTER 1

General Introduction

1. General Introduction

Pharmaceuticals, i.e., any drug used with medicinal purposes, have known an increase in their consumption in an epoch where both the length and quality of peoples' life are increasing. In this framework, major challenges related to the "green" credentials and sustainability of pharmaceutical industries and their products are a target of special attention.[1-5] The production processes in pharma industries often rely on the use of large amounts of a variety of organic solvents, that are often toxic and environmentally hazardous with a major impact on the life cycle analysis of their products.[6, 7] As patent by the high E factors (the mass ratio of waste to desired product and atom efficiency in kg waste/kg product) determined for chemical industries, the production of fine chemicals (5-50 kg waste *per* kg product) and pharmaceuticals (25->100 kg waste *per* kg product) has an enormous environmental impact.[5] Moreover, the persistency of pharmaceuticals in the environment is becoming threatening. Either by direct disposal or by human excreta, several drugs have been identified in soils and water, with severe impact upon ecosystems,[4, 8] namely the newsworthy case of wild fish developing intersex due to endocrine disruption caused by drugs' occurrence in rivers.[9] To accomplish a greener and more sustainable pharmacy seems to be the route to overcome such shortcomings.[10] From raw materials used to synthesis and manufacturing, from use to after-use fate, all stages of pharmaceuticals' life cycle should be looked at with a "greener" perspective.[11] Green Chemistry[12] has promoted some changes in chemical and pharmaceutical industries worldwide, in particular regarding (i) wastes generation prevention/minimization – principles 1 and 2 – and (ii) safety of the processes and chemicals involved and products designed – principles 3, 4, 5 and 10.[13]

In 2015, the European Commission launched an action called *Closing the loop - New circular economy package*,[14] with opportunities from both environmental and economic origin. To reduce environmental degradation and to mitigate climate change are key objectives to improve life quality and human health. Thus, a mindset shift started to occur in industry: a "take-make-use-dispose" economy, where linear flows of materials are undertaken in production processes, needs to be converted into a circular economy, where products and processes are developed in the light of resource efficiency and

recycling.[13, 14] Within a circular economy, goods that no longer serve can be transformed into resources/raw materials, so that waste minimization is accomplished.[15] For the inevitable waste generated, valorization is the most sustainable option. For that, the European Commission is welcoming industries to re-think the way they generate wastes, design their products and choose their raw materials.[16] Under this scenario, prevention, re-use and recycling of the wastes is encouraged, the durability of the products is a priority and trustable recovered raw-materials are advisable.[16] Industry may thus benefit from lower dependency from external resources and lower production costs as well as lower carbon footprint.[13, 15] Even though being challenging, this change means creating value from materials that industries used to discard, with clear economic, environmental and social advantages. Circular economy is an inevitable path for pharmaceutical industry to act according to its ultimate goals, i.e., enhance human health and well-being.

In order to meet green chemistry[12] and sustainability[17] recommendations and to move towards a circular economy,[13] modifications and innovations have been introduced in several production processes across the pharmaceutical industry. Key strategies were adopted: (i) the modification of synthetic routes substituting nefarious chemicals (raw materials, solvents, auxiliaries) by renewable or more benign ones, (ii) the substitution of multiple-step reactions by single-step ones and/or (iii) the implementation of recovery and recycling routes.[1, 13, 18] Organic solvents are employed in all steps involved in pharmaceuticals' production processes (synthesis, separation and formulation), being a major cause of hazards and wastes in the pharmaceutical industry.[6, 7] Furthermore, the final pharmaceutical products are thus likely to be contaminated, so that the proper selection of the solvents is crucial for yields and product quality achieved.[7, 19] At the forefront, the selection of solvents resembling the traditional ones but with more appealing environmental credentials (e.g., pentane and hexanes by heptane, benzene by toluene) was endorsed.[20] With environmental concerns in mind, FDA has approved related legislation, so that benzene was excluded from pharmaceutical industry and other highly pollutant solvents, such as hexane and toluene, should be exclusive to unavoidable cases.[21] Solvents such as water (e.g.,[22]) and ethanol (e.g.,[23]) are highly recommended. Alternative solvents have been highlighted in the frame of

pharmaceutical industries as advantageous options, since they are more benign, easy to recycle and less prone to contaminate the final product and the environment.[24] Alternative solvents encompass water, supercritical fluids, fluorous solvents, ionic liquids (ILs) and deep eutectic solvents (DES), among others.[24]

Adopting the strategies outlined above, pharma companies are thus benefiting from wastes, environmental footprint and costs minimization as well as improved workers safety. In 1998, Pfizer has embarked on an endeavor where several manufacturing processes, some of them entailing top selling drugs, were modified using green chemistry metrics. The traditional route to obtain sertraline hydrochloride (Zoloft), the most prescribed antidepressant worldwide, used titanium tetrachloride, a toxic, corrosive and air-unstable liquid, as "dehydrating" agent.[23] The production of titanium byproducts needed to be carefully managed, so that additional energy, inputs, costs and risks to the workers were involved.[23] The innovative process implemented uses ethanol as the main solvent and a more selective catalyst, allowing (i) to pass from a three-step to a single-step reaction, (ii) to create a safer synthetic route, (iii) to diminish the quantities of starting materials and solvents and (iv) to recycle the materials and the catalyst into the process.[23] The transformation of the sildenafil citrate (Viagra) manufacturing process followed, where the high quality of the final pharmaceutical was maintained at the same time that (i) safer reagents, (ii) lower number of reaction steps and (iii) lower number of solvents used and their recovery were accomplished.[25] The "greener" process allowed lower energy inputs and an improved E-factor of 6 kg waste *per* kg product.[25] Although out of industrial atmosphere, Bica and co-workers[26] came up with an innovative strategy to isolate a precursor of Tamiflu from natural sources resorting to a class of alternative solvents, ILs. Later on, the traditional synthesis of pregabalin (Lyrica), one of the most prescribed drugs around the world, was modified by developing enzymatic-based process with reaction steps conducted in water as the solvent.[22] The implementation of this new process allowed reducing waste when compared to the former method used, with improvements on the E factor from 86 down to 9.[22] Within a period of 13 years, Pfizer was able to reduce by 90% the amounts of solvents used and by 50% the raw materials.[22, 27] With similar rationales, Merck and Codexis developed an enzymatic process for the

synthesis of sitagliptin (Januvia) which enabled the operation under milder conditions, the removal of all metals involved during production and the reduction of the waste generated. [28] Also Roche excluded the highly toxic thionyl chloride from oseltamivir phosphate (Tamiflu) synthetic route and simplified the process by decreasing the amount of reaction steps.[29] By its side, AstraZeneca has implemented a solvent recovery unit as a strategy to mitigate solvents as a major hazardous waste stream. Such a strategy was responsible for (i) reduction in production costs by solvent recycling and reuse and (ii) minimization of total waste generation,[30] placing AstraZeneca in the spotlight of circular economy examples. Alongside, "Kalundborg Symbiosis",[31] a consortium of eight distinct companies, implemented a circular economy-based mentality to its activity. The production processes rely on what they call a "full resource utilization", where by-products of one company serve as a resource for another creating shared value.[31]

1.1. Scopes and Objectives

This thesis proposes alternative routes for the extraction and purification of drugs as an attempt to improve the sustainability of pharmaceutical processes and to move towards a circular economy strategy. The development of the processes was done in the light of Green Chemistry, Sustainability and Circular Economy, as outlined in Figure 1.1.

In Chapter 2, a circular economy-based approach is suggested to face the challenge of dealing with pharmaceuticals at the end of their life cycle. The development of sustainable ways to valorize domestic pharmaceutical wastes, i.e., unspent or outdated medicines, as an alternative to incineration was carried by (i) the recovery of active ingredients to be further applied in chemical-related industries as starting materials and (ii) using cleaner processes based on water and ILs (alternative solvents). The enhanced solvency of ILs is highlighted by the IL-mediated extraction and purification techniques used (solid-liquid extractions – ***section 2.1.1.***, aqueous biphasic systems (ABS) - ***section 2.1.2.*** and three-phase partitioning systems (TPP)– ***section 2.1.3.***). Particular emphasis will be given to processes involving real pharmaceutical samples (i.e., pills) and focusing on the isolation of the target drugs.

In Chapter 3, the age-long problem of producing enantiopure drugs rather than their racemic mixtures is addressed. Cleaner, simpler and tunable processes for the separation of racemic drugs were planned based on the use of two classes of alternative solvents: chiral ILs (CILs) and chiral DES. CILs were introduced in ABS as both the solvent and chiral selector - ***sections 3.1.1.*** and ***3.1.2.*** Finally, DES were considered as new chiral agents in enantioseparations, by shedding light upon the role of chirality on DES formation – ***section 3.2.1.***

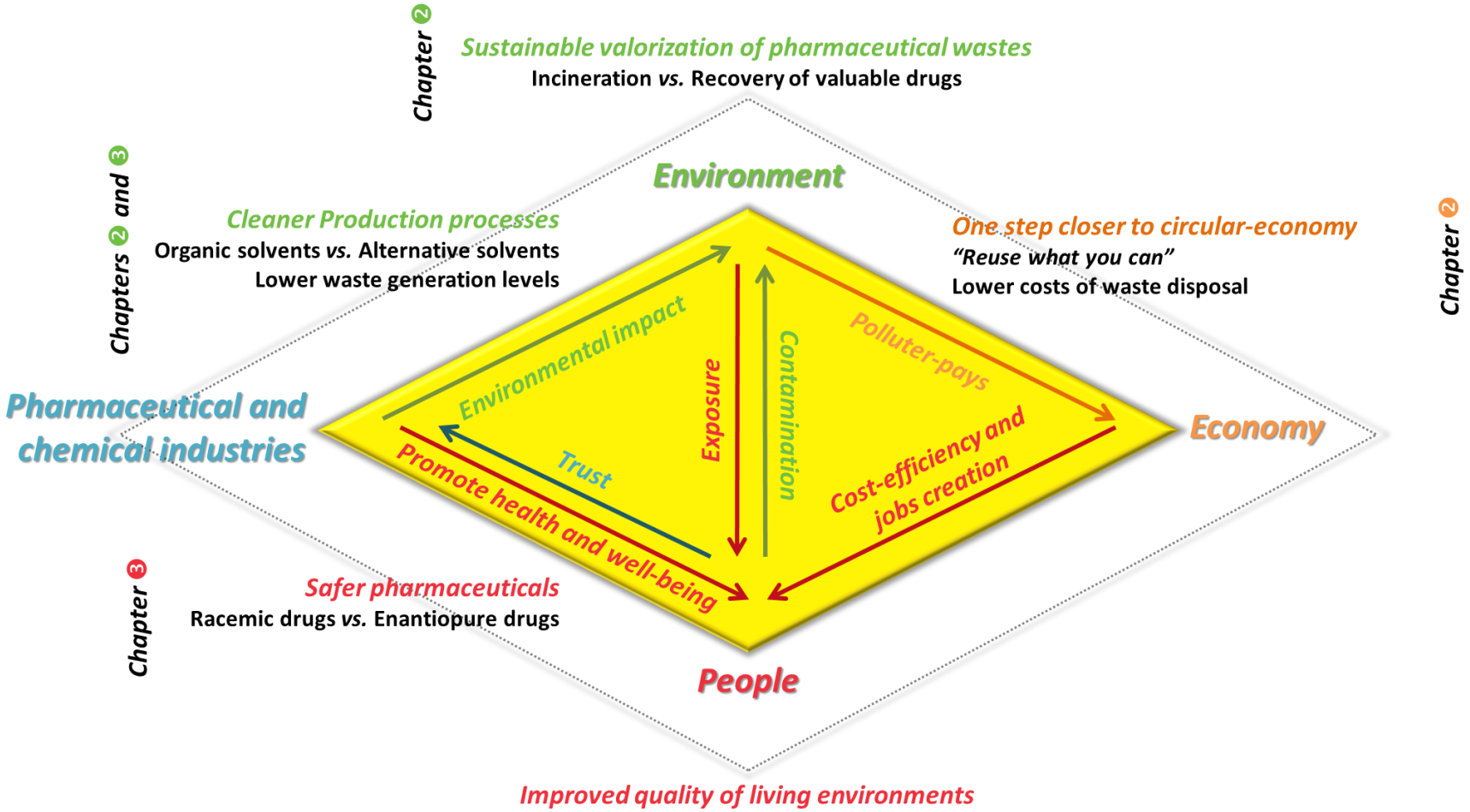

Figure 1.1. Overview of the present thesis.

References

[1] Alfonsi, K.; Colberg, J.; Dunn, P. J.; Fevig, T.; Jennings, S.; Johnson, T. A.; Kleine, H. P.; Knight, C.; Nagy, M. A.; Perry, D. A., et al. Green chemistry tools to influence a medicinal chemistry and research chemistry based organisation. *Green Chemistry* **2008,** *10* (1), 31-36.

[2] Manley, J. B., Introduction: The Five Ws of Pharmaceutical Green Chemistry. In *Green Chemistry Strategies for Drug Discovery*, The Royal Society of Chemistry: 2015; pp 1-12.

[3] Roschangar, F.; Sheldon, R. A.; Senanayake, C. H. Overcoming barriers to green chemistry in the pharmaceutical industry - the Green Aspiration Level™ concept. *Green Chemistry* **2015,** *17* (2), 752-768.

[4] Kümmerer, K. The presence of pharmaceuticals in the environment due to human use – present knowledge and future challenges. *Journal of Environmental Management* **2009,** *90* (8), 2354-2366.

[5] Sheldon, R. A. The E factor 25 years on: the rise of green chemistry and sustainability. *Green Chemistry* **2017,** *19* (1), 18-43.

[6] Constable, D. J. C.; Jimenez-Gonzalez, C.; Henderson, R. K. Perspective on Solvent Use in the Pharmaceutical Industry. *Organic Process Research & Development* **2007,** *11* (1), 133-137.

[7] Grodowska, K.; Parczewski, A. Organic solvents in the pharmaceutical industry. *Acta Poloniae Pharmaceutica* **2010,** *67* (1), 3-12.

[8] Calisto, V.; Esteves, V. I. Psychiatric pharmaceuticals in the environment. *Chemosphere* **2009,** *77* (10), 1257-1274.

[9] Sanchez, W.; Sremski, W.; Piccini, B.; Palluel, O.; Maillot-Maréchal, E.; Betoulle, S.; Jaffal, A.; Aït-Aïssa, S.; Brion, F.; Thybaud, E., et al. Adverse effects in wild fish living downstream from pharmaceutical manufacture discharges. *Environment International* **2011,** *37* (8), 1342-1348.

[10] Kummerer, K. Sustainable from the very beginning: rational design of molecules by life cycle engineering as an important approach for green pharmacy and green chemistry. *Green Chemistry* **2007,** *9* (8), 899-907.

[11] Kümmerer, K., Why Green and Sustainable Pharmacy? In *Green and Sustainable Pharmacy*, Kümmerer, K.; Hempel, M., Eds. Springer Berlin Heidelberg: Berlin, Heidelberg, 2010; pp 3-10.

[12] Anastas, P. T.; Warner, J. C., *Green chemistry: theory and practice*. Oxford university press: 2000.

[13] Sheldon, R. A. Green chemistry and resource efficiency: towards a green economy. *Green Chemistry* **2016,** *18* (11), 3180-3183.

[14] Bourguignon, D. Closing the loop - New circular economy package. http://www.europarl.europa.eu/RegData/etudes/BRIE/2016/573899/EPRS_BRI(2016)573899_EN.pdf. (accessed May 5, 2018).

[15] Stahel, W. R. The circular economy. *Nature* **2016,** *531*, 435–438.

[16] Vice-President Katainen's keynote speech at the 2016 European Circular Economy Conference. https://ec.europa.eu/commission/commissioners/2014-2019/katainen/announcements/vice-president-katainens-keynote-speech-2016-european-circular-economy-conference_en (accessed May 26, 2018).

[17] Glavič, P.; Lukman, R. Review of sustainability terms and their definitions. *Journal of Cleaner Production* **2007,** *15* (18), 1875-1885.

[18] Dunn, P. J.; Wells, A. S.; Williams, M. T., Future Trends for Green Chemistry in the Pharmaceutical Industry. In *Green Chemistry in the Pharmaceutical Industry*, Wiley-VCH Verlag GmbH & Co. KGaA: 2010; pp 333-355.

[19] Kolář, P.; Shen, J.-W.; Tsuboi, A.; Ishikawa, T. Solvent selection for pharmaceuticals. *Fluid Phase Equilibria* **2002,** *194-197*, 771-782.

[20] Capello, C.; Fischer, U.; Hungerbuhler, K. What is a green solvent? A comprehensive framework for the environmental assessment of solvents. *Green Chemistry* **2007,** *9* (9), 927-934.

[21] FDA, Q3C — Tables and List Guidance for Industry. https://www.fda.gov/downloads/drugs/guidances/ucm073395.pdf (accessed May 5, 2018).

[22] Dunn, P. J. Pharmaceutical Green Chemistry process changes - how long does it take to obtain regulatory approval? *Green Chemistry* **2013,** *15* (11), 3099-3104.

[23] Taber, G. P.; Pfisterer, D. M.; Colberg, J. C. A new and simplified process for preparing N-[4-(3, 4-dichlorophenyl)-3, 4-dihydro-1 (2H)-naphthalenylidene] methanamine and a telescoped process for the synthesis of (1 S-cis)-4-(3, 4-dichlorophenol)-1, 2, 3, 4-tetrahydro-N-methyl-1-naphthalenamine mandelate: key intermediates in the synthesis of sertraline hydrochloride. *Organic Process Research & Development* **2004,** *8* (3), 385-388.

[24] Kerton, F. M.; Marriott, R., *Alternative solvents for green chemistry*. Royal Society of Chemistry: 2013.

[25] Dunn, P. J.; Galvin, S.; Hettenbach, K. The development of an environmentally benign synthesis of sildenafil citrate (Viagra[trade mark sign]) and its assessment by Green Chemistry metrics. *Green Chemistry* **2004,** *6* (1), 43-48.

[26] Ressmann, A. K.; Gaertner, P.; Bica, K. From plant to drug: ionic liquids for the reactive dissolution of biomass. *Green Chemistry* **2011,** *13* (6), 1442-1447.

[27] Ritter, S. K. Greening Up Process Chemistry. *Chemical & Engineering News* **2010,** *88* (43), 45-47.

[28] Examples of Green Chemistry. https://www.acs.org/content/acs/en/greenchemistry/what-is-green-chemistry/examples.html. (accessed Feb 8, 2016).

[29] Carr, R.; Ciccone, F.; Gabel, R.; Guinn, M.; Johnston, D.; Mastriona, J.; Vandermeer, T.; Groaning, M. Streamlined process for the esterification and ketalization of shikimic acid en route to the key precursor for oseltamivir phosphate (Tamiflu™). *Green Chemistry* **2008,** *10* (7), 743-745.

[30] Environmental Sustainability. https://www.astrazeneca.com/content/dam/az/our-company/Sustainability/Environmental-Sustainability.pdf. (accessed May 5, 2018).

[31] Kalundborg Symbiosis Business Strategy. http://www.symbiosis.dk/en/business-strategy/ (accessed May 26, 2018).

CHAPTER 2

Recovery of drugs from pharmaceutical wastes

2. Recovery of drugs from pharmaceutical wastes

The direct household disposal of medicines may result from the end of the shelf life of drugs making them improper for consumption, the inadequate size of the packages and alterations in posology, or even failure to follow the therapeutic guidelines.[1, 2] Around Europe, large amounts of pharmaceutical wastes have been generated and, in some cases, incorrectly disposed. During 2015, in England, it was estimated that over 1 million of health products prescribed were dispensed every day, which represents a 50 % increase since 2005.[3] Other surveys, although they may seem outdated, mirror this alarming scenario, which varies with countries. For instance, in 2011, Belgium collected 572 tons of unwanted drugs, with an average increase of 2.5 % *per* year; around 223 tons of pharmaceutical wastes were recovered in 2012 by the Hungarian national system for collection and disposal of household pharmaceuticals, which is increasing over 7 % *per* year; Lithuania, in turn, lacks a responsible agency for this purpose since 2009, the year in which 31 tons of pharmaceutical wastes were received.[4] With the latter case being an exception, most countries have nowadays their own national collection system, which is responsible for the collection, storage, transport and removal of pharmaceutical wastes. Moreover, efforts are being directed to educate and inform population as a way to improve disposal routines.[5]

Portugal, particularly, has its waste management being carried by VALORMED, which collected around 1000 tons of pharmaceutical wastes (package and medicines) in 2015. After directing the waste to sorting centres, recyclable materials are separated from the medicines, which are incinerated for energetic valorization.[6] In addition to its high costs of construction, operation and maintenance, this valorization route fails to match Green and Sustainable Chemistry recommendations[7, 8] due to its hazardous nature related to intensive emission of pollutant gases and carcinogenic substances. The way by which incineration prevents the entrance of pharmaceuticals into the environment is the complete disintegration of the active ingredients at high temperature conditions between 1500 and 2000 ^{o}C.[9] In addition, the complete destruction of the waste neglects the opportunity of recovering valuable active ingredients. Indeed, circa 90 % of the active ingredients is still in its active form even past the expiration date.[10]

The major drawbacks presented by the management of household pharmaceutical wastes are thus urgent to be faced. Envisioning a circular economy,[11] the direct extraction and purification of drugs from pharmaceutical wastes represents a promising alternative to incineration. The recovered compounds will serve in a wide range of applications in the chemical industry (e.g., as starting materials for other chemicals or as industrial or commercial standards). So, it is of great interest the development of novel strategies that combine the extraction and purification of drugs from pharmaceutical wastes. In the light of Green Chemistry,[7] the implementation of alternative solvents represents an appealing solution. In particular, ILs have been highlighted as highly performant, economically viable and safer solvents in the extraction and purification of drugs.[12]

2.1. Ionic liquids as alternative solvents in the extraction and purification of drugs

This section is based on Ventura, S. P. M.; e Silva, F. A.; Quental, M. V.; Mondal, D.; Freire, M. G.; Coutinho, J. A. P. Ionic-Liquid-Mediated Extraction and Separation Processes for Bioactive Compounds: Past, Present, and Future Trends. *Chemical Reviews* **2017**, *117* (10), 6984–7052.

Contributions: S.P.M.V., M.G.F. and J.A.P.C. conceived and directed this work. Francisca A. e Silva, M.V.Q. and D.M. wrote the chapters included in this review, with vital contributions from S.P.M.V., M.G.F. and J.A.P.C.. Francisca A. e Silva. wrote those comprising Lipids and Other Hydrophobic Compounds, Nucleic Acids and Drugs and Pharmaceuticals, the latter being included in this chapter. Furthermore, Francisca A. e Silva was responsible for bringing all chapters together and drawing all Figures.

ILs are alternative solvents, since recently envisioned as promising substitutes to the molecular solvents widely used in pharmaceutical industry. These are salts of low melting point, usually below 100 ^{o}C,[13] and are commonly composed of a large organic cation and an anion that can be of either organic or inorganic nature. The low melting temperatures of ILs are a result of the lack of symmetry in their ions and their low-charge density, which lead to weaker Coulombic interactions and weaker cohesive energies in the solid phase when compared to high melting temperature salts.[13-16] Besides their outstanding thermal, chemical and electrochemical stabilities, lack of flammability and negligible volatility (avoiding their release into the atmosphere), ILs have found the spotlight in the development of novel extraction and purification approaches due to their excellent solvation ability and stabilizing properties.[17-21] Furthermore, their high structural versatility represented by their “designer solvent” nature[22] allows the design of task-specific solvents thus surpassing the poor selectivities exhibited by traditional organic solvents. In the processing of pharmaceuticals and beyond their use as solvents in extraction and purification approaches, ILs have been used in the synthesis of several

drugs, as novel routes for drug delivery, as suitable media for polymorphic drugs, as well as in the formulation of novel liquid active pharmaceutical ingredients of boosted bioavailability.[23, 24]

ILs are envisaged as powerful solvents for the extraction of several important molecules, in particular drugs, due to the unique array of intermolecular interactions that they can establish. Numerous authors have devoted their attention to the determination of the solubility of active pharmaceutical ingredients in ILs as the basis for the development of IL-based separation and purification processes. Currently, the spectrum of compounds investigated is broad, ranging from cardioactive prototype drugs[25] to antibiotics,[26-30] non-steroidal anti-inflammatory drugs (NSAIDs),[27, 28, 31] analgesic,[31, 32] anthelmintic,[32] and androgen[32] compounds. Most of these systematic studies focus on the use of hydrophobic ILs composed of nitrogen-[25, 26, 29-32] or phosphorus-[27, 28] based cations, and anions such as $[NTf_2]^-$[25-27, 29, 30] and $[PF_6]^-$,[31, 32] while only few works have reported the use of hydrophilic ILs.[25, 32] Rogers and co-workers,[33] in a study of drug delivery, recently shown that ILs, if cautiously designed, can boost the water solubility of poorly soluble active pharmaceutical ingredients. This concept can be thus extended to the extraction and purification of drugs using aqueous IL solutions.

This section overviews more efficient separation routes for pharmaceutical drugs by taking advantage of the unique characteristics of the ILs. Three main approaches are found in the literature: (i) liquid-liquid extraction (LLE), where hydrophobic ILs are generally adopted as substitutes for conventional organic solvents, (ii) ABS composed of ILs and salts, polymers or amino acids, sometimes combined with previous solid-liquid extraction steps, and (iii) crystallization in ILs or IL-enriched media. Separation and purification processes in aqueous media are the most widely adopted approaches. Distinct types of compounds were the target of separation and purification by each of these techniques, with antibiotics standing out as the compounds attracting the most attention. Besides antibiotics, NSAIDs, analgesics, vasodilators, fibrates, hypnotics, anticonvulsants and immunosupressants are within the drugs studied. The name and abreviation of the IL cation and anion combinations considered in this overeview is provided in Table 2.1.

The utilization incidence of distinct combinations of IL ions reveals that 1-alkyl-3-methylimidazolium-based ILs are the most well-investigated, although an appreciable usage of more benign ammonium-based cations, i.e., $[N_{wxyz}]^+$ and $[Ch]^+$, began over the past few years. $[BF_4]^-$, Cl^- and $[PF_6]^-$ are the anions most frequently paired with $[C_nC_1im]^+$. The more recent use of organic-acid-derived anions, namely $[C_1CO_2]^-$, $[Glut]^-$, $[Lev]^-$ and $[Suc]^-$, should however be noted, indicative of a promising trend towards the use of more biocompatible ILs in separation processes for drug production.

Table 2.1. Name and abreviation of the IL cation-anion combinations considered in this overview.

Cation		**Anion**	
Name	**Abbreviation**	**Name**	**Abbreviation**
1,3-diallylimidazolium	$[aaim]^+$	Alkylphosphonate	$[C_nPO_3]^-$
1,3-dihexyloxymethylimidazolium	$[(C_6H_{13}OCH_2)_2im]^+$	Alkylsulphate	$[C_nSO_4]^-$
1-alkyl-1-methylpyrrolidinium	$[C_nC_1pyrr]^+$	Bicarbonate	$[Bic]^-$
1-alkyl-2,3-dimethylimidazolium	$[C_nC_1C_1im]^+$	Bis(trifluoromethylsulfonyl)imide	$[NTf_2]^-$
1-alkyl-3-methylimidazolium	$[C_nC_1im]^+$	Bromide	Br^-
1-alkylpyridinium	$[C_npyr]^+$	Carboxylate	$[C_nCO_2]^-$
1-allyl-3-alkylimidazolium	$[aC_nim]^+$	Chloride	Cl^-
1-benzyl-3-methylimidazolium	$[C_7H_7C_1im]^+$	Dihydrogencitrate	$[DHCit]^-$
1-hexyloxymethyl-3-methylimidazolium	$[(C_6H_{13}OCH_2)C_1im]^+$	Dihydrogenophosphate	$[H_2PO_4]^-$
1-hydroxyalkyl-3-methylimidazolium	$[(OH)C_nC_1im]^+$	Glutarate	$[Glut]^-$
Cholinium [*N,N,N*-trimethyl-*N*-(2-hydroxyethyl)ammonium	$[Ch]^+$	Hexafluorophosphate	$[PF_6]^-$
N-Alkyl-*N,N*-dimethyl-*N*-(2-hydroxyethyl)ammonium	$[N_{11n(2OH)}]^+$	Levulinate	$[Lev]^-$
N-methyl-*N,N,N*-trioctylammonium	$[N_{1888}]^+$	Succinate	$[Suc]^-$
tetraalkylammonium	$[N_{nnnn}]^+$	Tetrafluoroborate	$[BF_4]^-$
Tetraalkylphosphonium	$[P_{nnnn}]^+$	Trifluoromethanesulfonate	$[CF_3SO_3]^-$

Liquid-liquid extractions

Cull et al.[34] were the first to report the use of ILs in the LLE of pharmaceuticals aiming at overcoming the potential hazards of organic solvents. The authors[34] used a $[C_4C_1im][PF_6]$ + water biphasic system to extract erythromycin A, a macrolide antibiotic industrially produced by aerobic fermentation, showing that the use of ILs could be as efficient as butyl acetate. This pioneering work triggered a new trend of seeking novel IL + water biphasic extraction systems for antibiotics. Table 2.2 presents the systems reported in the literature for such a goal. Based on the data reviewed, a scheme of a general process based on these LLE systems is outlined in Figure 2.1.

In 2005, Soto et al.[35] proposed the application of biphasic $[C_8C_1im][BF_4]$ + water systems for the extraction of two other antibiotics, amoxicillin and ampicillin. The partition coefficient results achieved (from 0.17 to 20.34) indicated a clear dependency of the antibiotics partition on the pH, due to their anionic (at pH 8) or zwitterionic (at pH 4) forms. Manic et al.[36] successfully extracted erythromycin A from an aqueous solution using $[C_4C_1pyrr][NTf_2]$. The major achievement of this work was that forty times less volume of the IL than that of an aqueous solution was used in ten successive cycles to achieve an overall yield higher than 80%. High pressure CO_2 was used to isolate circa of 76% of erythromycin,[36] this being one of the few examples where the recovery of pharmaceuticals from the IL-rich phase was attempted. After proving the chemical stability of the extracted antibiotic with ILs, the authors designed a valuable extraction process (represented in Figure 2.1A) with potential for industrial applications.

Biphasic IL + water systems composed of two hydrophobic imidazolium-based ILs ($[(C_6H_{13}OCH_2)_2im][NTf_2]$ and $[(C_6H_{13}OCH_2)C_1im][BF_4]$), at different pH values, were investigated by Domańska and collaborators[37] for the extraction of nitrofurantoin, an antibiotic prescribed for the treatment of infections of the urinary tract. The nitrofurantoin exhibited preferential partitioning towards the IL phase, except when $[(C_6H_{13}OCH_2)C_1im][BF_4]$ was employed at pH ≥3.13. The best conditions were obtained with the IL $[(C_6H_{13}OCH_2)_2im][NTf_2]$ and low pH (partition coefficient of 19.7), where the partitioning was explained based on a balanced contribution of π···π stacking, lone pair electrons, permanent dipoles and electrostatic interactions.[37]

Penicillin G, a microbially-produced antibiotic, was also the target of extraction by $[C_nC_1im][PF_6]$ (n = 4, 6 and 8) in two works by Matsumoto et al.[38] and Liu et al.[39] Matsumoto et al.[38] also included $[N_{1888}]Cl$ in their study, whereby this IL, at pH 6, led to the largest quantities of penicillin G extracted, and where the authors[38] suggested an anion exchange mechanism between the Cl^- and the antibiotic (which possesses a dissociation constant of 2.76). However, no real support for this assumption was provided by the authors,[38] since the tests carried out to prove their hypothesis led to inconclusive results. The isolation of antibiotics from $[N_{1888}]Cl$ was also attempted, but with no success.[38] However, inconsistent results were reported by Liu and collaborators[39] using $[C_nC_1im][PF_6]$ (n = 4, 6 and 8) ILs. In this work, $[C_4C_1im][PF_6]$ at pH 2 led to higher extraction performances (partition coefficient of circa 10 and extraction efficiency >80%). In this work, a simple isolation of the antibiotic (>95%) from the IL phase was achieved using a weak base (potassium bicarbonate). Notably, this system was successfully employed for the antibiotic extraction from its fermentation broth, with enhanced selectivity for contaminant removal than that achieved with the conventional process employing butyl acetate.[39] This last step is of high relevance, given that most authors carry out extraction studies with aqueous solutions spiked with pharmaceuticals, and do not prove the feasibility of the developed processes with real matrices. Figure 2.1B shows a schematic representation of the integrated process proposed by the authors.[39]

A later study by Wang and co-workers[40] focused on the development of non-toxic IL-based extraction systems. For this purpose, the naturally occurring cholinium cation was used for the preparation of hydrophobic ILs of increasing alkyl chain length, i.e., $[N_{11n(2OH)}]^+$ (n = 4, 6, 8 and 10) combined with the $[NTf_2]^-$ anion.[40] Four distinct drugs were investigated, namely the NSAIDs ibuprofen and indomethacin, the analgesic drug phenacetin, and the anesthetic and analgesic agent lidocaine. After the optimization of the extraction volume phase ratio and the equilibrium time, the impact of pH, the chemical structure of the ILs, and temperature upon the partitioning of the drugs was assessed. Depending on the drug under investigation, distinct effects were noticed: the indomethacin migration to the IL phase was significantly limited by higher pH conditions; enhanced performances were obtained for both ibuprofen and indomethacin by

increasing the IL alkyl side chain length, which is in contrast to the pattern observed for lidocaine; and finally, the extraction mechanism of ibuprofen is endothermic. Finally, the authors[40] highlighted the importance of isolating the pharmaceuticals from the ILs by removing more than 65% of indomethacin through pH changes (with 0.1 mol.L^{-1} NaOH), allowing the authors to envisage an integrated process similar to that represented in Figure 2.1C.

In a recent work, Vitasari et al.[41] have successfully separated the similar drugs progesterone and pregnenolone by IL-based LLE. The number of solvents able to solubilize these two steroids is limited, making ILs excellent candidates for such an application. The search for suitable systems was performed in three steps: (i) selection of suitable organic solvents by COSMO-RS, (ii) experimental determination of organic solvent-fluorinated IL combinations able to form two liquid phases, and (iii) determination of the IL concentration in the organic solvent phase.[41] The *tert*-butyl methyl ether-[C_4C_1im][BF_4] mixture was elected as the ideal system to pursue studies on the partitioning of progesterone and pregnenolone. A selectivity of 2.1 was reached and the purification of progesterone was successfully conducted by simulating a countercurrent extraction process.[41]

During the manufacturing process in any pharmaceutical industry, the final produced drugs cannot contain impurities and should obey the standards imposed by legal guidelines. Encouraged by such a necessity, Rogers and co-workers[42] proposed an IL-based separation strategy for an intermediate of the aliskiren synthesis from an interfering ammonium salt formed during the reaction. Aliskiren is a direct renin inhibitor used to treat high blood pressure. By investigating hydrophobic *vs.* hydrophilic ILs, distinct biphasic systems were created: [C_2C_1im][C_1CO_2] + ethyl acetate, [C_2C_1im][C_1CO_2] + *n*-heptane, [C_2C_1im][NTf_2] + *n*-heptane, and [C_2C_1im][NTf_2] + water. The solubilities of the reactants (a lactone and 3-amino-2,2-dimethylpropanamide), amide products and ammonium salts in both ILs and the three solvents were measured, and based on the results obtained, the [C_2C_1im][NTf_2] + water biphasic system was selected to separate the standard mixture. At the end of the process, the purities of both lactone and amide products were not as high as desired due to contamination issues with the hydrophobic

IL. Hence, the authors were forced to adopt the $[C_2C_1im][C_1CO_2]$ + ethyl acetate biphasic system, given the possibility of being able to remove $[C_2C_1im][C_1CO_2]$ from the lactone and amide product (both hydrophobic) by a simple washing step with water, as sketched in Figure 2.1C. Both regenerated lactone and amide were separated with high purity and the remaining reactant and ammonium salt were precipitated and recovered by washing the standard mixture with water. When applying this procedure to an actual reaction mixture (composed of reactants, products and some by-products), an additional step consisting of washing the regenerated amide with *n*-heptane was needed to remove the residual by-products.[42]

Also for the intermediate R-phenylacetylcarbinol, the replacement of toluene in LLE by the use of ILs was investigated. Computer aided molecular design was used, due to its time- and money-saving advantages over common systematic experimental studies.[43]

To summarize, two-phase systems with hydrophobic ILs + water are by far the most studied for the separation of drugs, as only one work[42] addressing hydrophilic ILs in combination with organic solvents for separation purposes exists. It is well-documented that hydrophobic ILs are more toxic than the hydrophilic ones and some of them are water-unstable, e.g., with the $[BF_4]^-$ anion. Even so, a recent trend towards the use of water-stable and more benign ILs has been observed in recent years.

Isolation strategies, with vital relevance for future industrial applications, although not conducted in most of the works herein reviewed, were however contemplated by some researchers. This more complex strategy allows researchers to obtain the target product free of IL (step 3 of Figure 2.1) and the recycled IL for further use (step 4 of Figure 2.1). Also missing in most reported works is an assessment of the chemical stability and pharmacological activities of the drugs extracted as a way of reinforcing the promising status of IL-based technologies for the purification of pharmaceuticals.

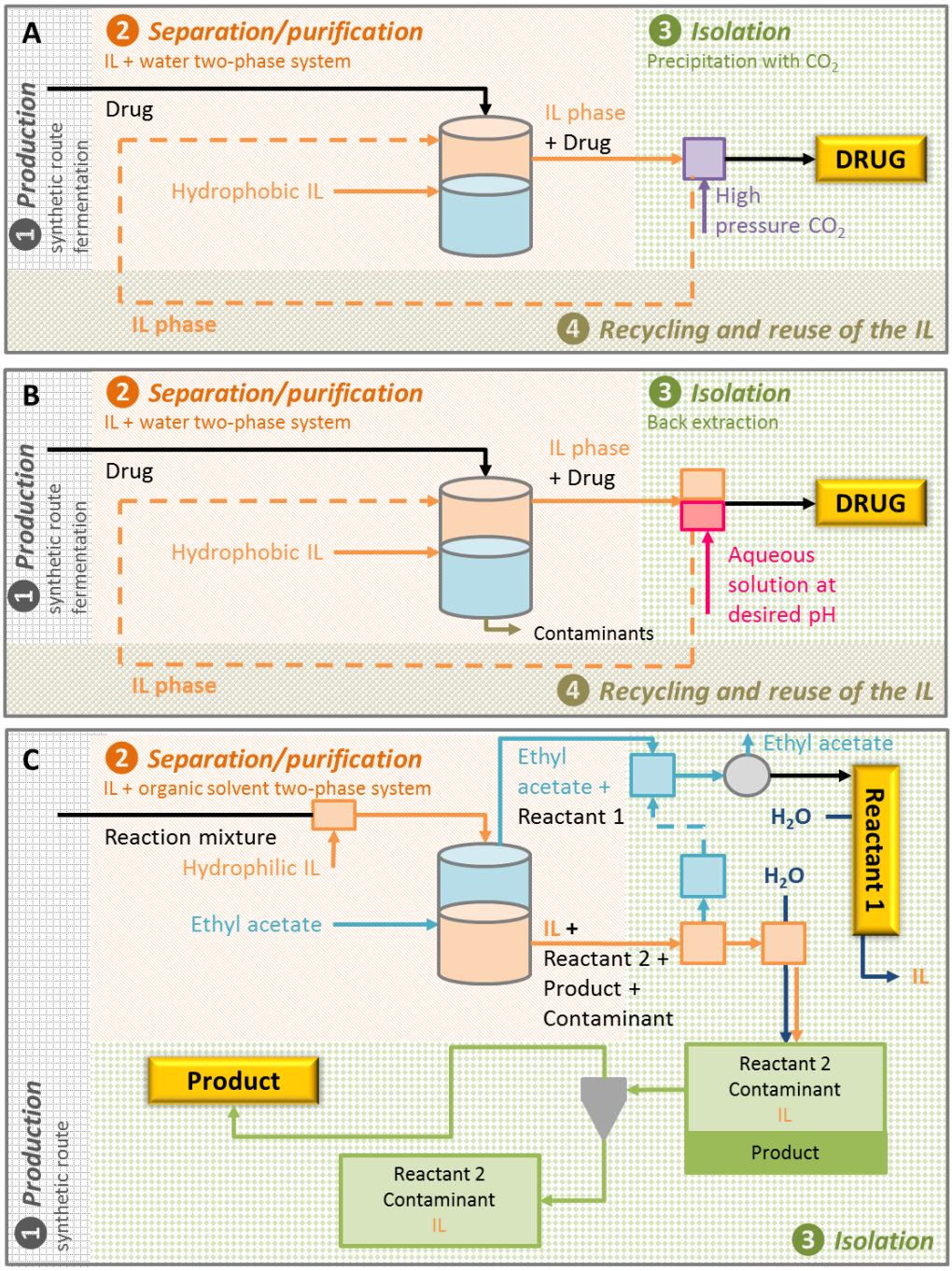

Figure 2.1. Schematic representation of the integrated process comprising the production, separation/purification, recovery of the target molecule and recycling of solvents in two-phase LLE comprising ILs. A and B correspond to processes where an induced precipitation with CO_2[36] and back-extraction[39, 40] approaches were used to recover the pharmaceuticals, while C represents the process of purification of an intermediate of aliskiren synthesis.[42]

Table 2.2. Extraction and separation of pharmaceuticals using LLE with hydrophobic ILs.

Pharmaceutical	**System used**	**Isolation strategy**
Amide (intermediate) and ammonium salt (contaminant): aliskiren synthesis	$[C_2C_1im][NTf_2]$ + water,[42] $[C_2C_1im][C_1CO_2]$ + ethyl acetate[42]	Washing with water and precipitation[42]
Amoxicillin	$[C_8C_1im][BF_4]$ + water[35]	
Ampicillin	$[C_8C_1im][BF_4]$ + water[35]	
Erythromicin A	$[C_4C_1im][PF_6]$ + water,[34] $[C_4C_1pyrr][NTf_2]$ + water[36]	High pressure CO_2[36]
Ibuprofen	$[N_{114(2OH)}][NTf_2]$ + water,[40] $[N_{116(2OH)}][NTf_2]$ + water,[40] $[N_{118(2OH)}][NTf_2]$ + water,[40] $[N_{1110(2OH)}][NTf_2]$ + water[40]	
Indomethacin	$[N_{114(2OH)}][NTf_2]$ + water,[40] $[N_{116(2OH)}][NTf_2]$ + water,[40] $[N_{118(2OH)}][NTf_2]$ + water,[40] $[N_{1110(2OH)}][NTf_2]$ + water[40]	Back extraction with NaOH[40]
Lidocaine	$[N_{114(2OH)}][NTf_2]$ + water,[40] $[N_{116(2OH)}][NTf_2]$ + water,[40] $[N_{118(2OH)}][NTf_2]$ + water,[40] $[N_{1110(2OH)}][NTf_2]$ + water[40]	
Nitrofurantoin	$[(C_6H_{13}OCH_2)C_1im][BF_4]$ + water,[37] $[(C_6H_{13}OCH_2)_2im]$ $[NTf_2]$ + water[37]	
Penicillin G	$[C_4C_1im][PF_6]$ + water,[38, 39] $[C_6C_1im][PF_6]$ + water,[38, 39] $[C_8C_1im][PF_6]$ + water,[38, 39] $[N_{1888}]Cl$ + water[38]	Back extraction with potassium bicarbonate[39]
Phenacetin	$[N_{114(2OH)}][NTf_2]$ + water,[40] $[N_{116(2OH)}][NTf_2]$ + water,[40] $[N_{118(2OH)}][NTf_2]$ + water,[40] $[N_{1110(2OH)}][NTf_2]$ + water[40]	
Progesterone and pregnenolone	$[C_4C_1im][BF_4]$ + *tert*-butyl methyl ether[41]	

Aqueous biphasic systems

More environmentally friendly routes for the purification of pharmaceuticals appeared with the use of IL-based ABS or IL aqueous solutions. The first report on the extraction of drugs using IL-based ABS dates from 2005,[44] in which the authors successfully extracted two opium drugs, the analgesic morphine (maximum extraction efficiency achievable of 67%) and the vasodilator papaverine (maximum extraction efficiency achievable of 96%) using ABS formed by $[C_4C_1im]Cl$ and K_2HPO_4. A summary of the ABS and IL aqueous solutions studied is reported in Table 2.3 and some representative processes are depicted in Figure 2.2.

It is probably not surprising that most works deal with antibiotics, tetracycline being the most studied. Ma et al.[45] first applied ABS constituted by $[C_4C_1im][BF_4]$ plus NaH_2PO_4 to the purification of tetracycline. Since then, other systems were investigated aiming at using water-stable[46, 47] and more benign ILs,[48, 49] as well as other phase-forming agents besides salts,[46-48] in particular polymers.[49] Extraction efficiencies consistently higher than 80% were achieved when either K_2HPO_4[46] or Na_2CO_3[47] were used as the salting-out agents in several IL-based ABS. However, there were systems formed by more benign cholinium-based ILs that led to a distinct behavior. Shahriari et al.[48] reported for the first time ABS comprised of this type of IL with K_3PO_4. They showed that both tetracycline and its hydrochloride salt present distinct partition trends between the two phases. Although observing a preferable partition of antibiotics towards the IL-rich phase, when using [Ch][Glut] the opposite behavior was observed. The partition was explained in light of the aptitude of K_3PO_4 for salting-out, with [Ch][Glut] being the exception.[48] Another work[49] employed PEG 600 and cholinium-based ILs to generate ABS for the pre-purification of tetracycline from the fermentation broth of *Streptomyces aureofaciens*. While Shahriari et al.[48] reported a preferential partition of tetracycline towards the IL-rich phase, Pereira et al.[49] demonstrated that in polymer-IL-based ABS the antibiotic partitions preferentially towards the polymer-rich phase. Again, it was observed that the IL structure has a significant impact on the partition behavior. Even though conventional ABS composed of a polymer and a salt (PEG + Na_2SO_4) and of two salts ([Ch]Cl + K_3PO_4) revealed better performance in extracting tetracycline, the main

advantage afforded by using PEG and cholinium-based ILs relies on their boosted biocompatibility and biodegradability. The most relevant results reported by Pereira et al.[49] comprise the evaluation of the applicability of these systems for the pre-purification of tetracycline from its production medium, i.e., a fermentation broth, highlighting therefore the potential of IL-based ABS to be applied to real systems. The authors[49] finally discussed the possibility of varying the partition tendencies for either salt- or PEG-rich phases to create purification and back-extraction approaches, anticipating an integrated process similar to that represented in Figure 2.2A.

Penicillin G has been studied as a target compound in three published works comprising the use of IL-based ABS. In these studies, $[C_4C_1im]Cl$,[50] $[C_4C_1im][BF_4]$[51] and $[C_4C_1im]Br$[52] were used, with NaH_2PO_4 or Na_2HPO_4 as the salting-out agent, and two distinct lines of research were adopted: while Liu and co-workers[50] extracted penicillin G from a filtered fermentation broth with efficiencies higher than 90%, Jiang and collaborators[51] addressed the approaches applied to isolate this antibiotic by adding an hydrophobic IL, as described in Figure 2.2B. In addition to tetracycline and penicillin G, other antibiotics were also studied, namely ciprofloxacin and its hydrochloride salt,[48, 53] cephalexin[54] and chloramphenicol.[55, 56] Of particular interest is the work of Han et al.[55] which followed an emergent green tendency of applying a less toxic and more biodegradable organic salt, such as $K_2C_4H_4O_6$, as a replacement for the typically used inorganic salts.

In 2014, Coutinho's research group[57] published a pioneering work where ABS composed of ILs were applied in the valorization of pharmaceutical wastes. This work served as the starting point of this thesis project as it looked at these residues as a rich source of active pharmaceutical ingredients, which are currently disposed of by incineration. The authors[57] attempted the extraction of paracetamol directly from expired pills to further serve as starting materials or standards in several industries. For this purpose, novel ABS composed of tetraalkylammonium halides and three salts, namely $C_6H_5K_3O_7/C_6H_8O_7$ and K_2HPO_4/KH_2PO_4 buffers and K_2CO_3, were investigated. After an optimization study comprising the ammonium IL chemical structure, salt, tie-line

length and pH, carried out with the pure compound, the best conditions were then used to extract paracetamol from *Ben-u-ron® 500* pills, yielding complete extraction.

While significant progress was made in the recovery of pharmaceuticals by implementing IL-based ABS, as described above, both favorable trends and failures similar to those observed at the level of the hydrophobic IL + water two-phase systems were observed. A trend towards the creation of more benign systems is already noticeable in both IL and phase-forming agents. Although inorganic salts remain the first choice as phase-forming agents of ABS, organic salts and polymers are gaining favor in the IL-based ABS community as greener and more sustainable options. In some works, the isolation of the target pharmaceuticals and drugs was evaluated and different strategies were presented. However, the development of strategies to recover and reuse the ILs and other expensive phase-forming components is still infrequent. The stability of target pharmaceuticals, and their crystalline structure and polymorph formation when recovered from IL matrices, are additional factors that deserve more attention. Finally, none of the discussed studies evaluated the potential scale-up of the developed technologies, which remains a minor or unaddressed topic.

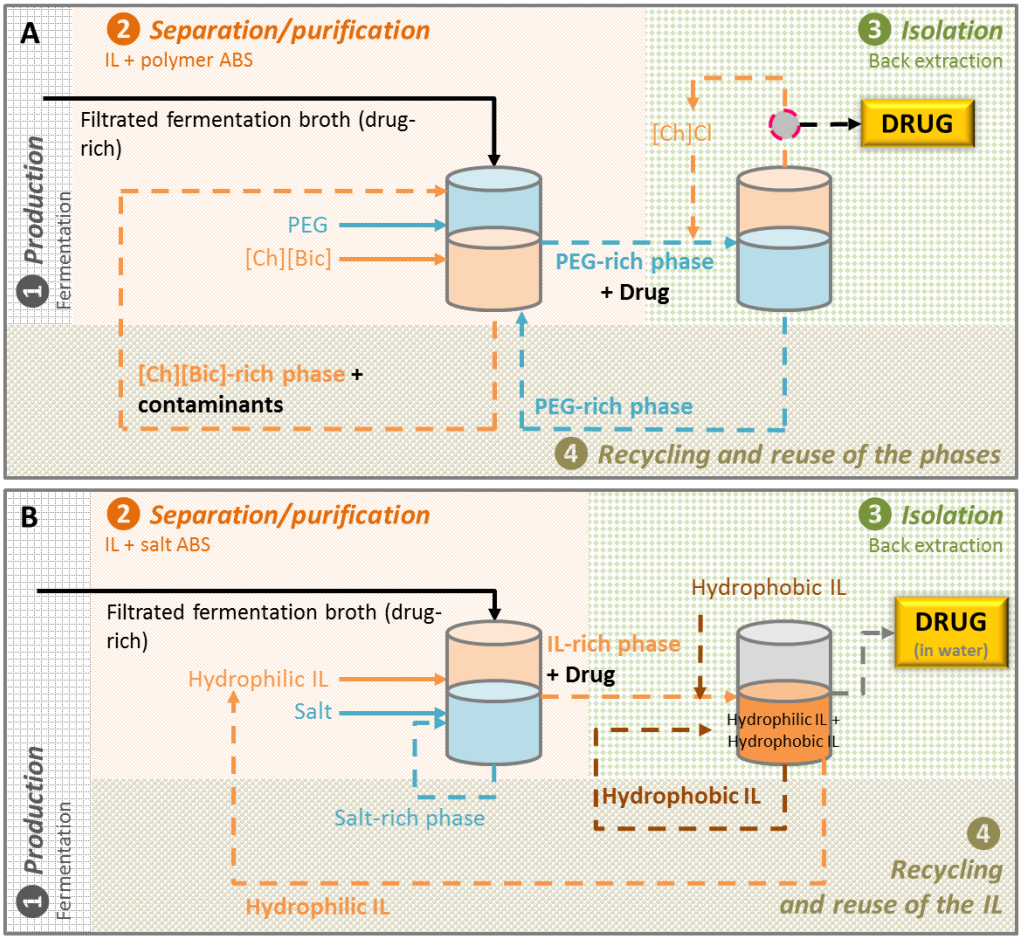

Figure 2.2. Schematic representation of integrated processes for the recovery of drugs, comprising the production, separation/purification of the drug and excipients, isolation of the drug and recycling of the phase-forming components in IL-based ABS. (A) Process with ABS with both separation/purification and back-extraction steps;[49] and (B) Process where both hydrophilic and hydrophobic ILs are used for the separation/purification and isolation of target pharmaceuticals.[51]

Table 2.3. Extraction and separation of pharmaceuticals using IL-based ABS or aqueous solutions of ILs.

Pharmaceutical	**System used**	**Isolation strategy**
Cephalexin	$[C_4C_1im][BF_4]$ + $ZnSO_4$[54]	
Chloramphenicol	$[C_4C_1im]Cl$ + $K_2C_4H_4O_6$,[55] $[C_6C_1im]Cl$ + $K_2C_4H_4O_6$,[55] $[C_7H_7C_1im]Cl$ + $K_2C_4H_4O_6$,[55] $[HOC_6C_1im]Cl$ + K_3PO_4,[56] $[HOC_6C_1im]Cl$ + K_2HPO_4,[56] $[HOC_6C_1im]Cl$ + K_2CO_3[56]	
Ciprofloxacin (or its hydrochloride salt form)	[Ch][Glut] + K_3PO_4,[48] [Ch][Suc] + K_3PO_4,[48] [Ch][Lev] + K_3PO_4,[48] [Ch][C_1CO_2] + K_3PO_4,[48] [Ch]Cl + K_3PO_4,[48] $[C_4C_1im][CF_3SO_3]$ + Lysine[53]	
Morphine	$[C_4C_1im]Cl$ + K_2HPO_4[44]	
Papaverine	$[C_4C_1im]Cl$ + K_2HPO_4[44]	
Paracetamol	$[N_{4444}]Cl$ + $C_6H_5K_3O_7/C_6H_8O_7$ pH 7,[57] $[N_{3333}]Cl$ + $C_6H_5K_3O_7/C_6H_8O_7$ pH 7,[57] $[N_{2222}]Cl$ + $C_6H_5K_3O_7/C_6H_8O_7$ pH 7,[57] $[N_{4444}]Br$ + $C_6H_5K_3O_7/C_6H_8O_7$ pH 7,[57] $[N_{3333}]Br$ + $C_6H_5K_3O_7/C_6H_8O_7$ pH 7,[57] $[N_{2222}]Br$ + $C_6H_5K_3O_7/C_6H_8O_7$ pH 7,[57] $[N_{2222}]Br$ + K_2HPO_4/KH_2PO_4 pH 7,[57] $[N_{2222}]Br$ + K_2CO_3,[57] $[N_{2222}]Br$ + $C_6H_5K_3O_7/C_6H_8O_7$ pH 5,[57] $[N_{2222}]Br$ + $C_6H_5K_3O_7/C_6H_8O_7$ pH 6,[57] $[N_{2222}]Br$ + $C_6H_5K_3O_7/C_6H_8O_7$ pH 8[57]	
Penicillin G	$[C_4C_1im]Cl$ + NaH_2PO_4,[50] $[C_4C_1im][BF_4]$ + NaH_2PO_4[51] and $[C_4C_1im]Br$ + Na_2HPO_4[52]	Hydrophobic IL + water LLE[51]
Tetracycline (or its hydrochloride salt form)	$[C_4C_1im][BF_4]$ + NaH_2PO_4,[45] $[C_4C_1im]Cl$ + K_2HPO_4,[46] $[C_2C_1im]Cl$ + Na_2CO_3,[47] $[C_4C_1im]Cl$ + Na_2CO_3,[47] $[C_6C_1im]Cl$ + Na_2CO_3,[47] $[aC_1im]Cl$ + Na_2CO_3,[47] $[C_4C_1pyrr]Cl$ + Na_2CO_3,[47] $[P_{4444}]Cl$ + Na_2CO_3,[47] [Ch][Glut] + K_3PO_4,[48] [Ch][Suc] + K_3PO_4,[48] [Ch][Lev] + K_3PO_4,[48] [Ch][C_1CO_2] + K_3PO_4,[48] [Ch]Cl + K_3PO_4,[48] [Ch]Cl + PEG 600,[49] [Ch][C_1CO_2] + PEG 600,[49] [Ch][Bic] + PEG 600,[49] [Ch][DHCit] + PEG 600,[49] [Ch][H_2PO_4] + PEG 600[49]	Back extraction with serial combination of distinct cholinium-PEG-based ABS[49]

Crystallization in IL media

Crystallization is vital in several processes within the pharmaceutical industry, and ILs have been also investigated for this purpose. This technique was often selected by the authors addressing the isolation of the target compounds from the IL matrix resultant from the processes described above. Table 2.4 provides an overview of all crystallization strategies conducted in IL media. In this field, Kroon et al.[58] demonstrated the possibility of using supercritical CO_2 as anti-solvent, by lowering the solubility in $[C_4C_1im][BF_4]$ of N-acetyl-(*S*)-phenylalanine methyl ester, the product resulting from the asymmetric hydrogenation of methyl-(*Z*)-α-acetamido cinnamate. This work[58] further opened the way to testing the conditions of crystallization of methyl-(*Z*)-α-acetamido cinnamate, an intermediate in the production of Levodopa, a drug used against Parkinson's disease, from $[C_4C_1im][BF_4]$.[59] The authors measured the phase behavior of the ternary system composed of $[C_4C_1im][BF_4]$, CO_2 and methyl-(*Z*)-α-acetamido cinnamate. It was concluded that CO_2 can act as either co-solvent or anti-solvent in distinct concentration regions. Low concentrations of CO_2 (30 mol%) yielded a higher solubility of methyl-(*Z*)-α-acetamido cinnamate in $[C_4C_1im][BF_4]$ + CO_2 than in pure IL, whilst at high CO_2 concentrations (40 mol% and 50 mol%) the opposite behavior is observed. Using these results, two possible strategies to crystallize this Levodopa intermediate from the IL were proposed: (i) by a thermal shift or (ii) by a crystallization phenomenon induced by CO_2.[59] After testing the CO_2 solubility in systems containing $[C_4C_1im][BF_4]$ and three organic solutes of pharmaceutical relevance and showing that these affect the phase behavior of the initial binary system ($[C_4C_1im][BF_4]$ + CO_2),[60] Kühne et al.[61] presented another study wherein improvements on the naproxen synthetic route, a broadly used NSAID, were the main target of research. The phase behavior (solid-liquid and liquid-vapor transitions) of the ternary system formed by $[C_4C_1im][BF_4]$, CO_2 and naproxen suggests that the CO_2 presence (in the range of 10 to 50 mol%) in combination with increasing pressures prompts the complete dissolution of naproxen in the pure IL. Moreover, when the CO_2 concentration is further increased within the aforementioned regime, lower temperatures are needed to dissolve the drug in $[C_4C_1im][BF_4]$.[61] Unfortunately, due to experimental limitations, the anti-solvent phenomenon was not observed; nevertheless,

an expectation of its occurrence at CO_2 concentrations of 60 mol% was suggested. Finally, it was envisaged that by tuning the amount of CO_2 dissolved in the system it is possible to obtain either homogenous or heterogeneous solid + liquid systems that are operationally convenient for naproxen reactions or separations, respectively.[61]

Myerson's group[62] published an innovative work focused on the purification of paracetamol by crystallization. The main idea consisted of the manipulation of the hydrogen bonding interactions for tailoring the solubility of paracetamol and its main impurities (4-aminophenol, 4-nitrophenol and 4'-chloroacetanilide) in IL media. ILs composed of anions of increasing hydrogen bond basicity ($[NTf_2]^-$, $[BF_4]^-$ and $[C_1CO_2]^-$) and hydrogen bond acidity ($[C_4pyr]^+$, $[C_4C_1im]^+$, $[C_2C_1im]^+$ and $[OHC_2C_1im]^+$) were tested, whereby it was found that the hydrogen bond basicity of the anion plays the dominant role in the crystallization of paracetamol. $[C_2C_1im][C_1CO_2]$ showed the best ability to solubilize paracetamol. Due to its high viscosity, IL mixtures formed by $[C_2C_1im][C_1CO_2]$ and the less viscous $[C_2C_1im][NTf_2]$ were also investigated.[62] The ability of $[C_2C_1im][C_1CO_2]_x[NTf_2]_{1-x}$ to solubilize paracetamol and 4-aminophenol linearly correlates with the $[C_1CO_2]^-$ concentration. Spectroscopic studies demonstrated that paracetamol shields the $[C_1CO_2]^-$ anion, while proving the importance of hydrogen bonding in the dissolution phenomenon. Three strong hydrogen-bond-donating compounds (ethanol, acetic acid and 1,1,1,3,3,3-hexafluoroisopropanol) were studied as anti-solvents. The latter provided the most promising results, inducing a strong decrease of the solubility of paracetamol. With its use, the co-precipitation of only one impurity, the weakest hydrogen bonding impurity 4-aminophenol, was observed. This study provided novel insights on the importance of understanding the molecular interactions acting in IL media to design efficient crystallization processes and represents the only report available on IL mixtures for processing drugs.[62]

Two distinct perspectives of anti-solvent precipitation strategies in IL media were presented by Viçosa et al.[63] – in the preparation of ultrafine particles – and by An and Kim[64, 65] – in polymorphic design. Indeed, in addition to the separation and purification of the desired drugs, these works addressed other important questions occurring during the formulation and processing of pharmaceuticals. Rifampicin, being a sparingly water

soluble antibiotic, has its bioavailability restricted and the preparation of ultrafine particles may be promising.[63] Preliminary tests proved that raw rifampicin was more soluble in $[C_2mim][C_1PO_3]$ than in other solvents, while in mixtures of this IL and phosphate buffer (KH_2PO_4 + NaOH at pH 6.8) the solubility drastically decreases. These results support the choice of phosphate buffer as the anti-solvent in the preparation of ultrafine rifampicin particles. Notably, the particles were prepared with great purity (93 to 108%) and improved dissolution rate.[63]

The polymorphic design of active pharmaceutical ingredients plays a key role in the pharmaceutical domain and it often depends on the crystallization conditions. As ILs can establish a wider range of interactions when compared to traditional solvents, they have been studied for this application by An and Kim.[64, 65] Currently used to treat chronic hepatitis B, adefovir dipivoxil was the object of these two works. In a first attempt,[64] the combination of $[aC_2im][BF_4]$ and water as the solvent and anti-solvent, respectively, was able to produce novel polymorphs of the target antiviral drug that are unachievable with conventional organic solvents. In a second study,[65] the authors used pairs of distinct ILs, one of which working as the solvent ($[aC_2im][BF_4]$) and the other ($[C_4C_1C_1im][BF_4]$, $[aaim][BF_4]$, $[C_2C_1im][C_2SO_4]$, $[aC_2im]Br$ and $[aaim]Br$) as the anti-solvent. Despite the fact that some combinations did not induce crystallization or only produced the usual polymorph, $[aC_2im][BF_4]$ + $[C_4C_1mim][BF_4]$ generated exceptional interactions with adefovir dipivoxil and led to the formation of a new polymorph.[65]

The anti-solvent crystallization methods reviewed herein are summarized in Figure 2.3A. These processes may run into some operational obstacles related to the presence of IL, soluble contaminants and anti-solvent, which hamper the recycling and reuse of the IL. Cooling crystallization is thus foreseen by some authors as a favorable method of processing active pharmaceutical ingredients, as sketched in Figure 2.3B. Smith et al.[66] studied paracetamol cooling crystallization in two IL media, namely $[C_4C_1im][PF_6]$ and $[C_6C_1im][PF_6]$. By the proper manipulation of three variables (i.e., type of solvent, paracetamol concentration and crystal growth method), new crystal habits different from those commonly obtained with organic solvents were observed. Aiming at developing purification processes, Myerson's group[67] selected $[C_2C_1im][NTf_2]$, a thermally stable and

low-viscosity IL, as the ideal solvent to perform cooling crystallization of active pharmaceutical ingredients. Twelve pharmaceuticals divided into the following classes were studied: analgesics (paracetamol), fibrates (fenofibrate), NSAIDs (ibuprofen, acetylsalicylic acid, salicylic acid and naproxen), antibiotics (itraconazole, griseofulvin and amoxicillin), hypnotics (etomidate), anticonvulsants (rufinamide) and immunosuppressants (cyclosporine). Ten of these drugs were miscible with the IL, the exceptions being represented by ibuprofen and amoxicillin, the latter being thermally unstable. Distinct solubility profiles were observed, even for compounds with close melting points, suggesting the occurrence of specific interactions between the IL and the active pharmaceutical ingredient. From the results collected, the solubility of many of these drugs varies from low (at room temperature) to extremely high (at higher temperatures), highlighting the promising capability of $[C_2C_1im][NTf_2]$ as a solvent for cooling crystallization processes. To provide a proof of this concept, this approach was applied to the purification of paracetamol in the presence of its most common impurities. Ultimately, and comparing the data obtained with those obtained through the anti-solvent approach,[62] pharmaceuticals with higher yields and purity levels were obtained.[67]

From all works reviewed in this section, there are two main approaches to induce the crystallization of pharmaceuticals: precipitation with anti-solvents and cooling crystallization. The supremacy of hydrophobic ILs is transversal to these articles and only one article assessed the use of IL mixtures (to tailor the viscosity of the solvent). In this sense, more studies need to be carried out, not only by using different ILs as solvents, but also considering conditions other than temperature, for example the pH (to manipulate the speciation of the drugs) and pressure (to control the solubility of the drugs), without neglecting the understanding of the specific interactions taking place in the IL media, which are crucial to the identification of task-specific solvents. The characterization of the crystals also needs to be taken into account, principally regarding the crystal size distribution, crystal shape and polymorphic forms produced, since these are crucial parameters to attest the quality and industrial potential of the crystallization process. Crystallization is itself important for drug purification, but when integrated with the

remaining techniques described can lead to even more outstanding results. For instance, in most of the LLE approaches discussed above, one of the major drawbacks identified was the lack of attempts at the recovery of the target pharmaceuticals from the IL-rich phase, which, when combined with crystallization-induced approaches, can allow the design of integrated and effective purification processes for pharmaceuticals.

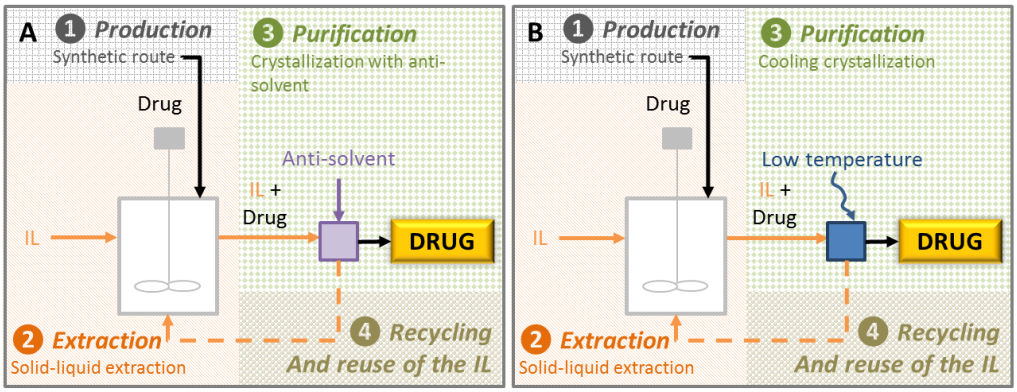

Figure 2.3. Schematic representation of the integrated processes proposed, comprising production, extraction and purification through crystallization using anti-solvents (A)[59, 61-65] or cooling crystallization (B),[66, 67] and the recycling of the IL.

Table 2.4. Separation and isolation of pharmaceuticals by crystallization methods in IL media.

Pharmaceutical	**IL**	**Crystallization approach**
4-aminophenol, 4-nitrophenol and 4'-chloroacetanilide (contaminants): production of paracetamol	$[C_2C_1im][C_1CO_2]_x[NTf_2]_{1-x}$ (IL mixture),[62] $[C_2C_1im][NTf_2]$[67]	
Acetylsalicylic acid	$[C_2C_1im][NTf_2]$[67]	Cooling crystallization[67]
Adefovir dipivoxil	$[aC_2im][BF_4]$[64, 65]	Precipitation with water[64] and with ILs $[C_4C_1C_1im][BF_4]$, $[aaim][BF_4]$, $[C_2C_1im][C_2SO_4]$, $[aC_2im]Br$ and $[aaim]Br$ as anti-solvents[65]
Cyclosporine	$[C_2C_1im][NTf_2]$[67]	Cooling crystallization[67]
Etomidate	$[C_2C_1im][NTf_2]$[67]	Cooling crystallization[67]
Fenofibrate	$[C_2C_1im][NTf_2]$[67]	Cooling crystallization[67]
Griseofulvin	$[C_2C_1im][NTf_2]$[67]	Cooling crystallization[67]
Itraconazole	$[C_2C_1im][NTf_2]$[67]	Cooling crystallization[67]
Methyl-(Z)-α-acetamido cinnamate (intermediate): production of Levodopa	$[C_4C_1im][BF_4]$[59]	Thermal shift,[59] precipitation with CO_2 as anti-solvent[59]
Naproxen	$[C_4C_1im][BF_4]$,[61] $[C_2C_1im][NTf_2]$[67]	Precipitation with CO_2 as anti-solvent,[61] cooling crystallization[67]
Paracetamol	$[C_2C_1im][C_1CO_2]_x[NTf_2]_{1-x}$ (IL mixture),[62] $[C_4C_1im][PF_6]$,[66] $[C_6C_1im][PF_6]$,[66] $[C_2mim][NTf_2]$[67]	Precipitation with 1,1,1,3,3,3-hexafluoroisopropanol as anti-solvent,[62] cooling crystallization[66, 67]
Rifampicin (ultrafine particles)	$[C_2C_1im][C_1PO_3]$[63]	Precipitation with KH_2PO_4/NaOH pH 6.8 as anti-solvent[63]
Rufinamide	$[C_2C_1im][NTf_2]$[67]	Cooling crystallization[67]
Salicylic acid	$[C_2C_1im][NTf_2]$[67]	Cooling crystallization[67]

Scopes and Objectives

Before starting this thesis, in 2014, we have reported the recovery of paracetamol from solid wastes using IL-based ABS.[57] Although contributing toward a circular economy and a greener pharmaceutical waste management, this work was of more fundamental basis rather than fully directed to the real application. A proof of concept was successfully achieved, where paracetamol was recovered from Ben-U-Ron 500 pills with extraction efficiencies of 100 %. Yet, the development of an integrated process lagged behind.

Following the same line of study, this chapter aims at extending the technologies available for drug recovery from wastes, covering distinct classes of drugs (NSAIDs – ***section 2.1.1.*** and ***2.1.3.*** – and antidepressants – ***section 2.1.2.***), as well as their inherent properties (pKa, log$K_{o/w}$ and water solubility). The creation of such technologies entailed major stages (Figure 2.4), viz. extraction and/or purification of the target drug as well as its isolation from the solvent used, which were here carefully studied and optimized. The optimal conditions were used to conceptualize integrated processes allowing to showcase the environmental and economic relevance of such a valorization route.

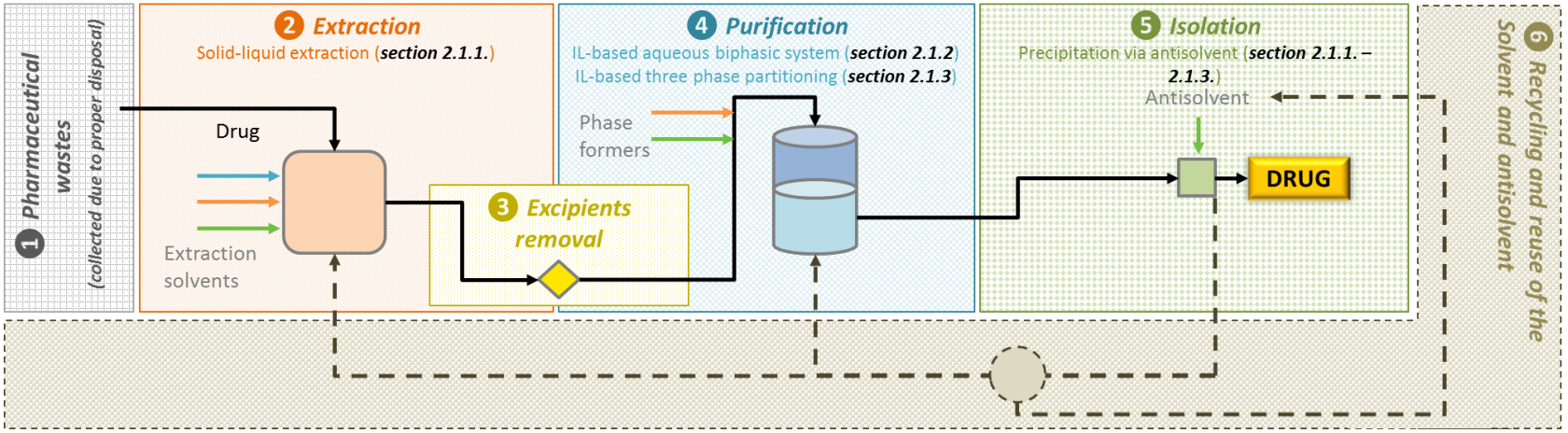

Figure 2.4. General representation of the valorization route proposed in this thesis.

References

[1] Mendes, Z.; Crisóstomo, S.; Marques, F. B.; Martins, A. P.; Rodrigues, V.; Ribeiro, C. F. Desperdício de medicamentos no ambulatório em Portugal. *Revista Portuguesa de Clinica Geral* **2010,** *26*, 12–20.

[2] Trueman, P.; Lowson, K.; Blighe; Meszaros, A.; Wright, D.; Glanville, J.; Taylor, D.; Newbould, J.; Bury, M.; Barber, N., et al. Evaluation of the Scale, Causes and Costs of Waste Medicines. *Report of DH funded national project. York Health Economics Consortium and The School of Pharmacy, University of London: York and London.* **2010**.

[3] Prescriptions Dispensed in the Community England 2005-2015. http://content.digital.nhs.uk/catalogue/PUB20664/pres-disp-com-eng-2005-15-rep.pdf (accessed Jan 30, 2017).

[4] Unused Pharmaceuticals Where Do They End Up?. https://noharm-europe.org/sites/default/files/documents-files/2616/Pharm%20Report_WEB.pdf (accessed Jan 30, 2017).

[5] Vollmer, G., Disposal of Pharmaceutical Waste in Households – A European Survey. In *Green and Sustainable Pharmacy*, Kümmerer, K.; Hempel, M., Eds. Springer Berlin Heidelberg: Berlin, Heidelberg, 2010; pp 165-178.

[6] Valormed. Resumo do Relatório de Actividades 2015. http://www.valormed.pt/uploads/files/RESUMO_Relatorio%20de%20Actividades%202015_FINAL.pdf (accessed Jan 30, 2017).

[7] Anastas, P. T.; Warner, J. C., *Green chemistry: theory and practice*. Oxford university press: 2000.

[8] Glavič, P.; Lukman, R. Review of sustainability terms and their definitions. *Journal of Cleaner Production* **2007,** *15* (18), 1875-1885.

[9] Santoleri, J. J.; Theodore, L.; Reynolds, J., *Introduction to hazardous waste incineration*. John Wiley & Sons: 2000.

[10] Natarajan, J.; Altan, S.; Raghavarao, D. Expiration Dating of Pharmaceutical Compounds in Relation to Analytical Variation, Degradation Rate, and Matrix Designs. *Drug Information Journal* **1997,** *31* (2), 589-595.

[11] Bourguignon, D. Closing the loop - New circular economy package. http://www.europarl.europa.eu/RegData/etudes/BRIE/2016/573899/EPRS_BRI(2016)573899_EN.pdf. (accessed May 5, 2018).

[12] Shamshina, J. L.; Berton, P.; Wang, H.; Zhou, X.; Gurau, G.; Rogers, R. D., Ionic Liquids in Pharmaceutical Industry. In *Green Techniques for Organic Synthesis and Medicinal Chemistry*, 2018.

[13] Seddon, K. R. Ionic Liquids for Clean Technology. *Journal of Chemical Technology & Biotechnology* **1997,** *68* (4), 351-356.

[14] Earle, M. J.; Seddon, K. R. Ionic liquids. Green solvents for the future. *Pure and Applied Chemistry* **2000,** *72* (7), 1391-1398.

[15] Wilkes, J. S. A short history of ionic liquids-from molten salts to neoteric solvents. *Green Chemistry* **2002,** *4* (2), 73-80.

[16] Pereiro, A. B.; Araújo, J. M. M.; Oliveira, F. S.; Bernardes, C. E. S.; Esperanca, J. M. S. S.; Canongia Lopes, J. N.; Marrucho, I. M.; Rebelo, L. P. N. Inorganic salts in purely ionic liquid media: the development of high ionicity ionic liquids (HIILs). *Chemical Communications* **2012,** *48* (30), 3656-3658.

[17] Chiappe, C.; Pieraccini, D. Ionic liquids: solvent properties and organic reactivity. *Journal of Physical Organic Chemistry* **2005,** *18* (4), 275-297.

[18] Naushad, M.; Alothman, Z. A.; Khan, A. B.; Ali, M. Effect of ionic liquid on activity, stability, and structure of enzymes: A review. *International Journal of Biological Macromolecules* **2012,** *51* (4), 555-560.

[19] Vijayaraghavan, R.; Izgorodin, A.; Ganesh, V.; Surianarayanan, M.; MacFarlane, D. R. Long-Term Structural and Chemical Stability of DNA in Hydrated Ionic Liquids. *Angewandte Chemie International Edition* **2010,** *49* (9), 1631-1633.

[20] Wilkes, J. S. Properties of ionic liquid solvents for catalysis. *Journal of Molecular Catalysis A: Chemical* **2004,** *214* (1), 11-17.

[21] Olivier-Bourbigou, H.; Magna, L.; Morvan, D. Ionic liquids and catalysis: Recent progress from knowledge to applications. *Applied Catalysis A: General* **2010,** *373* (1–2), 1-56.

[22] Freemantle, M. Designer Solvents. Ionic liquids may boost clean technology development. *Chemical & Engineering News Archive* **1998,** *76* (13), 32-37.

[23] Ventura, S. P. M.; Silva, F. A. e.; Quental, M. V.; Mondal, D.; Freire, M. G.; Coutinho, J. A. P. Ionic liquid-mediated extraction and purification of bioactive compounds: Past, Present and Future Trends. *Chemical Reviews* **2017,** *117* (10), 6984–7052.

[24] Marrucho, I.; Branco, L.; Rebelo, L. Ionic liquids in pharmaceutical applications. *Annual review of chemical and biomolecular engineering* **2014,** *5*, 527-546.

[25] Resende de Azevedo, J.; Letourneau, J.-J.; Espitalier, F.; Ré, M. I. Solubility of a New Cardioactive Prototype Drug in Ionic Liquids. *Journal of Chemical & Engineering Data* **2014,** *59* (6), 1766-1773.

[26] Melo, C. I.; Bogel-Łukasik, R.; Nunes da Ponte, M.; Bogel-Łukasik, E. Ammonium ionic liquids as green solvents for drugs. *Fluid Phase Equilibria* **2013,** *338*, 209-216.

[27] Faria, R. A.; da Ponte, M. N.; Bogel-Łukasik, E. Solubility studies on the system of trihexyl(tetradecyl)phosphonium bis[(trifluoromethyl)sulfonyl]amide) ionic liquid and pharmaceutical and bioactive compounds. *Fluid Phase Equilibria* **2015,** *385*, 1-9.

[28] Faria, R. A.; Bogel-Łukasik, E. Solubilities of pharmaceutical and bioactive compounds in trihexyl(tetradecyl)phosphonium chloride ionic liquid. *Fluid Phase Equilibria* **2015,** *397*, 18-25.

[29] Forte, A.; Melo, C. I.; Bogel-Łukasik, R.; Bogel-Łukasik, E. A favourable solubility of isoniazid, an antitubercular antibiotic drug, in alternative solvents. *Fluid Phase Equilibria* **2012,** *318*, 89-95.

[30] Manic, M. S.; Najdanovic-Visak, V. Solubility of erythromycin in ionic liquids. *The Journal of Chemical Thermodynamics* **2012,** *44* (1), 102-106.

[31] Smith, K. B.; Bridson, R. H.; Leeke, G. A. Solubilities of Pharmaceutical Compounds in Ionic Liquids. *Journal of Chemical & Engineering Data* **2011,** *56* (5), 2039-2043.

[32] Mizuuchi, H.; Jaitely, V.; Murdan, S.; Florence, A. T. Room temperature ionic liquids and their mixtures: Potential pharmaceutical solvents. *European Journal of Pharmaceutical Sciences* **2008,** *33* (4), 326-331.

[33] McCrary, P. D.; Beasley, P. A.; Gurau, G.; Narita, A.; Barber, P. S.; Cojocaru, O. A.; Rogers, R. D. Drug specific, tuning of an ionic liquid's hydrophilic-lipophilic balance to improve water solubility of poorly soluble active pharmaceutical ingredients. *New Journal of Chemistry* **2013,** *37* (7), 2196-2202.

[34] Cull, S. G.; Holbrey, J. D.; Vargas-Mora, V.; Seddon, K. R.; Lye, G. J. Room-temperature ionic liquids as replacements for organic solvents in multiphase bioprocess operations. *Biotechnology and Bioengineering* **2000,** *69* (2), 227-233.

[35] Soto, A.; Arce, A.; Khoshkbarchi, M. K. Partitioning of antibiotics in a two-liquid phase system formed by water and a room temperature ionic liquid. *Separation and Purification Technology* **2005,** *44* (3), 242-246.

[36] Manic, M. S.; da Ponte, M. N.; Najdanovic-Visak, V. Recovery of erythromycin from aqueous solutions with an ionic liquid and high-pressure carbon dioxide. *Chemical Engineering Journal* **2011,** *171* (3), 904-911.

[37] Domańska, U.; Pobudkowska, A.; Bocheńska, P. Extraction of Nitrofurantoin Using Ionic Liquids. *Journal of Chemical & Engineering Data* **2012,** *57* (7), 1894-1898.

[38] Matsumoto, M.; Ohtani, T.; Kondo, K. Comparison of solvent extraction and supported liquid membrane permeation using an ionic liquid for concentrating penicillin G. *Journal of Membrane Science* **2007,** *289* (1), 92-96.

[39] Liu, Q.; Li, Y.; Li, W.; Liang, X.; Zhang, C.; Liu, H. Efficient Recovery of Penicillin G by a Hydrophobic Ionic Liquid. *ACS Sustainable Chemistry & Engineering* **2016,** *4* (2), 609-615.

[40] Pei, Y.; Zhang, J.; Song, X.; Zhao, M.; Wang, J. Partition Behavior of Drug Molecules in Cholinium-Based Ionic Liquids. *Separation Science and Technology* **2015,** *50* (11), 1641-1646.

[41] Vitasari, C. R.; Gramblička, M.; Gibcus, K.; Visser, T. J.; Geertman, R.; Schuur, B. Separating closely resembling steroids with ionic liquids in liquid–liquid extraction systems. *Separation and Purification Technology* **2015,** *155*, 58-65.

[42] Wang, H.; Gurau, G.; Kelley, S. P.; Myerson, A. S.; Rogers, R. D. Hydrophobic vs. hydrophilic ionic liquid separations strategies in support of continuous pharmaceutical manufacturing. *RSC Advances* **2013,** *3* (25), 10019-10026.

[43] Harini, M.; Jain, S.; Adhikari, J.; Noronha, S. B.; Yamuna Rani, K. Design of an ionic liquid as a solvent for the extraction of a pharmaceutical intermediate. *Separation and Purification Technology* **2015,** *155*, 45-57.

[44] Li, S. H.; He, C. Y.; Liu, H. W.; Li, K. A.; Liu, F. Ionic liquid-salt aqueous two-phase system, a novel system for the extraction of abused drugs. *Chinese Chemical Letters* **2005,** *16* (8), 1074-1076.

[45] Ma, C.-H.; Wang, L.; Yan, Y.-S.; Che, G.-B.; Yin, Y.-S.; Wang, R.-Z.; Li, D.-Y. Extraction of tetracycline via ionic liquid two-phase system. *Chemical Research in Chinese Universities* **2009,** *25* (6), 832-835.

[46] Pang, J.; Han, C.; Chao, Y.; Jing, L.; Ji, H.; Zhu, W.; Chang, Y.; Li, H. Partitioning Behavior of Tetracycline in Hydrophilic Ionic Liquids Two-Phase Systems. *Separation Science and Technology* **2015,** *50* (13), 1993-1998.

[47] Marques, C. F. C.; Mourão, T.; Neves, C. M. S. S.; Lima, Á. S.; Boal-Palheiros, I.; Coutinho, J. A. P.; Freire, M. G. Aqueous biphasic systems composed of ionic liquids and sodium carbonate as enhanced routes for the extraction of tetracycline. *Biotechnology Progress* **2013,** *29* (3), 645-654.

[48] Shahriari, S.; Tome, L. C.; Araujo, J. M. M.; Rebelo, L. P. N.; Coutinho, J. A. P.; Marrucho, I. M.; Freire, M. G. Aqueous biphasic systems: a benign route using cholinium-based ionic liquids. *RSC Advances* **2013,** *3* (6), 1835-1843.

[49] Pereira, J. F. B.; Vicente, F.; Santos-Ebinuma, V. C.; Araújo, J. M.; Pessoa, A.; Freire, M. G.; Coutinho, J. A. P. Extraction of tetracycline from fermentation broth using aqueous two-phase systems composed of polyethylene glycol and cholinium-based salts. *Process Biochemistry* **2013,** *48* (4), 716-722.

[50] Liu, Q.; Yu, J.; Li, W.; Hu, X.; Xia, H.; Liu, H.; Yang, P. Partitioning Behavior of Penicillin G in Aqueous Two Phase System Formed by Ionic Liquids and Phosphate. *Separation Science and Technology* **2006,** *41* (12), 2849-2858.

[51] Jiang, Y.; Xia, H.; Guo, C.; Mahmood, I.; Liu, H. Phenomena and Mechanism for Separation and Recovery of Penicillin in Ionic Liquids Aqueous Solution. *Industrial & Engineering Chemistry Research* **2007,** *46* (19), 6303-6312.

[52] Jiang, Y.; Xia, H.; Yu, J.; Guo, C.; Liu, H. Hydrophobic ionic liquids-assisted polymer recovery during penicillin extraction in aqueous two-phase system. *Chemical Engineering Journal* **2009,** *147* (1), 22-26.

[53] Domínguez-Pérez, M.; Tomé, L. I. N.; Freire, M. G.; Marrucho, I. M.; Cabeza, O.; Coutinho, J. A. P. (Extraction of biomolecules using) aqueous biphasic systems formed by ionic liquids and aminoacids. *Separation and Purification Technology* **2010,** *72* (1), 85-91.

[54] Li, Y. F.; Han, J.; Wang, Y.; Ma, J. J.; Yan, Y. S. Partitioning of Cephalexin in Ionic Liquid Aqueous Two-Phase System Composed of 1-Butyl-3-Methylimidazolium Tetrafluoroborate and ZnSO4. *Journal of Chemistry* **2013,** *2013*, 5.

[55] Han, J.; Wang, Y.; Chen, C.; Kang, W.; Liu, Y.; Xu, K.; Ni, L. (Liquid+liquid) equilibria and extraction capacity of (imidazolium ionic liquids+potassium tartrate) aqueous two-phase systems. *Journal of Molecular Liquids* **2014,** *193*, 23-28.

[56] Zhang, W.; Zhang, G.; Han, J.; Yan, Y.; Chen, B.; Sheng, C.; Liu, Y. Phase equilibrium and chloramphenicol partitioning in aqueous two-phase system composed of 1-hydroxylhexyl-3-methylimidazolium chloride–salt. *Journal of Molecular Liquids* **2014,** *193*, 226-231.

[57] e Silva, F. A.; Sintra, T.; Ventura, S. P. M.; Coutinho, J. A. P. Recovery of paracetamol from pharmaceutical wastes. *Separation and Purification Technology* **2014,** *122*, 315-322.

[58] Kroon, M. C.; van Spronsen, J.; Peters, C. J.; Sheldon, R. A.; Witkamp, G.-J. Recovery of pure products from ionic liquids using supercritical carbon dioxide as a co-solvent in extractions or as an anti-solvent in precipitations. *Green Chemistry* **2006,** *8* (3), 246-249.

[59] Kroon, M. C.; Toussaint, V. A.; Shariati, A.; Florusse, L. J.; van Spronsen, J.; Witkamp, G.-J.; Peters, C. J. Crystallization of an organic compound from an ionic liquid using carbon dioxide as anti-solvent. *Green Chemistry* **2008,** *10* (3), 333-336.

[60] Kuhne, E.; Peters, C. J.; van Spronsen, J.; Witkamp, G.-J. Solubility of carbon dioxide in systems with [bmim][BF4] and some selected organic compounds of interest for the pharmaceutical industry. *Green Chemistry* **2006,** *8* (3), 287-291.

[61] Kuhne, E.; Santarossa, S.; Witkamp, G.-J.; Peters, C. J. Phase equilibria in ternary mixtures of the ionic liquid bmim[BF4], (S)-naproxen and CO2 to determine optimum regions for green processing. *Green Chemistry* **2008,** *10* (7), 762-766.

[62] Weber, C. C.; Kunov-Kruse, A. J.; Rogers, R. D.; Myerson, A. S. Manipulation of ionic liquid anion-solute-antisolvent interactions for the purification of acetaminophen. *Chemical Communications* **2015,** *51* (20), 4294-4297.

[63] Viçosa, A.; Letourneau, J.-J.; Espitalier, F.; Inês Ré, M. An innovative antisolvent precipitation process as a promising technique to prepare ultrafine rifampicin particles. *Journal of Crystal Growth* **2012,** *342* (1), 80-87.

[64] An, J.-H.; Kim, J.-M.; Chang, S.-M.; Kim, W.-S. Application of Ionic Liquid to Polymorphic Design of Pharmaceutical Ingredients. *Crystal Growth & Design* **2010,** *10* (7), 3044-3050.

[65] An, J.-H.; Kim, W.-S. Antisolvent Crystallization Using Ionic Liquids As Solvent and Antisolvent for Polymorphic Design of Active Pharmaceutical Ingredient. *Crystal Growth & Design* **2013,** *13* (1), 31-39.

[66] Smith, K. B.; Bridson, R. H.; Leeke, G. A. Crystallisation control of paracetamol from ionic liquids. *CrystEngComm* **2014,** *16* (47), 10797-10803.

[67] Weber, C. C.; Kulkarni, S. A.; Kunov-Kruse, A. J.; Rogers, R. D.; Myerson, A. S. The Use of Cooling Crystallization in an Ionic Liquid System for the Purification of Pharmaceuticals. *Crystal Growth & Design* **2015,** *15* (10), 4946-4951

.

2.1.1. Recovery of ibuprofen from pharmaceutical wastes using ionic liquids

This section is based on e Silva, F. A.; Caban, M.; Stepnowski, P.; Coutinho, J. A. P.; Ventura, S.P.M. Recovery of ibuprofen from pharmaceutical wastes using ionic liquids. *Green Chemistry* **2016**, *18* (13), 3749-3757.

Contributions: S.P.M.V. and J.A.P.C. conceived and directed this work. Francisca A. e Silva and M.C. acquired the experimental data. In particular, Francisca A. e Silva acquired all data regarding the extraction and isolation of ibuprofen. Francisca A. e Silva, M.C., S.P.M.V. and J.A.P.C. interpreted the experimental data. Francisca A. e Silva and S.P.M.V. wrote the manuscript with contributions from the remaining authors.

Abstract

This work aims at developing a process to valorise pharmaceutical wastes through the recovery of pharmaceutical active compounds. The ibuprofen extraction and isolation from solid pharmaceutical wastes is here used as a case study and an integrated approach comprising the ibuprofen solid-liquid extraction, the removal of the insoluble excipients present in the pills, the target drug recovery and the recycling of the aqueous solutions is proposed. The present work is centred on the optimization of the first (solid-liquid extraction) and third (drug recovery) steps above mentioned. For the solid-liquid extraction step, various IL aqueous solutions were tested, being the tetrabutylammonium chloride ($[N_{4444}]Cl$) adopted to further optimize the process. A solution composed of 45 wt% of $[N_{4444}]Cl$ + 5 wt% of citrate buffer + 50 wt% of H_2O led to the highest ibuprofen extraction efficiency (EE_{IBU} = 97.92 ± 2.65 %) while in the absence of citrate the extraction efficiency was somewhat lower (EE_{IBU} = 93.53 ± 0.62 %). The polishing task was affected by the type of aqueous solution utilized during the solid-liquid extraction step: in presence of citrate buffer water was not prone to induce significant ibuprofen precipitation (maximum RE_{IBU} of 34.71 ± 4.00 %) being the KCl aqueous solution the best option (maximum RE_{IBU} of 87.97 ± 1.00 %); when no citrate buffer is used water can be

used as anti-solvent with maximum RE_{IBU} of 91.60 ± 0.19 % while KCl aqueous solutions lead to RE_{IBU} up to 97.07 ± 0.14 %. Based on these results an integrated process is proposed for the ibuprofen recovery and isolation aimed at adding value to pharmaceutical wastes.

Introduction

Recent works have shown the ability of aqueous solutions of ILs in the extraction of value-added compounds from biomass[1] as a result of their hydrotropic nature as revealed by Cláudio et al.[2] Moreover, they have also been successfully applied in the purification of a wide range of (bio)molecules,[3] including drugs.[4] Based on these previous works a more sustainable route for the valorisation of pharmaceutical wastes is here investigated. For this purpose, aqueous solutions of ILs combined with the potassium citrate buffer (from now on referred to as citrate buffer) normally used as hydrotrope in the pharmaceutical industry[5-7] will be studied. Initially, an evaluation of the performance of three ILs will be carried aiming at perceiving its capacity to extract ibuprofen, a hydrophobic NSAID, sparingly soluble in water, from a real pharmaceutical matrix (*i.e.*, pills). After identifying the most efficient IL, this will be applied in an optimization study regarding the selection of the optimal IL/citrate buffer ratio to enhance the extractive capacity of the aqueous solution. Finally, the isolation/recovery of ibuprofen from the aqueous solution will be described. A conceptual integrated process for the extraction and purification of the NSAIDs, as well as the solvent recovery will be proposed.

Experimental

Materials

The ILs studied were tetrabutylammonium chloride, $[N_{4444}]Cl$ (purity ≥ 97 wt%), 1-butyl-3-methylimidazolium chloride, $[C_4C_1im]Cl$ (purity = 99 wt%) and benzyldimethyl(2-hydroxyethyl)ammonium chloride, [BzCh]Cl (purity ≥ 97 wt%), which were supplied by Sigma-Aldrich, Iolitec and Fluka, respectively. The potassium citrate tribasic monohydrate, $C_6H_5K_3O_7•H_2O$ (purity = 99 wt%) and citric acid monohydrate, $C_6H_8O_7•H_2O$ (purity = 100

wt%), used to prepare the citrate buffer at pH 7, were acquired at Acros Organics and Fischer-Scientific, respectively. The ibuprofen (IBU) pills, Brufen® 200 [*active principle:* ibuprofen, 200 mg per 1 capsule; *excipients:* microcrystalline cellulose, sodium croscarmellose, lactose monohydrate, colloidal silicon dioxide anhydrous, sodium lauryl sulfate, magnesium stearate, hypromellose 2910 (5 cp), hypromellose 2910 (6 cp), talc and titanium dioxide], were purchased from a local pharmacy (Aveiro, Portugal). The molecular structures of the three ionic liquids and ibuprofen are depicted in Figure 2.5. Potassium chloride, KCl (purity = 99.5 wt%) was supplied by Chem-Lab.

The mobile phase used in the HPLC analysis was composed of ammonium acetate, $NH_4C_2H_3O_2$ (purity ≥ 99.99 wt%) and acetic acid, $C_2H_4O_2$ (purity ≥ 99.99 wt%), both from Sigma-Aldrich, HPLC grade acetonitrile, C_2H_3N from HiPerSolv Chromanorm and ultrapure water treated using a Milli-Q 185 water purification apparatus. Syringe filters (0.45 µm) and regenerated cellulose membrane filters (0.45 µm) respectively acquired at Specanalitica and Sartorius Stedim Biotech, were used during the filtration steps.

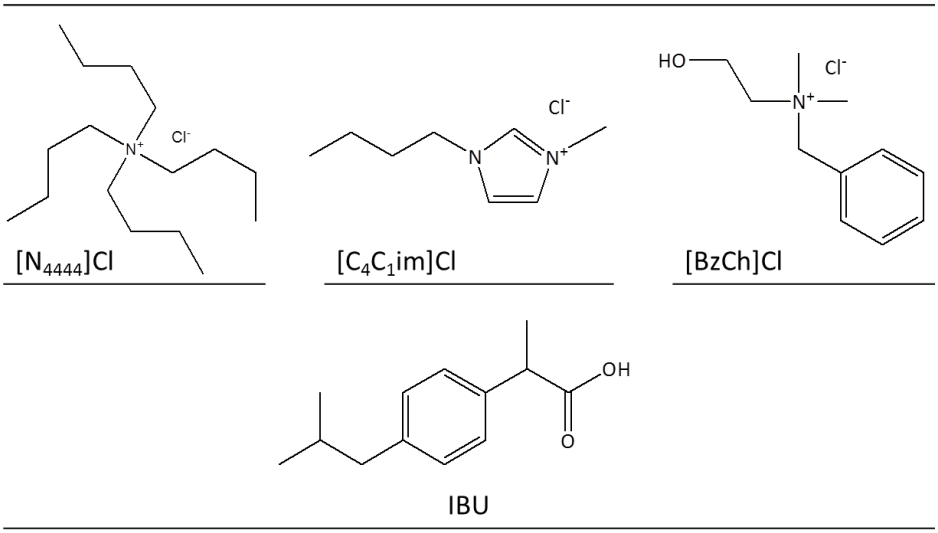

Figure 2.5. Chemical structures and acronyms of the ILs and NSAID (ibuprofen) investigated in this work.

Solid-liquid extraction

For the initial evaluation of the ILs structure on their ability to extract ibuprofen, solutions composed of 45 wt% of each IL ($[C_4C_1im]Cl$, $[N_{4444}]Cl$ and [BzCh]Cl) + 0 or 5 wt%

of citrate buffer + 55 or 50 wt% of H_2O were prepared. The best IL was then fixed for the evaluation of the impact of $[N_{4444}]Cl$ + citrate buffer compositions on the extractive performance. The compositions represented in Table 2.5 were investigated during these optimization studies. The citrate buffer at pH 7 was prepared by adding the appropriate amounts of potassium citrate tribasic and citric acid at circa 50 wt% according to a well-established protocol.[8] It should be underlined that when the amount of citrate buffer added in each experiment is defined, it describes the salt and acid contents ($C_6H_5K_3O_7$ + $C_6H_8O_7$), meaning without the water content. All the aqueous solutions' compositions selected were placed at the monophasic region of the ternary phase diagrams reported for ABS composed of $[N_{4444}]Cl$,[4] $[C_4C_1im]Cl$[9] and [BzCh]Cl[10] + citrate buffer at pH 7. By taking into consideration the total mass of ibuprofen and excipients present in the grinded pill (as described in the pharmaceutical flyer), 20 mg of ibuprofen were added to 3 mL of each solution. All extraction assays were conducted under constant stirring at a controlled temperature of 298 (± 1) K during at least 12 hours. After this period, the solutions were filtrated using syringe filters in order to remove all the solids in suspension, being the ibuprofen content further assayed in the clean solution by HPLC-DAD. Triplicates were performed in order to estimate the average extraction efficiencies attained using each one of the aqueous solutions and the respective standard deviations (σ).

The extraction efficiencies of ibuprofen (EE_{IBU}, %) were calculated according to Equation 2.1.:

$$EE_{IBU}, \% = \frac{m_{aq\ sol}^{IBU}}{m_0^{IBU}} \times 100 \qquad (\textbf{\textit{Equation 2.1}})$$

where $m_{aq\ sol}^{IBU}$ and m_0^{IBU} are the mass of ibuprofen on the aqueous solution after the solid-liquid extraction assay and filtration stage and that initially added to the system, respectively.

Table 2.5. Compositions of the $[N_{4444}]Cl$ and citrate buffer salt aqueous solutions tested during the optimization studies of solid-liquid extraction.

100 × mass fraction composition (wt%)		
$[N_{4444}]Cl$	**Citrate buffer salt**	**H_2O**
0	0	100
15	0	85
25	0	75
35	0	65
45	0	55
50	0	50
55	0	45
0	5	95
0	15	85
0	25	75
0	35	65
15	5	80
25	5	70
35	5	60
45	5	50
25	10	65
10	25	65
15	15	70
5	15	80

Ibuprofen purification

The ibuprofen purification assays were carried out by means of precipitation with an anti-solvent. For that purpose, aqueous solutions of KCl at 25 wt% or water were added in the proportions 1:1, 1:2, 1:3, 1:4 and 1:5 (volume of drug extract:volume of anti-solvent) to the extract obtained from the solid-liquid extraction (with 45 wt% of $[N_{4444}]Cl$ + 5 wt% of citrate buffer + 50 wt% of H_2O and with 45 wt% of $[N_{4444}]Cl$ + 55 wt% of H_2O). After the addition of the anti-solvent, the solutions became cloudy due to the formation of a precipitate, which was then filtrated using syringe filters. The concentration of ibuprofen remaining in solution was further assessed by HPLC-DAD. All the assays were

performed in triplicate to determine the recovery efficiencies of ibuprofen and the corresponding standard deviations (σ).

The recovery efficiencies of ibuprofen (RE_{IBU}, %) from the aqueous solutions were calculated following Equation 2.2.

$$RE_{IBU}, \% = 100 - \left(\frac{m_{anti-solvent}^{IBU}}{m_{aq\ sol}^{IBU}} \times 100\right) \qquad (\textbf{\textit{Equation 2.2}})$$

where $m_{anti-solvent}^{IBU}$ and $m_{aq\ sol}^{IBU}$ are the mass of ibuprofen present in the filtered solution after the addition of the anti-solvent and that on the initial aqueous solution after the solid-liquid extraction assay and filtration step, respectively.

Ibuprofen quantification

The concentration of ibuprofen was determined by HPLC-DAD using an analytical method developed and validated by us. The liquid chromatograph HPLC Elite LaChrom (VWR Hitachi) was composed of a diode array detector (DAD) l-2455, column oven l-2300, auto-sampler l-2200 and pump l-2130. A 5 µm, 250 mm × 4 mm i.d. C_{18} reversed-phase column (LiChrospher 100 RP-18) linked to a 5 µm, 4 mm × 4 mm guard column with the same stationary phase was used. The column oven and the autosampler operated at controlled temperatures of 27 and 25 °C, respectively. The mobile phase was formed by an organic phase, i.e., C_2H_3N, and an aqueous phase, i.e., 5 mM of $NH_4C_2H_3O_2$ at pH 4.02 (the pH adjustment was done by the addition of $C_2H_4O_2$) and 5 wt% of C_2H_3N. The separation was conducted in gradient elution mode as follows: 0 - 4 min 30% of C_2H_3N, 4-11 min from 30 to 60% of C_2H_3N, 11-18 min 60% of C_2H_3N, 18-21 min from 60 to 30% of C_2H_3N, 21-24 min 30% of C_2H_3N, at a flow rate of 1 mL.min^{-1} and using an injection volume of 10 µL. DAD was set to measure at 230 nm. Each sample was analysed at least two times. The validation parameters acquired through an external standard method were the following: retention time of 16.48 min, R^2 of 0.9999, linearity range of 10 – 750 µg mL^{-1} (stock solutions prepared in C_2H_3N), LOQ of 10 µg mL^{-1} (with assumed precision lower than 5% and accuracy between 80 – 120 %), LOD of 1 µg mL^{-1} (using signal:noise ratio of 3), accuracy intra-day of 83.1 – 101.0 %, accuracy inter-day of 88.7 – 109.7 %, precision intra-day of 0.15 – 3.00 % and precision inter-day of 0.01 – 1.93 %. The samples

coming from the solid-liquid experiments or isolation assays were diluted in a mixture of C_2H_3N and H_2O in a volumetric ratio of 30:70, when required.

Results and discussion

The conception and development of an integrated process for the efficient and sustainable extraction and isolation of ibuprofen from pharmaceutical wastes is the objective of this work. The conceptual process diagram proposed comprising four main steps ***1)*** Solid-liquid extraction using aqueous solutions of ILs, ***2)*** Removal of the insoluble contaminants, e.g., excipients, by filtration, ***3)*** Recovery of the ibuprofen through precipitation by an anti-solvent, and ***4)*** Recycling of the aqueous solutions and reuse of the anti-solvent, is depicted in Figure 2.6.

This work will focus on the optimization of steps ***1)*** and ***3)*** of the proposed process. Regarding step ***1)***, an initial evaluation aimed at selecting the most suitable IL cation was performed in presence or absence of citrate buffer. Subsequently, the most effective IL was used to carry out a study aimed at optimizing the conditions for the solid-liquid extraction process. Having established those variables, the concentrations of KCl aqueous solution and water, used as anti-solvents in step ***3)***, which maximize the recovery of ibuprofen, are gauged.

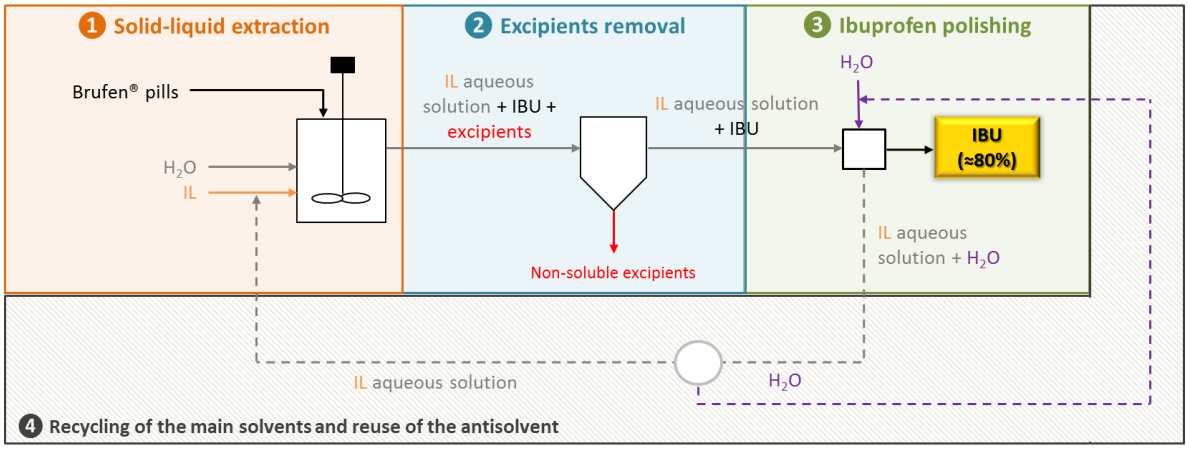

Figure 2.6. Schematic representation of the integrated process of extraction, purification, ibuprofen recovery and recycling of the main solvents based on the use of $[N_{4444}]Cl$ aqueous solutions and water as the solvent and anti-solvent, respectively.

Selecting the best ionic liquid

The capability of three ILs with cations of distinct nature, namely $[N_{4444}]Cl$, $[C_4C_1im]Cl$ and [BzCh]Cl, for extracting ibuprofen from solid wastes was assessed. These were chosen taking into account our previous experience in solid-liquid and LLE using aqueous solutions of ILs[3, 11] and studies on the hydrotropic nature of IL cations[2] while trying to keep the anion as simple as possible (chloride) to minimize the process operational costs and environmental risk. These cations were combined with the citrate buffer, a known anionic hydrotropic agent used in the pharmaceutical industry[5-7] allowing the study of the synergies of the two compounds in the extraction process. Figure 2.7 shows the results obtained using solutions composed of 45 wt% of IL + 0 or 5 wt% of citrate buffer + 50 or 55 wt% of H_2O along with those gathered using only H_2O and 5 wt% of citrate buffer. The detailed data obtained is provided in Table A1 in Appendix A. The ability of *(i)* ILs and *(ii)* ILs + citrate buffer aqueous solutions to extract ibuprofen can be ranked as follows: water < [BzCh]Cl < 5 wt% citrate buffer ≈ $[C_4C_1im]Cl$ << $[C_4C_1im]Cl$ + citrate buffer < [BzCh]Cl + citrate buffer < $[N_{4444}]Cl$ < $[N_{4444}]Cl$ + citrate buffer.

While both citrate buffer and the ILs show an higher capacity to the extraction of ibuprofen than water alone, only $[N_{4444}]Cl$ or the combined action of the citrate buffer with the ILs achieves extraction efficiencies higher than 90 %. The synergetic effect is quite dramatic on the $[C_4C_1im]Cl$ + citrate buffer and [BzCh]Cl + citrate buffer systems, and less important for the $[N_{4444}]Cl$ as this salt alone is able to achieve very high extraction efficiencies (EE_{IBU} = 93.73 ± 1.62 %) that are somewhat enhanced by the presence of the citrate buffer (EE_{IBU} = 97.92 ± 2.65 %). The information on ILs as hydrotropic agents is still scarce,[2] and thus it is difficult to anticipate how they will impact upon the solubility of a compound and, consequently, on their extraction. Previous studies show that the same hydrotrope may affect similar molecules very differently[2]. In this work,[2] the authors have shown that the hydrotropy could be a synergistic phenomenon with the cation and the anion working together to enhance the solubility of a given solute. Moreover, they mentioned that nor the π···π interactions nor the formation of complexes were enough to explain the hydrotropic nature of the ILs, since the non-aromatic were also responsible for the enhancement of the solubility of

both vanillin and gallic acid, neither the formation of complexes was proved by UV spectroscopy analysis[2]. However, and contrarily to what happened in our recent paper,[2] the results here obtained can be interpreted in the light of the hydrophobic interactions known to be relevant in the hydrotropic agents action.[2]

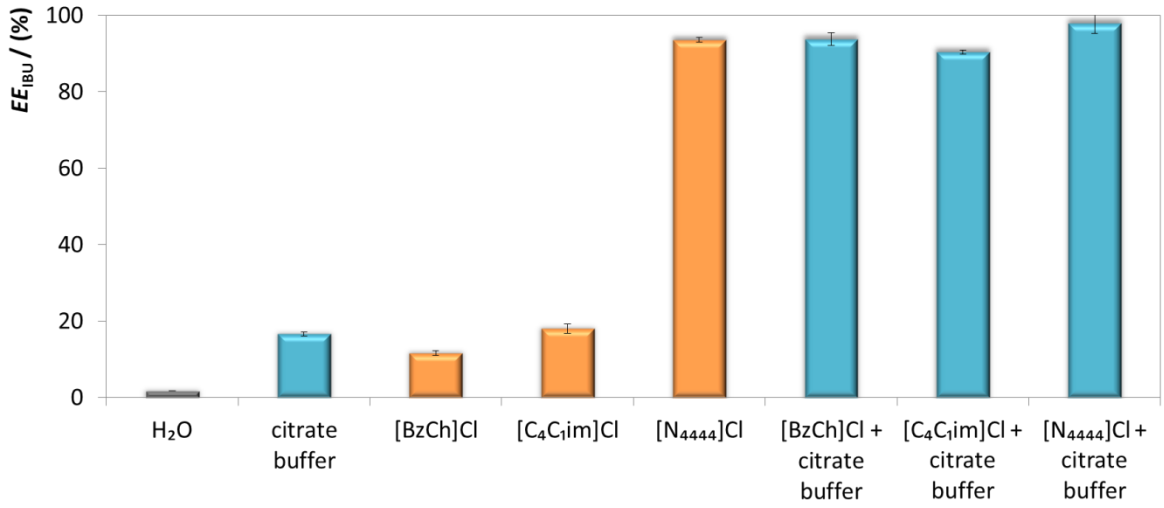

Figure 2.7. Extraction efficiencies of ibuprofen (EE_{IBU}, %) achieved in the solid-liquid extractions carried out with aqueous solutions of three ILs (45 wt%) in absence (orange bars) and presence (blue bars) of 5 wt% of citrate buffer. The data obtained for the experiments with water and citrate buffer at 5 wt% are depicted for comparison purposes.

The extraction efficiencies of the ILs alone correlate well with the ILs hydrophobicity. Ibuprofen being a hydrophobic drug, as suggested by its octanol-water partition coefficient (log K_{ow} of 2.48[12]), has its solubility enhanced in aqueous solutions of the most hydrophobic IL, $[N_{4444}]Cl$. The other ILs being more hydrophilic exhibit similar but much lower extraction efficiencies (EE_{IBU} = 11.58 ± 0.63 % for [BzCh]Cl and EE_{IBU} = 17.94 ± 1.20 % for $[C_4C_1im]Cl$). A similar dependency of ibuprofen's extraction with the IL hydrophobicity was observed by Pei et al. in LLE systems.[13] Since all three ILs investigated are water-miscible in an extended concentration range, their hydrophobicity was inferred from two perspectives: their log K_{ow} (values retrieved from Chemspider[14]) and their ability to undergo liquid-liquid demixing in ABS. Taking into account the octanol-

water partition coefficient values, $[N_{4444}]Cl$ possesses a log K_{ow} of 1.32, indicating its higher affinity for the octanol phase and thus, its higher hydrophobicity. The remaining two ionic compounds, i.e., $[C_4C_1im]Cl$ and [BzCh]Cl, with negative log K_{ow} values of -2.15 and -2.94, respectively, are identified as more hydrophilic than the ammonium. Moreover, and consistent with this pattern is their improved ability to generate ABS with salts according to the following hierarchy, $[C_4C_1im]Cl \approx [BzCh]Cl << [N_{4444}]Cl$[10], which is also based on the increased hydrophobicity of the ILs' cations.[3] Given the good extraction capabilities demonstrated by the $[N_{4444}]Cl$ it will be here selected for further optimization studies described below.

Optimization of the ratio $[N_{4444}]Cl$: citrate buffer

Based on its ability for extracting ibuprofen from the *Brufen® 200* pills, both in presence or absence of citrate buffer as well as its low cost[1] and toxicity,[15] $[N_{4444}]Cl$ was selected to conduct a concentration optimization study. Aqueous solutions formed by the addition of distinct amounts of $[N_{4444}]Cl$ and/or citrate buffer at pH 7 at concentrations where no liquid-liquid phase separation occurs[4] were tested. The data gathered in this study is represented in Figure 2.8. To simplify the analysis and discussion of the results, these were grouped according to the impact of $[N_{4444}]Cl$ and citrate buffer on the solid-liquid extraction efficiency, either individually or combined. These results are compiled in Table A2 in Appendix A. The results plotted in Figure 2.8 show that high concentrations of $[N_{4444}]Cl$ (in the range of 35 – 55 wt%) and low concentrations of citrate buffer (in the range of 0 – 10 wt%) are the conditions that favour ibuprofen extraction. A synergistic effect of the hydrotropic effect of $[N_{4444}]Cl$ and of citrate buffer is observed.

The conditions that maximize the extraction efficiencies, while minimizing the cost of the extraction solution are composed by 45 wt% of $[N_{4444}]Cl$ and 5 wt% of citrate buffer and by $[N_{4444}]Cl$ alone (a concentration of 45 wt% was adopted as it allows direct comparison at the same time that keeps the extractive performance higher than 90 %). These will be used in subsequent studies concerning the definition of the operating conditions for the proposed conceptual process for the recovery of ibuprofen from pharmaceutical wastes.

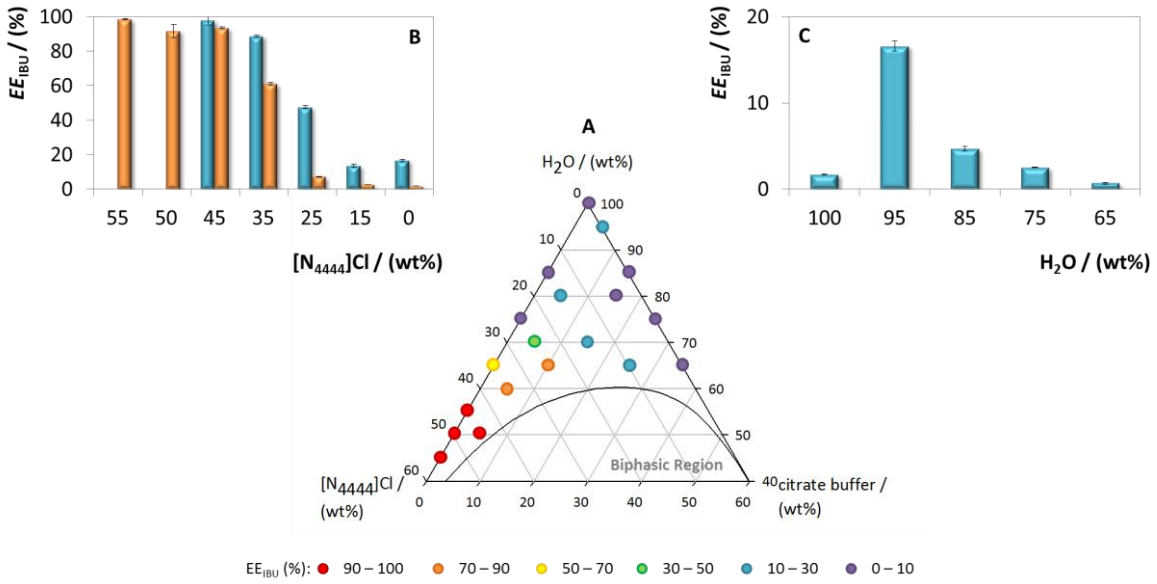

Figure 2.8. Extraction efficiencies of ibuprofen (EE_{IBU}, %) attained for the optimization study of the solid-liquid extraction carried out with aqueous solution of [N_{4444}]Cl and citrate buffer (A). The black line[4] denotes the boundary between the monophasic and the biphasic regions. To facilitate the results perception, the extraction efficiencies of ibuprofen (EE_{IBU}, %) results were grouped according to *i)* the [N_{4444}]Cl concentration impact (55, 50, 45, 35, 25, 15 and 0 wt%) in the presence (5 wt%) (blue bars) and absence (0 wt%) (orange bars) of citrate buffer (B) and *ii)* the citrate concentration effect (0, 5, 15, 25 and 35 wt%, i.e., 100, 95, 85, 75 and 65 wt% of H_2O) in the absence of [N_{4444}]Cl (blue bars) (C).

Precipitating agents for ibuprofen recovery

The recovery of ibuprofen (Task 3 of the integrated process proposed – Figure 2.6) from the extraction solutions with concentrations previously fixed at 45 wt% of [N_{4444}]Cl + 5 wt% of citrate buffer + 50 wt% of H_2O and 45 wt% of [N_{4444}]Cl + 55 wt% of H_2O was studied using KCl and water as the precipitating agents and attempting at optimizing their concentration. The KCl was selected to avoid introducing new ionic species into the solution, since K^+ and Cl^- were already part of the extraction system. An aqueous solution of KCl at 25 wt% was added in different proportions of 1:1, 1:2, 1:3, 1:4 and 1:5, these ratios representing the volume of extract:volume of KCl aqueous solution. The same

procedure was adopted for water as the anti-solvent. The recovery results obtained are graphically displayed in Figure 2.9, whilst the detailed data is reported in Table A3 in Appendix A. At first glance, the influence of citrate buffer present in the solid-liquid extraction solution is notorious, as it hampers the precipitation phenomenon. Recovery efficiencies of ibuprofen up to 97.07 ± 0.14 % and 91.60 ± 0.19 % were achieved by the addition of KCl aqueous solutions in a proportion of 1:5 and of water in a ratio of 1:3, respectively, having as starting point the extraction conducted with 45 wt% of $[N_{4444}]Cl$ + 55 wt% of H_2O. Lower maximums of 87.97 ± 1.00 % and 34.71 ± 4.00 % of recovery efficiencies of ibuprofen were instead assessed when applying KCl and water in the same ratios aforementioned, using the initial solution containing 5 wt% of citrate buffer. This boosted aptitude of water to precipitate ibuprofen from the solutions free of citrate buffer is justified by the hydrophobic character of this drug. Another aspect of relevance is the enhanced power of KCl aqueous solution as anti-solvent, more preponderant for higher volumes of anti-solvent added and in the presence of citrate buffer in solution. The change in the ionic strength of the medium, and the speciation in solution caused by the introduction of KCl in the system reduce the interactions between ibuprofen and the components of the extractive solution leading to its precipitation. Arising from these data is the possibility of creating/destroying strong hydrotropes (i.e., citrate salts and ILs) with the cautious choice of the solvent and anti-solvent adopted.

The precipitates obtained were submitted to ^1H NMR spectroscopy along with separated samples of the main component of the aqueous solution, $[N_{4444}]Cl$, and the ibuprofen pure standard. Separated analysis were performed for the powders isolated from the processes starting with either $[N_{4444}]Cl$ + citrate buffer or $[N_{4444}]Cl$ aqueous solutions at the level of the solid-liquid extraction. The NMR spectra are provided in Figure A1 in Appendix A, demonstrating the presence of ibuprofen with purities of circa 70 % and 80% on a molar basis, respectively, due to the contamination with IL. This suggests the need of a further polishing step, that, given the differences in solubility between ibuprofen and the $[N_{4444}]Cl$, could be a simple washing step with cold water to remove the IL content from the drug precipitate.

Although water-insoluble (or poorly soluble) excipients contained in *Brufen 200* pills were likely removed in step *2)* by filtration (microcrystalline cellulose, sodium croscarmellose, colloidal silicon dioxide anhydrous, magnesium stearate, talc and titanium dioxide), attention must be called to the possibility of co-extracting water-soluble compounds (lactose monohydrate, sodium lauryl sulfate, hypromellose). As discussed above, it is known that ILs may have a significant impact upon the solubilities of a wide range of solutes,[2, 11, 16] and the presence of traces of some insoluble excipients cannot be fully discarded. The presence of such contaminants, even if anticipated as being present in very low concentrations, will affect the ibuprofen final purity. Beyond $[N_{4444}]Cl$, no other organic contamination was found in considerable extent by ^{1}H NMR spectra analysis (Figure A1 in Appendix A), supporting the idea that the main bulk of excipients was removed.

In spite of the improved extraction and recovery efficiencies of ibuprofen obtained on a process based on $[N_{4444}]Cl$ + citrate buffer and precipitations with aqueous solution and KCl, respectively as the solvent and the anti-solvent, this was dropped as the desirable approach due to the higher degree of operational complexity (cf. Figure A2 in Appendix A). Remarkably, the selection of water as the anti-solvent in the integrated process represented in Figure 2.6 gives rise to a simpler approach for which no need for a further step of KCl removal is required. Having most of ibuprofen recovered from the $[N_{4444}]Cl$ aqueous solution, this can be recycled and reused within the integrated process herein proposed (step *4*). For that, it would be necessary to remove the excess amount of water added during step *3)* through evaporation or a membrane-based process. It should be pointed that the ibuprofen content remaining in solution even after the precipitation step (around 8.4 % of the IBU feed into the process) will be recycled to step *1)*, then increasing the ibuprofen content at the feed and enhancing the recovery in the following steps until a steady state is reached where the ibuprofen feed into the process equals its amount recovered in each cycle.

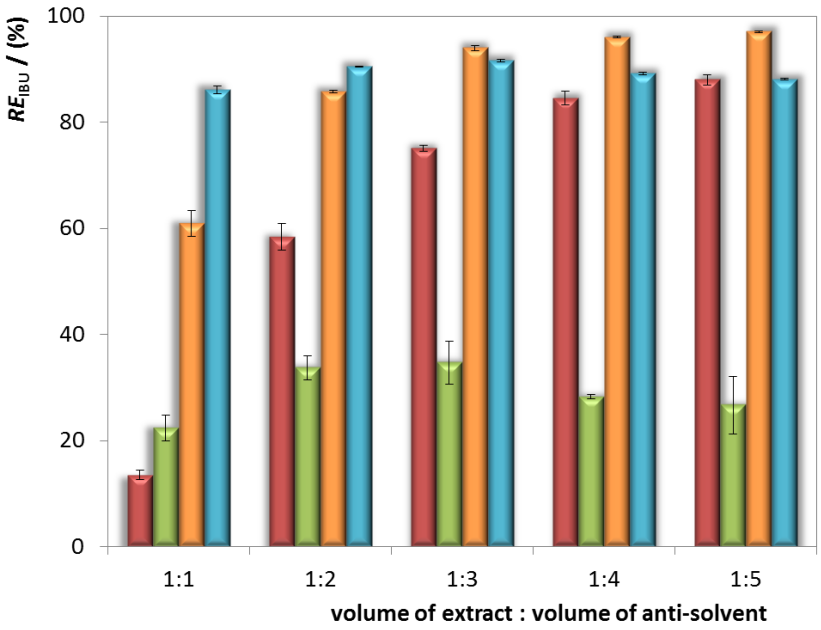

Figure 2.9 Recovery efficiencies of ibuprofen (RE_{IBU}, %) attained for the isolation assays carried out by adding distinct proportions of anti-solvent: aqueous solution of KCl at circa 25 wt% to the solid-liquid extraction aqueous solutions composed of 45 wt% of $[N_{4444}]Cl$ with citrate buffer (red bars) and without citrate buffer (orange bars); water to the solid-liquid extraction aqueous solutions composed of 45 wt% of $[N_{4444}]Cl$ with citrate buffer (green bars) and without citrate buffer (blue bars).

The industrial relevance of the process here proposed can be gauged from the overview of processes for ibuprofen production or purification previously reported presented hereafter. Firstly prepared and patented in 1961, ibuprofen has seen its production processes evolving in the light of the Green Chemistry principles. The former synthetic route involved six steps, including the use of aluminium trichloride, which cannot be reused, to trigger the reaction.[17] The massive amounts of wastes generated along with the excessive quantities of aluminium trichloride required forced changes to this synthetic route. A "greener route" developed by BASF decreases both the (i) waste generation (i.e., uses small amounts of the recyclable catalyst hydrofluoric acid as an alternative to aluminium trichloride) and the (ii) synthesis complexity (only three steps) at the same time that manufacturers' profits are enhanced.[17] An isolation method of ibuprofen from tablets was patented in 1994.[18] According to the inventors,[18] recycling

ibuprofen reduces wastes and costs, but it is only worthwhile if ibuprofen is separated from the excipients in a low cost process. The process proposed involves alkanes or cycloalkanes as solvents at temperatures higher than 35 ^{o}C, a filtration step to remove undissolved solids, followed by the ibuprofen separation from the solvent through crystallization or solvent evaporation and by the solvent recycling and reuse.[18] Another approach proposed addresses the purification of ibuprofen from reaction product mixtures and relays on the use of selective ibuprofen crystallization from a hydrocarbon solvent, keeping the impurities in solution.[19] The mixtures need to be pre-treated (heating and/or washing) and/or to be submitted to sequential crystallizations for impurities removal. Overall, the process here proposed allows replacing the volatile organic solvents by an IL aqueous solution and operating at ambient conditions, thus representing a greener approach to this problem.

Conclusions

The current study addresses the development of a conceptual process, and the optimization of its most relevant steps, for the recovery of ibuprofen from solid pharmaceutical wastes. The proposed integrated process comprises four steps, starting from the solid-liquid extraction of ibuprofen from the pharmaceutical solid wastes using aqueous solutions of [N_{4444}]Cl (at concentration of 45 wt%) [step ***1)***]; followed by the step ***2)***, the elimination of the insoluble excipients by filtration; and then the processes of the recovery of ibuprofen using water as anti-solvent [step ***3)***], and the recycle and reuse of the aqueous solution and the anti-solvent [step ***4)***]. This work is focused on the optimization of steps ***1)*** and ***3)*** evaluating the best IL and optimal concentrations to maximize the extractions and recovery. The results here reported show that it is possible to achieve up to 97.92 ± 2.65 % and 97.07 ± 0.14 % of ibuprofen extraction and recovery efficiency from the pills, respectively. Known the optimization results scenario, the most adequate integrated process was selected on the basis of a balance between performance of extraction, the purity achievable and the operational simplicity. From both economic and environmental points of view, the promising and competitive status of the integrated process developed can be forecasted. The possibility of valorising a

valueless feedstock together with the transversal nature of the integrated process here proposed supports its industrial relevance.

References

[1] Passos, H.; Freire, M. G.; Coutinho, J. A. P. Ionic liquid solutions as extractive solvents for value-added compounds from biomass. *Green Chemistry* **2014,** *16* (12), 4786-4815.

[2] Cláudio, A. F. M.; Neves, M. C.; Shimizu, K.; Canongia Lopes, J. N.; Freire, M. G.; Coutinho, J. A. P. The magic of aqueous solutions of ionic liquids: ionic liquids as a powerful class of catanionic hydrotropes. *Green Chemistry* **2015,** *17* (7), 3948-3963.

[3] Freire, M. G.; Claudio, A. F. M.; Araujo, J. M. M.; Coutinho, J. A. P.; Marrucho, I. M.; Lopes, J. N. C.; Rebelo, L. P. N. Aqueous biphasic systems: a boost brought about by using ionic liquids. *Chemical Society Reviews* **2012,** *41* (14), 4966-4995.

[4] e Silva, F. A.; Sintra, T.; Ventura, S. P. M.; Coutinho, J. A. P. Recovery of paracetamol from pharmaceutical wastes. *Separation and Purification Technology* **2014,** *122*, 315-322.

[5] Pareek, V.; Tambe, S.; Bhalerao, S. Role of different hydrotropic agents in spectrophotometric and chromatographic estimation of Cefixime. *International Journal of Pharmacy and Biological Sciences* **2010,** *1* (3), 1-10.

[6] Dharmendira Kumar, M.; Nagendra Gandhi, N. Effect of Hydrotropes on Solubility and Mass Transfer Coefficient of Methyl Salicylate. *Journal of Chemical Engineering Data* **2000,** *45* (3), 419-423.

[7] Dhinakaran, M.; Morais, A. B.; Gandhi, N. N. Extraction of vanillin through hydrotropy. *Asian Journal of Chemistry* **2013,** *25* (1), 231-236.

[8] Zafarani-Moattar, M. T.; Hamzehzadeh, S. Effect of pH on the phase separation in the ternary aqueous system containing the hydrophilic ionic liquid 1-butyl-3-methylimidazolium bromide and the kosmotropic salt potassium citrate at T = 298.15 K. *Fluid Phase Equilibria* **2011,** *304* (1–2), 110-120.

[9] Passos, H.; Trindade, M. P.; Vaz, T. S. M.; da Costa, L. P.; Freire, M. G.; Coutinho, J. A. P. The impact of self-aggregation on the extraction of biomolecules in ionic-liquid-

based aqueous two-phase systems. *Separation and Purification Technology* **2013,** *108*, 174-180.

[10] Sintra, T. E.; Cruz, R.; Ventura, S. P. M.; Coutinho, J. A. P. Phase diagrams of ionic liquids-based aqueous biphasic systems as a platform for extraction processes. *Journal of Chemical Thermodynamics* **2014,** *77*, 206-213.

[11] Cláudio, A. F. M.; Ferreira, A. M.; Freire, M. G.; Coutinho, J. A. P. Enhanced extraction of caffeine from guarana seeds using aqueous solutions of ionic liquids. *Green Chemistry* **2013,** *15* (7), 2002-2010.

[12] Scheytt, T.; Mersmann, P.; Lindstädt, R.; Heberer, T. 1-Octanol/Water Partition Coefficients of 5 Pharmaceuticals from Human Medical Care: Carbamazepine, Clofibric Acid, Diclofenac, Ibuprofen, and Propyphenazone. *Water Air Soil and Pollution* **2005,** *165* (1-4), 3-11.

[13] Pei, Y.; Zhang, J.; Song, X.; Zhao, M.; Wang, J. Partition Behavior of Drug Molecules in Cholinium-Based Ionic Liquids. *Separation Science and Technology* **2015,** *50* (11), 1641-1646.

[14] Chemspider - The free chemical database at http://www.chemspider.com (accessed March 3, 2016).

[15] Munoz, M.; Domínguez, C. M.; de Pedro, Z. M.; Quintanilla, A.; Casas, J. A.; Ventura, S. P. M.; Coutinho, J. A. P. Role of the chemical structure of ionic liquids in their ecotoxicity and reactivity towards Fenton oxidation. *Separation and Purification Technology* **2015,** *150*, 252-256.

[16] McCrary, P. D.; Beasley, P. A.; Gurau, G.; Narita, A.; Barber, P. S.; Cojocaru, O. A.; Rogers, R. D. Drug specific, tuning of an ionic liquid's hydrophilic-lipophilic balance to improve water solubility of poorly soluble active pharmaceutical ingredients. *New Journal of Chemistry* **2013,** *37* (7), 2196-2202.

[17] Poliakoff, M.; Licence, P. Sustainable technology: Green chemistry. *Nature* **2007,** *450* (7171), 810-812.

[18] Lakin, M. B.; Shockley, T. H.; Zey, E. G. Isolation of ibuprofen from tablets. **1994**, US Patent No. US 5300301 A.

[19] Zey, E. G.; Shockley, T. H.; Ryan, D. A.; Moss, G. L. Method for purification of ibuprofen comprising mixtures. **1992**, US Patent No. US 5151551 A.

2.1.2. Recovery of an antidepressant from pharmaceutical wastes using ionic liquid-based aqueous biphasic systems

This section is based on Zawadzki, M.; e Silva, F.A.; Domańska, U.; Coutinho, J. A. P.; Ventura, S. P. M. Recovery of an antidepressant from pharmaceutical wastes using ionic liquid-based aqueous biphasic systems. *Green Chemistry* **2016**, *18* (12), 3527-3536.

Contributions: S.P.M.V. and J.A.P.C. conceived and directed this work. Francisca A. e Silva and M.Z. acquired the experimental data. In particular, Francisca A. e Silva acquired data regarding the partition and isolation of amitriptyline. Francisca A. e Silva, M.Z. S.P.M.V. and J.A.P.C. interpreted the experimental data. Francisca A. e Silva, M.Z. and S.P.M.V. wrote the manuscript with contributions from the remaining authors.

Abstract

This work is aimed at developing a sustainable process for the recovery of valuable drugs from pharmaceutical wastes by using IL-based ABS. Since in pharmaceutical wastes, excipients consist on the major contaminants, the search for selective routes for their elimination is of primordial relevance, and for that purpose, IL-based ABS were here evaluated. The effects of different process parameters, namely the IL nature, the pH and the mixture composition used in the extraction system were studied and the process optimized to maximize the extraction of the antidepressant from pharmaceutical wastes. Moreover, the maximum amount of amitriptyline able to be processed using such systems was assessed. The set of ABS investigated herein revealed high extraction performance, as indicated by the outstanding logarithmic functions of the amitriptyline partition coefficients ranging from 2.41 ± 0.05 to >2.5 and extraction efficiencies between 66 ± 1 % to 100. The best ABS and conditions were considered in the development of an integrated multi-step purification process. The process here proposed comprises three main stages: the solid-liquid extraction of the antepressant from *ADT 25* pills, its purification using the optimal IL-based ABS and the antidepressant isolation by

precipitation with anti-solvent. After the removal of most water insoluble excipients in the first step, with the selected IL-based ABS it was possible to further eliminate water soluble contaminants. A high capability of extraction and purification, leading to the selective separation of amitriptyline hydrochloride from the main contaminants contained in solid pharmaceutical wastes was achieved. Finally, through precipitation with the anti-solvent the isolation of the amitriptilyne in a pure state was successfully accomplished.

Introduction

Antidepressants are one of the most intensively prescribed pharmaceutical classes throughout the globe.[1] The prescription of antidepressants was around 300,000 packaging in Portugal in 2001 and this number is growing.[2] This group of drugs has been detected in surface and treated drinking waters, wastewater treatment plants and aquatic organisms' tissues, showing its huge environmental persistency and signs of possible bioaccumulation.[3] Besides, this class of pharmaceuticals is one of the hottest considering their market price. The free access data available is representative of their global market, revealing a total revenue of 8.7 billion U.S. dollars, considering the top antidepressant drugs sold in the United States between July of 2011 and June of 2012.[4]

Recently, the successful use of ABS to recover paracetamol from pharmaceutical wastes was reported.[5] Following the same line of research, the main objective of this work is to recover and purify an antidepressant from its solid wastes through the application of IL-based ABS for its purification, thus enlarging the spectrum of active pharmaceutical ingredients recovered by this approach. ABS composed of phosphonium- and quaternary ammonium-based ILs together with distinct phosphate-based salts and buffers were selected to ascertain the partitioning behavior of amitriptyline hydrochloride (here used as an antidepressant model compound). Finally, the best systems were integrated in a multi-stage process for the extraction, purification and isolation (or polishing) of amitriptyline hydrochloride directly from the pharmaceutical waste.

Experimental

Materials

Amitriptyline hydrochloride (Ami, 1-Propanamine,3-(10,11-dihydro-5H-dibenzo[a,d]cyclohepten-5-ylidene)-N,N-dimethyl- hydrochloride, CAS number 549-18-8, purity ≥ 98 wt%) was purchased at Sigma-Aldrich (see Figure 2.10A). The ILs used in this study belong to two distinct families, the quaternary ammonium such as tetrabutylammonium bromide, $[N_{4444}]Br$ (purity ≥ 98 wt%) and tetrabutylammonium chloride, $[N_{4444}]Cl$ (purity ≥ 97 wt%) both purchased at Sigma-Aldrich; and the phosphonium such as tetrabutylphosphonium bromide, $[P_{4444}]Br$ (purity = 95.2 wt%), tributylmethylphosphonium methylsulfate, $[P_{4441}][C_1SO_4]$ (purity = 98.6 wt%) and triisobutyl(methyl)phosphonium tosylate, $[P_{i(444)1}][Tos]$ (purity = 99 wt%), all kindly supplied by Cytec. Their chemical structures and abbreviation names are shown in Figure 2.10B. The purity of each IL was further checked through ^{1}H and ^{13}C NMR spectroscopy and found to match the purity levels given by the suppliers. The salts used were potassium phosphate tribasic, K_3PO_4 (purity ≥ 98 wt%) and potassium phosphate monobasic, KH_2PO_4 (purity ≥ 99.5 wt%), both from Sigma-Aldrich, and potassium phosphate dibasic, K_2HPO_4 (purity ≥ 98 wt%), purchased at JMVP, Portugal. For the HPLC-UV-Vis mobile phase, the ammonium acetate (purity ≥ 99.99%) and acetic acid (purity ≥ 99.99 %) were acquired at Sigma-Aldrich, the triethylamine (HPLC grade) was acquired at Fischer Chemical and the acetonitrile (HPLC grade) was purchased at HiPerSolv CHROMANORM. Potassium hydroxide (KOH, pure) was purchased at Pronalab. The water used was double distilled, passed by a reverse osmosis system and further treated with a Milli-Q plus 185 water purification apparatus.

The pharmaceutical drug *ADT 25 mg* was produced in Portugal by Wynn Industrial Pharma, S. A. and obtained from a local pharmacy (Aveiro, Portugal).

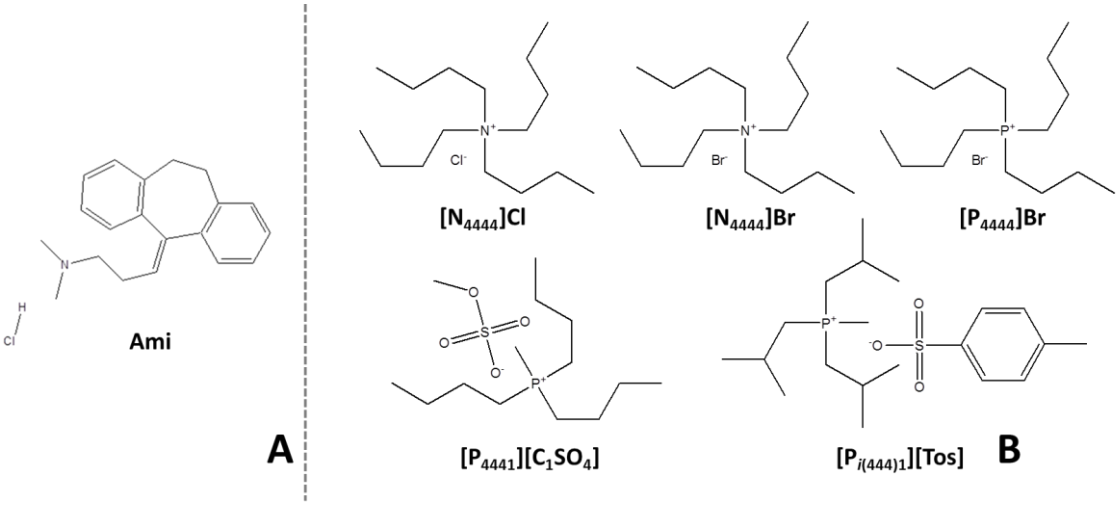

Figure 2.10. Chemical structure of amitriptyline hydrochloride (A) and the ILs studied (B).

Phase diagrams and tie-lines

The ternary phase diagrams for the systems $[P_{i(444)1}][Tos] + K_2HPO_4/KH_2PO_4 + H_2O$, $[P_{4441}][C_1SO_4] + K_2HPO_4/KH_2PO_4 + H_2O$, $[N_{4444}]Br + K_2HPO_4/KH_2PO_4 + H_2O$, $[P_{4444}]Br + K_2HPO_4/KH_2PO_4 + H_2O$, $[P_{4444}]Cl + K_2HPO_4/KH_2PO_4 + H_2O$ and $[N_{4444}]Cl + K_3PO_4 + H_2O$ were already established in previous works.[6, 7] Aiming at completing the array of IL-based ABS evaluated in this work, additional experimental ternary phase diagrams for the systems composed of $[N_{4444}]Br + K_2HPO_4 + H_2O$, $[N_{4444}]Br + K_3PO_4 + H_2O$ and $[N_{4444}]Cl + K_2HPO_4 + H_2O$ were determined through the cloud point titration method,[8] at 298 (±1) K and atmospheric pressure. The experimental binodal curves were correlated using the Merchuk equation[9] (Equation B1 provided in Appendix B).

The tie-lines (TLs) were measured through a well-established gravimetric method firstly reported by Asenjo and collaborators[9] and widely used and validated by us for IL-based ABS.[5-8] A ternary mixture of IL + salt + H_2O at the biphasic region was prepared, vigorously stirred and allowed to reach the thermodynamic equilibrium by the separation of phases for at least 18 hours at 298 (±1) K. After the separation of the coexisting phases, they were carefully separated and weighed with a precision of ± 10^{-4} g. The TLs were determined by the application of the lever-arm rule through the relationship between the weight of the top (IL-rich) phase and that of the overall system. For the calculation of each TL, a system of four equations and four unknown variables was solved (Equations B2 – B5 described in more detail in the Appendix B). The tie-line length (TLL) was determined

as the Euclidean distance between the IL-rich (top) and salt-rich (bottom) phases compositions (Equation B6 of Appendix B).

Quantification of amitriptyline hydrochloride

The liquid chromatograph HPLC Gilson was equipped with a UV-Vis detector 156 and a pump 321. The analytical column (100×4.6 mm) and precolumn were composed of a LiChrosphere 100 RP-C18 (5 µm) sorbent and were acquired at Merck. The mobile phase consisted of an aqueous phase (A) containing 21.5 mM acetic acid, 5 mM ammonium acetate buffer, 0.1 wt% of trimethylamine (pH 4.8) and 5 wt % acetonitrile (to prevent bacteria growth), and an organic phase (B) composed of pure acetonitrile. The separation was carried out under isocratic conditions with a mobile phase ratio of 50% of phase B, using a flow rate of 1 $mL.min^{-1}$. The quantification was based upon internal calibration using the respective peak areas, being two calibration curves prepared for higher and lower concentration regimes. The injection volume was 20 µL and the UV-Vis detector was set to measure at 240 nm. The validation parameters of the analytical method prepared are given in Appendix B, Table B1. The retention time of amitriptyline depends on the type of IL employed, being those with bromide anion responsible for lower values (5.3 min for chloride-based *vs.* 3.4 min for bromide-based).

Optimization study of amitriptyline hydrochloride partition

The optimization of the extraction of amitriptyline hydrochloride from aqueous solution was carried using three variables: the IL, the pH (by varying the salt) and the mixture point compositions (along the same tie line). For each optimization assay, 5 g total mixtures of IL + salt + water + amitriptyline hydrochloride (≈ 10^{-3} g) were prepared by weighing the appropriate amounts of each component (within an uncertainty of 10^{-4} g). The mixtures were vigorously stirred and the systems were placed at 298 (±1) K for at least 18 hours to assure the complete separation of the two aqueous phases. Those were separated and collected for the measurement of weight (with an uncertainty of 10^{-4} g) and volume (with an uncertainty of 0.1 mL) and for amitriptyline quantification. Under these conditions, the top and bottom phases correspond to, respectively, an IL-rich and a

salt-rich layer. Each system was done in triplicate (the standard deviations are reported along with the extraction parameters determined) and at least three injections *per* sample were performed. Moreover, the maximum amount of antidepressant able to be processed by this technology was assessed by following the same procedure described above with few modifications. Mixtures composed of 10 wt% $[N_{4444}]Br$ + 25 wt% K_3PO_4 and varying amounts of amitriptyline hydrochloride, from 2.53 up to 100.6 mg (which correspond to 0.51 up to 20.9 mg *per* gram of ABS), were added.

The extraction efficiency (EE_{Ami}, %) was calculated using Equation 2.3:

$$EE_{Ami}, \% = \frac{[Ami]_{IL} \times V_{IL}}{m_{Ami}} \times 100 \qquad \textbf{(Equation 2.3)}$$

where m_{Ami} is the mass of amitriptyline hydrochloride initially added to prepare the ABS and $[Ami]_{IL}$ and V_{IL} are the amitriptyline hydrochloride concentration and the volume of the IL-rich (top) phase, respectively.

The logarithmic functions of the partition coefficients, $\log K_{Ami}$, have been calculated as the ratio between the concentration of amitriptyline hydrochloride found in the IL-rich (top), $[Ami]_{IL}$, and in the salt-rich (bottom) phases, $[Ami]_{Salt}$, represented by Equation 2.4:

$$logK_{Ami} = log\left(\frac{[Ami]_{IL}}{[Ami]_{Salt}}\right) \qquad \textbf{(Equation 2.4)}$$

Table 2.6. Description of the mixture compositions and respective extraction efficiencies (EE_{Ami}), logarithmic function of the partition coefficients (logK_{Ami}) of amitriptyline hydrochloride and the corresponding standard deviations (σ) for the IL-based ABS used during the optimization studies.

IL	Salt	pH	$[IL]_M$ / (wt%)	$[Salt]_M$ / (wt%)	$[water]_M$ / (wt%)	$EE_{Ami} \pm \sigma$ (%)	log$K_{Ami} \pm \sigma$
$[P_{i(444)1}][Tos]$	K_2HPO_4/KH_2PO_4	6.6	30.03	15.07	54.90	95 ± 1	>2.5
$[P_{4441}][C_1SO_4]$	K_2HPO_4/KH_2PO_4	6.6	29.86	14.98	55.16	98 ± 4	2.41 ± 0.05
$[N_{4444}]Br$	K_2HPO_4/KH_2PO_4	6.6	37.50	10.55	51.95	100	>2.5
			30.01	15.01	54.98	93 ± 3	>2.5
			20.10	21.05	58.85	99 ± 6	>2.5
			10.06	26.98	62.96	98 ± 5	>2.5
	K_2HPO_4	9.6	30.00	15.06	54.94	97 ± 3	>2.5
	K_3PO_4	13.2	30.05	15.11	54.84	97.5 ± 0.6	>2.5
$[P_{4444}]Br$	K_2HPO_4/KH_2PO_4	6.6	29.80	14.99	55.21	96 ± 2	>2.5
			19.99	19.60	60.41	97 ± 3	>2.5
			9.99	23.30	66.71	94 ± 4	>2.5
$[N_{4444}]Cl$	K_2HPO_4/KH_2PO_4	6.6	27.34	13.79	58.87	100	>2.5
	K_2HPO_4	9.6	29.67	15.03	55.30	100	>2.5
	K_3PO_4	13.2	29.88	15.05	55.07	100	>2.5
			20.14	20.91	58.92	100	>2.5
			10.06	27.09	62.85	100	>2.5

Recovery and isolation of amitriptyline hydrochloride from *ADT 25 mg*

The extraction of amitriptyline hydrochloride from *ADT 25 mg* was carried out in a multi-stage process designed specifically for that purpose. In the first step, a solid-liquid extraction with water was performed, where amitriptyline hydrochloride was recovered from powdered *ADT 25 mg* tablets (under constant stirring, for 24 hours). Then, the liquid solution (*ADT* pill solution) was centrifuged and filtrated (diameter of the pore 0.45 µm), in order to remove any insoluble excipients from the drug. The amitriptyline hydrochloride solution previously filtrated was subsequently used in the preparation of the IL-based ABS previously selected from the optimization data as the best extraction systems. The systems elected were composed of 10.0 wt% of $[N_{4444}]Br$ + 27.1 wt% K_2HPO_4/KH_2PO_4 at pH 6.6, 10.0 wt% of $[N_{4444}]Br$ + 25.1 wt% K_3PO_4 at pH 13.2, 10.0 wt% of $[P_{4444}]Br$ + 23.5 wt% K_2HPO_4/KH_2PO_4 at pH 6.6 and 10.0 wt% $[N_{4444}]Cl$ + 27.0 wt% K_3PO_4, where the filtrated extract was added in the appropriate amount to achieve 57 mg of amitriptyline hydrochloride in the 10 g total extraction system. The last step, i.e., the polishing or isolation of amitriptyline hydrochloride from the IL-rich phase was performed by applying two distinct approaches: (i) for the phases from the system $[N_{4444}]Br + K_3PO_4$ and $[N_{4444}]Cl + K_3PO_4$ both at pH 13.2, phases were diluted 6 times with pure water; (ii) for the system $[N_{4444}]Br + K_2HPO_4/KH_2PO_4$ at pH 6.6 and $[P_{4444}]Br + K_2HPO_4/KH_2PO_4$ pH 6.6, the phases were diluted 6 times with an aqueous solution containing 5 wt% KOH. After proper dilution, the IL-rich phases became cloudy and after 24 hours at 277 (± 1) K, a precipitate was formed. After centrifugation of each sample, the concentration of amitriptyline hydrochloride in the solution obtained was measured. The isolation efficiency (IE_{Ami}, %) was calculated based on the concentrations of amitriptyline hydrochloride in the IL-rich (top) phase before ($[Ami]_{IL}$) and after the precipitation step ($[Ami]_{IL}^{A.P}$, considering the dilution factor due to anti-solvent addition) as shown in Equation 2.5.

$$IE_{Ami}, \% = \left(1 - \frac{[Ami]_{IL}^{A.P.}}{[Ami]_{IL}}\right) \times 100 \qquad (\textbf{\textit{Equation 2.5}})$$

pH assessment

The pH values of the salt solutions were monitored at 298 (± 1) K using a Mettler Toledo S47 SevenMulti^{TM} dual meter pH equipment with uncertainty of ± 0.02.

Results and discussion

The main objective of this work is the development of a new process based in IL-based ABS for the recovery of amitriptyline hydrochloride from pharmaceutical residues (*ADT 25 mg*). In this context, this work starts with an initial optimization of the ABS (carried out with a commercial standard of the antidepressant), aiming at the analysis and interpretation of the extraction results and driving forces behind the partition of the antidepressant drug. From the insights gathered in the optimization task, the best systems will be further studied in the definition of an integrated process of purification which will contemplate the extraction of the active drug from the solid pharmaceutical wastes, its purification by using the most efficient ABS in terms of extraction efficiency and purification performance and then the isolation of the antidepressant compound from the solvents used in the ABS preparation.

Partition of amitriptyline hydrochloride with ABS

The applicability of the IL-based ABS to the recovery of amitriptyline hydrochloride has been investigated by the optimization of several parameters, namely the IL structure, pH and mixture composition. An overview of the results obtained for the extraction parameters along with the conditions tested is reported in Table 2.6. The results indicate the complete partition of amitriptyline hydrochloride for the IL-rich phase, as confirmed by the large partition coefficients logarithmic functions obtained, generally higher than 2.5. This excellent capability to extract amitriptyline hydrochloride is corroborated by the remarkable extraction efficiency data obtained, that varied between 93 ± 3 % and 100 %. Its preferential distribution towards the IL-top phase, the most hydrophobic layer in these systems, is related to the lipophilic nature of this tricyclic antidepressant, in accordance with its high octanol-water partition coefficient (log$K_{o/w}$ of 4.85[10]). In order to facilitate the analysis of each experiment, the results are represented in Figures 2.11 to 2.13, which are organized according to the effect of ILs' structural features (Figure 2.11), pH (Figure 2.12) and mixture composition (Figure 2.13).

The study of the IL structure effect on the extractive performance of amitriptyline hydrochloride was carried using ABS composed of circa 30 wt% of IL + 15 wt% of K_2HPO_4/KH_2PO_4 (pH 6.6). Results, presented in Figure 2.11, indicate that $[N_{4444}]Cl$ is the best choice to efficiently extract this drug (EE_{Ami} of 100 % and $\log K_{Ami}$ > 2.5). When comparing the influence of the cation structure, based on two ILs sharing the Br^- anion, $[P_{4444}]Br$ and $[N_{4444}]Br$, it is possible to observe a slightly higher ability of the $[P_{4444}]^+$ (which is more hydrophobic than $[N_{4444}]^+$) to extract the antidepressant (again, the partition phenomenon seems to be controlled by the relative lipophilic/hydrophilic nature of the phases). The other phosphonium-based ILs ($[P_{4441}][C_1SO_4]$ and $[P_{i(444)1}][Tos]$) display extraction efficiencies similar to those of $[P_{4444}]Br$. The picture emerging from these results indicates that, although the phosphonium-based compounds seem to be better candidates, the careful optimization of the cation/anion combination is a key issue in the successful preparation of an adequate extraction system as gauged from the enhanced results obtained by applying the $[N_{4444}]Cl$. Moreover, it is not only the extraction and partition parameters obtained that should be taken into account, but also the cost, environmental impact and chemical characteristics of the ILs involved in these systems. Although slightly more corrosive, the halide-based compounds ($[N_{4444}]Br$, $[N_{4444}]Cl$ and $[P_{4444}]Br$) are cheaper[11] and less toxic[12] (especially when compared to the $[P_{i(444)1}][Tos]$). An additional benefit of ammonium-based cations utilization compared to their phosphonium-based congeners is both their lower cost[11] and toxicity.[13] ILs based on ammonium cations and halide anions were thus selected.

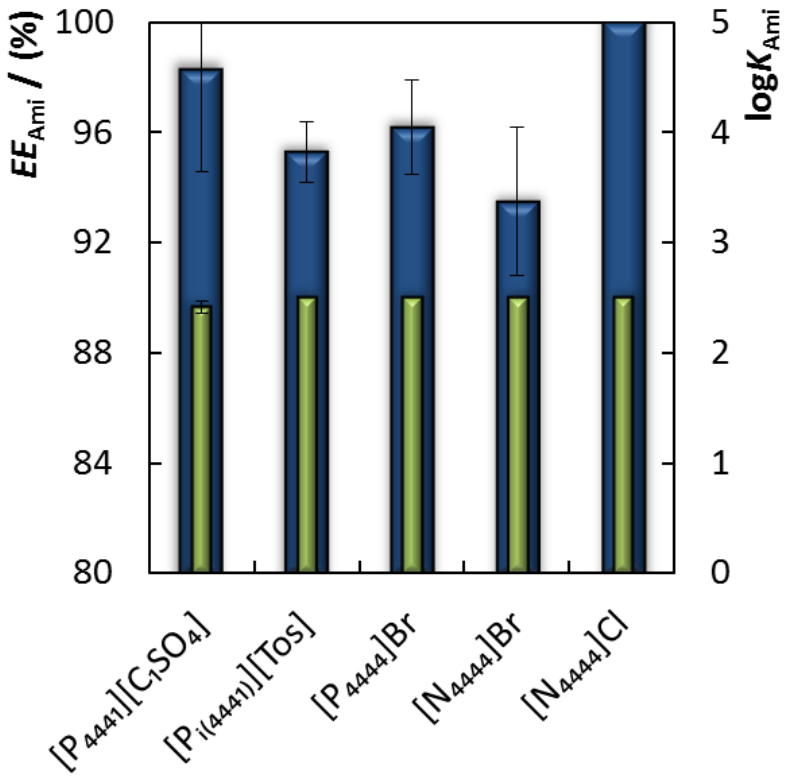

Figure 2.11. Effect of ILs' structural features on the extraction efficiencies (EE_{Ami} – blue bars) and logarithmic function of the partition coefficients ($\log K_{Ami}$ – green bars) of amitriptyline hydrochloride using IL-based ABS composed of around 30 wt% of IL + 15 wt% of K_2HPO_4/KH_2PO_4 (pH 6.6). In the case of $[N_{4444}]Cl$-based ABS, the composition considered was 27.4 wt% IL + 13.7 wt% of K_2HPO_4/KH_2PO_4 and water, due to experimental restrictions occurring at higher concentrations. Error bars correspond to standard deviations (σ).

The effect of pH on the extraction process was conducted using systems composed of $[N_{4444}]Br$ or $[N_{4444}]Cl$, by varying the salting-out species, K_3PO_4 at pH 13.2, K_2HPO_4 at pH ≈ 9.6 and K_2HPO_4/KH_2PO_4 at pH ≈ 6.6. For this purpose, additional binodal curves for the systems composed of $[N_{4444}]Br$ + K_2HPO_4, $[N_{4444}]Br$ + K_3PO_4 and $[N_{4444}]Cl$ + K_2HPO_4 were determined in order to fulfill the series of ABS at distinct pH values. The data in mass fraction units of the ternary phase diagrams (Tables B2-B4), Merchuk parameters (Table B5) and information on the TLs and TLLs (Table B6) are provided in Appendix B. It was verified that the main effects induced by the changes at the level of the IL's structural features and "salting-out" agents are in agreement with those well-described in literature

(decreasing order of ABS formation ability: K_3PO_4 > K_2HPO_4 and $[N_{4444}]Br$ > $[N_{4444}]Cl$).[14] The influence of the pH on the charge of amitriptyline, and on its subsequent extraction partition, was also analyzed. Speciation of this molecule as a function of pH is presented in Figure B1 in the Appendix B.[15] Amitriptyline has an amine group in its structure that can become protonated, and change its hydrophilicity (pKa = 9.41[16]). The three salts investigated here provided totally different pH to this heterocyclic drug: pH ≈ 6.6 where amitriptyline is in its ionized form, pH ≈ 9.6 in which only around of 60 % of the species in solution are in their protonated form and pH ≈ 13.2, where amitriptyline is its neutral form.[15] It is known that these charge modifications can affect the partitioning on the ABS, as the solubility in water of amitriptyline in its non-ionized form decreases drastically when compared with the charged form.[17] The results related to the pH effect on the extraction efficiencies of this antidepressant are presented in Figure 2.12. It is noticed that the pH does not affect the extraction performance of $[N_{4444}]Cl$-based ABS, being constant at values of 100 %, and has a small effect for the systems based on the $[N_{4444}]Br$, in which this value slightly increases from 93 ± 3 % (at pH ≈ 6.6) to 97 ± 3 % (at pH ≈ 9.6) closer to 97.5 ± 0.6 % (at pH ≈ 13.2). Also from the partition coefficients results, where their logarithmic functions were larger than 2.5, it is observed that, even changing the pH, the antidepressant always migrates extensively towards the top phase. This can only be explained by a process dominated by the salting-out from the salt-rich phase induced by the phosphate salts, coupled to the change in solvation resulting from the loss of electrostatic interactions as the drug with increasing pH becomes neutral, decreasing its solubility in water and increasing its lipophilicity. Moreover, the extraction performance achieved for the $[N_{4444}]Cl$-based ABS (pH ≈ 6.6) is higher than that obtained for the $[N_{4444}]Br$-based ABS (pH 6.6), however, at higher pH values this tendency is attenuated. This may be a direct consequence of the higher lipophilic character of $[N_{4444}]Br$ when compared with the $[N_{4444}]Cl$, conjugated with the poorer water content in the $[N_{4444}]Br$-rich phase. Indeed, a longer TLL was achieved for $[N_{4444}]Br$ than for $[N_{4444}]Cl$, taking into account the results for the same mixture point composition, i.e., higher amounts of IL and lower water contents in the IL-rich phase (for more details in the TLs see Table B6 in Appendix B).

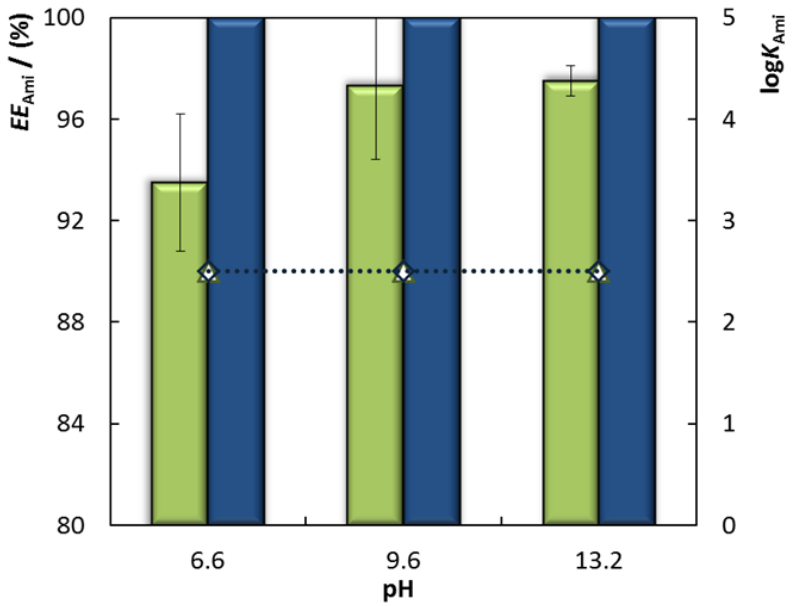

Figure. 2.12. Effect of pH on the extraction efficiencies (EE_{Ami} – bars) and logarithmic function of the partition coefficient ($\log K_{Ami}$ – symbols) of amitriptyline hydrochloride using IL-based ABS composed of 30 wt% of $[N_{4444}]Br$ (green bars and triangles) or 27 or 30 wt% of $[N_{4444}]Cl$ (blue bars and diamonds) + 14 or 15 wt% of phosphate-based salts. Error bars correspond to standard deviations (σ).

The influence of different mixture points, along the same TL, on the partitioning behavior of amitriptyline hydrochloride was also investigated in this study. Here, the main objective is to tune the volume ratio of the coexisting aqueous phases, by reducing as much as possible the IL-rich phase volume in order to yield a concentration of amitriptyline as high as possible. For this purpose, mixture compositions laying on the same TL for $[N_{4444}]Br + K_2HPO_4/KH_2PO_4 + H_2O$, $[P_{4444}]Br + K_2HPO_4/KH_2PO_4 + H_2O$ and $[N_{4444}]Cl + K_3PO_4 + H_2O$ were prepared. The extraction parameters obtained are presented in Figure 2.13 and show that both the extraction efficiencies and partition coefficients were persistently high, with no significant changes (EE_{Ami} > 93 ± 3 % for $[N_{4444}]Br + K_2HPO_4/KH_2PO_4 + H_2O$, > 94 ± 4 % for $[P_{4444}]Br + K_2HPO_4/KH_2PO_4 + H_2O$ and ≈ 100 % for $[N_{4444}]Cl + K_3PO_4 + H_2O$ and $\log K_{Ami}$ > 2.5 for the entire set of systems). Systems composed of smaller top phases are thus better alternatives, not only from an operational point of view (improved extractive performances at the same time that facilitate further isolation

strategies), but also from an economic perspective since the amounts of the IL used are minimized.

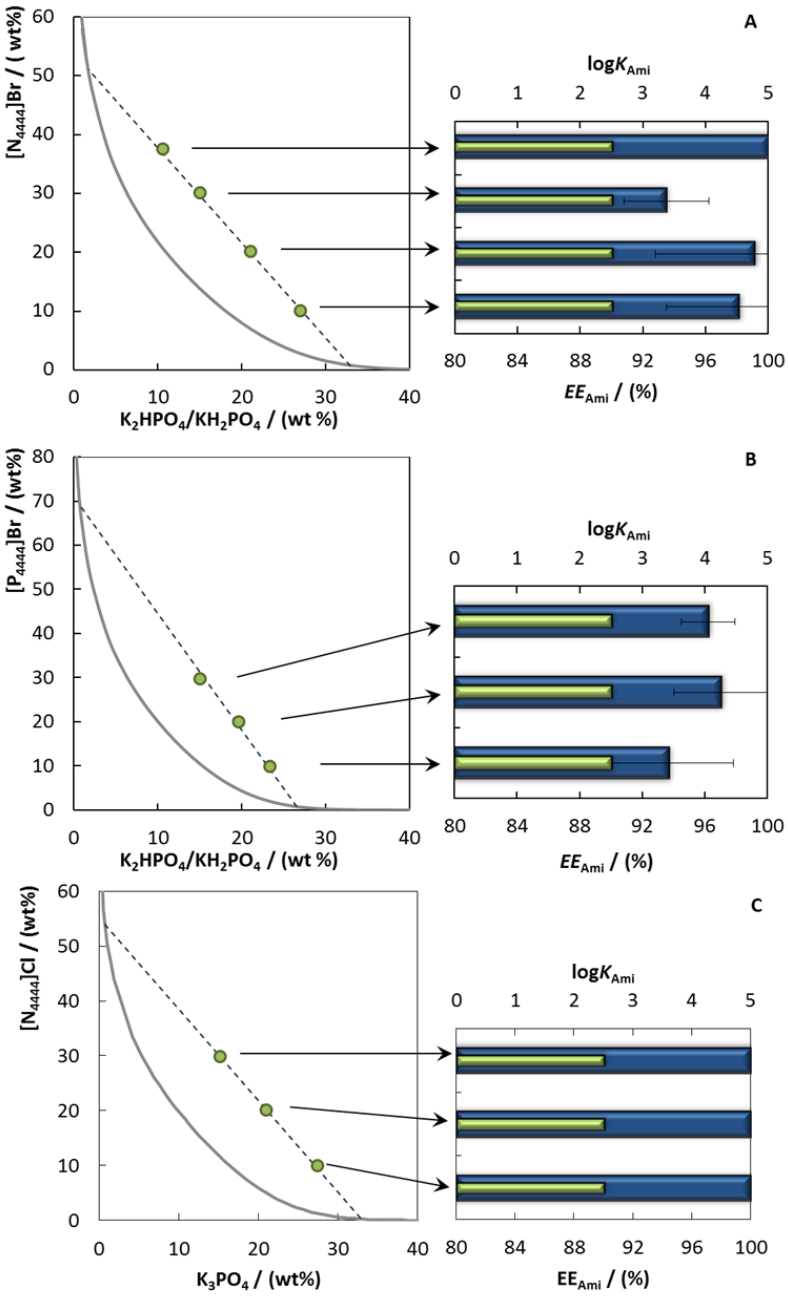

Figure 2.13. Representation of the experimental binodal curve (solid line), tie-line (dashed line) and mixture compositions (green circles),extraction efficiencies (EE_{Ami}, blue bars) and logarithmic functions of the partition coefficients (logK_{Ami}, green bars) attained for the systems $[N_{4444}]Br + K_2HPO_4/KH_2PO_4 + H_2O$ (A), $[P_{4444}]Br + K_2HPO_4/KH_2PO_4 + H_2O$ (B) and $[N_{4444}]Cl + K_3PO_4 + H_2O$ (C). Error bars correspond to standard deviations (σ).

Given the promising extraction results afforded by the use of alkaline pH environments and lower IL-rich phase volumes, systems composed of circa 10 wt% $[N_{4444}]Br$ + 25 wt% K_3PO_4 + 65 wt% H_2O + distinct concentrations of antidepressant, were chosen to evaluate the maximum capacity of the present technology. The results obtained are depicted in Figure 2.14 and show that the extraction efficiency increases with the amitriptyline concentration in the ABS (the detailed conditions and data are provided in Appendix B – Table B7). Then, a maximum EE_{Ami} = 97 ± 3 % is reached *at* circa 50 mg of amitriptyline fed in the ABS, followed by a significant decrease (down to 66 ± 1%) – Figure 2.14A. Contrarily, the logarithmic function of the partition coefficients does not depend on the amitriptyline concentration, being > 2.5 (strong tendency to partition towards the IL-rich phase). The increase of the amitriptyline hydrochloride concentration in the ABS leads to its accumulation in IL-rich phase, until saturation (C_{Ami} = 93.5 mg of amitriptyline hydrochloride *per* g of IL-rich phase, as shown in Figure 2.14B). As the amitriptyline hydrochloride concentration is further increased in the system, the formation of a third layer between the IL-rich phase and salt-rich phase is observed, which is likely the reason for the drop in the extraction efficiencies (due to drug precipitation/losses) and thus can be considered as an indication of the maximum capacity of the current technology.

Table 2.7. Mixture compositions of the IL-based ABS, extraction efficiencies (EE_{Ami}) and isolation efficiencies (IE_{Ami}) attained during the multi-stage process developed, aiming at the recovery of amitriptyline hydrochloride from the drug *ADT 25 mg*.

IL-based ABS	**$[IL]_M$ / (wt%)**	**$[Salt]_M$ / (wt%)**	**$[water]_M$ / (wt%)**	**$EE_{Ami} \pm \sigma$ (%)**	**$IE_{Ami} \pm \sigma$ (%)**
$[N_{4444}]Br + K_2HPO_4/KH_2PO_4$	10.07	27.14	62.79	98.5 ± 0.7	98.73 ± 0.07
$[N_{4444}]Br + K_3PO_4$	10.40	25.08	64.52	95± 6	96.9 ± 0.1
$[P_{4444}]Br + K_2HPO_4/KH_2PO_4$	10.08	23.47	66.45	92 ± 1	97 ± 1
$[N_{4444}]Cl + K_3PO_4$	10.09	26.89	63.01	100	95 ± 2

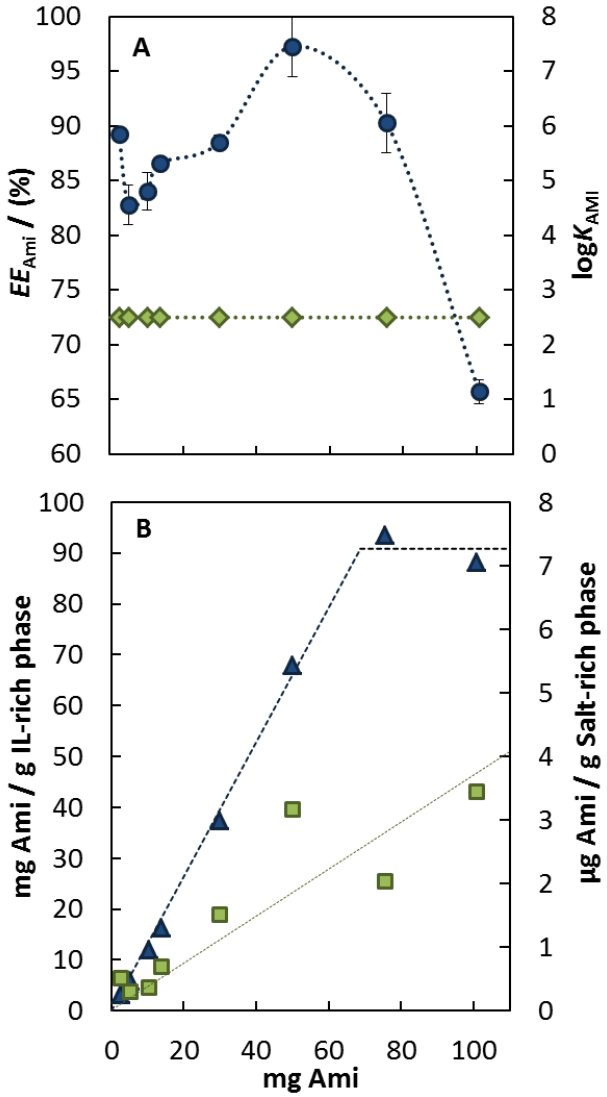

Figure 2.14. Influence of the amitriptyline hydrochloride amount on the (A) extraction efficiency (EE_{Ami}, blue circles) and logarithmic function of the partition coefficient (logK_{Ami}, green diamonds) and (B) amount of the antidepressant included in the IL-rich (top) phase (blue triangle) and salt-rich (bottom) phase (green square), using the system $[N_{4444}]Br + K_3PO_4 + H_2O$. The lines are only for eye guide.

Recovery and isolation of amitriptyline hydrochloride from *ADT 25 mg*

After development of the amitriptyline hydrochloride purification process by the refinement of several IL-based ABS, their application to a real pharmaceutical waste-based matrix, i.e., *ADT 25 mg* pills, was carried out. A multi-stage process was set up including a solid-liquid extraction step followed by the physical separation of insoluble

excipients, a purification stage involving the use of the best IL-based ABS selected in the optimization step and, finally, the isolation of the target drug. The proposed process diagram is depicted in Figure 2.15. The solid-liquid extraction was performed using water as the principal solvent, in which amitriptyline hydrochloride is highly soluble. The grinded pills were added to water and kept under stirring for 24 hours in order to extract the total amount of the antidepressant. Afterwards, the resulting extract was submitted to two physical separation methods (filtration and centrifugation) to remove any insoluble excipients present in the aqueous extract rich in the antidepressant. At the end of these steps, the expected final concentration of amitriptyline hydrochloride (circa 31 $g.dm^{-3}$) was theoretically determined based on the total amount of active ingredient in each pill (information retrieved from medicine flyers) and the number of pills added to the solid-liquid extracting agent. The actual concentration attained was confirmed by HPLC-UV-Vis by us, which was then regularly considered during the calculations of the efficiencies in the following steps.

The filtered aqueous extract obtained from the solid-liquid extraction, is rich in amitriptyline and other compounds, namely calcium hydrogenophosphate dehydrate and tartrazine, two of the excipients used in *ADT 25 mg* formulation with large solubility in water (information detailed by Infarmed for the medicine used in this work). Thus, the purification task was developed taking into account the most efficient IL-based ABS (considering the extraction efficiency results) according to optimization studies (10 wt% $[N_{4444}]Br$ + 25 wt% K_3PO_4 + 65 wt% H_2O, 10 wt% $[N_{4444}]Br$ + 27 wt% K_2HPO_4/KH_2PO_4 + 63 wt% H_2O, 10 wt% $[P_{4444}]Br$ + 23 wt% K_2HPO_4/KH_2PO_4 + 67 wt% H_2O and 10 wt% $[N_{4444}]Cl$ + 27 wt% K_3PO_4 + 63 wt% H_2O). These results are shown in Table 2.7 and reveal that the extraction efficiency and the logarithmic function of the partition coefficients always exceed 92 ± 1 % and 2.5, respectively, results also consistent with those assessed in the optimization step using the commercial standard.

During the purification of the antidepressant from the medicine *ADT 25 mg* using the $[N_{4444}]Br$ and $[N_{4444}]Cl$ + K_3PO_4 + H_2O systems, a white precipitate was formed in the interphase, contrarily to what was observed during the optimization studies with the pure standard (formation of two clear phases). In this context and to exclude any possibility of

amitriptyline losses, the aqueous phases were separated and its concentration assessed by HPLC-UV-Vis. The extraction efficiency was 95 % or 100 %, respectively, meaning that this technology keeps its high performance and that the precipitate is not significantly composed by amitriptyline hydrochloride. This probably means that at this pH, some soluble excipients (simultaneously extracted during the solid-liquid extraction step) precipitate, allowing for a first step of purification considering the physical elimination of some of the contaminants from the amitriptyline rich-phase.

The last step consisted on the isolation of the target antidepressant from the top (IL-rich) phase, through the manipulation of the pH to cause the inherent decrease of solubility of the antidepressant, when it is present in its neutral form. For that purpose, an aqueous solution of KOH was added to the IL-rich phase in the case of the K_2HPO_4/KH_2PO_4 (pH ≈ 6.6)-based systems or only water in K_3PO_4-based ABS (as the inherent pH of these systems guarantees the presence of amitriptyline hydrochloride as a neutral species). It should be mentioned that this pH-driven isolation was conducted at low temperature of 277 (±1) K, a suitable way to further decrease the solubility of the antidepressant, thus enhancing its crystallization. In general, the isolation step was successfully developed as the isolation efficiencies (IE_{Ami}) obtained for the three systems were higher than 95 ± 2 %.

At the end, the highest extraction and isolation efficiencies were observed for the ABS composed of $[N_{4444}]Br + K_2HPO_4/KH_2PO_4$ and $[N_{4444}]Cl + K_3PO_4$ and the lowest values were attained using $[P_{4444}]Br + K_2HPO_4/KH_2PO_4$. The promising performance of the systems composed of $[N_{4444}]Br$ and $[N_{4444}]Cl + K_3PO_4 + H_2O$ should be highlighted as it allows an "extra" purification step (precipitation of excipients extracted along with the target antidepressant during the solid-liquid extraction) and a simpler precipitation procedure (no need for additional species in solution, contrarily to the remaining systems that required the addition of KOH).

For the proposed process to be of industrial relevance, the recovery and reuse of the main phase components must be considered after the purification and polishing steps. It is here proposed that the two phases are recycled by the application of H_3PO_4 for the neutralization of the phase (from which the amitriptyline hydrochloride was isolated)

to neutralize the small content of KOH added in the polishing step and then the phase can be re-introduced in the preparation of the ABS, as described in the process diagram of Figure 2.15. The other phase, practically free of amitriptyline hydrochloride and rich in excipients, can be treated by a step of ultrafiltration to remove the high molecular weight excipients and then directly reused in the preparation of ABS. It is also highlighted that the concentration of excipients/contaminants is residual at this stage and thus the reuse of the phase components is facilitated.

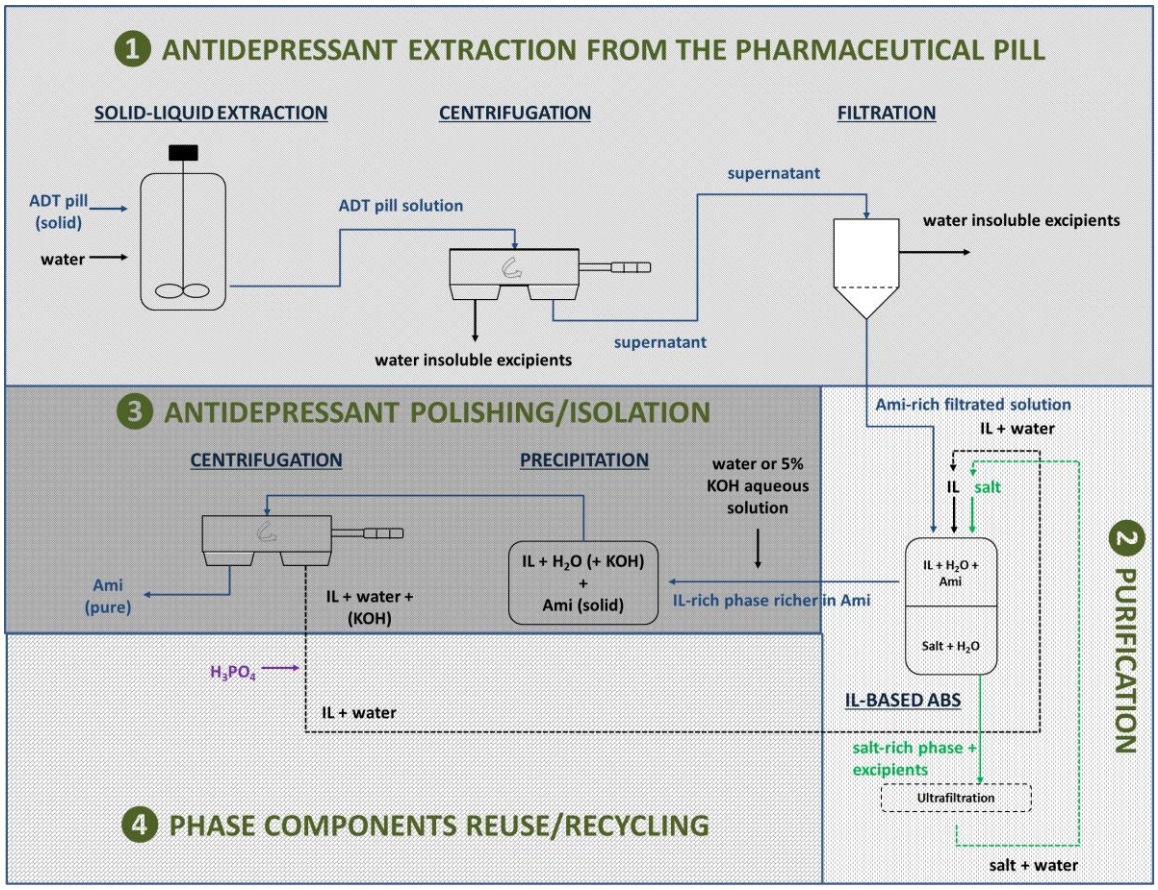

Figure 2.15. Schematic representation of the integrated process diagram comprising the following steps: solid-liquid extraction of the antidepressant from the pharmaceutical pills, purification of amitriptyline hydrochloride from the antidepressant drug *ADT 25 mg* considering the excipients used in its formulation as the main contaminants and polishing process of the antidepressant; in here, we are describing the process of isolation of the antidepressant from the presence of the phase components of the ABS. The recovery and reuse of the main phase components is also represented.

Conclusions

A novel process for the extraction of amitriptyline hydrochloride able to selectively separate it from its main contaminants (i.e., *ADT 25* pills' excipients) present in the pharmaceutical wastes was successfully developed. It comprises a solid-liquid extraction step (where most of the water insoluble excipients were removed), the purification using IL-based ABS (where the water soluble excipients were eliminated), and the isolation of the target antidepressant (where the amitriptyline hydrochloride was recovered from the solvent matrix). The extraction step was optimized using various IL + phosphate salts-based ABS, where the IL nature, the type of phosphate salt (which induced distinct pH media) and the mixture composition were varied. During this task, it was concluded that the antidepressant partition occurs towards the top (IL-rich) phase ($\log K_{Ami} > 0$) with very high extraction efficiencies, ranging from 66 ± 1 to 100%. The most appropriate conditions for the partition phenomenon were selected based not only on the extractive performances, but also on the predicted cost and environmental impact of the ABS formation agents. In this context, the halide-based ILs, two extreme pH environments (K_2HPO_4/KH_2PO_4 and K_3PO_4) and mixture compositions containing low quantities of *at* circa 10 wt% of IL corresponding to short volume top phases, were selected as the best solvents and conditions to be adopted in the development of the process of purification considering the use of a multi-step process comprising the extraction, purification and isolation of amitriptyline hydrochloride from the pharmaceutical residues of *ADT 25*. At the end, the process herein designed was shown to be efficient for both extraction (92 ± 1 % < EE_{AMI} < 100 %) and isolation (95 ± 2 % < IE_{AMI} < 98.73 ± 0.07 %) steps regarding the recovery of amitriptyline hydrochloride. The essential role of the pH (above amitriptyline hydrochloride's pK_a – 9.41) in both purification and isolation stages is shown in this work. In stages of some water soluble excipients are precipitated, while in the second stage a simple isolation procedure of amitriptyline hydrochloride from the top (IL-rich) phase is obtained. With this work new perspectives for the recovery of valuable drugs from pharmaceutical wastes (very low cost raw materials) are being created, converting them from toxic liabilities into a source of valuable chemicals thus minimizing the life cycle impact of these compounds.

References

[1] Antidepressants: global trends; http://www.theguardian.com/news/2013/nov/20/mental-health-antidepressants-global-trends, 2013.

[2] Evolução do consumo de antidepressivos em Portugal Continental de 1995 a 2001: Impacto das medidas reguladoras; Infarmed: http://www.infarmed.pt/portal/page/portal/INFARMED/MONITORIZACAO_DO_MERCADO/OBSERVATORIO/INTRODUCAO_DE_FICHEIROS/rel_antidepressivos.pdf, 2002.

[3] Calisto, V.; Esteves, V. I. Psychiatric pharmaceuticals in the environment. *Chemosphere* **2009,** *77* (10), 1257-1274.

[4] Top antidepressant drugs in the United States based on revenue in 2011-2012 (in million U.S. dollars); Statistica - The Statistics Portal: http://www.statista.com/statistics/242644/revenues-of-top-depression-drugs-in-the-us-2011-2012/, 2012.

[5] e Silva, F. A.; Sintra, T.; Ventura, S. P. M.; Coutinho, J. A. P. Recovery of paracetamol from pharmaceutical wastes. *Separation and Purification Technology* **2014,** *122*, 315-322.

[6] Sintra, T. E.; Cruz, R.; Ventura, S. P. M.; Coutinho, J. A. P. Phase diagrams of ionic liquids-based aqueous biphasic systems as a platform for extraction processes. *Journal of Chemical Thermodynamics* **2014,** *77*, 206-213.

[7] Passos, H.; Sousa, A. C. A.; Pastorinho, M. R.; Nogueira, A. J. A.; Rebelo, L. P. N.; Coutinho, J. A. P.; Freire, M. G. Ionic-liquid-based aqueous biphasic systems for improved detection of bisphenol A in human fluids. *Analytical Methods* **2012,** *4* (9), 2664-2667.

[8] Neves, C. M. S. S.; Ventura, S. P. M.; Freire, M. G.; Marrucho, I. M.; Coutinho, J. A. P. Evaluation of Cation Influence on the Formation and Extraction Capability of Ionic-Liquid-Based Aqueous Biphasic Systems. *Journal of Physical Chemistry B* **2009,** *113* (15), 5194-5199.

[9] Merchuk, J. C.; Andrews, B. A.; Asenjo, J. A. Aqueous two-phase systems for protein separation: Studies on phase inversion. *Journal of Chromatography B Biomedical Sciences and Applications.* **1998,** *711* (1–2), 285-293.

[10] Faassen, F.; Vogel, G.; Spanings, H.; Vromans, H. Caco-2 permeability, P-glycoprotein transport ratios and brain penetration of heterocyclic drugs. *International Journal of Pharmaceutics* **2003,** *263* (1–2), 113-122.

[11] Passos, H.; Freire, M. G.; Coutinho, J. A. P. Ionic liquid solutions as extractive solvents for value-added compounds from biomass. *Green Chemistry* **2014,** *16* (12), 4786-4815.

[12] Ventura, S. P. M.; Marques, C. S.; Rosatella, A. A.; Afonso, C. A. M.; Gonçalves, F.; Coutinho, J. A. P. Toxicity assessment of various ionic liquid families towards Vibrio fischeri marine bacteria. *Ecotoxicology and Environmental Safety* **2012,** *76*, 162-168.

[13] Carvalho, P. J.; Ventura, S. P. M.; Batista, M. L. S.; Schröder, B.; Gonçalves, F.; Esperança, J.; Mutelet, F.; Coutinho, J. A. P. Understanding the impact of the central atom on the ionic liquid behavior: Phosphonium vs ammonium cations. *Journal of Chemical Physics* **2014,** *140* (6), 064505.

[14] Freire, M. G.; Cláudio, A. F. M.; Araújo, J. M. M.; Coutinho, J. A. P.; Marrucho, I. M.; Lopes, J. N. C.; Rebelo, L. P. N. Aqueous biphasic systems: a boost brought about by using ionic liquids. *Chemical Society Reviews* **2012,** *41* (14), 4966-4995.

[15] Chemspider - The free chemical database at http://www.chemspider.com (accessed Oct 10, 2014).

[16] Yazdi, A. S.; Razavi, N.; Yazdinejad, S. R. Separation and determination of amitriptyline and nortriptyline by dispersive liquid–liquid microextraction combined with gas chromatography flame ionization detection. *Talanta* **2008,** *75* (5), 1293-1299.

[17] Hansen, S.; Pedersen-Bjergaard, S.; Rasmussen, K., *Introduction to pharmaceutical chemical analysis*. John Wiley & Sons: 2011.

2.1.3. Recovery of non-steroidal anti-inflammatory drugs from wastes using ionic liquid-based three-phase partitioning systems

This section is based on e Silva, F. A.; Caban, M.; Kholany, M.; Stepnowski, P.; Coutinho, J. A. P.; Ventura, S.P.M. Recovery of non-steroidal anti-inflammatory drugs from wastes using ionic liquid-based three-phase partitioning systems. *ACS Sustainable Chemistry and Engineering* **2018**, *6* (4), 4574–4585.

Contributions: S.P.M.V. and J.A.P.C. conceived and directed this work. Francisca A. e Silva, M.C. and M.K. acquired the experimental data. In particular, Francisca A. e Silva acquired data regarding the partition of the drugs. Francisca A. e Silva, M.C. S.P.M.V. and J.A.P.C. interpreted the experimental data. Francisca A. e Silva, M.C. and S.P.M.V. wrote the manuscript with contributions from the remaining authors.

Abstract

Aiming at outlining new strategies for the valorization of solid pharmaceutical wastes as viable alternatives to incineration, this work proposes the use of IL-based TPP systems. Ibuprofen, naproxen and ketoprofen, all belonging to the class of NSAIDs, were adopted as model compounds. An integrated process has been conceptualized based on three steps: 1 – extraction and purification of NSAIDs using the IL-based TPP systems; – 2 – drug isolation by precipitation with anti-solvents; – 3 – recycle and reuse of the solvents. With the optimization of steps 1 and 2 as objects of this investigation, ABS composed of three distinct ILs (tetrabutylammonium chloride, 1-butyl-3-methylimidazolium chloride and benzyldimethyl(2-hydroxyethyl)ammonium chloride) and potassium citrate buffer were studied. The corresponding IL-based TPP systems were further applied in the purification of each NSAID, and different anti-solvents (citric acid aqueous solutions for ibuprofen and naproxen and aluminium sulphate aqueous solutions for ketoprofen) were evaluated as precipitating agents to isolate each drug. The success of the process developed is demonstrated by the extraction efficiencies higher than 84 ± 8 % attained in step 1 and isolation efficiencies higher than 76 ± 2 % in step 2. The stability of the three NSAIDs in IL-based aqueous matrices was additionally checked by

using a protocol adapted from the OECD guidelines. The economic efficiency and environmental benignity of the process herein developed is underlined, based not only on the low cost of the solvents chosen, but also on the possibility of recycling and reusing the phase-forming components and anti-solvents employed.

Introduction

The highly aqueous-rich environment of IL-based ABS along with the interfacial partition of targeted compounds in TPP systems has originated a novel separation platform, the IL-based TPP systems.[1] While conventional TPP resorts to organic solvents,[2] the introduction of ABS improves the process biocompatibility. Moreover, IL-based TPP are able to keep all the ABS advantages with an extra degree of operational simplicity linked to the purification stage, where the formation of an interface enriched in target compounds or contaminants in a purer state occurs.[1] IL-based TPP has been successfully applied in the one-step purification of several biomolecules, particularly proteins and amino acids, showing some advantages when compared with the common ABS and IL-based ABS.[1, 3-5] In a series of works devoted to IL-based TPP systems, Alvarez-Guerra and collaborators[1, 3, 4] recovered up to 99% of lactoferrin from waste streams and defined some efficient ways to recycle and reuse the IL. CIL-based TPP systems find also application in enantiomeric separations. As shown by Wu et al.,[5] under optimized conditions, it was possible to tune the partition of the two enantiomeric forms of phenylalanine. The L-enantiomer precipitates in the interface, while the D-enantiomer partitions to the IL-rich phase.

In this sense, this work aims at the optimization and implementation of a new process for the purification of NSAIDs from wastes taking into account the IL-based ABS characteristics, but instead using IL-based TPP systems. The spectrum of active ingredients (ibuprofen, naproxen and ketoprofen, used as model NSAIDs) and of technologies available is here extended. ABS composed of three different ILs conjugated with the potassium citrate buffer were used to perform the partition studies of the model NSAIDs. Beyond the investigation of the IL's impact on the ABS extraction performance, other operational conditions were studied [viz. NSAID content, temperature, pH and tie-line length (TLL)]. Meanwhile, and using the characteristics of the systems under study,

the development of IL-based TPP systems was investigated. Thus, to recover ibuprofen, naproxen and ketoprofen directly from their waste-based matrices in a single-step (where the excipients are eliminated at the liquid-liquid interface), the IL-based TPP systems were optimized. At the end, these IL-based TPP were integrated in a process, where the isolation (i.e., polishing) of the three drugs is contemplated. The stability of the three NSAIDs in ILs or ILs + salts aqueous solutions was also assessed through the implementation of a new protocol adapted from OECD guidelines. Thus, this work allowed the development and optimization of an alternative and efficient process for the recovery of drugs from pharmaceutical wastes, transversal to other active ingredients and more complex waste mixtures/solutions. Moreover, the process allowed inferring on the suitableness of the IL-based TPP technology, not solely centered on its performance but also addressing the target molecule integrity.

Experimental

Materials

NSAIDs standards for ketoprofen (CAS number 22071-15-4) (≥ 98 %; Sigma-Aldrich, China), naproxen (CAS number 22204-53-1) (≥ 97 %; Sigma-Aldrich, USA) and ibuprofen (CAS number 15687-27-1) (≥ 98 %; Sigma-Aldrich, China) were purchased from Sigma-Aldrich. The corresponding pills were acquired in a local pharmacy (Aveiro, Portugal), being their specifications (viz. NSAIDs' content and the excipients' profile) shown in Table C1 from Appendix C. The ILs tested were tetrabutylammonium chloride $[N_{4444}]Cl$ (97 %, Sigma-Aldrich), 1-butyl-3-methylimidazolium chloride, $[C_4C_1im]Cl$ (99 %, IoLiTec, Ionic Liquids Technology) and the benzyldimethyl(2-hydroxyethyl)ammonium chloride [BzCh]Cl (97 %; Fluka). Depicted in Figure 2.16 are the NSAIDs and ILs chemical structures along with the abbreviations adopted. Citric acid monohydrate $C_6H_8O_7 \bullet H_2O$ (100 %) was from Fisher-Scientific, potassium citrate tribasic monohydrate $C_6H_5K_3O_7 \bullet H_2O$ (99 %) was supplied by Acros Organics and aluminium sulphate hexadecahydrate $Al_2(SO_4)_3 \bullet 16H_2O$ (≥ 95 %) was purchased at Sigma-Aldrich.

For the HPLC-DAD mobile phase, ammonium acetate $NH_4C_2H_3O_2$ (≥ 99.99%; Sigma-Aldrich, Japan), acetic acid (≥ 99.99 %; Sigma-Aldrich, USA), acetonitrile (HPLC gradient

grade; HiPerSolv CHROMANORM) and ultrapure water (treated with a Mili-Q 185 water apparatus) were used. Syringe filters (0.45 µm of pore size; Specanalitica, Portugal) and membrane filters (0.22 µm; Sartorius Stedim Biotech, Germany) were applied in the filtration steps.

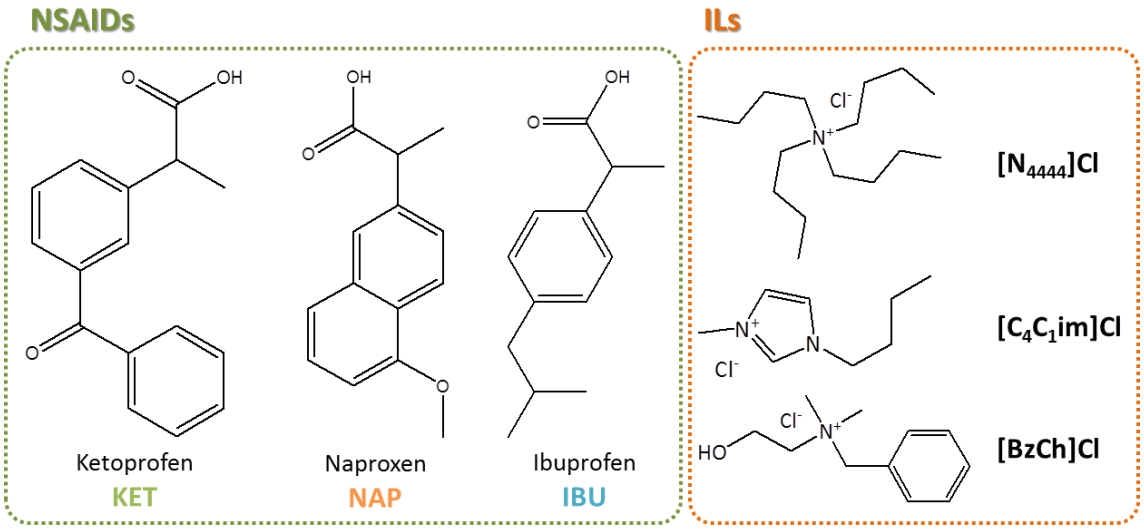

Figure 2.16. Chemical structures and abbreviations of the studied NSAIDs and ILs.

NSAIDs partitioning optimization studies using IL-based ABS

ABS composed of ILs with potassium citrate buffer were evaluated in what regards their ability to extract NSAIDs from pharmaceutical wastes. The corresponding ternary phase diagrams can be found in literature,[6-8] these being considered when selecting the compositions of the ABS and calculating the corresponding tie-lines (TLs) and TLLs. The TLs were determined through the Asenjo and collaborators[9] method, which was already adopted and validated by our research group for IL-based ABS.[6-8] TLLs are the Euclidean distance between the top and bottom phase compositions.

The influence of several operational conditions was assessed, namely IL structure, NSAID content, temperature, pH and TLL. The ABS preparation was carried by weighing the appropriate amounts of each component and NSAID according to Table 2.8. NSAIDs were added to the ABS (5 g of total mass) as a mixture composed of equal amounts of ibuprofen, ketoprofen and naproxen standard powders (at final contents of each NSAID of approximately 1, 2 and 4 mg *per* g of ABS). The systems were vigorously stirred and

placed at the desired temperature at least during 18 hours to reach equilibrium and to achieve the complete partition of the NSAIDs. In order to obtain the distinct pH values evaluated during the ABS optimization studies, potassium citrate buffer at pH 7 and 8, prepared according to tabulated values,[10] was used, while pH 9 was afforded by the use of potassium citrate tribasic.

After the appearance of two clear phases, their separation was carried followed by the measurement of their weight and volume. In the end, these systems resulted in one IL-rich and one salt-rich phase as the top and bottom layers, respectively. At least three repetitions of each system were performed. Both the top and bottom phases were analyzed by HPLC-DAD after filtration using syringe filters of 0.45 μm pore (to remove suspended solids) and appropriate dilution: for the top phase, 25 times in a mixture of water:ACN (70:30, v/v), 5 times in water was the dilution adopted for the salt-rich layers (three injections per sample). In order to evaluate the extractive performance of these systems, two parameters were calculated, namely the extraction efficiency of each NSAID (EE_{NSAID}, %) – Equation 2.6 – and their recovery toward the IL-rich (top) phase (R_T, %) – Equation 2.7.

$$EE_{NSAID}, \% = \frac{[NSAID]_T \times V_T}{m_0} \times 100 \qquad \textbf{(Equation 2.6)}$$

$$R_T, \% = \frac{[NSAID]_T \times V_T}{[NSAID]_T \times V_T + [NSAID]_B \times V_B} \times 100 \qquad \textbf{(Equation 2.7)}$$

$[NSAID]_T$ and $[NSAID]_B$ are the concentrations of each NSAID (ibuprofen, naproxen or ketoprofen) found in the top and bottom phases, V_T and V_B are the volumes of the top and bottom phases and m_0 is the mass of each NSAID initially added in the ABS preparation. Both EE_{NSAID} (%) and R_T (%) are reported as the average values with the corresponding standard deviations.

Table 2.8. Conditions studied and mass fraction compositions (in weight percentage) used during the ABS optimization studies.

Operational condition	**IL**	**Salt**	**NSAIDs content / (mg *per* g of ABS)**	**pH**	***T* (±1) / (°C)**	**100 × mass fraction composition / (wt%)**		
						IL	**Salt**	**Water**
IL structure	$[C_4C_1im]Cl$	$C_6H_5K_3O_7/C_6H_8O_7$	4	7	25	30	30	40
	[BzCh]Cl	$C_6H_5K_3O_7/C_6H_8O_7$	4	7	25	35	30	35
	$[N_{4444}]Cl$	$C_6H_5K_3O_7/C_6H_8O_7$	4	7	25	30	30	40
NSAID content	$[C_4C_1im]Cl$	$C_6H_5K_3O_7/C_6H_8O_7$	1	7	25	30	30	40
	$[C_4C_1im]Cl$	$C_6H_5K_3O_7/C_6H_8O_7$	2	7	25	30	30	40
	$[C_4C_1im]Cl$	$C_6H_5K_3O_7/C_6H_8O_7$	4	7	25	30	30	40
Temperature	$[C_4C_1im]Cl$	$C_6H_5K_3O_7/C_6H_8O_7$	4	7	15	30	30	40
	$[C_4C_1im]Cl$	$C_6H_5K_3O_7/C_6H_8O_7$	4	7	25	30	30	40
	$[C_4C_1im]Cl$	$C_6H_5K_3O_7/C_6H_8O_7$	4	7	35	30	30	40
	$[C_4C_1im]Cl$	$C_6H_5K_3O_7/C_6H_8O_7$	4	7	45	30	30	40
pH	$[C_4C_1im]Cl$	$C_6H_5K_3O_7/C_6H_8O_7$	4	7	25	30	30	40
	$[C_4C_1im]Cl$	$C_6H_5K_3O_7/C_6H_8O_7$	4	8	25	30	30	40
	$[C_4C_1im]Cl$	$C_6H_5K_3O_7$	4	≈9	25	30	30	40
TLL	$[C_4C_1im]Cl$	$C_6H_5K_3O_7/C_6H_8O_7$	4	7	25	30	30	40
	$[C_4C_1im]Cl$	$C_6H_5K_3O_7/C_6H_8O_7$	4	7	25	33	28	39
	$[C_4C_1im]Cl$	$C_6H_5K_3O_7/C_6H_8O_7$	4	7	25	35	26.5	38.5

Recovery of NSAIDs from pharmaceutical wastes

NSAIDs extraction by applying IL-based TTP systems. When applying the IL-based ABS to the pills, the extraction of each NSAID was performed separately in a single-step, i.e., the non-soluble excipients settled in the interface allowing their separation from the target active ingredients forming IL-based TPP. Their visual appearance is depicted in Figure C1 in Appendix C. The mass of each pill containing the NSAID was determined taking into account the total mass of NSAID present in the grinded pill and excluding that of excipients (data verified in the medicine flyers). So, using *Naproxeno Generis* (≈25% of excipients) and *Brufen* (≈25% of excipients) pills, 20 mg of naproxen and ibuprofen was added (4 mg *per* g of ABS), whereas for *Profenid Retard* (≈61% of excipients due to the prolonged release character of this medicine) the addition of 10 mg of ketoprofen was done (2 mg *per* g of ABS). During the phase separation, the excipients-rich interface was discarded. All the remaining procedure and calculations were the same as those adopted throughout the NSAIDs partitioning optimization studies using IL-based ABS.

NSAIDs isolation through precipitation. NSAIDs isolation from the IL-rich phase was conducted through precipitation with anti-solvents, namely citric acid and aluminium sulfate aqueous solutions. From the three distinct types of ABS investigated, the one composed of ≈ 30 wt% of $[C_4C_1im]Cl$, 30 wt% of salt and 40 wt% of water containing the same amounts of pills aforementioned was elected. It should be stressed that with *Profenid Retard* the pills quantities were doubled in order to facilitate this task. In a first attempt, aqueous solutions of citric acid at 25 wt% were added in ratios of top phase volume to volume of anti-solvent of 1:4 (given the conditions tested in our previous work[11]). Due to the impossibility of precipitating ketoprofen with citric acid aqueous solutions, an aqueous solution of aluminium sulfate at 15 wt% was instead employed in a broader range of ratios (1:4, 1:6, 1:8, 1:10 and 1:12). After the addition of the anti-solvent, a precipitate was formed, which induced a turbidity into the resulting solution. This was then filtrated using syringe filters with the concentration of the target NSAID remaining in solution determined using HPLC-DAD. Triplicates were consistently done,

allowing determining the average isolation efficiencies of each NSAID (IE_{NSAID}, % - Equation 2.8) and the corresponding standard deviations (σ).

$$IE_{NSAID}, \% = 100 - \left(\frac{m_{NSAID}^{Antisolv}}{m_{NSAID}^{T}} \times 100 \right) \quad \textbf{(Equation 2.8)}$$

In Equation 2.8, $m_{NSAID}^{Antisolv}$ and m_{NSAID}^{T} denote the mass of NSAID present in the filtered phase after the addition of the anti-solvent and that initially existing in the top phase, respectively.

NSAIDs stability in ILs and IL-salt aqueous solutions

A protocol for stability assessment was carried based on the OCDE 111e guideline and further applied to the analysis of the impact of the IL structure, media pH, salt presence/absence and temperature of incubation impact on the NSAIDs stability. Four sets of experiments were conducted as described on Table 2.9, always with aqueous solutions composed of 45 wt% of IL, $[C_4C_1im]Cl$, [BzCh]Cl or $[N_{4444}]Cl$. The first three sets comprised aqueous solutions in presence of potassium citrate buffer at pH ≈ 5 or 7 (the same source for preparation guidelines as that aforementioned was consulted[10]) and potassium citrate tribasic monohydrate, representing a pH of circa 9, at 5 wt% of salt composition. These compositions were adopted in order to mimic the IL-rich phase of an ABS. No salt was added in the fourth set of experiments. In all tests, a total of ≈ 3 mg of each NSAID was dissolved in 3 g of aqueous solution, and stirred for 1 hour. Each sample was divided into three portions: one taken at the beginning of experiments without any treatment (St_0) and the remaining two incubated in the dark at 25 or 50 (±1) °C for five days (St_{25} and St_{50}, respectively). At the end, these samples were analyzed by HPLC-DAD following the procedure of filtration previously described, adequate dilution in water:ACN (70:30, v/v) and injection. The relative stability (St_{NSAID}, in percentage) was calculated as the ratio between the NSAID peak areas in St_{25} or St_{50} and that in St_0 sample times 100.

NSAIDs quantification

Similar chromatographic conditions as those reported in our previous work were used.[11] The liquid chromatograph HPLC Elite LaChrom (VWR Hitachi) consisted of a diode

array detector (DAD) l-2455, column oven l-2300, auto-sampler l-2200 and pump l-2130. The analytical column used was purchased from Merck and it was composed of a sorbent LiChrospher 100 RP-18 (5µm) and cartridge LiChroCART 250-4 HPLC-Cartridge. Both the pre-column, in a special holder, and the main column possess the same type of stationary phase. The aqueous phase (A) contained 5 mM of ammonium acetate and was adjusted to pH 4.02 by adding acetic acid. Then, 5% of the ACN was added. Phase A was filtrated using membrane filters and further degassed in an ultrasound bath. The organic phase (B) contained the gradient grade ACN and it was degassed by ultrasonication. The separation was carried out using a gradient elution mode, according to the following program: 0 - 4 min 30% of B, 4-11 min from 30 to 60% of B, 11-18 min 60% of B, 18-21 min from 60 to 30% of B, 21-24 min 30% of B, using flow rate 1 $mL.min^{-1}$. The column temperature was adjusted to 27 ^{o}C and the autosampler to 25 ^{o}C. DAD was set to measure the spectrum from 200 to 400 nm and three specific wavelengths: 230 nm for ibuprofen and 245 or 270 nm for ketoprofen and naproxen depending on the sample type, as detailed in Table C2 from Appendix C. The injection volume was 10 µL or 25 µL if the sample was the top or bottom phase, respectively.

The instrumental validation was based on an external standard method. Two instrumental calibration curves were determined. Stock mixtures of the three NSAIDs at 1 $mg.mL^{-1}$ in ACN, further submitted to serial dilutions, were prepared for validation purpose. Accuracy was determined by comparison of the real concentrations of the NSAIDs and the values determined by the equipment. Precision corresponds to the relative standard deviations between injections. Accuracy and precision were determined in intra- and inter-day modes. The limit of quantification was the lowest concentrations of analytes used in the calibration curves, with a precision < 5 % and accuracy between 80-120%. The limit of detection was established using a signal/noise (S/N) ratio of 3. The quantification method and validation for ibuprofen at the higher concentration range was already reported in a previous work.[11] All the details regarding the validation parameters are shown in Table C2 from Appendix C.

pH measurements

The pH of the potassium citrate buffers and phase A of the HPLC mobile phase were measured using an HI 9321 Microprocessor pH meter equipment (Hanna Instruments) at 25 (±1) ^{o}C and within ± 0.02 pH units.

Results and discussion

The applicability of IL-based TPP systems to the purification of ketoprofen, ibuprofen and naproxen from pharmaceutical wastes was here studied. Firstly, an optimization study using commercial standards of each NSAID and testing the parent IL-based ABS was carried out. Then, the capability to directly extract and refine these NSAIDs from real matrices, i.e., solid state pills, in a single step by applying the IL-based TPP was assessed. As previously mentioned, IL-based TPP systems use the same systems as IL-based ABS.[1] Taking this into account, all information on the TLs used in the first part of this work is provided in Table C3 in Appendix C, namely the weight fraction composition (in wt%) of each compound composing the biphasic mixture and the coexisting phases, as well as the TLLs.

The optimization studies were centered on assessing the influence of the ILs nature, temperature, pH and TLL upon the partition of the three NSAIDs in ABS. Three structurally different ionic compounds were tested, [N_{4444}]Cl, [BzCh]Cl and [C_4C_1im]Cl, allowing screening distinct physical, chemical and biological properties. These were selected based on our previous know-how on designing extraction approaches applying ILs[12] to purify drugs.[6, 11] At the same time that the anion structure was kept simplistic offering benefits from an operational and economic point of view, the range of cations elected allows inspecting distinct partition environments (due to their distinct hydrophobic nature).[7] Moreover, and according to the well-established acute toxicity levels,[13] all ILs are non-toxic towards the marine bacteria *Vibrio fischeri* (EC_{50} of 519 mg.L^{-1}, 1498 mg.L^{-1} and 472 mg.L^{-1} for [C_4C_1im]Cl, [BzCh]Cl and [N_{4444}]Cl, respectively[14-16]). Also, all bearing the cheap Cl^- anion and two being quaternary ammonium-based, the ILs here elected may be considered as cost-effective.[17] The highly biodegradable character[10] and wide application in the pharmaceutical industry[18] of citrate-based salts encouraged the citrate buffer use as phase-forming component. Moreover, it was also previously shown that the combined use of this triad of ILs with citrate buffer in aqueous

solution enhanced the solubilization of ibuprofen in water in comparison to water itself, thus yielding good extraction efficiencies.[11] This fact allowed the use of high amounts (i.e., circa 20 mg in 5 g of total mass) of these NSAIDs, which are characterized by a low water solubility ([IBU] = 21 mg L^{-1}; [NAP] = 15.9 mg L^{-1}; [KET] = 51 mg L^{-1} – values at 25 ^{o}C)[19], to perform the partition studies. This was confirmed for all the NSAIDs here tested with experiments performed using the system based on [C_4C_1im]Cl and potassium citrate buffer at pH 7. Actually, for the NSAID amounts tested at circa 1 and 2 mg of each NSAID *per* g of ABS the results yielded similar EE_{NSAID} and R_T values to those obtained at higher NSAIDs content, respectively, 91.9 ± 0.1 % < EE_{KET} < 99 ± 3 %, 90 ± 3 % < EE_{NAP} < 98 ± 2 % and 87 ± 1 % < EE_{IBU} < 98 ± 3 % and R_T > 98.2 ± 0.1 % (cf. Figure 2.17 and Table C4 in Appendix C). This feature overcomes the limitation of ABS application when large amounts of waste are applied and the target active ingredient possesses a low solubility in water. The results exposed and discussed below suggest that it was possible to extract large amounts of NSAIDs, well above their saturation in water, with EE_{NSAID} and R_T higher than 80 % and 97 %, respectively.

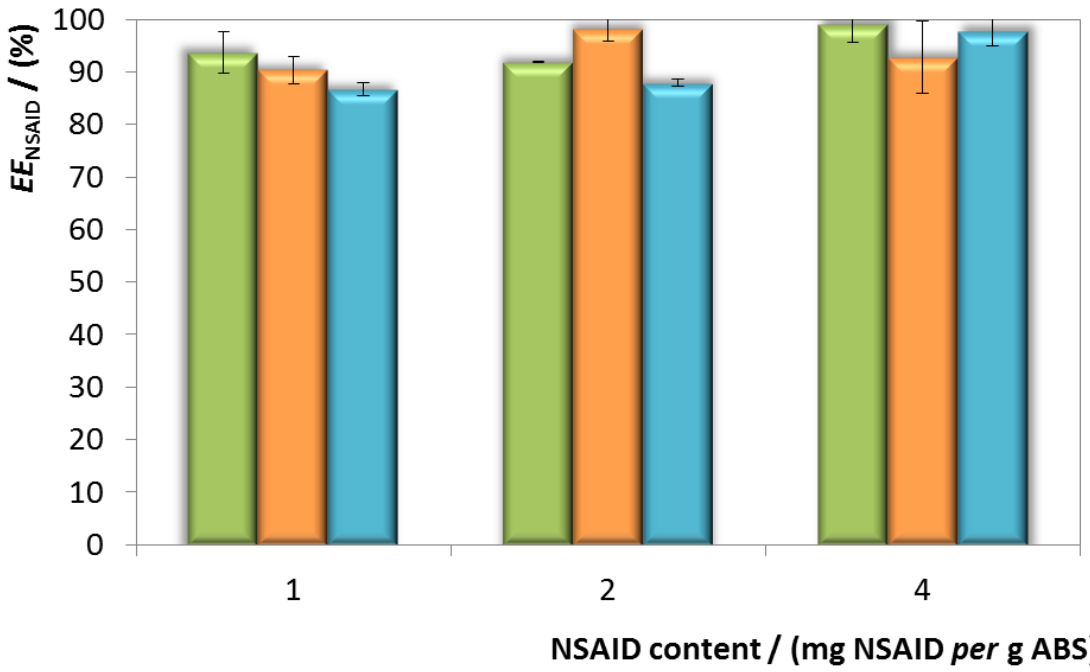

Figure 2.17. Impact of NSAIDs content on the extraction efficiency (EE_{NSAID}, %) of ketoprofen (green bars), naproxen (orange bars) and ibuprofen (blue bars) using ABS composed of 30 wt% of [C_4C_1im]Cl and 30 wt% of potassium citrate buffer at pH 7.

NSAIDs partition studies using IL-based ABS

The parameters determined to evaluate the extraction performance of the IL-salt ABS employed, namely the extraction efficiency for each NSAID (EE_{NSAID}, %) and the recovery towards the top phase (R_T, %) are reliable indicators to measure the success of the process here developed. The graphical representation of the relationship between EE_{NSAID} calculated for the three NSAIDs and distinct IL-based ABS are depicted in Figure 2.18, while the detailed numerical results, for both EE_{NSAID} and R_T, are given in Table C5 in Appendix C. In general, EE_{NSAID} values were higher than 80 %, showing the capacity of the studied IL-salt-based ABS to concentrate the NSAID in just one phase. In fact, the EE_{NSAID} vary from 90 ± 10 % to 100 %, 85 ± 6 % to 93 ± 7 %, and 89 ± 8 % to 98 ± 3 %, for ketoprofen, naproxen and ibuprofen, respectively.

The partition in these IL-based ABS results from a complex set of interactions between the NSAIDs and the phase-forming components, i.e., the interactions of *"NSAIDs-ILs"*, *"NSAIDs-citrate"* and/or *"NSAIDs-water".* At first glance, the preferential migration of the NSAIDs to the top (IL-rich) phase can be easily explained by their octanol-water partition coefficient values – Log P (3.97 for ibuprofen, 3.12 for ketoprofen and 3.18 for naproxen).[20] These parameters indicate the NSAIDs affinity for more hydrophobic environments (log P > 0). Hydrophobic interactions were shown to play a significant role in the partition behaviour of other molecules in IL-based ABS, namely proteins[21, 22] and other drugs.[23, 24] This tendency is corroborated by recoveries to the top phase higher than 98.7 ± 0.7 % for all NSAIDs (Table C5 in the Appendix C). Actually, these pharmaceutical active ingredients have similar structures and characteristics leading to similar extraction efficiencies using any of the IL-salt-based ABS under investigation.

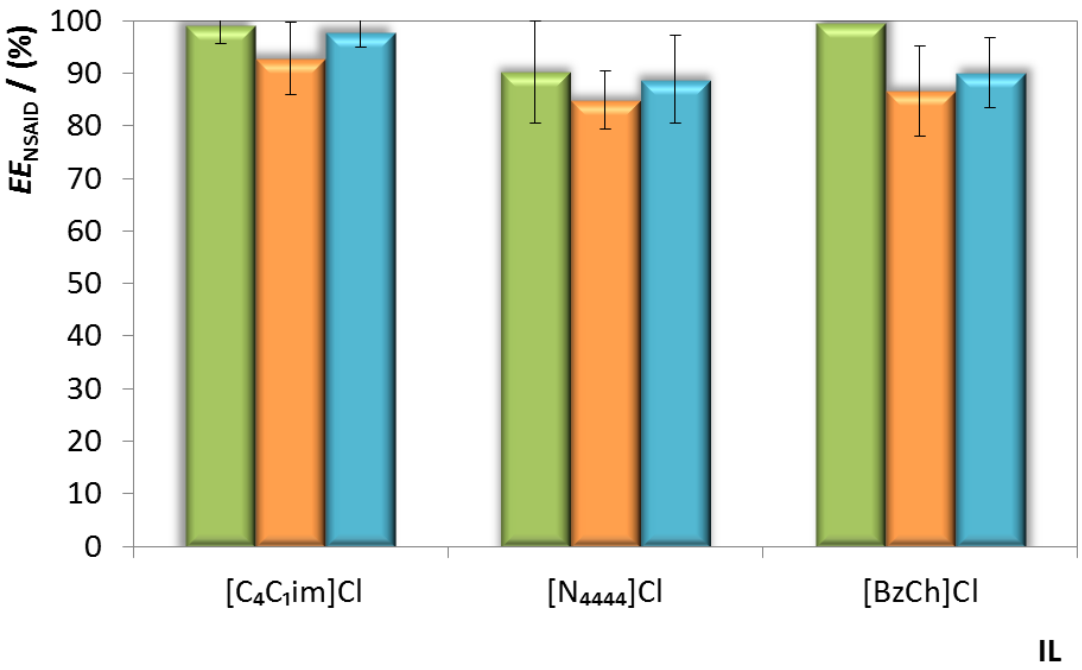

Figure 2.18. Impact of IL structure on the extraction efficiency (EE_{NSAID}, %) of ketoprofen (green bars), naproxen (orange bars) and ibuprofen (blue bars) using ABS composed of 30 wt% or 35 wt% of IL and 30 wt% of potassium citrate buffer.

In order to gain further details on the operational conditions affecting the extraction of NSAIDs using IL-based ABS, temperature, pH and TLL were also studied. As all IL-based ABS evaluated yielded similar performances, the system containing $[C_4C_1im]Cl$ was considered to assess the impact of such conditions. Figures 2.19 to 2.21 show the effects obtained for the extraction efficiencies of the three NSAIDs, being the detailed numerical data presented in Tables C6 to C8 in Appendix C. The conclusion emerging from the results obtained reveals that temperature, pH and TLL, although having distinct effects on the migration of NSAIDs in $[C_4C_1im]Cl$-based ABS, do not drastically influence their migration affinity, as represented by the data of $EE_{NSAID} > 80 \pm 3$ % and $R_T > 97.4 \pm 0.9$ %.

Temperature, varied between 15 °C and 45 °C with intervals of 10 °C, was shown to have a marginal effect on the extraction of ibuprofen, ketoprofen and naproxen (cf. Figure 2.19 and Table C6 in Appendix C). A diversified scenario is found in literature, where the temperature may lead to either null (as here) or significant (positive/negative) impacts on the extraction performance of IL-based ABS depending on the operational

conditions under study (e.g., IL, target molecule, phase formers pair, among others).[25-29] Due to the negligible temperature impact found and the possibility of minimizing energetic and operational costs, the room temperature was further maintained.

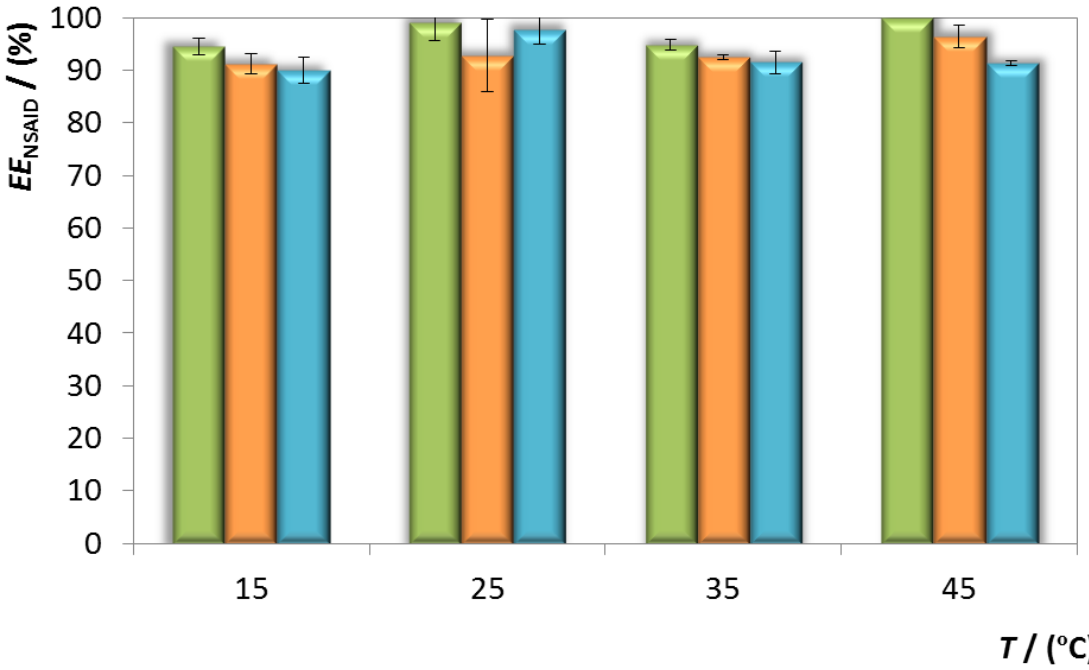

Figure 2.19. Impact of temperature on the extraction efficiency (EE_{NSAID}, %) of ketoprofen (green bars), naproxen (orange bars) and ibuprofen (blue bars) using ABS composed of 30 wt% of $[C_4C_1im]Cl$ and 30 wt% of potassium citrate buffer.

The pH effect was also evaluated by selecting potassium citrate buffer at pH 7 and 8 along with potassium citrate tribasic at pH ≈ 9. A wider range of pH was not studied due to the weak ability of the $[C_4C_1im]Cl$-based ABS to undergo phase separation at pH lower than 7.[30] It is well-known that electrostatic interactions triggered by pH changes may display significant impacts in the partition of ionizable solutes, allowing the control of their migration patterns.[31-34] However, this profile is highly dependent on the molecules addressed, in particular for NSAIDs, as unveiled by Almeida et al.[35, 36] Using IL-based ABS containing either aluminium sulphate (pH ≈ 2.4 – 2.9) or potassium citrate tribasic (pH ≈ 9), the authors showed that regardless of the pH, a major partition of the NSAIDs to the most hydrophobic (IL-rich) phase occurs. So, the same happened in this work, for which the preferential migration of the NSAIDs to the IL-rich phase was constantly observed

(EE_{NSAID} > 85 ± 4 % and R_T > 98.7 ± 0.7 %). As depicted in Figure 2.20 (detailed data is presented in Appendix C as Table C7), higher pH values lead to slightly poorer extraction efficiencies, mostly when potassium citrate tribasic (pH ≈ 9) is used. Since the charge of the three NSAIDs is kept constant and negative within the pH range evaluated, no major differences are observed for the migration of NSAIDs to the IL-rich phase (99 ± 3 % > EE_{KET} > 89.1 ± 0.8 %; 93 ± 7 % > EE_{NAP} > 86.5 ± 0.6 % and 98 ± 3 % > EE_{IBU} > 85 ± 4 %). Considering the 10% of maximum variation of the extraction efficiency values, pH 7 was maintained in further studies.

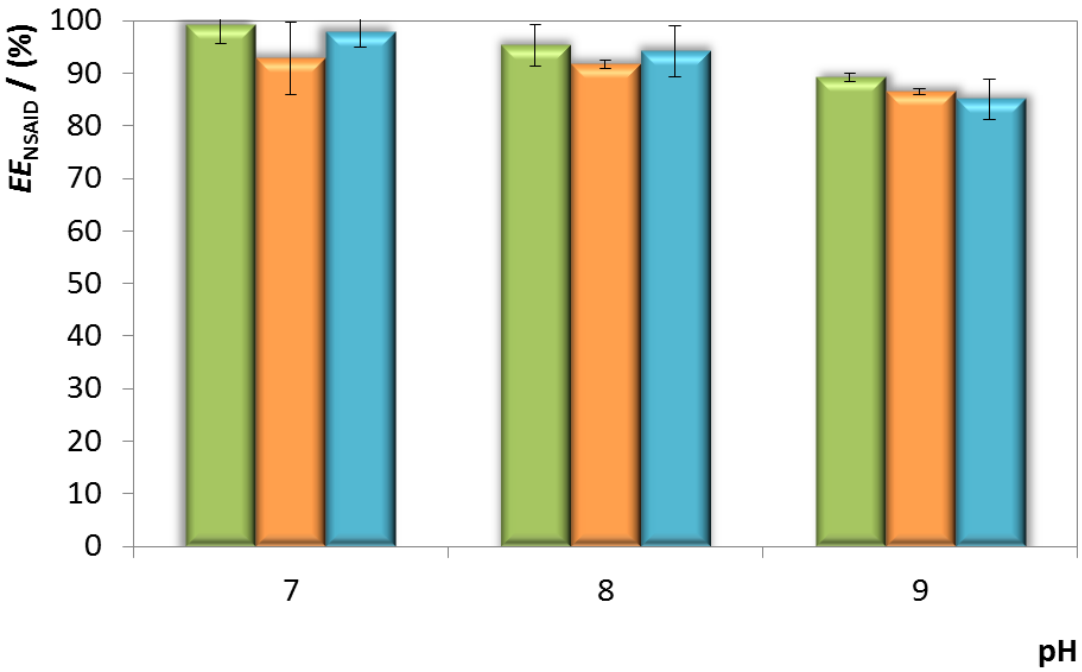

Figure 2.20. Impact of pH on the extraction efficiency (EE_{NSAID}, %) of ketoprofen (green bars), naproxen (orange bars) and ibuprofen (blue bars) using ABS composed of 30 wt% of $[C_4C_1im]Cl$ and 30 wt% of potassium citrate buffer (pH 7 and pH 8) or potassium citrate tribasic salt (pH ≈9).

Finally, the TLL influence on the NSAIDs partition was assessed by varying the compositions of $[C_4C_1im]Cl$ and potassium citrate buffer at pH 7 (30 wt%/30 wt%, 33 wt%/28 wt% and 35 wt%/26.5 wt%). The shortest the TLL is, the lowest are the amounts of IL and salt present in both phases and the highest are the water contents (cf. Table C3 in Appendix C). The evaluation of such a parameter allowed inferring on the role of $[water]_T$ on the NSAIDs partition. By increasing the TLL, under the conditions tested (IL =

[C_4C_1im]Cl, salt = potassium citrate buffer, NSAID content = 4 mg *per* g of ABS, pH = 7 and *T* = 25 °C), circa 20% decline in the NSAIDs extraction efficiency was verified. In other words, the higher the $[water]_T$, the higher the EE_{NSAID} (99 ± 3 % > EE_{KET} > 85 ± 3 %, 93 ± 7 % > EE_{NAP} > 83 ± 3 % and 98 ± 3 % > EE_{IBU} > 80 ± 3 %) – see Figure 2.21 (the detailed data is also presented in Appendix C as Table C8). This allowed concluding that slightly lower amounts of IL can be used to maximize the recovery of the NSAIDs.

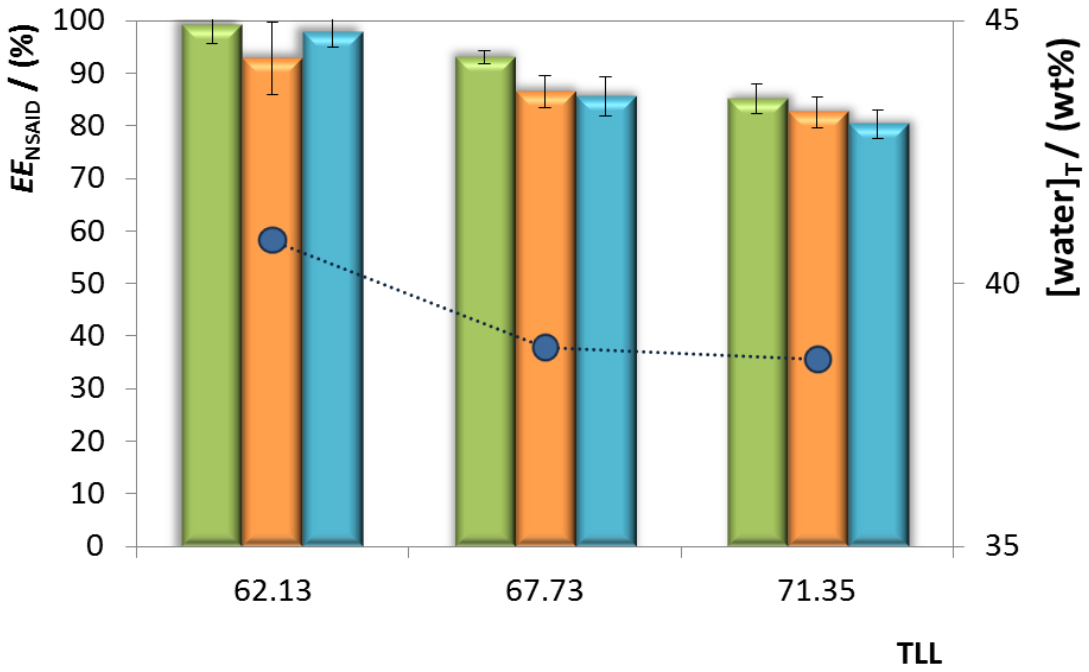

Figure 2.21. Impact of TLL on the extraction efficiency (EE_{NSAID}, %) of ketoprofen (green bars), naproxen (orange bars) and ibuprofen (blue bars) using ABS composed of variable amounts of [C_4C_1im]Cl and potassium citrate buffer at pH 7. The weight fraction of water present in the top phase ($[water]_T$, wt%) is also shown (circles connected by the dashed line).

Insights into the stability of NSAIDs in IL- and IL-salt-based aqueous matrices

In a scenario where three NSAIDs are successfully extracted and recovered from wastes to be further used for other applications, their chemical stability is a matter of great concern to assure the quality of the final product. It should therefore be assumed that the chemical environment afforded by the IL enriched (top) phase, i.e., a milieu made of IL and water bearing tiny amounts of citrate buffer salt (Table C3 in Appendix C), must

guarantee no degradation or by-product formation. Actually, if in the case of biomolecules such as proteins, their greater susceptibility to stability or activity losses prompts detailed studies,[22, 37-39] in the case of simpler and synthetic molecules this issue has been disregarded. In this sense, a stability protocol adapted from the OECD guidelines was used to test the NSAIDs stability. This test was adopted due to its simplicity and adequacy of the parameters (temperature, energy, UV radiation and pH) evaluated, when compared with other possible options, e.g., Stability Testing of Active Substances and Pharmaceutical Products from the World Health Organization (WHO) or the Q1A(R2) Stability Testing of New Drug Substances and Products from the Food and Drugs Administration (FDA). The protocol used in this work was compared with the original from OECD (111e) in Table C9 in Appendix C, thus leading to a simpler way of determining the chemicals stability in aqueous matrices of ILs. Taking into account the TLs determined (Table C3 in Appendix C) aqueous solutions containing 45 wt% of each IL and 5 wt% of salt were used to mimic the top phase environment allowing a direct comparison between systems. Bringing together the four sets of experiments it was possible to carefully assess the impact of IL structure, pH, salt and temperature of incubation on the NSAIDs stability.

The mean values of relative stability with standard deviations for the three NSAIDs under all the described conditions are reported in Table 2.9. It is clear that the set of NSAIDs did not lose stability during the five days of experiments, independently of their chemical structure, IL structure, pH, temperature or salt presence. Remarkable stability values consistently higher than 93.4 ± 0.1 % were achieved.

In spite of the limited solubility of these NSAIDs in water, the results obtained attest their stability in this solvent. This results from the fact that their simple structure lacks easily dissociated functional groups, e.g., esters and amides.[40] Furthermore, ketoprofen was proven to be more stable in neutral than in acidic conditions,[41] whilst ibuprofen was prone to lose its stability only in acidic conditions.[42] This evidence may explain the slight loss of stability of ibuprofen in presence of potassium citrate buffer at pH 5with $[N_{4444}]Cl$ (cf. Table 2.9). These results point IL-salt-based ABS as mild routes for the extraction of these NSAIDs from pharmaceutical wastes, contrarily to what is being

reported in literature about the photo-, bio- and ultrasonic degradation of naproxen, ibuprofen and ketoprofen.[43-50]

NSAIDs recovery from pharmaceutical wastes using IL-based TPP

IL-based ABSs exhibited a very good ability to extract the three target NSAIDs while preserving their chemical stability. They will thus serve as useful tools to conceptualize an integrated process of NSAIDs purification envisaging the pharmaceutical wastes valorization. Based on a similar approach to that followed by IL-based ABS, TPP constituted by the same triad of neoteric solvents were further employed as a way of simultaneously extracting NSAIDS (IL-rich phase) and separating the excipients (interface). The extraction in a one-step by IL-based TPP was attempted (***step 1***), and an anti-solvent-like isolation strategy for the three drugs was further investigated (***step 2***). Figure 2.22 provides a schematic representation of the conceptual process proposed. Although not studied in the present work, the recycling and reuse of both ABS components and anti-solvents (***step 3***) was also represented as it is considered essential for the economic and environmental sustainability of the process.[51, 52]

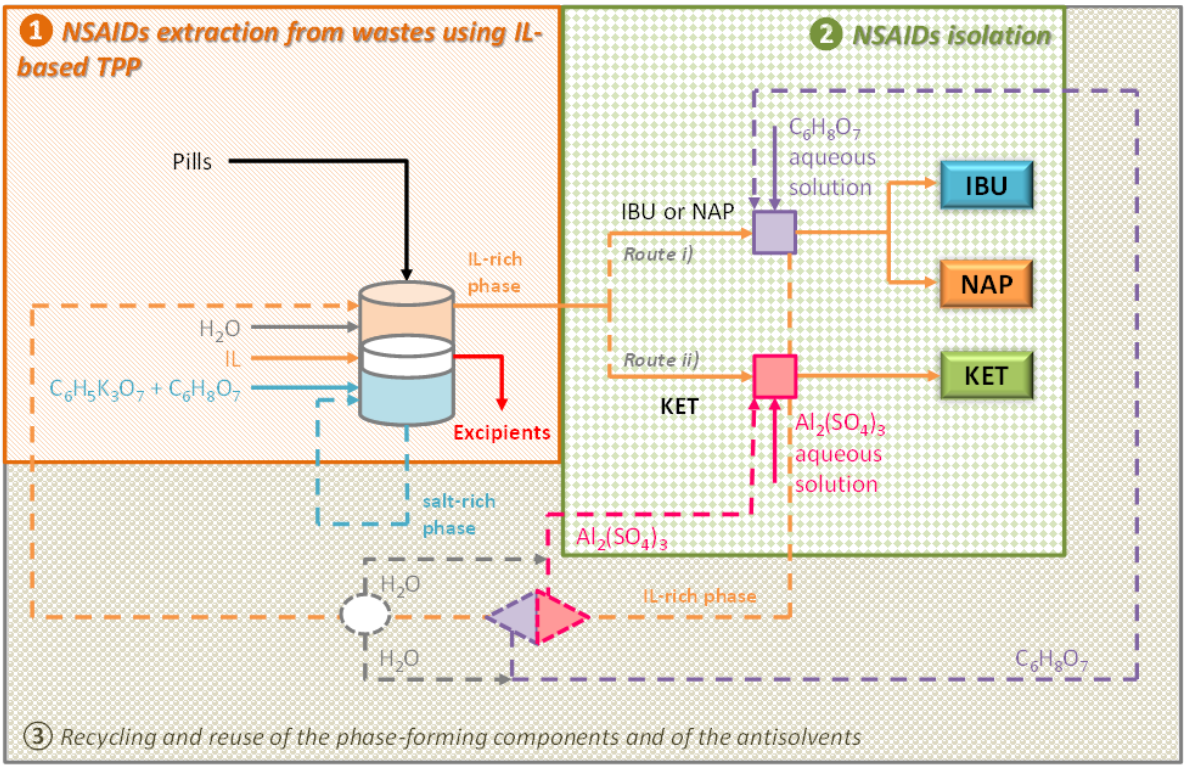

Figure 2.22. Schematic representation of the integrated process of NSAIDs purification (step 1) and isolation (step 2), including a hypothetical recycling of both the ABS components and the anti-solvents employed (step 3). Route i) represents the approach adopted for ibuprofen and naproxen isolation while Route ii) depicts the strategy developed for the ketoprofen isolation. Dashed lines were used for the hypothetical routes of recycling and reusing the solvents and anti-solvents.

Table 2.9. Mass fraction compositions (in wt%) of the matrices adopted to study the stability of the three NSAIDs along with the conditions tested and percentage stabilities (St_{NSAID}, %) plus the corresponding standard deviations (σ).

IL	Salt	[IL] / (wt%)	[Salt] / (wt%)	[water] / (wt%)	*T* (±1) / (°C)	St_{IBU} / (%)	St_{NAP} / (%)	St_{KET} / (%)
1st set								
$[C_4C_1im]Cl$	Potassium citrate buffer (pH 5)	45	5	50	25	100	100	100
					50	100	98.2 ± 0.8	100
$[N_{4444}]Cl$		45	5	50	25	98 ± 1	99 ± 3	100
					50	93.4 ± 0.1	100	100
[BzCh]Cl		45	5	50	25	100	100	100
					50	100	99 ± 3	99 ± 2
2nd set								
$[C_4C_1im]Cl$	Potassium citrate buffer (pH 7)	45	5	50	25	100	100	99 ± 3
					50	99.8 ± 0.7	99.8 ± 0.2	99 ± 4
$[N_{4444}]Cl$		45	5	50	25	97 ± 2	99 ± 2	99 ± 2
					50	98 ± 1	100	100
[BzCh]Cl		45	5	50	25	100	99 ± 2	100
					50	100	98 ± 2	99 ± 2
3rd set								
$[C_4C_1im]Cl$	Potassium citrate tribasic (pH ≈ 9)	45	5	50	25	100	99 ± 4	99 ± 2
					50	99.2 ± 0.9	99 ± 4	98 ± 4
$[N_{4444}]Cl$		45	5	50	25	100	99 ± 1	100
					50	98 ± 1	97.3 ± 0.3	100
[BzCh]Cl		45	5	50	25	100	98 ± 3	100

					50	100	96 ± 4	100
4th set								
$[C_4C_1im]Cl$		45	0	55	25	100	100	100
					50	100	100	100
$[N_{4444}]Cl$	-	45	0	55	25	100	99 ± 3	99.4 ± 0.3
					50	99 ± 2	100	100
[BzCh]Cl		45	0	55	25	100	100	100
					50	100	100	100

Step 1: Application of IL-based TPP systems to purify the NSAIDs. The results presented in Figure 2.23 (for more details see Table C10 in Appendix C) pinpoint the remarkable performance of IL-based TPP in the single-step extraction and purification of ibuprofen, ketoprofen and naproxen from their pharmaceutical matrices. Despite the slightly less effective extraction efficiencies obtained from the solid state pills when compared with those obtained with the model systems (cf. Figure 2.18), it should be pointed out that successful performances were also attained using the IL-based TPP systems ($EE_{NSAID} \geq 84 \pm 8$ %). R_T values higher than 97.8 ± 0.3% (Table C10 in the Appendix C) corroborate such evidence. However, it should be noticed that EE_{NSAID} values lower than 100 % do not necessarily indicate the preferential NSAIDs partition between phases, but may represent some losses of the drugs to the excipient-rich interface formed. In this work, no significant interferences were detected, due to the nature of the excipients present in the pills and the conditions defined for the quantification method. As examples, the ethyl phthalate composing the pill containing ketoprofen (Table C1 in Appendix C) was checked in the top (IL-rich) phase, and its presence was not detected in the chromatograms. The cellulose-derivative excipients, despite their potential dissolution by ILs[53], were also eliminated as contaminants because at 25 ^{o}C (the temperature of the extraction process), ILs may only cause the cellulose to be wet.[54] Finally, the titanium dioxide that, despite its high affinity for ILs (or top-IL-rich phase),[55] has a limited solubility in water and was also discarded as main contaminant. Thus, the main bulk of excipients settle in the interface due to its low-solubility in the water/aqueous phases of ABS.

The design of these IL-based TPP systems allowed the purification of each NSAID under study by the exclusion of the excipients that settled on the interface of the IL-salt-based ABS. This allowed the purification of ketoprofen, ibuprofen and naproxen in a single-step. These results suggest that IL-salt-based TPP systems are a suitable approach for the recovery of active ingredients from pharmaceutical wastes.

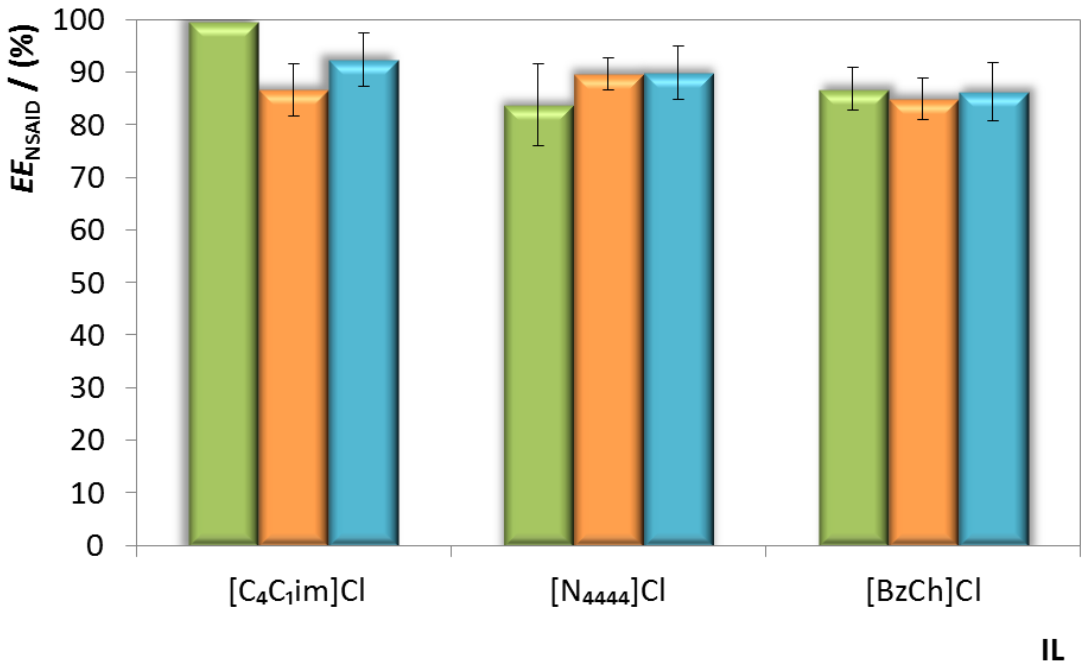

Figure 2.23. Results obtained for the extraction efficiency (EE_{NSAID}, %) of ketoprofen (green bars), naproxen (orange bars) and ibuprofen (blue bars) from pharmaceutical pills using IL-based TPP systems composed of 30 or 35 wt % IL and 30 wt% potassium citrate buffer.

Step 2: Isolation of NSAIDs from IL-salt-based ABS through precipitation with anti-solvents. High extraction performances were obtained when the separation of the three NSAIDs from the real waste-based matrix was attempted. Envisaging the industrial potential of this process, an isolation strategy to remove the phase formers was defined. Precipitation through the addition of an anti-solvent was the approach selected due to its simple operation and scalability.[56] Although equivalent extraction parameters were gauged, the ABS composed of $[C_4C_1im]Cl$ was selected as the most efficient (cf. Figure 2.23). Due to the distinct solubility in water of each NSAID,[19] specific precipitation agents were selected. The results are represented in Figure 2.24 and in Table C11 in Appendix C (mean values and standard deviations). Initially, citric acid aqueous solutions at 25 wt% were selected as the ideal anti-solvent due to the good isolation results attained of 79 ± 2 % and 79 ± 3 % for ibuprofen and naproxen, respectively. Moreover, using this anti-solvent, the introduction of additional species was avoided, which simplifies the process.[11] It seems here that the combined action of water and citric acid is ruling the

precipitation phenomena: if on one hand both ibuprofen and naproxen are practically insoluble in water,[19] on the other hand both are acidic drugs (pKa of 4.91 for ibuprofen and 4.15 for naproxen[20]) having their solubility enhanced at higher pH values due to ionization.[57, 58]

Since ketoprofen did not precipitate in the same conditions, it was necessary to develop a different strategy for its isolation. Aluminium sulphate aqueous solutions were studied and a broader range of top phase and anti-solvent volume ratios was tested, namely 1:4, 1:6, 1:8, 1:10 and 1:12. The reason behind this choice was the strong "salting-out" effect and high acidic character of this salt.[59] It was confirmed to work well as a precipitation agent leading to isolation efficiencies from 76 ± 2 % to 87.9 ± 0.3 %, depending of the volume of anti-solvent added. Besides the ketoprofen limited solubility in water and pKa value (4.45[20]), changes in the ionic strength and species in the media by the introduction of aluminium sulphate also hampered the "*ketoprofen-IL-citrate buffer-water*" interactions thus leading to ketoprofen precipitation. This result is in agreement with that observed for the isolation of ibuprofen from an IL + citrate buffer aqueous solution by the addition of potassium chloride.[11] Important to be highlighted is the fact that the NSAIDs content remaining in solution (21 % of either ibuprofen or naproxen and around 12 % of ketoprofen) after the precipitation could be recycled to ***step 1***. The target NSAID content at the feed stream will enlarge, thus improving the isolation in ***step 2*** up to a point where the amount of NSAID is the same as that recovered in each cycle.

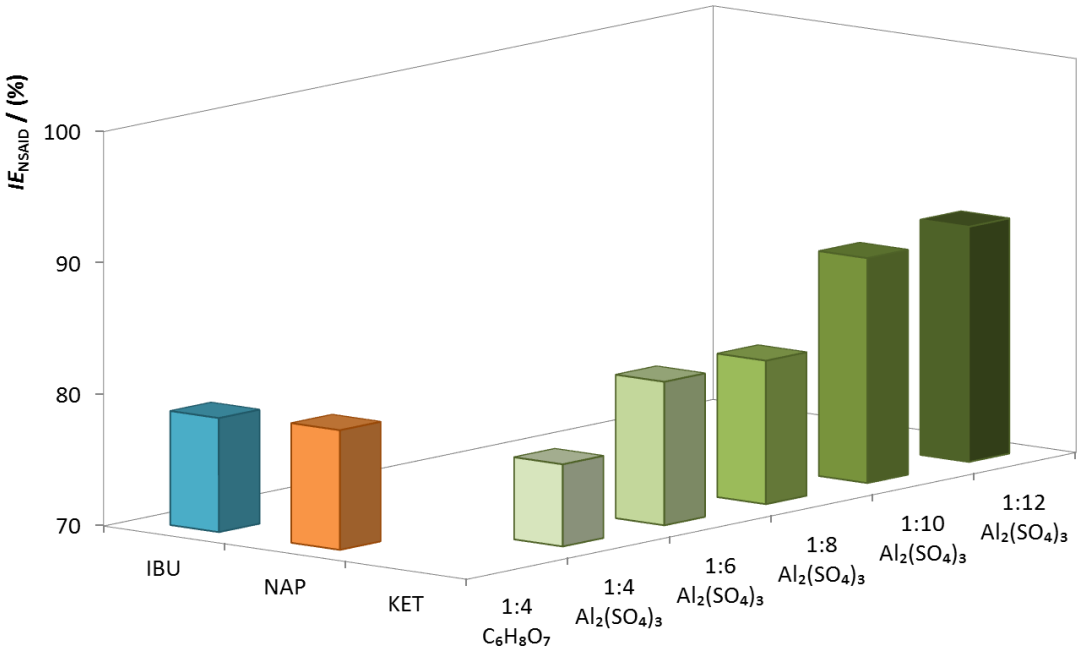

Figure 2.24. Results obtained for the isolation efficiency (IE_{NSAID}, %) of each NSAID using distinct anti-solvents.

The process herein conceptualized (Figure 2.22) represents another step towards the creation of a set of effective technologies for the recovery of NSAIDs from pharmaceutical matrices. The sustainability of the proposed process is promising when compared to others reported in literature. Some processes were suggested aimed at recovering naproxen,[60] ketoprofen[61] and ibuprofen[62] from pharmaceutical formulations, e.g., suppositories, topical creams and tablets. Even though speeding up the recovery process, the use of microwave-assisted methods (e.g., microwave irradiation of 2450 MHz)[60, 61] and/or high temperatures (≥ 35 °C,[62] 65 °C[61] and 70 °C[60]) generate high energetic inputs. In all three works, the use of volatile organic solvents, such as methanol,[60] acetone[61] and alkanes[62] as part of the extraction solvent constrained the safety and benignity of the processes developed. Instead, in this work, volatile organic solvents were replaced by benign ILs in aqueous environment with no additional energetic costs arising from neither irradiation nor heating. Yet, the use of ILs as a way to improve the green credentials of NSAIDs processing is not new. 1-ethyl-3-methylimidazolium bis(trifluoromethanesulfonyl)imide for example, further abbreviated

as [C_2mim][NTf_2], was evaluated as a crystallization solvent for ibuprofen and naproxen.[63] [C_2mim][NTf_2] was able to solubilize naproxen at elevated temperatures (≈ 125 °C), while failing to solubilize ibuprofen independently of the temperature used.[63] Recently, our group developed a simple process to recover ibuprofen,[11] replacing the use of volatile organic solvents by an IL aqueous solution and operating under ambient conditions. However, this approach is not the most adequate when more complex waste mixtures/solutions are used and, consequently, when more than one active ingredient needs to be simultaneously recovered and separated from the excipients. Compared to the process developed in the present work, and also some other previously published by us,[11] such approaches are not as flexible as ours for the different NSAIDs, require more expensive and less biocompatible ILs and utilize harsh temperature/pressure conditions.

Conclusions

An alternative approach for the purification of three NSAIDs, namely ibuprofen, naproxen and ketoprofen, was here designed by applying IL-based TPP systems. Three steps were contemplated in the conceptual integrated process proposed: a ***step 1*** of extraction and purification of the target drugs using IL-based TPP systems, a ***step 2*** aimed at the isolation (i.e., polishing) of each target compound by anti-solvent induced precipitation, and a ***step 3*** of recycling and reuse of the solvents employed. After the ***step 1*** of optimization using pure standards, where ABS composed of ILs and the potassium citrate buffer revealed a very good capability to extract the three NSAIDs (80 ± 3 % < EE_{NSAID} < 100 %), IL-based ABS were transformed into TPP systems allowing the interfacial separation of the main contaminants (i.e., pills' excipients). A single-step purification process was proposed with extraction efficiencies on the range (84 ± 8 % < EE_{NSAID} < 100 %). The isolation of each of three NSAIDs was attempted by precipitation with anti-solvents. Two distinct strategies were outlined: one for naproxen and ibuprofen using citric acid aqueous solutions (to maintain the species in solution) and other for ketoprofen isolation employing aluminium sulphate aqueous solutions. Isolation efficiencies higher 76 ± 2 % were attained with the possibility of the phases being recycled to ***step 1***. Additionally, problems associated with possible stability losses in IL-rich media were mitigated, since ibuprofen, ketoprofen and naproxen have been proven

to be stable in these processing conditions. A sustainable and efficient alternative route for the recovery of drugs from pharmaceutical wastes transversal to other active ingredients was developed in this work, opening the opportunity for further application to more complex systems or matrices other than pills.

References

[1] Alvarez-Guerra, E.; Irabien, A. Ionic Liquid-Based Three Phase Partitioning (ILTPP) for Lactoferrin Recovery. *Separation Science and Technology* **2014,** *49* (7), 957-965.

[2] Przybycien, T. M.; Pujar, N. S.; Steele, L. M. Alternative bioseparation operations: life beyond packed-bed chromatography. *Current Opinion in Biotechnology.* **2004,** *15* (5), 469-478.

[3] Alvarez-Guerra, E.; Irabien, A. Ionic liquid-based three phase partitioning (ILTPP) systems for whey protein recovery: ionic liquid selection. *Journal of Chemical Technology and Biotechnology* **2015,** *90* (5), 939-946.

[4] Alvarez-Guerra, E.; Ventura, S. P. M.; Coutinho, J. A. P.; Irabien, A. Ionic liquid-based three phase partitioning (ILTPP) systems: Ionic liquid recovery and recycling. *Fluid Phase Equilibria.* **2014,** *371*, 67-74.

[5] Wu, H.; Yao, S.; Qian, G.; Yao, T.; Song, H. A resolution approach of racemic phenylalanine with aqueous two-phase systems of chiral tropine ionic liquids. *Journal of Chromatography A* **2015,** *1418*, 150-157.

[6] e Silva, F. A.; Sintra, T.; Ventura, S. P. M.; Coutinho, J. A. P. Recovery of paracetamol from pharmaceutical wastes. *Separation and Purification Technology* **2014,** *122*, 315-322.

[7] Sintra, T. E.; Cruz, R.; Ventura, S. P. M.; Coutinho, J. A. P. Phase diagrams of ionic liquids-based aqueous biphasic systems as a platform for extraction processes. *Journal of Chemical Thermodynamics* **2014,** *77*, 206-213.

[8] Passos, H.; Trindade, M. P.; Vaz, T. S. M.; da Costa, L. P.; Freire, M. G.; Coutinho, J. A. P. The impact of self-aggregation on the extraction of biomolecules in ionic-liquid-based aqueous two-phase systems. *Separation and Purification Technology* **2013,** *108*, 174-180.

[9] Merchuk, J. C.; Andrews, B. A.; Asenjo, J. A. Aqueous two-phase systems for protein separation: Studies on phase inversion. *Journal of Chromatography B Biomedical Sciences and Applications* **1998,** *711* (1–2), 285-293.

[10] Zafarani-Moattar, M. T.; Hamzehzadeh, S. Partitioning of amino acids in the aqueous biphasic system containing the water-miscible ionic liquid 1-butyl-3-methylimidazolium bromide and the water-structuring salt potassium citrate. *Biotechnology Progress* **2011,** *27* (4), 986-997.

[11] e Silva, F. A.; Caban, M.; Stepnowski, P.; Coutinho, J. A. P.; Ventura, S. P. M. Recovery of ibuprofen from pharmaceutical wastes using ionic liquids. *Green Chemistry* **2016,** *18* (13), 3749-3757.

[12] Freire, M. G.; Cláudio, A. F. M.; Araújo, J. M. M.; Coutinho, J. A. P.; Marrucho, I. M.; Lopes, J. N. C.; Rebelo, L. P. N. Aqueous biphasic systems: a boost brought about by using ionic liquids. *Chemical Society Reviews* **2012,** *41* (14), 4966-4995.

[13] http://www.unece.org/fileadmin/DAM/trans/danger/publi/ghs/ghs_rev01/English/04e_part4.pdf (accessed Nov 6, 2017).

[14] Muñoz, M.; Domínguez, C. M.; de Pedro, Z. M.; Quintanilla, A.; Casas, J. A.; Ventura, S. P. M.; Coutinho, J. A. P. Role of the chemical structure of ionic liquids in their ecotoxicity and reactivity towards Fenton oxidation. *Separation and Purification Technology* **2015,** *150*, 252-256.

[15] Ventura, S. P. M.; e Silva, F. A.; Gonçalves, A. M. M.; Pereira, J. L.; Gonçalves, F.; Coutinho, J. A. P. Ecotoxicity analysis of cholinium-based ionic liquids to Vibrio fischeri marine bacteria. *Ecotoxicology and Environmental Safety* **2014,** *102*, 48-54.

[16] Stolte, S.; Matzke, M.; Arning, J.; Boschen, A.; Pitner, W.-R.; Welz-Biermann, U.; Jastorff, B.; Ranke, J. Effects of different head groups and functionalised side chains on the aquatic toxicity of ionic liquids. *Green Chemistry* **2007,** *9* (11), 1170-1179.

[17] Passos, H.; Freire, M. G.; Coutinho, J. A. P. Ionic liquid solutions as extractive solvents for value-added compounds from biomass. *Green Chemistry* **2014,** *16* (12), 4786-4815.

[18] Bastin, R. J.; Bowker, M. J.; Slater, B. J. Salt Selection and Optimisation Procedures for Pharmaceutical New Chemical Entities. *Organic Process Research & Development* **2000,** *4* (5), 427-435.

[19] Pubchem, Open Chemistry Database - https://pubchem.ncbi.nlm.nih.gov/ (accessed Jan 20, 2018).

[20] DrugBank, Drug and Drug Target database - http://www.drugbank.ca/ (accessed Jan 7, 2016).

[21] Wu, C.; Wang, J.; Li, Z.; Jing, J.; Wang, H. Relative hydrophobicity between the phases and partition of cytochrome-c in glycine ionic liquids aqueous two-phase systems. *Journal of Chromatography A* **2013,** *1305*, 1-6.

[22] Pei, Y.; Wang, J.; Wu, K.; Xuan, X.; Lu, X. Ionic liquid-based aqueous two-phase extraction of selected proteins. *Separation and Purification Technology* **2009,** *64* (3), 288-295.

[23] Zawadzki, M.; e Silva, F. A.; Domańska, U.; Coutinho, J. A. P.; Ventura, S. P. M. Recovery of an antidepressant from pharmaceutical wastes using ionic liquid-based aqueous biphasic systems. *Green Chemistry* **2016,** *18* (12), 3459–3670.

[24] Jiang, Y.; Xia, H.; Guo, C.; Mahmood, I.; Liu, H. Phenomena and Mechanism for Separation and Recovery of Penicillin in Ionic Liquids Aqueous Solution. *Industrial & Engineering Chemistry Research* **2007,** *46* (19), 6303-6312.

[25] Cláudio, A. F. M.; Freire, M. G.; Freire, C. S. R.; Silvestre, A. J. D.; Coutinho, J. A. P. Extraction of vanillin using ionic-liquid-based aqueous two-phase systems. *Separation and Purification Technology* **2010,** *75* (1), 39-47.

[26] Li, S.; He, C.; Liu, H.; Li, K.; Liu, F. Ionic liquid-based aqueous two-phase system, a sample pretreatment procedure prior to high-performance liquid chromatography of opium alkaloids. *Journal of Chromatography B* **2005,** *826* (1), 58-62.

[27] Du, Z.; Yu, Y.-L.; Wang, J.-H. Extraction of Proteins from Biological Fluids by Use of an Ionic Liquid/Aqueous Two-Phase System. *Chemistry – A European Journal* **2007,** *13* (7), 2130-2137.

[28] He, C.; Li, S.; Liu, H.; Li, K.; Liu, F. Extraction of testosterone and epitestosterone in human urine using aqueous two-phase systems of ionic liquid and salt. *Journal of Chromatography A* **2005,** *1082* (2), 143-149.

[29] Chen, L.-L.; Li, F.-F.; Tan, Z.-J. Chiral separation of α-cyclohexylmandelic acid enantiomers using ionic liquid/salt aqueous two-phase system. *Chemical Papers* **2015,** *69* (11), 1465-1472.

[30] Ferreira, A. M.; Claudio, A. F. M.; Valega, M.; Domingues, F. M. J.; Silvestre, A. J. D.; Rogers, R. D.; Coutinho, J. A. P.; Freire, M. G. Switchable (pH-driven) aqueous biphasic systems formed by ionic liquids as integrated production-separation platforms. *Green Chemistry* **2017,** *19* (12), 2768-2773.

[31] Moody, M. L.; Huddleston, J. G.; Berton, P.; Zhang, J.; Rogers, R. D. The effects of pH on the partitioning of aromatic acids in a polyethylene glycol/dextran aqueous biphasic system. *Separation Science and Technology* **2017,** *52* (5), 843-851.

[32] e Silva, F. A.; Carmo, R. M.; Fernandes, A. P.; Kholany, M.; Coutinho, J. o. A.; Ventura, S. n. P. Using Ionic Liquids to Tune the Performance of Aqueous Biphasic Systems Based on Pluronic L-35 for the Purification of Naringin and Rutin. *ACS Sustainable Chemistry and Engineering* **2017,** *5* (8), 6409-6419.

[33] Cláudio, A. F. M.; Ferreira, A. M.; Freire, C. S. R.; Silvestre, A. J. D.; Freire, M. G.; Coutinho, J. A. P. Optimization of the gallic acid extraction using ionic-liquid-based aqueous two-phase systems. *Separation and Purification Technology* **2012,** *97*, 142-149.

[34] Claudio, A. F. M.; Marques, C. F. C.; Boal-Palheiros, I.; Freire, M. G.; Coutinho, J. A. P. Development of back-extraction and recyclability routes for ionic-liquid-based aqueous two-phase systems. *Green Chemistry* **2014,** *16* (1), 259-268.

[35] Almeida, H. F. D.; Freire, M. G.; Marrucho, I. M. Improved monitoring of aqueous samples by the preconcentration of active pharmaceutical ingredients using ionic-liquid-based systems. *Green Chemistry* **2017,** *19* (19), 4651-4659.

[36] Almeida, H. F.; Marrucho, I. M.; Freire, M. G. Removal of Nonsteroidal Anti-Inflammatory Drugs from Aqueous Environments with Reusable Ionic-Liquid-Based Systems. *ACS Sustainable Chemistry and Engineering* **2017,** *5* (3), 2428-2436.

[37] Taha, M.; e Silva, F. A.; Quental, M. V.; Ventura, S. P. M.; Freire, M. G.; Coutinho, J. A. P. Good's buffers as a basis for developing self-buffering and biocompatible ionic liquids for biological research. *Green Chemistry* **2014,** *16* (6), 3149-3159.

[38] Taha, M.; Quental, M. V.; Correia, I.; Freire, M. G.; Coutinho, J. A. P. Extraction and stability of bovine serum albumin (BSA) using cholinium-based Good's buffers ionic liquids. *Process Biochemistry* **2015,** *50* (7), 1158-1166.

[39] Desai, R. K.; Streefland, M.; Wijffels, R. H.; H. M. Eppink, M. Extraction and stability of selected proteins in ionic liquid based aqueous two phase systems. *Green Chemistry* **2014,** *16* (5), 2670-2679.

[40] Testa, B.; Mayer, J. M., *Hydrolysis in drug and prodrug metabolism*. Wiley-VCH Weinheim, Germany: 2003.

[41] Patil, P.; Wankhede, S.; Chaudhari, P. Stability-indicating HPTLC method for simultaneous determination of Ketoprofen, Methyl Paraben and Propyl Paraben in gel formulation. *Journal of Pharmacy Research* **2013,** *6* (9), 945-953.

[42] Reddy, Y. R.; Kumar, K. K.; Mukkanti, K.; Reddy, M. R. P. RP-UPLC method development and validation for the simultaneous estimation of ibuprofen and famotidine in pharmaceutical dosage form. *Pharmaceutical Methods* **2012,** *3* (2), 57-61.

[43] Marotta, R.; Spasiano, D.; Di Somma, I.; Andreozzi, R. Photodegradation of naproxen and its photoproducts in aqueous solution at 254 nm: A kinetic investigation. *Water Research* **2013,** *47* (1), 373-383.

[44] Jácome-Acatitla, G.; Tzompantzi, F.; López-González, R.; García-Mendoza, C.; Alvaro, J. M.; Gómez, R. Photodegradation of sodium naproxen and oxytetracycline hydrochloride in aqueous medium using as photocatalysts Mg-Al calcined hydrotalcites. *Journal of Photochemistry and Photobiology A: Chemistry* **2014,** *277*, 82-89.

[45] Borràs, E.; Llorens-Blanch, G.; Rodríguez-Rodríguez, C. E.; Sarrà, M.; Caminal, G. Soil colonization by Trametes versicolor grown on lignocellulosic materials: Substrate selection and naproxen degradation. *International Biodeterioration & Biodegradation* **2011,** *65* (6), 846-852.

[46] Im, J.-K.; Boateng, L. K.; Flora, J. R. V.; Her, N.; Zoh, K.-D.; Son, A.; Yoon, Y. Enhanced ultrasonic degradation of acetaminophen and naproxen in the presence of

powdered activated carbon and biochar adsorbents. *Separation and Purification Technology* **2014,** *123*, 96-105.

[47] Martínez, C.; Vilariño, S.; Fernández, M. I.; Faria, J.; L, M. C.; Santaballa, J. A. Mechanism of degradation of ketoprofen by heterogeneous photocatalysis in aqueous solution. *Applied Catalysis B: Environmental* **2013,** *142–143*, 633-646.

[48] Marco-Urrea, E.; Pérez-Trujillo, M.; Cruz-Morató, C.; Caminal, G.; Vicent, T. White-rot fungus-mediated degradation of the analgesic ketoprofen and identification of intermediates by HPLC–DAD–MS and NMR. *Chemosphere* **2010,** *78* (4), 474-481.

[49] Szabó, R. K.; Megyeri, C.; Illés, E.; Gajda-Schrantz, K.; Mazellier, P.; Dombi, A. Phototransformation of ibuprofen and ketoprofen in aqueous solutions. *Chemosphere* **2011,** *84* (11), 1658-1663.

[50] Méndez-Arriaga, F.; Torres-Palma, R. A.; Pétrier, C.; Esplugas, S.; Gimenez, J.; Pulgarin, C. Ultrasonic treatment of water contaminated with ibuprofen. *Water Research* **2008,** *42* (16), 4243-4248.

[51] Mai, N. L.; Ahn, K.; Koo, Y.-M. Methods for recovery of ionic liquids—A review. *Process Biochemistry* **2014,** *49* (5), 872-881.

[52] Ventura, S. P. M.; Coutinho, J. A. P., Toward the Recovery and Reuse of the ABS Phase-Forming Components. In *Ionic-Liquid-Based Aqueous Biphasic Systems: Fundamentals and Applications*, Freire, M. G., Ed. Springer Berlin Heidelberg: Berlin, Heidelberg, 2016; pp 285-315.

[53] Feng, L.; Chen, Z.-l. Research progress on dissolution and functional modification of cellulose in ionic liquids. *Journal of Molecular Liquids* **2008,** *142* (1–3), 1-5.

[54] Swatloski, R. P.; Spear, S. K.; Holbrey, J. D.; Rogers, R. D. Dissolution of Cellose with Ionic Liquids. *Journal of the American Chemical Society* **2002,** *124* (18), 4974-4975.

[55] Amjadi, M.; Samadi, A. Modified ionic liquid-coated nanometer TiO2 as a new solid phase extraction sorbent for preconcentration of trace nickel. *Colloids and Surfaces A: Physicochemical and Engineering Aspects* **2013,** *434*, 171-177.

[56] Beckmann, W., *Crystallization: Basic Concepts and Industrial Applications*. John Wiley & Sons: 2013.

[57] Rivera-Leyva, J. C.; García-Flores, M.; Valladares-Méndez, A.; Orozco-Castellanos, L. M.; Martínez-Alfaro, M. Comparative Studies on the Dissolution Profiles of Oral Ibuprofen Suspension and Commercial Tablets using Biopharmaceutical Classification System Criteria. *Indian Journal of Pharmaceutical Sciences* **2012,** *74* (4), 312-318.

[58] Bolten, D.; Lietzow, R.; Türk, M. Solubility of Ibuprofen, Phytosterol, Salicylic Acid, and Naproxen in Aqueous Solutions. *Chemical Engineering and Technology* **2013,** *36* (3), 426-434.

[59] Neves, C. M. S. S.; Freire, M. G.; Coutinho, J. A. P. Improved recovery of ionic liquids from contaminated aqueous streams using aluminium-based salts. *RSC Advances* **2012,** *2* (29), 10882-10890.

[60] Labbozzetta, S.; Valvo, L.; Bertocchi, P.; Manna, L. Focused microwave-assisted extraction and LC determination of the active ingredient in naproxen-based suppositories. *Journal of Pharmaceutical and Biomedical Analysis* **2005,** *39* (3), 463-468.

[61] Labbozzetta, S.; Valvo, L.; Bertocchi, P.; Alimonti, S.; Gaudiano, M. C.; Manna, L. Focused Microwave-Assisted Extraction and LC Determination of Ketoprofen in the Presence of Preservatives in a Pharmaceutical Cream Formulation. *Chromatographia* **2009,** *69* (3), 365-368.

[62] Lakin, M. B.; Shockley, T. H.; Zey, E. G. Isolation of ibuprofen from tablets; 1994; US Patent No US5300301A.

[63] Weber, C. C.; Kulkarni, S. A.; Kunov-Kruse, A. J.; Rogers, R. D.; Myerson, A. S. The Use of Cooling Crystallization in an Ionic Liquid System for the Purification of Pharmaceuticals. *Crystal Growth & Design* **2015,** *15* (10), 4946-4951.

CHAPTER 3

Chiral resolution of racemic drugs

3. Chiral resolution of racemic drugs

The search for effective pathways of producing enantiopure drugs has evolved in the last years, since the famous "thalidomide scandal". After the World War II, this immunomodulatory drug started to be marketed and widely prescribed to heal nausea and relieve vomiting in pregnant women. While sold as a racemic mixture, R-thalidomide (i.e., the eutomer) possessed the desired effect and the S-enantiomer (i.e., the distomer) was teratogenic and induced a large number of miscarriages and child deaths.[1, 2] In spite of being as similar as the two human hands and possessing identical physico-chemical properties (except for their optical rotation), biological systems can discriminate them. While one isomer induces the desired therapeutic action, the other can be less potent, bio-inert or even toxic.[1, 3, 4] Under this scenario, the responsible regulatiory entities worldwide became stricter in their policies and strongly recommend the development of enantiopure drugs.[5, 6] Even though some medicines can be commercialized and safely consumed as racemates (e.g., ibuprofen and warfarin), the pharmaceutical companies must provide much more detailed information upon approval requisition. That is, pharmacologic, pharmacokinetic and toxicological data for each enantiomer and respective racemic mixture must be provided. Hence, the pharmaceutical industry remains interested on efficient techniques to produce enantiopure drugs.

The current techniques being applied entail two main strategies, (i) the direct synthesis of the desired enantiomer and (ii) the synthesis of racemic mixtures followed by enantioseparation.[7, 8] The former is considered the most powerful approach. Still, it suffers from the high cost of the pure raw materials used, the stereospecific catalysts required, and the numerous reactions usually needed to attain the optical purity that standards impose. Furthermore, asymmetric synthesis entails laborious and prolonged development processes, with uncertain outcome.[9, 10] In turn, the latter, being of simpler, more flexible and cheaper nature has been increasingly envisaged as a promising alternative.[8, 11, 12] Chromatographic techniques and crystallization are, probably, the most used approaches for the resolution of racemic compounds.[8] Enantioselective crystallization is based on the distinct solubility of diastereomic salts or conglomerates formed. The technological simplicity, cost efficiency and easy coupling with other

techniques make crystallization of utmost industrial relevance. Still, the lack of compounds able to form conglomerates (estimated values of 5-10 %), the need for additional steps of enantiomeric enrichment to overcome the common low yields attained, and the inherent excessive solids' handling confine its application.[8, 12] Chromatography allows the separation of enantiomers within analytical columns by the formation of diastereomers. Although quick, broadly applicable and operationally flexible, chromatographic techniques are limited by the high cost and limited availability of chiral columns, low loading capacities and narrow scalability.[8, 12]

Enantioselective LLE (ELLE) techniques are attracting attention as alternatives for chiral resolution.[11] Beyond its simple operation and low cost, ELLE joins an easy scale-up and a broad applicability. Combining the principles of solvent extraction and enantiomeric recognition, ELLE requires the existence of at least one chiral selector, otherwise enantiomeric recognition does not occur. Briefly, the migration of such chiral selector between the two immiscible phases along with the "chiral selector-enantiomer" interactions control the enantiomers' separation in ELLE systems.[11] The enantiomeric recognition follows the three-point attachment model, where it is envisioned that the occurrence of three simultaneous "chiral selector-enantiomer" interactions come about (e.g., electrostatic, van der Waals, hydrogen bond, π-π stacking).[13] The most used chiral selectors are crown-ether-based, metal complexes or metalloids, β-cyclodextrin and its derivatives, and tartaric acid-inspired.[14-20] As a way to overcome the deficient performance sometimes exhibited by the implementation of a single chiral selector, the two later examples are frequently combined, due to their distinct solubility and recognition ability, in biphasic recognition approaches.[21-24] Tang et al.[24] proposed the combined use of β-cyclodextrin (water soluble) and L-tartrate (organic solvent soluble) derivatives in an organic solvent/water biphasic system to resolve racemic flurbiprofen. Among all screenings performed, 1,2-dichloroethane was the best solvent and trimethyl-β-cyclodextrin + L-iso-butyl tartrate appeared as the most promising pair of chiral selectors. As compared to the monophasic recognition chiral extraction (enantioselectivity of 1.16), biphasic recognition chiral recognition performed slightly better (enantioselectivity of 1.24). 1,2-dichloroethane/water liquid-liquid system was

again employed, instead for the chiral resolution of pantoprazole, with enhanced enantioselectivities with hydroxypropyl-β-cyclodextrin and diisobutyl tartrate as chiral selectors.[22] In comparison to the monophasic recognition chiral extraction, the optimal system yielded a much higher enantioselectivity (1.42 vs. 1.10). This system was further implemented in continuous mode in centrifugal contactor separators, with an achievable enantiomeric excess of 48 %.[25] Further reinforcing such a scenario, in other work,[26] it was possible to separate racemic mandelic acid with a 1-octanol/water liquid-liquid system with O,O'-di-benzoyl-(2S,3S)-4-toluoyl-tartaric acid and hydroxypropyl-β-cyclodextrin acting as chiral selectors. The addition of a second chiral selector to the organic phase improved the enantioselectivies from 1.333 up to 1.527. Envisaging their industrial application, processes other than pantoprazole chiral resolution[25] were already operated, for instance, in continuous mode centrifugal contactor separators or counter-current chromatography.[18, 27-31]

Still, the large quantities of volatile and nefarious organic solvents that ELLE uses fail to match the recommendations of the Green Chemistry and Sustainability guidelines.[32, 33] Under this scenario, there is a demand to turn enantioseparations into greener approaches. ABS may appear as good candidates to provide more biocompatible and versatile routes for enantioseparation. Not only the enhanced biocompatibility of these systems provided by the high water content contribute to such a status, but also the wide range of solutes, some of them bearing chiral centres, available to induce liquid-liquid demixing.[34-36]

The implementation of ABS to chiral resolution has been done resorting to two approaches. The most used relays on the addition of a chiral selector (not essential to two-phase formation),[37-53] while the other approach uses a chiral compound as both chiral selector and phase former.[54-58] The racemates separated with these water-rich systems cover drugs and their precursors (mandelic acid and its derivatives, phenylsuccinic acid, ofloxacin, flurbiprofen, zopiclone, among others) and amino acids [phenylalanine (Phe) and tryptophan (Trp)].[37-58] The first approach has been mainly focused on the use of β-cyclodextrin derivatives, copper-β-cyclodextrin complexes, tartaric acid derivatives, proteins and microbial cells as chiral selectors in polymer-salt,

polymer-polymer, polar organic solvents-salt, ILs-salt and micellar systems.[37-53] Promising enantioselectivities were achieved with several types of ABS for different racemic mixtures. The highest enantiomeric excess obtained so far (86.7 %) was achieved in a combinatorial process of enantioselective biotransformation and extraction of an histidine intermediate with an ABS composed of poly(ethylene) glycol, Na_2HPO_4 and microbial cells as chiral selectors.[49] Temperature-dependent micellar systems containing copper-β-cyclodextrin complexes as chiral selectors were able to extract mandelic acid with an enantiomeric excess of 67.91 %,[38] while the implementation of the biphasic recognition chiral extraction concept in ethanol-$(NH_4)_2SO_4$ has separated phenylsuccinic acid enantiomers with 57.86 % of optical purity.[42] Moreover, the protein bovine serum albumin in a poly(ethylene) glycol-dextran system exhibited an outstanding recognition ability for ofloxacin enantiomers yielding 62 % of enantiomeric excess.[46] The second approach, although it has lagged behind during the past years, is more technologically simple and facilitates the phase's formers recycling and the isolation of the target enantiomer. It usually resorts to β-cyclodextrin derivatives, chiral polymers of synthetic origin and CILs as phase formers in combination with polar organic solvents, salts and common polymers (e.g., dextran).[54-58] In polymeric ABS composed of dextran and a newly synthesized chiral polymer, poly(MAH-β-CD-co-NIPAAm), mandelic acid was obtained with 1.27 of enantioselectivity.[54] The recyclability and reuse of the phase formers was successfully achieved due to the thermosensitive nature of poly(MAH-β-CD-co-NIPAAm). The introduction of polar organic solvents-β-cyclodextrin derivatives ABS performed much better with both phenylsuccinic acid and zopiclone being enantioseparated with enantiomeric excesses of 31.7 % and 32.66 %, respectively (enantioselectivities of 2.1 and 2.58).[55, 56] So far, less appealing enantioselectivities have been obtained than those with the first approach. Still, there is much to be done concerning the pairs of phase formers frequently adopted. Indeed, the literature offers a wide range of ABS bearing chiral components as phase forming agents. For instance, ABS based on carbohydrates[59-62] or amino acids[63-66] paired with polymers, surfactants, polar organic solvents and ILs have been reported; yet, their application to chiral recognition was not yet attempted.

3.1. Chiral ionic liquids as alternative solvents for the separation of chiral compounds

Some of the parts included in this state of the art were taken from Ventura, S. P. M.; e Silva, F. A.; Quental, M. V.; Mondal, D.; Freire, M. G.; Coutinho, J. A. P. Ionic-Liquid-Mediated Extraction and Separation Processes for Bioactive Compounds: Past, Present, and Future Trends. *Chemical Reviews* **2017**, *117* (10), 6984–7052, where enantioseparations were considered.

Contributions: S.P.M.V., M.G.F. and J.A.P.C. conceived and directed this work. Francisca A. e Silva, M.V.Q. and D.M. wrote the chapters included in this review, with vital contributions from S.P.M.V., M.G.F. and J.A.P.C.. Francisca A. e Silva wrote those comprising Lipids and Other Hydrophobic Compounds, Nucleic Acids and Drugs and Pharmaceuticals, the latter being included in this chapter. Furthermore, Francisca A. e Silva was responsible for bringing all chapters together and drawing all Figures.

The designer solvent status of ILs creates the opportunity of using chiral structures as cations, anions or both.[67] Such a feature makes ILs as excellent candidates to overcome the current drawbacks of the aforementioned techniques. The first CIL, 1-butyl-3-methylimidazolium lactate, was synthesized in 1999 by Seddon and co-workers.[68] Ever since, many other chiral ILs were proposed, such as those based on carbohydrates,[69-71] amino acids[72-75] and other natural acids,[76, 77] alkaloids,[78] amino alcohols[79], terpenes[80] and thiourea.[81, 82] Given the ready availability of most of these natural (chiral) starting materials and the enhanced biocompatibility afforded, many applications were hitherto attempted. CILs have been applied as either solvents or catalysts in asymmetric synthesis, in spectroscopic techniques for chiral recognition and in chromatographic and electrophoretic techniques as stationary phases or additives.[83, 84] Still, the application of CILs in chiral separation techniques has been neglected as it will be notorious by the literature overviewed below. The name and abreviation of the cations and anions used hitherto in the formulation of CILs is presented in Table 3.1.

Table 3.1. Name and abreviation of the IL cation-anion combinations considered in this overview.

Cation		**Anion**	
Name	**Abbreviation**	**Name**	**Abbreviation**
Chiral			
pipecoloxylididinium	$[Pip]^+$	L-tartrate	$[L\text{-}Tar]^-$
alkyltropinium	$[C_n tro]^+$	L-prolinate	$[L\text{-}Pro]^-$
bis(alkyl)-alkaneditropinium	$[C_n tro\text{-}C_n\text{-}troC_n]^+$	L-phenylalaninate	$[L\text{-}Phe]^-$
(*R*)-3-(2-((1-hydroxybutan-2-yl)amino)-2-oxoethyl)-1-methyl-imidazolium	$[C_{10}H_{18}N_3O_2]^+$		
(R)-3-(2-(3-(1-hydroxybutan-2-yl)ureido)ethyl)-1-methyl-imidazolium	$[C_{11}H_{21}N_4O_2]^+$		
ethyl L-phenylalaninium	$[C_2(L\text{-}Phe)]^+$		
Achiral			
3,3´-(1,6-alkanedyl)bis(1-methylimidazolium)	$[C_1im\text{-}C_n\text{-}imC_1]^+$	Bis(trifluoromethylsulfonyl)imide	$[NTf_2]^-$
1-alkyl-3-methylimidazolium	$[C_nC_1im]^+$	Dicyanamide	$[N(CN)_2]^-$
		Hexafluorophosphate	$[PF_6]^-$
		Tetrafluoroborate	$[BF_4]^-$

Enantioselective liquid-liquid extractions

In 2013, the chiral separation of racemic mandelic acid using hydrophobic ILs + water systems was attempted.[85] The achiral ILs, $[C_8C_1im][BF_4]$ and $[C_4C_1im][PF_6]$, were used as the ionic phases with β-cyclodextrin derivatives as chiral selectors. The study suggested that $[C_4C_1im][PF_6]$ as the extraction solvent and hydroxypropyl-β-cyclodextrin as the chiral selector was the optimal combination. By decreasing temperature, pH and the concentration of enantiomers, and by increasing the chiral selector concentrations, improved enantioselectivities were obtained.[85]

In 2010, Tang and co-authors[86] employed, for the first time, functional amino-acid-based ILs as solvents and selectors for the LLE of racemic mixtures of amino acids [Phe, tyrosine (Tyr), histidine (His) and Trp]. With this class of ILs working both as solvent

and chiral selector and ethylacetate as a donor phase, it was possible to extract with higher efficiencies the L-enantiomers into the IL phase. This enantioselective enrichment was driven by a chiral ligand-exchange mechanism, since a minimum concentration of the target amino acid and chelant (Cu^{2+}) is necessary. Amino acid-based ILs proved to be excellent solvents since they display not only a chiral recognition ability (maximum enantiomeric excesses of 50.6 % for Phe), but they also extract more than 99 % of the amino acids from the ethylacetate phase.[86]

Zgonnik et al.[87] described a more environmentally friendly approach. Here, the most toxic molecular solvents were substituted by novel CILs synthesized in a simple and atom economic way. Starting by mixing $[P_{4444}]_2$[L-Tar] and $[C_8C_1im][NTf_2]$ ILs in water, methatesis occured, thus arising two-phases. The IL layer is $[P_{4444}][NTf_2]$-rich, while tartrate and $[C_8C_1im]$ ions (more hydrophilic) constitute the aqueous phase – "ILs ion cross-metathesis" was the denomination afforded to such an innovative process. After giving the proof of concept on "ILs ion cross-metathesis", the separation of racemic pipecoloxylidide was attempted (mixing in water $[Pip][NTf_2]$ and $[P_{4444}]_2$[L-Tar], as sketched in Figure 3.1). The preferential chiral recognition ability of the tartrate anions to the S-enantiomers (formation of [S-Pip][L-Tar]) allowed enantiomeric separation with an enantiomeric excess of 30 % for the water layer.[87] A summary of all ELLE reviewed is presented in Table 3.2.

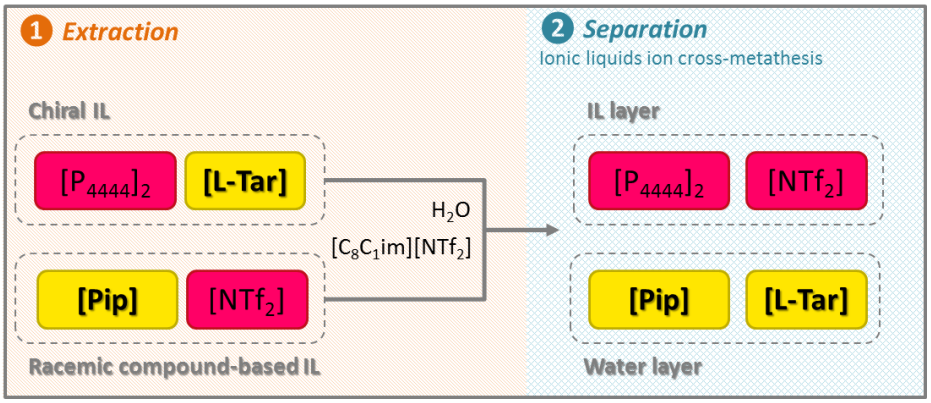

Figure 3.1. Schematic representation of ILs ion cross-metathesis for the chiral resolution of racemic mixtures of pharmaceuticals by ELLE.[87]

Table 3.2. Enantiomeric separation of racemic compounds using LLE with ILs.

Racemic compound	**System used**	**Chiral selector**	**Isolation strategy**
His	$[C_2C_1im][L\text{-}Pro]$ + ethyl acetate + $Cu(CH_3CO_2)_2$[86]	$[C_2C_1im][L\text{-}Pro]$ + Cu^{2+}[86]	Precipitation with HCl + washing with water[86]
Mandelic acid	$[C_8C_1im][BF_4]$ + H_2O + β-cyclodextrin derivatives,[85] $[C_4C_1im][PF_6]$ + H_2O + β-cyclodextrin derivatives[85]	β-cyclodextrin derivatives[85]	
Phe	$[C_nC_1im][L\text{-}Pro]$ + ethyl acetate (n = 2, 4, 6, 8) + $Cu(CH_3CO_2)_2$, $[C_2C_1im]Br$ + ethyl acetate + $Cu(CH_3CO_2)_2$[86]	$[C_nC_1im][L\text{-}Pro]$ + Cu^{2+}[86]	Precipitation with HCl + washing with water[86]
Pipecoloxylidide	$[P_{4444}]_2[L\text{-}Tar]$ + $[Pip][NTf_2]$ + H_2O + $[C_8C_1im][NTf_2]$ (co-solvent)[87]	$[L\text{-}Tar]^{2-}$[87]	
Trp	$[C_2C_1im][L\text{-}Pro]$ + ethyl acetate + $Cu(CH_3CO_2)_2$[86]	$[C_2C_1im][L\text{-}Pro]$ + Cu^{2+}[86]	Precipitation with HCl + washing with water[86]
Tyr	$[C_2C_1im][L\text{-}Pro]$ + ethyl acetate + $Cu(CH_3CO_2)_2$[86]	$[C_2C_1im][L\text{-}Pro]$ + Cu^{2+}[86]	Precipitation with HCl + washing with water[86]

Aqueous biphasic systems

Chen et al.[41] have recently addressed the use of IL-based ABS formed by $[C_4C_1im][BF_4]$, $[C_2C_1im][BF_4]$ and $[C_4C_1im][N(CN)_2]$ and the salt $(NH_4)_2SO_4$, adding hydroxypropyl-β-cyclodextrin as a chiral selector for enantiomers, for the separation of the mandelic acid derivative α-cyclohexylmandelic acid. In spite of the lack of chiral recognition of some systems, under optimal conditions (salt amount, temperature, pH and chiral selector content), the system composed of $[C_4C_1im][BF_4]$, $(NH_4)_2SO_4$ and hydroxypropyl-β-cyclodextrin granted the best separation factor (ratio of the partition coefficients of the two enantiomers) of 1.59.[41] Here, ILs are only employed as solvents and an additional chiral selector is required to afford a certain enantioselectivity.

Concerning the second approach, wherein CILs are used as phase former and chiral selector, a recent work revealed that imidazolium-based CILs can be used to separate racemic mixtures of amino acids (D-Phe and L-Phe), with a maximum

enantiomeric excess of 53 % reported.[57] The D-enantiomer interacts with ILs, remaining in the IL-rich phase, while the L-enantiomer migrates towards the Na_2SO_4-rich phase. ^1H NMR and density functional theory (DFT) calculations showed that hydrogen-bonding interactions between the carboxylate and amide groups and resonance-assisted hydrogen-bonding interactions between amino and hydroxyl groups play a pivotal role.[57] The applicability of such systems was further extended to other amino acids [aspartic acid (Asp), Isoleucine (Ile), serine (Ser), threonine (Thr), Trp and Tyr].[57] Given the potential of forming ABS combining ILs with amino acids,[63, 64] and although not attempted up to date as previously highlighted, a much simpler approach can be anticipated, namely on the use of chiral amino acids as phase promoters of ABS and on their use for the separation of racemic mixtures of amino acids.

IL-based TPP systems are usually achieved by the creation of an additional phase in the ABS, which corresponds to the desired precipitated product. ABS based on tropine CILs and inorganic salts were prepared for the enantiomeric separation of a racemic mixture of Phe,[58] as sketched in Figure 3.2. In this study, the phase behaviour of IL-based ABS was investigated along with the factors influencing the separation efficiency. When the amount of D-Phe and L-Phe reached approximately the range of 15–20 $mg.g^{-1}$ (concentration required for enantioselectivity), a TPP system was created composed of a top IL-rich phase, a middle phase with precipitated amino acids and a bottom salt-rich phase. In general, more hydrophobic ILs allow improved selectivities for the separation of racemic mixtures of Phe.[58] On the other hand, large amounts of salt and water compromise the IL enantioselectivity. Under the optimum conditions, the enantiomeric excess value of L-Phe in the middle phase of the IL-TPP was of 65 %, while the D-enantiomer remains at the IL-rich phase. The obtained results prompted the authors to conclude that this system could be a promising approach for the racemic resolution of amino acids.[58] Although other conditions like temperature and pH could be additionally evaluated to improve the selectivity, IL-TPP appears as a promising strategy for the separation of other enantiomers of high commercial interest. In this sense, and given the single report found for the separation of racemic compounds with IL-TPP systems, it is worthwhile to explore this technique since, in addition to the good results obtained, also

the target compounds recovery and ILs recycling is much easier to accomplish, allowing the development of cost-effective purification strategies. An overview of the IL-based ABS implemented for enantioseparations is provided in Table 3.3.

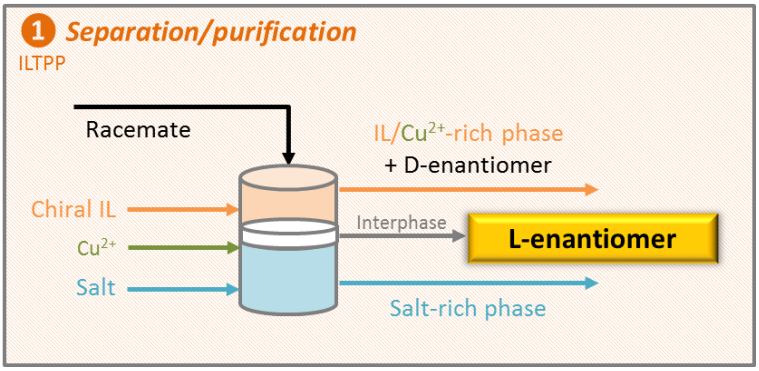

Figure 3.2. Schematic representation of IL-based TPP processes for the chiral resolution of racemic mixtures of amino acids.[58]

Table 3.3. Enantiomeric separation of racemic compounds using IL-based ABS and TPP.

Racemic compound	**System used**	**Chiral selector**	**Isolation strategy**
α-cyclohexylmandelic acid	$[C_4C_1im][BF_4]$ + $(NH_4)_2SO_4$ + H_2O + hydroxypropyl-β-cyclodextrin,[41]	hydroxypropyl-β-cyclodextrin[41]	
	$[C_2C_1im][BF_4]$ + $(NH_4)_2SO_4$ + H_2O + hydroxypropyl-β-cyclodextrin,[41]		
	$[C_4C_1im][N(CN)_2]$ + $(NH_4)_2SO_4$ + H_2O + hydroxypropyl-β-cyclodextrin[41]		
Asp	$[C_{10}H_{18}N_3O_2][PF_6]$ + Na_2SO_4 + H_2O[57]	$[C_{10}H_{18}N_3O_2][PF_6]$[57]	
Ile	$[C_{10}H_{18}N_3O_2][PF_6]$ + Na_2SO_4 + H_2O[57]	$[C_{10}H_{18}N_3O_2][PF_6]$[57]	
Phe	$[C_n$tro$][$L-Pro$]$ + K_2HPO_4 + H_2O (n= 2 – 8),[58]	$[C_n$tro$][$L-Pro$]$,[58]	Precipitation at liquid-liquid interface,[58] Precipitation with acetronitrile[57]
	$[C_8$tro$][$L-Pro$]$ + K_2HPO_4 + H_2O + $Cu(CH_3CO_2)_2$,[58]	$[C_{10}H_{18}N_3O_2][PF_6]$,[57]	
	$[C_8$tro$][$L-Pro$]$ + K_3PO_4 + H_2O,[58] $[C_8$tro$][$L-Pro$]$ + K_2CO_3 + H_2O,[58]	$[C_{11}H_{21}N_4O_2][PF_6]$[57]	
	$[C_{10}H_{18}N_3O_2][PF_6]$ + Na_2SO_4 + H_2O,[57]		

	$[C_{11}H_{21}N_4O_2][PF_6]$ $Na_2SO_4 + H_2O$[57]	+	
Ser	$[C_{10}H_{18}N_3O_2][PF_6]$ $Na_2SO_4 + H_2O$[57]	+	$[C_{10}H_{18}N_3O_2][PF_6]$[57]
Thr	$[C_{10}H_{18}N_3O_2][PF_6]$ $Na_2SO_4 + H_2O$[57]	+	$[C_{10}H_{18}N_3O_2][PF_6]$[57]
Trp	$[C_{10}H_{18}N_3O_2][PF_6]$ $Na_2SO_4 + H_2O$[57]	+	$[C_{10}H_{18}N_3O_2][PF_6]$[57]
Tyr	$[C_{10}H_{18}N_3O_2][PF_6]$ $Na_2SO_4 + H_2O$[57]	+	$[C_{10}H_{18}N_3O_2][PF_6]$[57]

Solid-liquid two-phase extraction

An approach of boosted operational simplicity, biocompatibility and quickness was recently proposed by the Song group.[88, 89] As overviewed in Table 3.4, the authors have used two classes of CILs, namely dicationic imidazolium-based[88] and dicationic tropine-based,[89] attempting the enantiomeric separation of racemic amino acids. Such new solid-liquid two-phase approaches combine aqueous solutions of CILs with copper salts as coordination agents to promote selective precipitation, as exemplified in Figure 3.3.[88, 89] L-Phe preferentially precipitated due to cooperative interactions with the IL and cooper ion, as further confirmed by NMR (^{1}H and NOESY), IR, molecular dynamics (MD) simulation and/or UV-Vis spectroscopy.[88, 89] Remarkable enantiomeric excesses higher than 98 % of L-Phe in the solid-phase were reported, whereas the D-enantiomer remained in the liquid layer with enantiopurities higher than 61.8 %.[88, 89] This approach facilitated the ultimate isolation of the target enantiomer from the IL, analogously to IL-based TPP, with the need of less complex systems. In the second work of this series,[89] the authors went further showcasing the possibility of industrial application by (i) performing scale-up studies, (ii) developing an integrated process entailing the recycling and reuse of the CIL, cooper salt and D/L-Phe remaining in solution – Figure 3.3 - and (iii) extending the applicability to other amino acids keeping the outstanding performances (e.g., enantiomeric excess for Trp of 99.7 %).[89]

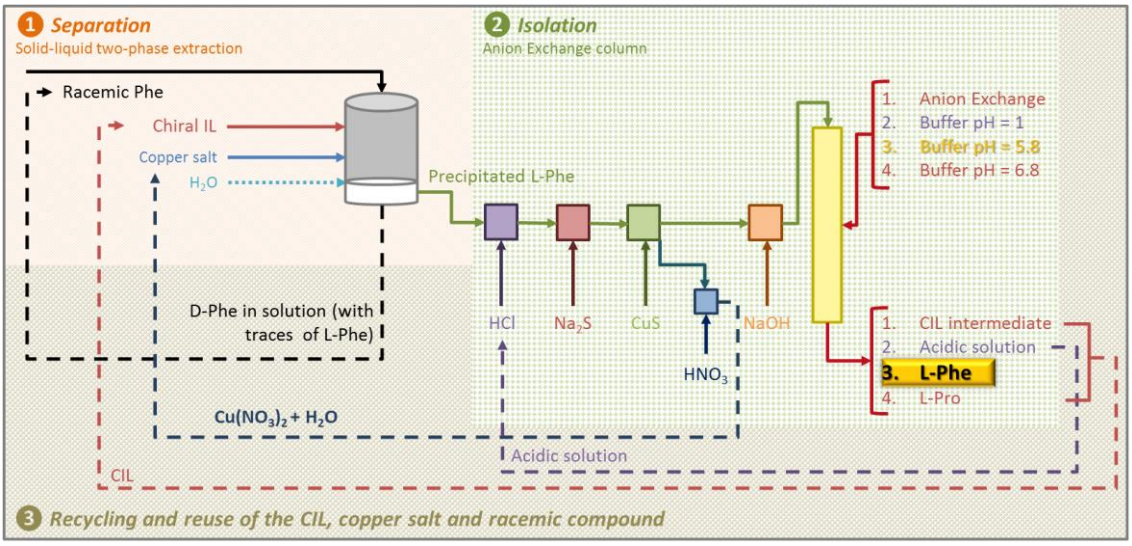

Figure 3.3. Schematic representation of IL-based solid-liquid two-phase processes for the selective separation of racemic amino acids.[89]

Table 3.4. Enantiomeric separation of racemic compounds using IL-based solid-liquid two-phase systems.

Racemic compound	System used	Chiral selector	Isolation strategy
Phe	$[C_n\text{tro-}C_n\text{-tro}C_n][\text{L-Pro}]_2$ (n = 3 to 6) + copper salts + H_2O,[89] $[C_1\text{im-}C_n\text{-im}C_1][\text{L-Pro}]_2$ + $Cu(CH_3CO_2)_2 + H_2O$[88]	$[\text{Tro-}C_n\text{-Tro}][\text{L-Pro}]_2\text{-}Cu^{2+}$,[89] $[C_1\text{im-}C_n\text{-im}C_1][\text{L-Pro}]_2\text{-}Cu^{2+}$[88]	Anion exchange [89]
Trp	$[C_n\text{tro-}C_3\text{-tro}C_n]$ $[\text{L-Pro}]_2$ + $Cu(NO_3)_2 + H_2O$[89]	$[\text{Tro-}C_3\text{-Tro}][\text{L-Pro}]_2\text{-}Cu^{2+}$[89]	
Tyr	$[C_n\text{tro-}C_3\text{-tro}C_n][\text{L-Pro}]_2$ + $Cu(NO_3)_2 + H_2O$[89]	$[\text{Tro-}C_3\text{-Tro}][\text{L-Pro}]_2\text{-}Cu^{2+}$[89]	
Benzene glycine	$[C_n\text{tro-}C_3\text{-tro}C_n][\text{L-Pro}]_2$ + $Cu(NO_3)_2 + H_2O$[89]	$[\text{Tro-}C_3\text{-Tro}][\text{L-Pro}]_2\text{-}Cu^{2+}$[89]	
Mandelic acid	$[C_n\text{tro-}C_3\text{-tro}C_n]$ $[\text{L-Pro}]_2$ + $Cu(NO_3)_2 + H_2O$[89]	$[\text{Tro-}C_3\text{-Tro}][\text{L-Pro}]_2\text{-}Cu^{2+}$[89]	

Solid-phase extraction

IL-based solid-phase extraction (SPE) methods aiming at extracting and separating racemic compounds, in particular amino acids, although scarce, cover three distinct approaches: (i) CILs immobilized on silica;[90, 91] (ii) CILs on the preparation of molecularly imprinted polymers (MIPs);[92] and (iii) silica-coated magnetic nanoparticles modified with CILs.[93] A synopsis of the systems reported in literature is given in Table 3.5. The first approach was studied by Marwani et al.[90] and Qian et al.[91] In the former,[90] a new CIL, $[C_2(L\text{-Phe})][NTf_2]$, was immobilized on silica for the D-Phe enantioselective separation from aqueous media. Data on adsorption isotherms revealed that the adsorption capacity of the solid support for D-Phe was of 97.35 % at pH 3.0. The feasibility of the methodology was ultimately validated by implementing it to real samples with satisfactory results.[90] In the later,[91] tropine-like CILs-Cu^{2+} complexes were immobilized on silica by chemical modification and further used to carry on adsorption studies on chromatographic column. The chiral resolution of two distinct amino acids, namely Phe and Trp, was attempted. In both cases, distinct adsorptions of D- and L-enantiomers onto the CIL-Cu^{2+}-modified column allowed fully separating the enantiomers (enantiomeric excess around 100 %).[91] Yang et al.,[92] on the other hand, turned their attention to the second approach by applying the oil-soluble 1-butyl-3-methylimidazolium α-aminohydrocinnamic acid ($[C_4C_1im][L\text{-Phe}]$) to prepare surfaces of MIPs in acetonitrile for the selective recognition of L-Phe. This approach is schematically displayed in Figure 3.4. Binding studies, such as adsorption kinetics, adsorption thermodynamics, SPE application, and the chiral resolution of racemic Phe mixtures were performed. Preferential adsorption of the L-Phe over the D enantiomer was shown. Additionally, this IL-based copolymerizing process in acetonitrile, when compared with the traditional imprinting process with acetonitrile/H_2O, created more binding sites and allowed a higher adsorption of L-Phe, resulting in the selective separation of L-Phe from other amino acids (L-Trp and L-His), with a recovery above 90.6 %. With these results, the authors suggested that $[C_4C_1im][Phe]$ imprinting polymers provide a new pathway for separating amino acids and their racemates.[92] The third approach was matter of study in the work of Liu et al.[93] by bonding the CIL $[C_2C_1im][L\text{-Pro}]$ onto silica-coated magnetic nanoparticles. Preliminary

studies involving the direct separation of five distinct racemic amino acids with such chiral magnetic nanospheres were performed. The good discriminating ability for racemic amino acids was patent by the optical rotation showed by the supernatants collected after contact with the chiral magnetic nanospheres. Trp was further used to conduct separation studies using the fabricated magnetic nanospheres by centrifugal chiral chromatography. Playing with the mobile phase composition and gradients, it was possible to separate the two Trp enantiomers from each other, with a peak resolution of 1.5. Beyond the good chiral resolution ability, CIL-based magnetic nanospheres showed great promise in the field due to the easy recycle via external magnetic field.[93]

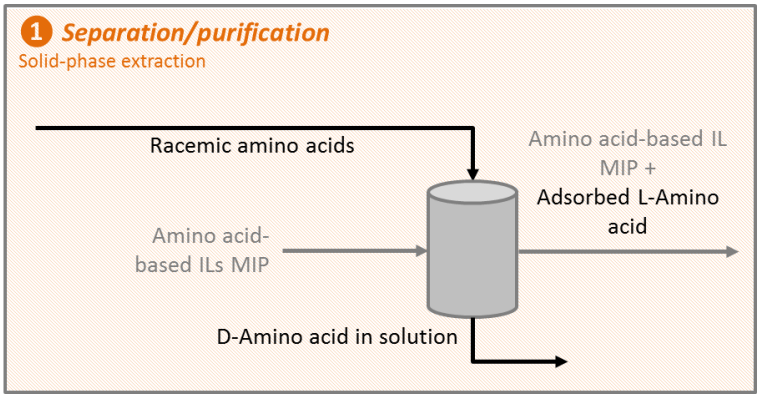

Figure 3.4. Schematic representation of IL-based SPE processes for the selective separation of enantiomeric mixtures of amino acids.[92]

Table 3.5. Enantiomeric separation of racemic compounds using IL-based solid-phase extraction.

Racemic compound	**System used**	**Chiral selector**
1-(2-Napthyl) ethanol	SiO_2-[C_2(L-Phe)][NTf_2][90]	[C_2(L-Phe)][NTf_2][90]
Arginine	Fe_3O_4@SiO_2@6-diisocyanatohexane-[C_2C_1im][L-Pro][93]	[C_2C_1im][L-Pro][93]
Cysteine	Fe_3O_4@SiO_2@6-diisocyanatohexane-[C_2C_1im][L-Pro][93]	[C_2C_1im][L-Pro][93]
Glutamine	Fe_3O_4@SiO_2@6-diisocyanatohexane-[C_2C_1im][L-Pro][93]	[C_2C_1im][L-Pro][93]
Leucine	Fe_3O_4@SiO_2@6-diisocyanatohexane-[C_2C_1im][L-Pro][93]	[C_2C_1im][L-Pro][93]
Phe	SiO_2-[C_2(L-Phe)][NTf_2],[90] SiO_2-[C_3Tro][L-Pro] – Cu^{2+},[91] [C_4C_1im][L-Phe]-MIP[92]	[C_2(L-Phe)][NTf_2],[90] [C_3Tro][L-Pro] – Cu^{2+},[91] [C_4C_1im][L-Phe][92]
Trp	SiO_2-[C_2(L-Phe)][NTf_2],[90] SiO_2-[C_3Tro][L-Pro]-Cu^{2+},[91] Fe_3O_4@SiO_2@6-diisocyanatohexane-[C_2C_1im][L-Pro][93]	[C_2(L-Phe)][NTf_2],[90] [C_3Tro][L-Pro] – Cu^{2+},[91] [C_2C_1im][L-Pro][93]

Scopes and Objectives

Many advances were made during decades to create safe and efficient methods for chiral resolution of drugs within a pharmaceutical industry frame. It is well-patent that asymmetric synthesis is the most powerful approach, with its importance being recognized by The Royal Swedish Academy of Sciences who awarded the Nobel Prize of Chemistry to three scientists on the field in 2001.[94] The shortcomings of such an approach have been, however, identified along the years, with the high costs and lengthy development processes and cumbersome operation hampering its broader application.[9, 10] Alternatives to asymmetric synthesis pass through the chiral resolution of racemic drugs by ELLE techniques, which are considered as simpler, more flexible and cheaper.[11] CILs-based ABS, although poorly explored for such a process, have been highlighted as representing a performant and greener route for enantioseparations.[57, 58]

Given the lack of knowledge on how CILs perform as chiral resolution agents and solvents in the separation of enantiomeric drugs and the restrictive array of CILs hitherto investigated,[57, 58] this thesis intends to expand the CIL-based ABS database and their applicability to enantioseparations. To accomplish such an aim, the "designer solvent" status of ILs will serve as motivation to design two sets of CILs-based ABS. Firstly, CILs with chirality at the cation core are used (***section 3.1.1.***) and secondly, where the anion will be the chiral structure (***section 3.1.2.***), which will expand the applicability of CIL-based ABS to either acidic or basic drugs. Furthermore, and to gather some insights on the enantioseparation ability of such systems, some optimization studies entailing a plethora of operational conditions, others than the CIL structure, were performed.

References

[1] Nunez, M. C.; Garcia-Rubino, M. E.; Conejo-Garcia, A.; Cruz-Lopez, O.; Kimatrai, M.; Gallo, M. A.; Espinosa, A.; Campos, J. M. Homochiral Drugs: A Demanding Tendency of the Pharmaceutical Industry. *Current Medicinal Chemistry* **2009,** *16* (16), 2064-2074.

[2] Miller, M. T.; Strömland, K. The study of malformations "by the company they keep". *Transactions of the American Ophthalmological Society* **1992,** *90*, 247-263.

[3] Nguyen, L. A.; He, H.; Pham-Huy, C. Chiral Drugs: An Overview. *International Journal of Biomedical Science : IJBS* **2006,** *2* (2), 85-100.

[4] Lin, G.-Q.; You, Q.-D.; Cheng, J.-F., *Chiral drugs: chemistry and biological action*. John Wiley & Sons: 2011.

[5] U.S. Food and Drug Administration. Development of New Stereoisomeric Drugs. http://www.fda.gov/Drugs/GuidanceComplianceRegulatoryInformation/Guidances/ucm122883.htm (accessed Feb 1, 2017).

[6] European Medicines Agency. Test Procedures And Acceptance Criteria For New Veterinary Drug Substances And New Medicinal Products: Chemical Substances. http://www.ema.europa.eu/docs/en_GB/document_library/Scientific_guideline/2009/10/WC500004339.pdf (accessed Feb 1, 2017).

[7] Boyd, D. R.; McKervey, M. A. Asymmetric synthesis. *Quarterly Reviews, Chemical Society* **1968,** *22* (2), 95-122.

[8] Heike, L.; Andreas, S. M. Processes To Separate Enantiomers. *Angewandte Chemie International Edition* **2014,** *53* (5), 1218-1250.

[9] Mane, S. Racemic drug resolution: a comprehensive guide. *Analytical Methods* **2016,** *8* (42), 7567-7586.

[10] Blaser, H.-U. Chirality and its implications for the pharmaceutical industry. *Rendiconti Lincei* **2013,** *24* (3), 213-216.

[11] Schuur, B.; Verkuijl, B. J. V.; Minnaard, A. J.; de Vries, J. G.; Heeres, H. J.; Feringa, B. L. Chiral separation by enantioselective liquid-liquid extraction. *Organic & Biomolecular Chemistry* **2011,** *9* (1), 36-51.

[12] Maier, N. M.; Franco, P.; Lindner, W. Separation of enantiomers: needs, challenges, perspectives. *Journal of Chromatography A* **2001,** *906* (1), 3-33.

[13] Davankov, V. A. The nature of chiral recognition: Is it a three-point interaction? *Chirality* **1997,** *9* (2), 99-102.

[14] Galan, A.; Andreu, D.; Echavarren, A. M.; Prados, P.; De Mendoza, J. A receptor for the enantioselective recognition of phenylalanine and tryptophan under neutral conditions. *Journal of the American Chemical Society* **1992,** *114* (4), 1511-1512.

[15] Steensma, M.; Kuipers, N. J. M.; de Haan, A. B.; Kwant, G. Influence of process parameters on extraction equilibria for the chiral separation of amines and amino-alcohols with a chiral crown ether. *Journal of Chemical Technology & Biotechnology* **2006,** *81* (4), 588-597.

[16] Tsukube, H.; Uenishi, J.-I.; Kanatani, T.; Itoh, H.; Yonemitsu, O. Enantioselective binding and extraction of zwitterionic amino acids by chiral lanthanide complexes. *Chemical Communications* **1996,** *0* (4), 477-478.

[17] Reeve, T. B.; Cros, J.-P.; Gennari, C.; Piarulli, U.; de Vries, J. G. A Practical Approach to the Resolution of Racemic N-Benzyl α-Amino Acids by Liquid–Liquid Extraction with a Lipophilic Chiral Salen–Cobalt(III) Complex. *Angewandte Chemie International Edition* **2006,** *45* (15), 2449-2453.

[18] Tang, K.; Wang, Y.; Zhang, P.; Huang, Y.; Dai, G. Process optimization of continuous liquid–liquid extraction in centrifugal contactor separators for separation of oxybutynin enantiomers. *Separation and Purification Technology* **2015,** *150*, 170-178.

[19] Ren, Z.; Zeng, Y.; Hua, Y.; Cheng, Y.; Guo, Z. Enantioselective Liquid–Liquid Extraction of Racemic Ibuprofen by l-Tartaric Acid Derivatives. *Journal of Chemical & Engineering Data* **2014,** *59* (8), 2517-2522.

[20] Kewen, T.; Panliang, Z.; Chunyue, P.; Hongjian, L. Equilibrium studies on enantioselective extraction of oxybutynin enantiomers by hydrophilic β-cyclodextrin derivatives. *AIChE Journal* **2011,** *57* (11), 3027-3036.

[21] Jiao, F. P.; Chen, X. Q.; Hu, W. G.; Ning, F. R.; Huang, K. L. Enantioselective extraction of mandelic acid enantiomers by L-dipentyl tartrate and β-cyclodextrin as binary chiral selectors. *Chemical Papers* **2007,** *61* (4), 326-328.

[22] Liu, J.-J.; Liu, C.; Tang, K.-W.; Zhang, P.-L. Biphasic recognition chiral extraction — novel way of separating pantoprazole enantiomers. *Chemical Papers* **2014,** *68* (5), 599-607.

[23] Tang, K.; Chen, Y.; Liu, J. Resolution of Zopiclone enantiomers by biphasic recognition chiral extraction. *Separation and Purification Technology* **2008,** *62* (3), 681-686.

[24] Tang, K.; Song, L.; Liu, Y.; Pan, Y.; Jiang, X. Separation of flurbiprofen enantiomers by biphasic recognition chiral extraction. *Chemical Engineering Journal* **2010,** *158* (3), 411-417.

[25] Wang, Y.; Tang, K.; Zhang, P.; Zhou, J.; Huang, Y.; Wen, P.; Sun, G. Continuous Separation of Pantoprazole Enantiomers by Biphasic Recognition Chiral Extraction in Centrifugal Contactor Separators. *Organic Process Research & Development* **2015,** *19* (9), 1082-1087.

[26] Kewen, T.; Jianmin, Y.; Kelong, H.; Guoli, Z. Biphasic recognition chiral extraction: A novel method for separation of mandelic acid enantiomers. *Chirality* **2009,** *21* (3), 390-395.

[27] Tang, K.; Wang, Y.; Zhang, P.; Huang, Y.; Hua, J. Optimization study on continuous separation of equol enantiomers using enantioselective liquid–liquid extraction in centrifugal contactor separators. *Process Biochemistry* **2016,** *51* (1), 113-123.

[28] Zhang, P.; Zhang, H.; Tang, K.; Yi, J.; Huang, Y. Influence of pH on enantioselective extraction of aromatic acid enantiomers in centrifugal contactor separators: Experiments and simulation. *Separation and Purification Technology* **2015,** *141*, 68-75.

[29] Tong, S.; Yan, J.; Guan, Y.-X.; Fu, Y.; Ito, Y. Separation of α-cyclohexylmandelic acid enantiomers using biphasic chiral recognition high-speed counter-current chromatography. *Journal of Chromatography A* **2010,** *1217* (18), 3044-3052.

[30] Xiong, Q.; Jin, J.; Lv, L.; Bu, Z.; Tong, S. Chiral ligand exchange countercurrent chromatography: Enantioseparation of amino acids. *Journal of Separation Science* **2018,** *41* (6), 1479-1488.

[31] Franco, P.; Blanc, J.; Oberleitner, W. R.; Maier, N. M.; Lindner, W.; Minguillón, C. Enantiomer Separation by Countercurrent Chromatography Using Cinchona Alkaloid Derivatives as Chiral Selectors. *Analytical Chemistry* **2002,** *74* (16), 4175-4183.

[32] Anastas, P. T.; Warner, J. C., *Green chemistry: theory and practice*. Oxford university press: 2000.

[33] Glavič, P.; Lukman, R. Review of sustainability terms and their definitions. *Journal of Cleaner Production* **2007,** *15* (18), 1875-1885.

[34] Freire, M. G.; Claudio, A. F. M.; Araujo, J. M. M.; Coutinho, J. A. P.; Marrucho, I. M.; Lopes, J. N. C.; Rebelo, L. P. N. Aqueous biphasic systems: a boost brought about by using ionic liquids. *Chemical Society Reviews* **2012,** *41* (14), 4966-4995.

[35] Soares, R. R. G.; Azevedo, A. M.; Van Alstine, J. M.; Aires-Barros, M. R. Partitioning in aqueous two-phase systems: Analysis of strengths, weaknesses, opportunities and threats. *Biotechnology Journal* **2015,** *10* (8), 1158-1169.

[36] Molino, J. V. D.; Viana Marques, D. d. A.; Pessoa Júnior, A.; Mazzola, P. G.; Gatti, M. S. V. Different types of aqueous two-phase systems for biomolecule and bioparticle extraction and purification. *Biotechnology Progress* **2013,** *29* (6), 1343-1353.

[37] Tan, L.; Long, Y.; Jiao, F.; Chen, X. Enantioselective extraction of mandelic acid enantiomers by aqueous two-phase systems of polyethylene glycol and ammonium sulfate containing β-cyclodextrin as chiral selector. *Journal of the Iranian Chemical Society* **2011,** *8* (4), 889-896.

[38] Xing, J.-M.; Li, F.-F. Chiral separation of mandelic acid by temperature-induced aqueous two-phase system. *Journal of Chemical Technology & Biotechnology* **2012,** *87* (3), 346-350.

[39] Li, F.-F.; Tan, Z.-J.; Guo, Z.-F. Enantioseparation of mandelic acid and α-cyclohexylmandelic acid using an alcohol/salt-based aqueous two-phase system. *Chemical Papers* **2014,** *68* (11), 1539-1545.

[40] Li, L.-H.; Li, F.-F. Chiral separation of α-cyclohexyl-mandelic-acid by aqueous two phase system combined with Cu2-β-cyclodextrin complex. *Chemical Engineering Journal* **2012,** *211-212*, 240-245.

[41] Chen, L.-L.; Li, F.-F.; Tan, Z.-J. Chiral separation of α-cyclohexylmandelic acid enantiomers using ionic liquid/salt aqueous two-phase system. *Chemical Papers* **2015,** *69* (11), 1465-1472.

[42] Chen, X.; Wang, J.; Jiao, F. Efficient enantioseparation of phenylsuccinic acid enantiomers by aqueous two-phase system-based biphasic recognition chiral extraction: Phase behaviors and distribution experiments. *Process Biochemistry* **2015,** *50* (9), 1468-1478.

[43] Zhuang, J.; Yang, W.; Chen, X.; Jiao, F. Enantioseparation of Phenylsuccinic Acid Enantiomers Using Aqueous Two-Phase Flotation and Their Determination by HPLC and UV Detection. *Chromatographia* **2014,** *77* (9), 679-685.

[44] Wang, J.; Chen, X.; Jiao, F. Enantioseparation of phenylsuccinic acid enantiomers based on aqueous two-phase system with ethanol/ammonium sulfate: phase diagrams optimization and partitioning experiments. *Journal of Inclusion Phenomena and Macrocyclic Chemistry* **2015,** *81* (3), 475-484.

[45] Jiao, F.; Wang, J.; Jiang, X.; Yang, H.; Shi, S.; Chen, X.; Yu, J. Biphasic recognition enantioseparation of ofloxacin enantiomers by an aqueous two-phase system. *Journal of Chemical Technology & Biotechnology* **2015,** *90* (12), 2234-2239.

[46] Arai, T.; Kuroda, H. Distribution behavior of some drug enantiomers in an aqueous two-phase system using counter-current extraction with protein. *Chromatographia* **1991,** *32* (1), 56-60.

[47] Chen, Z.; Zhang, W.; Wang, L.; Fan, H.; Wan, Q.; Wu, X.; Tang, X.; Tang, J. Z. Enantioseparation of Racemic Flurbiprofen by Aqueous Two-Phase Extraction With Binary Chiral Selectors of L-dioctyl Tartrate and L-tryptophan. *Chirality* **2015,** *27* (9), 650-657.

[48] Shinomiya, K.; Kabasawa, Y.; Ito, Y. Enantiomeric Separation of Commercial D,L-Kynurenine with an Aqueous Two-Phase Solvent System by Cross-Axis Coil Planet Centrifuge. *Journal of Liquid Chromatography & Related Technologies* **1998,** *21* (1-2), 135-141.

[49] Ni, Y.; Zhou, J.; Sun, Z. Production of a key chiral intermediate of Betahistine with a newly isolated Kluyveromyces sp. in an aqueous two-phase system. *Process Biochemistry* **2012,** *47* (7), 1042-1048.

[50] Chen, X.; Liu, L.; Jiao, F.; Wang, Z. Extraction of Phenylalanine Enantiomers by Aqueous Two Phase Systems Containing Combinatorial Chiral Selector. *Chinese Journal of Chemistry* **2012,** *30* (4), 965-969.

[51] Ekberg, B.; Sellergren, B.; Albertsson, P.-Å. Direct chiral resolution in an aqueous two-phase system using the counter-current distribution principle. *Journal of Chromatography A* **1985,** *333*, 211-214.

[52] Chen, X.-Q.; Dong, Q.-L.; Yu, J.-G.; Jiao, F.-P. Extraction of Tryptophan enantiomers by aqueous two-phase systems of ethanol and (NH4)2SO4. *Journal of Chemical Technology & Biotechnology* **2013,** *88* (8), 1545-1550.

[53] Tong, S.; Ito, Y.; Ma, Y. Enantioseparation of DL-tryptophan by spiral tube assembly counter-current chromatography and evaluation of mass transfer rate for enantiomers. *Journal of Chromatography A* **2014,** *1374*, 77-84.

[54] Tan, Z.; Li, F.; Zhao, C.; Teng, Y.; Liu, Y. Chiral separation of mandelic acid enantiomers using an aqueous two-phase system based on a thermo-sensitive polymer and dextran. *Separation and Purification Technology* **2017,** *172*, 382-387.

[55] Wang, J.; Liu, Q.; Rong, L.; Yang, H.; Jiao, F.; Chen, X. Enantioselective extraction of phenylsuccinic acid in aqueous two-phase systems based on acetone and β-cyclodextrin derivative: Modeling and optimization through response surface methodology. *Journal of Chromatography A* **2016,** *1467*, 490-496.

[56] Wang, J.; Yang, H.; Yu, J.; Chen, X.; Jiao, F. Macrocyclic β-cyclodextrin derivative-based aqueous-two phase systems: Phase behaviors and applications in enantioseparation. *Chemical Engineering Science* **2016,** *143*, 1-11.

[57] Wu, D.; Zhou, Y.; Cai, P.; Shen, S.; Pan, Y. Specific cooperative effect for the enantiomeric separation of amino acids using aqueous two-phase systems with task-specific ionic liquids. *Journal of Chromatography A* **2015,** *1395*, 65-72.

[58] Wu, H.; Yao, S.; Qian, G.; Yao, T.; Song, H. A resolution approach of racemic phenylalanine with aqueous two-phase systems of chiral tropine ionic liquids. *Journal of Chromatography A* **2015,** *1418*, 150-157.

[59] de Brito Cardoso, G.; Mourão, T.; Pereira, F. M.; Freire, M. G.; Fricks, A. T.; Soares, C. M. F.; Lima, Á. S. Aqueous two-phase systems based on acetonitrile and carbohydrates and their application to the extraction of vanillin. *Separation and Purification Technology* **2013,** *104*, 106-113.

[60] Ferreira, A. M.; Esteves, P. D. O.; Boal-Palheiros, I.; Pereiro, A. B.; Rebelo, L. P. N.; Freire, M. G. Enhanced tunability afforded by aqueous biphasic systems formed by fluorinated ionic liquids and carbohydrates. *Green Chemistry* **2016,** *18* (4), 1070-1079.

[61] Freire, M. G.; Louros, C. L. S.; Rebelo, L. P. N.; Coutinho, J. A. P. Aqueous biphasic systems composed of a water-stable ionic liquid + carbohydrates and their applications. *Green Chemistry* **2011,** *13* (6), 1536-1545.

[62] Sadeghi, R.; Ebrahimi, N.; Tehrani, M. D. Investigation of carbohydrates as non-charged, non-toxic and renewable soluting-out agent for polymer based aqueous biphasic systems implementation. *Polymer* **2016,** *98*, 365-377.

[63] Domínguez-Pérez, M.; Tomé, L. I. N.; Freire, M. G.; Marrucho, I. M.; Cabeza, O.; Coutinho, J. A. P. (Extraction of biomolecules using) aqueous biphasic systems formed by ionic liquids and aminoacids. *Separation and Purification Technology* **2010,** *72* (1), 85-91.

[64] Capela, E. V.; Quental, M. V.; Domingues, P.; Coutinho, J. A. P.; Freire, M. G. Effective separation of aromatic and aliphatic amino acid mixtures using ionic-liquid-based aqueous biphasic systems. *Green Chemistry* **2017,** *19* (8), 1850-1854.

[65] Chakraborty, A.; Sen, K. l-Proline Based Aqueous Biphasic System: Design and Application To Isolate the Alkaline Earths. *Journal of Chemical & Engineering Data* **2014,** *59* (4), 1288-1294.

[66] Sadeghi, R.; Hamidi, B.; Ebrahimi, N. Investigation of Amino Acid–Polymer Aqueous Biphasic Systems. *The Journal of Physical Chemistry B* **2014,** *118* (34), 10285-10296.

[67] Payagala, T.; Armstrong Daniel, W. Chiral ionic liquids: A compendium of syntheses and applications (2005–2012). *Chirality* **2011,** *24* (1), 17-53.

[68] J. Earle, M.; B. McCormac, P.; R. Seddon, K. Diels-Alder reactions in ionic liquids . A safe recyclable alternative to lithium perchlorate-diethyl ether mixtures. *Green Chemistry* **1999,** *1* (1), 23-25.

[69] Kumar, V.; Pei, C.; Olsen, C. E.; Schäffer, S. J. C.; Parmar, V. S.; Malhotra, S. V. Novel carbohydrate-based chiral ammonium ionic liquids derived from isomannide. *Tetrahedron: Asymmetry* **2008,** *19* (6), 664-671.

[70] Van Buu, O. N.; Aupoix, A.; Hong, N. D. T.; Vo-Thanh, G. Chiral ionic liquids derived from isosorbide: synthesis, properties and applications in asymmetric synthesis. *New Journal of Chemistry* **2009,** *33* (10), 2060-2072.

[71] Poletti, L.; Chiappe, C.; Lay, L.; Pieraccini, D.; Polito, L.; Russo, G. Glucose-derived ionic liquids: exploring low-cost sources for novel chiral solvents. *Green Chemistry* **2007,** *9* (4), 337-341.

[72] Chen, X.; Li, X.; Hu, A.; Wang, F. Advances in chiral ionic liquids derived from natural amino acids. *Tetrahedron: Asymmetry* **2008,** *19* (1), 1-14.

[73] Li, M.; De Rooy, S. L.; Bwambok, D. K.; El-Zahab, B.; DiTusa, J. F.; Warner, I. M. Magnetic chiral ionic liquids derived from amino acids. *Chemical Communications* **2009,** *0* (45), 6922-6924.

[74] Bao, W.; Wang, Z.; Li, Y. Synthesis of Chiral Ionic Liquids from Natural Amino Acids. *The Journal of Organic Chemistry* **2003,** *68* (2), 591-593.

[75] Ohno, H.; Fukumoto, K. Amino Acid Ionic Liquids. *Accounts of Chemical Research* **2007,** *40* (11), 1122-1129.

[76] Wang, Z.; Wang, Q.; Zhang, Y.; Bao, W. Synthesis of new chiral ionic liquids from natural acids and their applications in enantioselective Michael addition. *Tetrahedron Letters* **2005,** *46* (27), 4657-4660.

[77] Bonanni, M.; Soldaini, G.; Faggi, C.; Goti, A.; Cardona, F. Novel L-tartaric acid derived pyrrolidinium cations for the synthesis of chiral ionic liquids. *Synlett* **2009,** *2009* (5), 747-750.

[78] Heckel, T.; Winkel, A.; Wilhelm, R. Chiral ionic liquids based on nicotine for the chiral recognition of carboxylic acids. *Tetrahedron: Asymmetry* **2013,** *24* (18), 1127-1133.

[79] Vasiloiu, M.; Cervenka, I.; Gaertner, P.; Weil, M.; Schröder, C.; Bica, K. Amino alcohol-derived chiral ionic liquids: structural investigations toward chiral recognition. *Tetrahedron: Asymmetry* **2015,** *26* (18), 1069-1082.

[80] Malhotra, S. V.; Wang, Y.; Kumar, V. α-Pinene-Based New Chiral Ionic Liquids and their Application as Phase Transfer Catalysts in Enantioselective Addition of Diethylzinc to Aldehydes. *Letters in Organic Chemistry* **2009,** *6* (3), 264-268.

[81] Foreiter, M. B.; Gunaratne, H. Q. N.; Nockemann, P.; Seddon, K. R.; Stevenson, P. J.; Wassell, D. F. Chiral thiouronium salts: synthesis, characterisation and application in NMR enantio-discrimination of chiral oxoanions. *New Journal of Chemistry* **2013,** *37* (2), 515-533.

[82] Foreiter, M. B.; Gunaratne, H. Q. N.; Nockemann, P.; Seddon, K. R.; Srinivasan, G. Novel chiral ionic liquids: physicochemical properties and investigation of the internal rotameric behaviour in the neat system. *Physical Chemistry Chemical Physics* **2014,** *16* (3), 1208-1226.

[83] Bica, K.; Gaertner, P. Applications of Chiral Ionic Liquids. *European Journal of Organic Chemistry* **2008,** *2008* (19), 3235-3250.

[84] Soares, B.; Passos, H.; Freire, C. S. R.; Coutinho, J. A. P.; Silvestre, A. J. D.; Freire, M. G. Ionic liquids in chromatographic and electrophoretic techniques: toward additional improvements in the separation of natural compounds. *Green Chemistry* **2016,** *18* (17), 4582-4604.

[85] Yue, Y.; Jiang, X.-Y.; Yu, J.-G.; Tang, K.-W. Enantioseparation of mandelic acid enantiomers in ionic liquid aqueous two-phase extraction systems. *Chemical Papers* **2014,** *68* (4), 465-471.

[86] Tang, F.; Zhang, Q.; Ren, D.; Nie, Z.; Liu, Q.; Yao, S. Functional amino acid ionic liquids as solvent and selector in chiral extraction. *Journal of Chromatography A* **2010,** *1217* (28), 4669-4674.

[87] Zgonnik, V.; Zedde, C.; Genisson, Y.; Mazieres, M.-R.; Plaquevent, J.-C. Synthesis of chiral ionic liquids by ion cross-metathesis: en route to enantioselective water-ionic liquid extraction (EWILE), an eco-friendly variant of the ELLE process. *Chemical Communications* **2012,** *48* (26), 3185-3187.

[88] Huang, X.; Wu, H.; Wang, Z.; Luo, Y.; Song, H. High resolution of racemic phenylalanine with dication imidazolium-based chiral ionic liquids in a solid-liquid two-phase system. *Journal of Chromatography A* **2017,** *1479*, 48-54.

[89] Wang, Z.; Hou, Z.; Yao, S.; Lin, M.; Song, H. A new and recyclable system based on tropin ionic liquids for resolution of several racemic amino acids. *Analytica Chimica Acta* **2017,** *960*, 81-89.

[90] Marwani, H. M.; Bakhsh, E. M.; Al-Turaif, H. A.; Asiri, A. M.; Khan, S. B. Enantioselective separation and detection of D-phenylalanine based on newly developed chiral ionic liquid immobilized silica gel surface. *International Journal of Electrochemical Science* **2014,** *9*, 7948-7964.

[91] Qian, G.; Song, H.; Yao, S. Immobilized chiral tropine ionic liquid on silica gel as adsorbent for separation of metal ions and racemic amino acids. *Journal of Chromatography A* **2016,** *1429*, 127-133.

[92] Yang, L.; Hu, X.; Guan, P.; Li, J.; Wu, D.; Gao, B. Molecularly imprinted polymers for the selective recognition of l-phenylalanine based on 1-butyl-3-methylimidazolium ionic liquid. *Journal of Applied Polymer Science* **2015,** *132* (36).

[93] Liu, Y.; Tian, A.; Wang, X.; Qi, J.; Wang, F.; Ma, Y.; Ito, Y.; Wei, Y. Fabrication of chiral amino acid ionic liquid modified magnetic multifunctional nanospheres for centrifugal chiral chromatography separation of racemates. *Journal of Chromatography A* **2015,** *1400*, 40-46.

[94] Borman, S. Asymmetric Catalysis Wins: Chemistry Nobel honors Knowles, Noyori, Sharpless for chiral syntheses. *Chemical & Engineering News* **2001,** *79* (42), 5.

3.1.1. Aqueous biphasic systems using chiral ionic liquids bearing chiral cations for the enantioseparation of mandelic acid enantiomers

This section is based on e Silva, F. A.; Kholany, M.; Sintra, T. E.; Caban, M.; Stepnowski, P.; Ventura, S. P. M.; Coutinho, J. A. P. Aqueous biphasic systems using chiral ionic liquids for the enantioseparation of mandelic acid enantiomers. *Solvent Extraction and Ion Exchange* **2018**, *36* (5), accepted.

Contributions: J.A.P.C. conceived and directed this work. Francisca A. e Silva, M.K., T.E.S. and M.C. acquired the experimental data. In particular, Francisca A. e Silva acquired data on the partition of mandelic acid. Francisca A. e Silva, S.P.M.V. and J.A.P.C. interpreted the experimental data. Francisca A. e Silva and J.A.P.C. wrote the manuscript with contributions from the remaining authors.

Abstract

This work aims at extending the applicability of chiral ABS to enantioseparations by using CILs simultaneously as phase forming agents and chiral selectors. After determining the ternary phase diagrams of ABS composed of CILs and salts, these were used to ascertain the CIL structure on the ABS aptitude to separate mandelic acid enantiomers. Representative CIL-based ABS were further employed in optimization studies, where the mandelic acid content, temperature, tie-line length (TLL), salt and phases weight ratio were studied. The influence of these parameters is shown to be highly dependent on the CIL-based ABS, however the results here reported suggest that the key driving the enantioseparation in these ABS is a combination of the enantiorecognition ability of a given CIL with the solubility of mandelic acid in the corresponding CIL-rich phase.

Introduction

Given the limited application of CILs in the development of ABS for chiral resolution purposes,[1, 2] it is here intended to contribute towards the enlargement of CIL-based ABS database and to provide further insights on their enantioseparation aptitude.

Initially on this work, the phase diagrams of ABS composed of CILs based on quinine, L-proline and L-valine and three salts (viz. K_3PO_4, K_2HPO_4 and K_2CO_3) were determined. The low toxicity, significant water solubility and proved chiral recognition aptitude of this set of CILs recently synthesized by some of us showcase the interest of their implementation in chiral ABS.[3] Their enantioseparation aptitude was further evaluated and optimized using mandelic acid, a key precursor in chiral pharmaceuticals manufacturing, as model chiral compound.

Experimental

Materials

Six cationic CILs were synthesized in this work: 1-methyl quininium methylsulfate, $[C_1Qui][C_1SO_4]$; *N,N*-dimethyl-L-proline methyl ester iodide, $[C_1C_1C_1Pro]I$; *N,N*-dimethyl-L-proline methyl ester methylsulfate, $[C_1C_1C_1Pro][C_1SO_4]$; *N,N*-diethyl-L-proline ethyl ester bromide, $[C_2C_2C_2Pro]Br$; *N,N,N*-trimethyl-L-valinolium iodide, $[C_1C_1C_1Val]I$; and *N,N,N*-trimethyl-L-valinolium methylsulfate, $[C_1C_1C_1Val][C_1SO_4]$. For the synthesis, the reagents used were quinine, Qui (purity = 98%), iodomethane, CH_3I (purity = 99%), dimethyl sulfate, $(CH_3)_2SO_4$ (purity = 99%), dichloromethane anhydrous, CH_2Cl_2 (purity = 99.8%), ethanol, C_2H_5OH (purity = 99.8%), acetone, C_3H_6O (HPLC grade), potassium carbonate, K_2CO_3 (purity ≥ 99%), L-proline, L-Pro (purity = 99%), bromoethane, CH_3CH_2Br (purity = 98%), acetonitrile, CH_3CN (purity = 99.8%), chloroform, $CHCl_3$ (purity = 99%), L-valine, L-Val (purity = 98%), tetrahydrofuran anhydrous, C_4H_8O (purity = 99.9%), sodium borohydride, $NaBH_4$ (purity = 99%), sulfuric acid, H_2SO_4 (purity = 99.9%), methanol, CH_3OH (purity = 99%), ethyl acetate, $C_4H_8O_2$ (purity = 99.8%), potassium hydroxide, KOH (purity = 90%), formic acid, HCOOH (purity = 98%), formaldehyde, CH_2O (37 wt % in water solution) and hydrochloric acid, HCl (37 wt% in water solution) acquired from Sigma-Aldrich. The salts used in ABS were potassium phosphate tribasic, K_3PO_4 (purity = 97%), K_2CO_3 (purity ≥ 99%) and di-potassium hydrogen phosphate trihydrate, $K_2HPO_4{\cdot}3H_2O$ (extra pure) and were respectively purchased at Alfa-Aesar, Sigma-Aldrich and Scharlau. The enantiomers used were *R*-(-)-mandelic acid, *R*-MA (purity = 99%), and *S*-(+)-mandelic

acid, *S*-MA (purity = 99%), both supplied by Acros Organics. The chemical structures and abbreviations of the CILs and mandelic acid enantiomers are depicted in Figure 3.5.

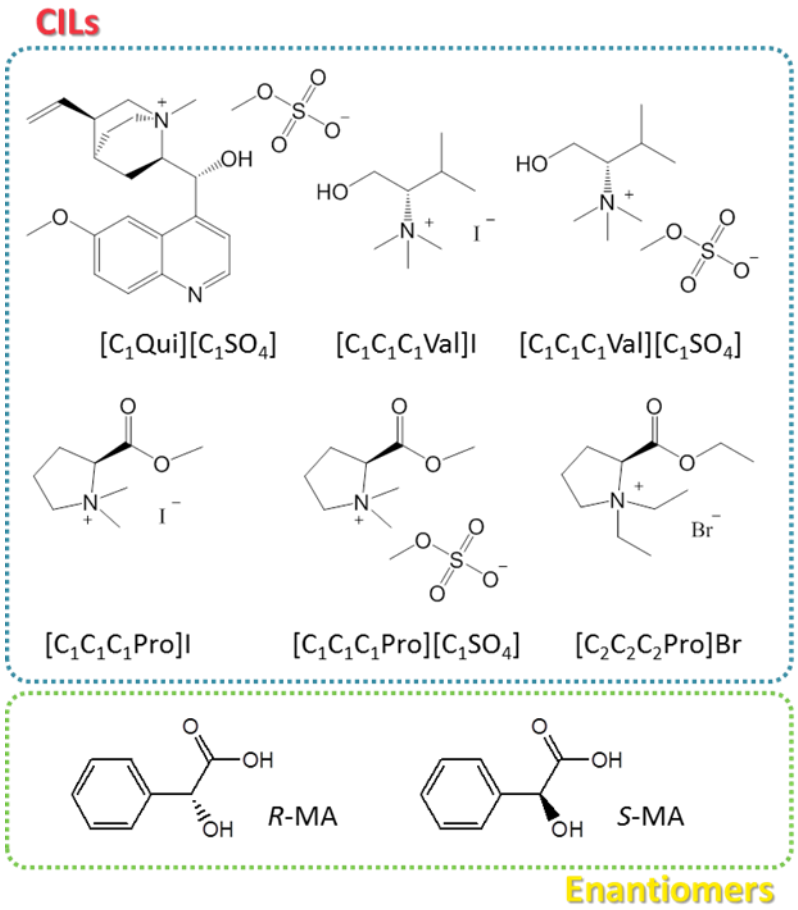

Figure 3.5. Chemical structures and abbreviations of the CILs and mandelic acid enantiomers investigated.

For the HPLC-DAD analysis of the mandelic acid enantiomers, copper (II) sulphate pentahydrate, $CuSO_4 \cdot 5H_2O$ (purity > 98%), L-phenylalanine, L-Phe (purity > 98%), purchased from AnalaR and Alfa Aesar, respectively, and methanol (HPLC grade), acquired from Fisher Chemical, were used for the mobile phase. Ammonia solution at 25% was obtained from Chem-Lab. Ultra-pure water (double distilled and then treated with a Milli-Q plus 185 water purification apparatus) was used for the HPLC analysis. Syringe filters (0.45 µm) and regenerated cellulose membrane filters (0.45 µm), acquired at Specanalitica and Sartorius, respectively, were used during filtration steps.

Synthesis of the chiral ionic liquids based on quinine, L-proline and L-valine

The six CILs here used were synthesized in our laboratory according to well-established protocols.[3] Briefly, an alkylation reaction between dimethyl sulphate and quinine yielding $[C_1Qui][C_1SO_4]$ was performed, L-valine-based CILs were obtained in a three step synthesis entailing reduction of L-valine, Eschweiler-Clark reaction and *N*-alkylation and L-proline-based CILs were synthesized by alkylation reactions between L-proline and iodomethane, bromoethane or dimethyl sulphate affording $[C_1C_1C_1Pro]I$, $[C_2C_2C_2Pro]Br$ or $[C_1C_1C_1Pro][C_1SO_4]$, respectively. Relevant features of CILs, namely melting temperature (T_m, °C), decomposition temperature (T_d, °C) and specific rotations ($[\alpha]_D^{25}$) can be consulted in Appendix D, Table D1.[3]

Determination of the phase diagrams and tie-lines

The ternary phase diagrams of the ABS composed of CILs and K_3PO_4, K_2CO_3 or K_2HPO_4 were determined through the cloud point titration method at 25 (± 1) °C.[4] To aqueous solutions containing circa 6-70 wt% of CILs, the alternate drop-wise addition of an aqueous solution of salt at circa 40 wt%-50 wt% and of pure water was performed under constant stirring. The repetition of this procedure allows, by turns, entering the biphasic region (turbid solution) and reaching the monophasic region (clear solution), respectively. By weight quantification (± 10^{-4} g) after the addition of each solution, the ternary systems compositions of the phase diagram were determined. The experimental binodal curves were fitted by Equation 3.1.[5]

$$[\mathrm{CIL}] = A\mathrm{e}^{[(B[\mathrm{salt}])^{0.5} - (C[\mathrm{salt}]^3)]} \qquad (\textbf{\textit{Equation 3.1}})$$

where [CIL] and [salt] are the CIL and salt weight fraction percentages, respectively, while *A*, *B* and *C* correspond to the fitting parameters. The tie-lines were gravimetrically determined, as originally proposed by Merchuk et al.[5] A ternary mixture composition formed by CIL + salt + water located at the biphasic region was prepared within ± 10^{-4} g, vigorously stirred and left to equilibrate at 25 (± 1) °C for at least 12 h. Both phases were then separated and weighed. The lever-arm rule by the relationship between the top CIL-rich phase and the overall system weights allowed calculating each tie-line. Detailed guidelines on the tie-lines determination can be found elsewhere.[4]

Separation of mandelic acid enantiomers using ABS

Mixture points localized in the biphasic region of the phase diagrams were selected to conduct studies on racemic mandelic acid enantioseparation. The systems were gravimetrically prepared (within ± 10^{-4} g) by adding the correct amounts of CIL, salt and water along with equal amounts of two aqueous solutions of *R*-mandelic acid and *S*-mandelic acid both prepared at the same concentrations (viz. 10, 50 or 100 $mg.mL^{-1}$) to yield the desired final content in the ABS. Throughout this work, the evaluation of distinct conditions was carried out: CIL's structure, enantiomers content, temperature, TLLs, salt and mixture points along the same TL. The overall mixture compositions and conditions are detailed in Appendix D, Table D2. The CILs were placed in contact with the mandelic acid enantiomers in aqueous solution for at least 12 h under constant stirring (300 rpm) at the desired temperature, to promote specific interactions between the CIL and the target enantiomers, as recommended elsewhere.[1] The salt was added after such a period to induce liquid-liquid demixing. To this a period of equilibration of at least 12 h under the desired temperature followed, to guarantee complete separation of the phases and partition of the enantiomers among phases. The phases, the top being CIL-rich and the bottom being salt-rich, were then separated and weighed (within ± 10^{-4} g). CIL-rich phases were submitted to HPLC-DAD analysis for mandelic acid enantiomers quantification. In order to estimate the average extraction/enantioseparation parameters and the corresponding standard deviations, triplicates were performed.

The percentage extraction efficiencies of *R* and *S*-mandelic acid ($EE_{\text{R-MA}}$ and $EE_{\text{S-MA}}$, %) were separately determined according to the Equation 3.2:

$$EE_{R/S-MA}, \% = \frac{\mathrm{m}^{\mathrm{CIL}}_{R/S-\mathrm{MA}}}{\mathrm{m}^{0}_{R/S-\mathrm{MA}}} \times 100 \qquad (\textbf{\textit{Equation 3.2}})$$

where $\mathrm{m}^{\mathrm{CIL}}_{R/S-\mathrm{MA}}$ is the mass of *R* or *S*-mandelic acid present in the CIL-rich phase and $\mathrm{m}^{0}_{R/S-\mathrm{MA}}$ is the mass of *R* or *S*-mandelic acid originally added to the ABS.

The enantiomeric excess (*e.e.*, %) present in the CIL-rich phase was calculated in accordance to Equation 3.3:

$$e.e., \% = \frac{\mathrm{m}^{\mathrm{CIL}}_{S-\mathrm{MA}} - \mathrm{m}^{\mathrm{CIL}}_{R-\mathrm{MA}}}{\mathrm{m}^{\mathrm{CIL}}_{S-\mathrm{MA}} + \mathrm{m}^{\mathrm{CIL}}_{R-\mathrm{MA}}} \times 100 \qquad (\textbf{\textit{Equation 3.3}})$$

in which $\mathrm{m}^{\mathrm{CIL}}_{S-\mathrm{MA}}$ and $\mathrm{m}^{\mathrm{CIL}}_{R-\mathrm{MA}}$ are the mass of *S* and *R*-mandelic acid present in the CIL-rich phase, respectively.

Mandelic acid enantiomers quantification

Mandelic acid enantiomers were quantified by HPLC-DAD using an analytical method adapted from Yue et al. with modifications.[6] The liquid chromatograph HPLC Elite LaChrom (VWR Hitachi) used for this purpose was equipped with a diode array detector (DAD) l-2455, column oven l-2300, auto-sampler l-2200 and pump l-2130. A C_{18} reversed-phase analytical column (LiChrospher 100 RP-18, 5 µm, 250 mm × 4 mm i.d.) linked to a guard column (5 µm, 4 mm × 4 mm) with the same stationary phase was used. The column oven and autosampler were operated at controlled temperature of 22 °C and 25 °C, respectively. The mobile phase was made up of water:methanol [85:15 (v/v)], 2 mM L-phenylalanine and 1 mM $CuSO_4$ at pH = 4.00 (± 0.02), adjusted by adding an ammonia aqueous solution at 5 wt%. The separation was carried out using isocratic elution at a flow rate of 0.8 $mL.min^{-1}$ and the injection volume was 20 µL. DAD was set to measure the spectrum from 200 to 600 nm, with a specific wavelength of 270 nm being used for *R*-mandelic acid and *S*-mandelic acid quantification. Calibration curves were previously determined using stock solutions prepared in water:methanol [85:15 (v/v)] at concentrations of 10 – 500 $\mu g.mL^{-1}$ of each enantiomer. The *R* enantiomer elutes first, at a retention time of around 11.7 min, followed by *S* eluting at approximately 13.2 min. The LOD and LOQ were, respectively, 5 $\mu g.mL^{-1}$ and 10 $\mu g.mL^{-1}$ for both enantiomers. Intra and inter-day precisions were 0.27-3.29 % and 1.39-1.88 % for *R*-MA and 0.79-5.59 % and 4.01-6.40 % for *S*-MA, respectively. Intra and inter-day accuracies were 95.8-127 % and 96.4-118.4 % for *R*-MA, while for *S*-MA they were of 97.3-126.2 % and 93.0-124.6%, respectively. The CIL-rich phases were diluted using water:methanol [85:15 (v/v)] and filtered using syringe filters (0.45 µm). At least two injections *per* sample were done.

Results and discussion

Ternary phase diagrams and tie-lines

The knowledge of the CIL-based ABS phase diagrams is essential for the development of enantioseparations. To accomplish this, the ternary phase diagrams composed of five CILs, $[C_1C_1C_1Val]I$, $[C_1C_1C_1Val][C_1SO_4]$, $[C_2C_2C_2Pro]Br$, $[C_1C_1C_1Pro]I$ and $[C_1Qui][C_1SO_4]$, and K_3PO_4, a strong salting-out agent,[4] were measured at 25 (± 1) °C. $[C_1C_1C_1Pro][C_1SO_4]$ was not able to form ABS with K_3PO_4. Two additional salts, K_2CO_3 and K_2HPO_4, were paired with $[C_2C_2C_2Pro]Br$ to evaluate the role of salt type upon ABS formation.

The ternary phase diagrams are shown in Figures 3.6 and 3.7 in weight fraction. All detailed experimental data related (ternary phase diagrams weight fraction compositions, Equation 3.1 regression parameters and TL information) are provided as Appendix D (Table D3 – Table D11). The ternary phase diagrams determined in this study provide information on the CILs and salt role upon ABS formation (Figures 3.6 and 3.7). The biphasic zone is placed above the binodal curve meaning that the broader this is the more prone is the CIL to form ABS.

As observed in Figure 3.6, the CILs' ability to form ABS with K_3PO_4 can be ranked as follows (at fixed CIL weight fraction composition of 10 wt%): $[C_1Qui][C_1SO_4]$ > $[C_1C_1C_1Val]I$ > $[C_1C_1C_1Val][C_1SO_4]$ > $[C_2C_2C_2Pro]Br$ > $[C_1C_1C_1Pro]I$. Within the CILs studied, it is possible to infer on both cation ($[C_1Qui][C_1SO_4]$ *vs.* $[C_1C_1C_1Val][C_1SO_4]$ *vs.* $[C_1C_1C_1Pro][C_1SO_4]$) and anion role ($[C_1C_1C_1Val]I$ *vs.* $[C_1C_1C_1Val][C_1SO_4]$) on the ABS formation. The cation effect is driven by the hydrophobicity-hydrophilicity of the cation, where the order $[C_1Qui]^+$ > $[C_1C_1C_1Val]^+$ > $[C_1C_1C_1Pro]^+$ directly correlates with the octanol-water partition coefficients of their precursors (log $K_{o/w}$ of 3.44, -0.08 and -0.10 for quinine, valinol and proline methyl ester, respectively[7]). In close agreement with previous studies,[4] the more hydrophobic the CIL the higher is its aptitude to form ABS. It should be highlighted that, although valinol and proline methyl ester possess similar log $K_{o/w}$, $[C_1C_1C_1Pro][C_1SO_4]$ failed to induce phase separation in presence of K_3PO_4. This can be attributed to the higher hydrophobicity of the cation when compared to the parent compound, due to alkylation:

while the addition of 3 methyl groups is done to valinol, only 2 methyl groups are added to proline methyl ester (cf. Figure 3.5).

In general, the ability of an IL anion to create ABS is related with the decrease in their hydrogen-bond accepting ability (*β*).[8, 9] The aforementioned rank places I^- as a better two-phase formation inducer than $[C_1SO_4]^-$, in good agreement with their relative position in the scale of hydrogen bond basicity of ILs proposed by Cláudio et al.[10] Although $[C_2C_2C_2Pro]Br$ *vs.* $[C_1C_1C_1Pro]I$ do not allow direct comparisons, it should be noted that Br^- is a stronger hydrogen-bond acceptor than I^-,[10] being thus expected to yield smaller biphasic regions. Since the opposite is observed, the effect of longer alkyl chains in $[C_2C_2C_2Pro]Br$ may overwhelm that of the anion nature (cf. Figure 3.5).

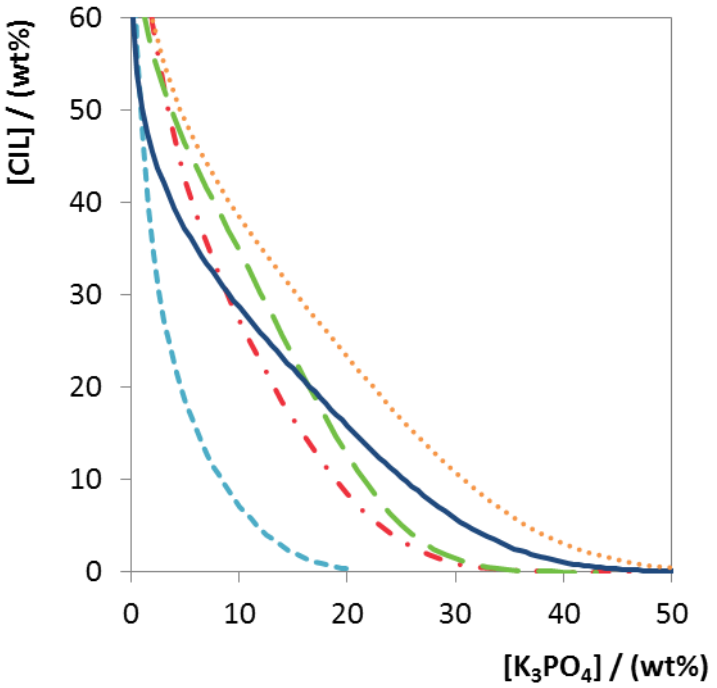

Figure 3.6. Phase diagrams of ABS composed of CILs and K_3PO_4 at 25 (± 1) °C: $[C_1Qui][C_1SO_4]$ (blue dashed line), $[C_1C_1C_1Val]I$ (red dashed-dotted line), $[C_1C_1C_1Val][C_1SO_4]$ (green dashed line), $[C_2C_2C_2Pro]Br$ (dark blue solid line) and $[C_1C_1C_1Pro]I$ (orange dotted line).

Figure 3.7 shows the ability of three salts to promote phase separation, which can be rated as follows (at fixed CIL weight fraction composition of 10 wt%): $K_3PO_4 \approx K_2HPO_4 >$

K_2CO_3. This ranking follows the Hofmeister series as previously established in the literature for ABS composed of ILs and salts.[11, 12]

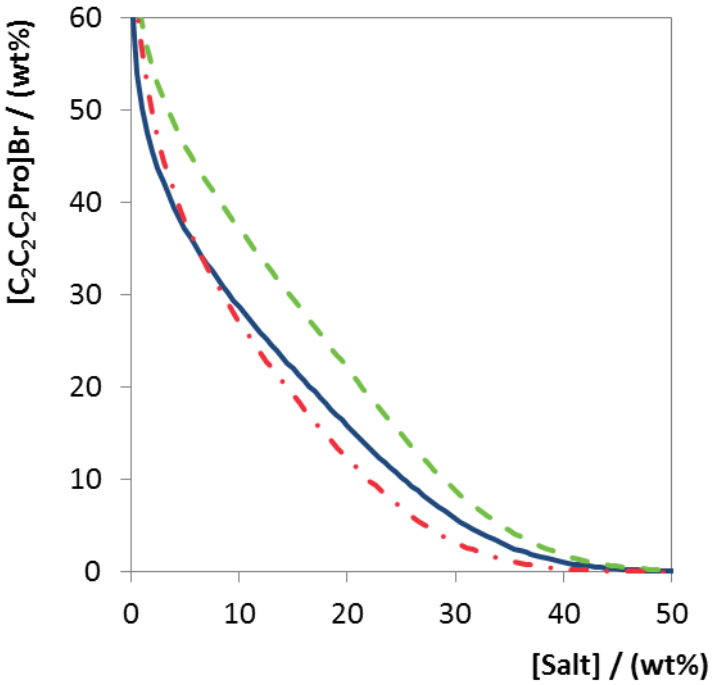

Figure 3.7. Phase diagrams of ABS composed of $[C_2C_2C_2Pro]Br$ and salts at 25 (± 1) °C: K_3PO_4 (dark blue solid line), K_2HPO_4 (red dashed-dotted line) and K_2CO_3 (green dashed line).

CILs-based ABS: evaluating the impact of CILs structures in enantioseparation

An initial screening comprising the five CIL-based ABS developed (Appendix D, Table D2) was done in order to understand the role of the cation/anion structures on the enantioseparation of *R*- and *S*- mandelic acid structures. The extraction efficiencies ($EE_{R\text{-}MA}$ and $EE_{S\text{-}MA}$) as well as enantiomeric excesses (*e.e.*) obtained are depicted in Figure 3.8 and detailed in Appendix D (Table D12). The $EE_{R/S\text{-}MA}$ values reveal a similar partition of mandelic acid between the two phases, or a preferential partition of mandelic acid for the salt-rich phase. Under the conditions adopted (initial biphasic mixture compositions, temperature and mandelic acid content – Table D2 in Appendix D), all CILs exhibited preferable chiral recognition for the *S*-mandelic acid over the *R* enantiomer, with modest *e.e.* (1.61 ± 0.92 % to 17.37 ± 1.92 %). Moreover, valine and proline-based CILs seem to be more promising than the quinine-based CIL.

In general, electrostatic interactions between mandelic acid and the CIL cations play an important role in the "three-point model"-based enantiorecognition process, since mandelic acid is deprotonated (pKa_1 = 3.75 and pKa_2 = 13.57, Figure D1 in Appendix D)[7] under the alkaline pH induced by K_3PO_4. Given the chemical structures of the CILs and mandelic acid (cf. Figure 3.5) and the results found, it seems that other interactions can act in the mandelic acid enantiomeric discrimination by valine and proline-based CILs. Moreover, and contrarily to what is reported in literature when aromatic chiral recognition agents and solutes are present,[13-15] in this specific case, π-π stacking does not seem to contribute to the enantioseparation of racemic mandelic acid, since $[C_1Qui][C_1SO_4]$ (the only CIL bearing aromatic rings) yielded the lowest *e.e.*.

It has been previously shown that factors other than the CIL structure may affect the enantioseparation ability and that such impact is dependent on the ABS phase formers.[1, 2] Bearing this in mind, optimization studies will be carried for two CILs, the least and the most performant ones, aiming to gain further insight on the phenomena governing enantioseparations in these CIL-based ABS.

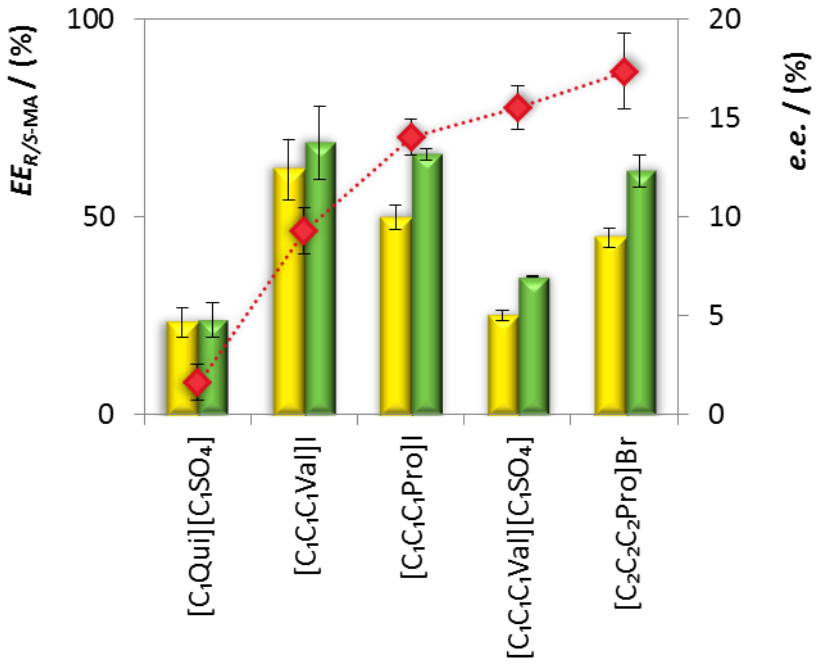

Figure 3.8. Extraction efficiencies ($EE_{R\text{-}MA}$, yellow bars and $EE_{S\text{-}MA}$, green bars) and enantiomeric excesses (*e.e.*, diamonds) obtained with five CIL-based ABS at 25 (± 1) °C.

$[C_1Qui][C_1SO_4]$-based ABS: evaluating the impact of mandelic acid content, temperature and TLL in enantioseparation

$[C_1Qui][C_1SO_4]$, here identified as the weakest enantiorecognition agent, was used for further optimization to understand whether its enantioseparation ability could be improved by modifying the operational conditions. Mandelic acid content, TLL (varied by changing the mixture point) and temperature were evaluated, as presented in Appendix D (Table D2). The results obtained are depicted in Figure 3.9 and detailed in Appendix D (Table D12) and suggest that, although having distinct effects on the extraction and separation of mandelic acid enantiomers, the parameters evaluated lead to better enantioseparations [from nearly 0 to a maximum *e.e.* of 7.88 ± 0.70 % obtained with $[C_1Qui][C_1SO_4]$-based ABS at 15 (± 1) °C].

While a decline of about 15 % on $EE_{R/S\text{-}MA}$ is observed, an increase of circa 3.8 times in *e.e.* occurs by raising mandelic acid content in the system (Figure 3.9A). So, the enantioseparation seems to be ruled by a compromise between the solubility of mandelic acid in the CIL-rich phase and the more favorable interactions between the CIL and *S*-mandelic acid. The TLL effect is marginal under the conditions studied in this work (Figure 3.9B). Temperature, in turn, has a significant impact in the $EE_{R/S\text{-}MA}$, likely as a result of the increasing solubility of mandelic acid in the CIL-rich phase at 45 °C (Figure 3.9C). Furthermore, Figure 3.9C provides support of a trade-off between $EE_{R/S\text{-}MA}$ and *e.e.* parameters. *e.e.* is higher for lower temperatures (e.g., 15 °C) where the molecular motions are slower, thus favoring the "*S*-mandelic acid-$[C_1Qui][C_1SO_4]$" interactions. The same behavior was previously observed in a work on the chiral separation of phenylalanine enantiomers with CIL-based ABS.[1]

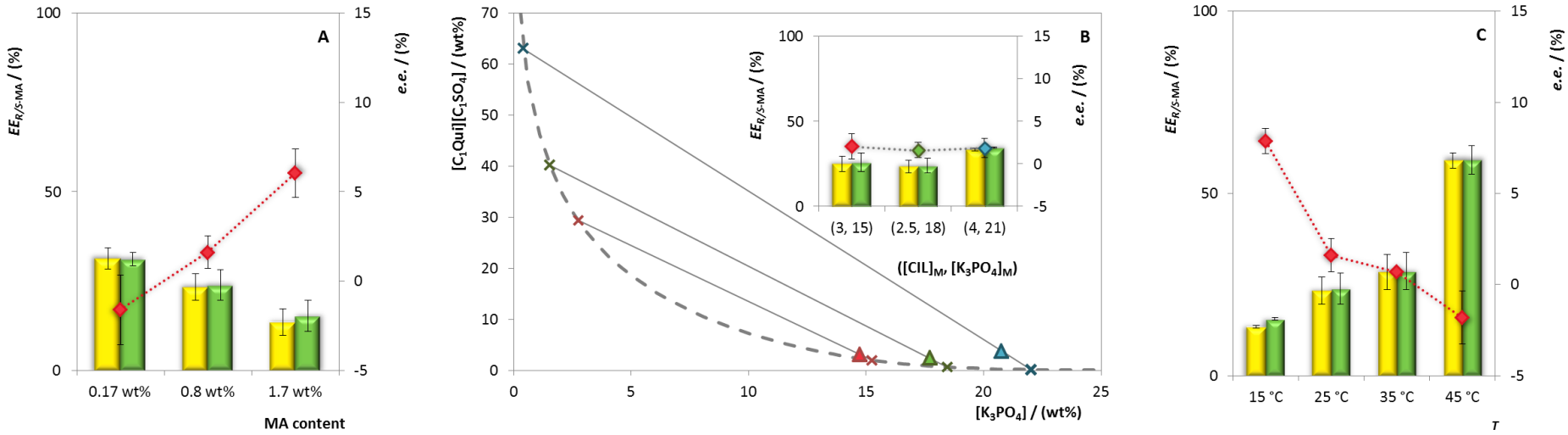

Figure 3.9. Impact of mandelic acid content (A), TLL (B) and temperature (C) on the extraction efficiencies ($EE_{R\text{-}MA}$, yellow bars and $EE_{S\text{-}MA}$, green bars) and enantiomeric excesses (*e.e.*, diamonds) obtained with ABS composed of $[C_1Qui][C_1SO_4]$ and K_3PO_4.

$[C_2C_2C_2Pro]Br$-based ABS: evaluating the impact of mandelic acid content, temperature, TLL, salt and phases' weight ratio in enantioseparation

Since the best enantioseparations were achieved with $[C_2C_2C_2Pro]Br$ and $[C_1C_1C_1Val][C_1SO_4]$, the role of the operational conditions on the performance of these ABS was further studied. The $[C_2C_2C_2Pro]Br$ was used as a model chiral selector to evaluate the influence of mandelic acid content, temperature, TLL, salt and the phases' weight ratio, as specified in Table D2 in Appendix D. Figure 3.10 overviews the results obtained with ABS composed of $[C_2C_2C_2Pro]Br$ and K_3PO_4 and reveals a complex scenario regarding the impact of distinct operational conditions upon mandelic acid enantioseparation (detailed data provided in Appendix D, Table D12). When mandelic acid content is increased from 0.17 wt% to 1.7 wt% in the ABS, a 37% drop in $EE_{R/S\text{-}MA}$ is observed. The maximum enantioseparation is achieved at intermediate mandelic acid concentration (*e.e.* = 17.37 ± 1.92 %) - Figure 3.10A - this seeming to be the optimal mandelic acid/CIL compositions to favor "$[C_2C_2C_2Pro]Br$-*S*-mandelic acid" interactions. A shift towards *R*-enantiomer higher partitions to the CIL-rich phase seems to occur (negative *e.e.* values are merely indicative of a *R*-mandelic acid enriched mixture) at cost of *e.e.* at the lowest (*e.e.* of 4.91 ± 1.34 %) and highest (*e.e.* of 6.40 ± 2.92 %) concentrations ascertained. Although this behavior may seem odd, similar results are found in literature, showing that low to intermediate concentrations are enantioseparation boosters.[16-20] It should however be emphasized that the type of system, chiral selector, operational conditions and racemic compound may lead to different dependencies.[2, 6, 21, 22] The lowest concentration of mandelic acid investigated seems to restrict the occurrence of "$[C_2C_2C_2Pro]Br$-*S*-mandelic acid" interactions, thus limiting enantioseparation.[2]

The TLL influences both the extraction and enantioseparation performance of $[C_2C_2C_2Pro]Br$-based ABS, as shown in Figure 3.10B. Mixture points yielding longer TLLs, i.e., higher concentrations of both CIL and K_3PO_4 in both top and bottom phases, respectively, promote the extraction of mandelic acid towards the CIL-rich phase. This may be explained in the light of hydrophobic interactions occurring between the mandelic

acid and the $[C_2C_2C_2Pro]Br$ in the top phase. However, enantioseparations are less efficient under such conditions, indicating that the relative amounts of CIL/salt in the top phase and mandelic acid in the system are crucial to design efficient CIL-based ABS. Contrarily to what was observed for $[C_1Qui][C_1SO_4]$, the temperature does not significantly affect $EE_{R/S\text{-}MA}$ or *e.e.* (Figure 3.10C). Therefore, both the solubility of mandelic acid in the $[C_2C_2C_2Pro]Br$-rich phase and the specific interactions taking place between the CIL and the *S*-enantiomer seem to be unaffected on the temperature range studied.

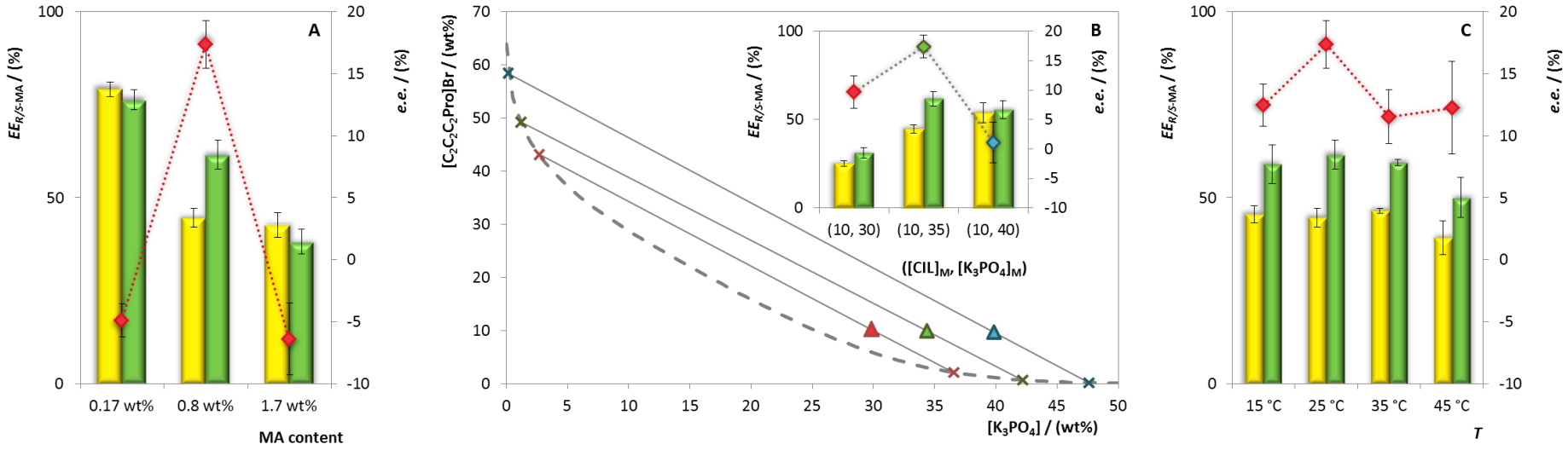

Figure 3.10. Impact of mandelic acid content (A), TLL (B) and temperature (C) on the extraction efficiencies ($EE_{R\text{-}MA}$, yellow bars and $EE_{S\text{-}MA}$, green bars) and enantiomeric excesses (*e.e.*, diamonds) obtained with ABS composed of $[C_2C_2C_2Pro]Br$ and K_3PO_4.

The action of two additional salts (K_2HPO_4 and K_2CO_3) on the enantioseparation ability of $[C_2C_2C_2Pro]Br$-based ABS was evaluated. It has been widely shown that the salt used has an important influence in the extraction and separation of a solute using ABS,[4] in particular if enantiomeric separations are targeted.[2] Figure 3.11 shows that also here the enantioseparation is dependent on the salt used. Under the conditions assessed, K_3PO_4 ranks first (*e.e.* = 17.37 ± 1.92 %), followed by K_2CO_3 (*e.e.* = 5.79 ± 0.12 %), while K_2HPO_4 completely failed to separate mandelic acid enantiomers (*e.e.* = 0.82 ± 0.18 %) (detailed data provided in Appendix D, Table D12). These salts create an alkaline pH in ABS ($pH^{CIL}_{K_2HPO_4}$ = 8.32 ± 0.02, $pH^{CIL}_{K_2CO_3}$ = 11.68 ± 0.02 and $pH^{CIL}_{K_3PO_4}$ = 12.99 ± 0.02), so that mandelic acid is deprotonated (pKa_1 = 3.75 and pKa_2 = 13.57)[7]. In presence of K_3PO_4 mandelic acid deprotonates displaying a distribution of approximately 79 % and 21% for mono- and divalent ions, respectively.[7] The amount of divalent ions further decreases with decreasing pH, down to around 1.34 % (K_2CO_3) and completely vanishes at pH 9.2 (Figure D1 in Appendix D).[7] Better recognition ability seems to be accomplished when divalent mandelic acid ions are present in solution, in agreement with previous insights gathered in the chiral separation of mandelic acid in micellar systems containing copper-β-cyclodextrin-complexes as chiral selector.[23] Alongside, mandelic acid partitions majorly to the CIL-rich phase (more hydrophobic) when K_2HPO_4 is used ($EE_{R\text{-MA}}$ = 81.90 ± 5.59 % and $EE_{S\text{-MA}}$ = 81.63 ± 5.08 %), while an almost equivalent distribution of mandelic acid between the two phases is observed for K_3PO_4 ($EE_{R\text{-MA}}$ = 44.62 ± 2.50 % and $EE_{S\text{-MA}}$ = 61.58 ± 3.96 %) and K_2CO_3 ($EE_{R\text{-MA}}$ = 55.13 ± 0.03 % and $EE_{S\text{-MA}}$ = 62.61 ± 2.31 %). Divalent mandelic acid is more polar than its monovalent congener, what may explain this extraction profile. It should be highlighted that the enantioseparation in these ABS may be additionally influenced by specific interactions promoted by the salt ions or distinct solubility profiles exhibited by mandelic acid in the corresponding ABS phases.

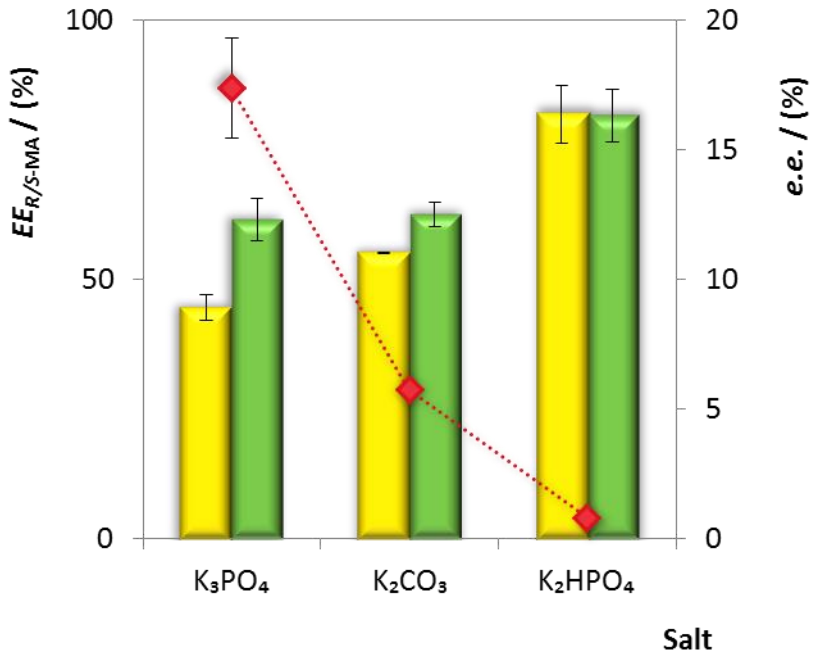

Figure 3.11. Impact of salt on the extraction efficiencies ($EE_{R\text{-}MA}$, yellow bars and $EE_{S\text{-}MA}$, green bars) and enantiomeric excesses (*e.e.*, diamonds) obtained with $[C_2C_2C_2Pro]Br$-based ABS.

The body of results hitherto reported provides some evidence that the performance of CIL-based ABS in the enantioseparation of mandelic acid may be improved by manipulating the solubility of mandelic acid in the CIL-rich phase. At first glance, the preferential partition of the *S*-enantiomer to the $[C_2C_2C_2Pro]Br$-rich phase is enhanced by constraining the mandelic acid solubility. To confirm this hypothesis, partition studies were carried out along the same TL for two distinct ABS (K_3PO_4- and K_2HPO_4-based), meaning that different weight ratios were used while the phases compositions were kept constant (Figure 3.12 and Table D12 from Appendix D). As shown in Figure 3.12A for the K_3PO_4-based ABS, almost complete partition of mandelic acid towards the $[C_2C_2C_2Pro]Br$-rich phase occurs for systems possessing larger CIL-rich phases ($EE_{R\text{-}MA}$ = 87.17 ± 7.70 % - 94.51 ± 5.94 % and $EE_{S\text{-}MA}$ = 86.63 ± 8.15 % - 92.81 ± 5.79 %). When the phases weight ratio is decreased, the CIL-rich phase becomes saturated, as revealed by the decreasing of mandelic acid partition ($EE_{R\text{-}MA}$ = 37.32 ± 2.74 % and $EE_{S\text{-}MA}$ = 48.10 ± 2.62). In previous studies distinct solubility profiles of the phenylalanine enantiomers in CILs phases were also observed.[1, 24] A completely distinct pattern was

observed by replacing K_3PO_4 by K_2HPO_4, where neither $EE_{R/S\text{-}MA}$ nor *e.e.* significantly vary along the tie line (Figure 3.12B), what must be related with the effect of the pH upon the charge of the mandelic acid as discussed above.

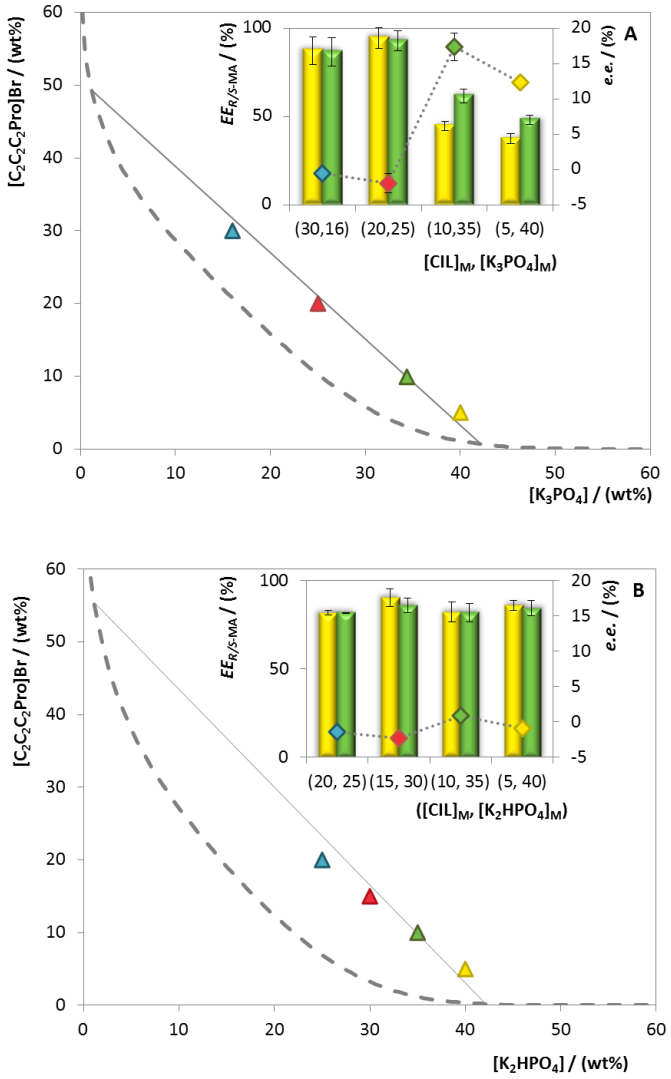

Figure 3.12. Extraction efficiencies ($EE_{R\text{-}MA}$, yellow bars and $EE_{S\text{-}MA}$, green bars) and enantiomeric excesses (*e.e.*, diamonds) obtained with ABS composed of $[C_2C_2C_2Pro]Br$ + K_3PO_4 (A) and $[C_2C_2C_2Pro]Br$ + K_2HPO_4 (B) at 25 (±1) °C and at distinct initial compositions along the same TL: binodal curve (dashed line), TL (solid line) and initial mixture composition (triangles).

Critical assessment of chiral ABS application in the enantioseparation of mandelic acid

As aforementioned, the satisfactory compromise between cost-effectiveness, broad applicability, easy operation and scale-up[25, 26] has placed ABS in the spotlight. Four works using chiral ABS for chiral separation of mandelic acid enantiomers were previously reported. While most are based on the introduction of an extra chiral agent to the ABS,[19, 23, 27] one proposes the use of chiral phase formers.[18] The phase formers are focused on polymer-salt,[19] alcohol-salt[27] and micellar systems[23] incorporating β-cyclodextrin derivatives as well as on polymer-polymer introducing a chiral compound acting as both phase former and chiral agent.[18] The enantioseparation ability is commonly evaluated by determining *e.e.* (Eq. 3) and/or enantioselectivity (α, the ratio between the partition coefficients of mandelic acid enantiomers). Overall, the enantioseparation abilities hitherto reported are highly dependent on the type of ABS and conditions adopted: ethanol-$(NH_4)_2SO_4$ + sulfonated-β-cyclodextrin with α = 1.69 and *e.e.* = 16 %;[27] poly(ethylene) glycol-$(NH_4)_2SO_4$ + β-cyclodextrin with α = 2.46 and *e.e.* = 42 %;[19] and Triton X-114 + copper-β-cyclodextrin complex with *e.e.* = 68 %.[23] Yet, the implementation of chiral phase formers yields less efficient enantioseparations (α = 1.27).[18] With this strategy, also employed in this work, the technological simplicity, target enantiomer polishing and ABS constituents recycling and reuse are enhanced.[18] Moreover, with the ability to overcome technological limitations of polymeric ABS[18] (e.g., viscosity of the phases, limited hydrophobicity-hydrophilicity range and difficulty to find pairs of polymers able to form ABS), the CIL-based ABS here developed are somehow more efficient (maximum *e.e.* of 17.37 ± 1.92 %). In addition, the possibility of using chiral cationic and/or anionic groups[28] affords the opportunity of designing specific CILs structures able to interact more specifically with some particular enantiomeric structures, avoiding the use of complex extraction systems, since these can act simultaneously as chiral selectors and solvents. Most purification systems reported in literature lack specificity towards the enantiomers structures, which leads to low specificity on their separations. Moreover, ILs can be combined with a large range of phase formers to generate ABS,[4] providing an extra degree of tailoring the enantioseparations. Such features offer unique opportunities to plan ABS to match specific enantioseparations.[4] Finally, some CILs show great promise in the field as they can be synthesized by simple,

practical and benign routes,[28] using natural precursors[28] and available in large scale.[29] However, given the limited understanding on their enantiorecognition mechanisms, the design of efficient chiral ABS platforms still relies on case-by-case studies and the broad applicability of ABS for these separations remains challenging.

Conclusions

On the search for alternative enantioseparation techniques, this work proposes the implementation of CILs as chiral phase formers in ABS to resolve racemic mandelic acid. The ternary phase diagrams of ABS constituted by five CILs bearing chirality in the cation and salts were ascertained under ambient conditions, with the hydrophobicity of the CIL cation and the salting out aptitude of the salt dictating the two-phase separation aptitude. After an initial screening where all five CILs were ranked according to their relative ability to separate mandelic acid enantiomers, a maximum *e.e.* of 17.37 ± 1.92 % was achieved with $[C_2C_2C_2Pro]Br$. The most and least promising CILs were object of detailed optimization, comprising the parameters mandelic acid content, temperature, TLL, salt and phases' weight ratio. With the CIL structure playing a central role, all remaining conditions were shown to influence the enantioseparation. Such impacts are highly dependent on the ABS nature: while temperature was the main factor improving the enantioseparation ability of $[C_1Qui][C_1SO_4]$-based ABS, $[C_2C_2C_2Pro]Br$-based ABS was mainly influenced by the salt used and the phases weight ratio. Based on the optimization results it seems that the saturation of the CIL-rich phase rules the enantioseparation: *S*-mandelic acid (the enantiomer with higher affinity for this set of CILs) remains in the CIL-rich phase, while *R*-mandelic acid partitions to the K_3PO_4-rich phase.

References

[1] Wu, D.; Zhou, Y.; Cai, P.; Shen, S.; Pan, Y. Specific cooperative effect for the enantiomeric separation of amino acids using aqueous two-phase systems with task-specific ionic liquids. *Journal of Chromatography A* **2015,** *1395*, 65-72.

[2] Wu, H.; Yao, S.; Qian, G.; Yao, T.; Song, H. A resolution approach of racemic phenylalanine with aqueous two-phase systems of chiral tropine ionic liquids. *Journal of Chromatography A* **2015,** *1418*, 150-157.

[3] Sintra, T. E. Synthesis of more benign ionic liquids for specific applications. PhD Thesis, University of Aveiro, 2017.

[4] Freire, M. G.; Cláudio, A. F. M.; Araújo, J. M. M.; Coutinho, J. A. P.; Marrucho, I. M.; Lopes, J. N. C.; Rebelo, L. P. N. Aqueous biphasic systems: a boost brought about by using ionic liquids. *Chemical Society Reviews* **2012,** *41* (14), 4966-4995.

[5] Merchuk, J. C.; Andrews, B. A.; Asenjo, J. A. Aqueous two-phase systems for protein separation: Studies on phase inversion. *Journal of Chromatography B Biomedical Sciences and Applications* **1998,** *711* (1), 285-293.

[6] Yue, Y.; Jiang, X.-Y.; Yu, J.-G.; Tang, K.-W. Enantioseparation of mandelic acid enantiomers in ionic liquid aqueous two-phase extraction systems. *Chemical Papers* **2014,** *68* (4), 465-471.

[7] Chemspider - The free chemical database at http://www.chemspider.com (accessed Feb 10, 2018).

[8] Cláudio, A. F. M.; Ferreira, A. M.; Shahriari, S.; Freire, M. G.; Coutinho, J. A. P. Critical Assessment of the Formation of Ionic-Liquid-Based Aqueous Two-Phase Systems in Acidic Media. *Journal of Physical Chemistry B* **2011,** *115* (38), 11145-11153.

[9] Passos, H.; Dinis, T. B. V.; Cláudio, A. F. M.; Freire, M. G.; Coutinho, J. A. P. Hydrogen bond basicity of ionic liquids and molar entropy of hydration of salts as major descriptors in the formation of aqueous biphasic systems. *Physical Chemistry Chemical Physics* **2018**, *20* (20), 14234-14241.

[10] Cláudio, A. F. M.; Swift, L.; Hallett, J. P.; Welton, T.; Coutinho, J. A. P.; Freire, M. G. Extended scale for the hydrogen-bond basicity of ionic liquids. *Physical Chemistry Chemical Physics* **2014,** *16* (14), 6593-6601.

[11] Shahriari, S.; Neves, C. M. S. S.; Freire, M. G.; Coutinho, J. A. P. Role of the Hofmeister Series in the Formation of Ionic-Liquid-Based Aqueous Biphasic Systems. *Journal of Physical Chemistry B* **2012,** *116* (24), 7252-7258.

[12] Li, S.; He, C.; Liu, H.; Li, K.; Liu, F. Ionic liquid-based aqueous two-phase system, a sample pretreatment procedure prior to high-performance liquid chromatography of opium alkaloids. *Journal of Chromatography B* **2005,** *826* (1), 58-62.

[13] Kacprzak, K.; Maier, N.; Lindner, W. Unexpected enantioseparation of mandelic acids and their derivatives on 1,2,3-triazolo-linked quinine tert-butyl carbamate anion exchange-type chiral stationary phase. *Journal of Separation Science* **2010,** *33* (17-18), 2590-2598.

[14] Chen, S. The enantioseparation of amino acids on a teicoplanin chiral stationary phase using non-aqueous mobile phases after pre-column derivatization with sulfur-containing reagents: the considerations of mobile phase composition and analyte structure variation on resolution enhancement. *Biomedical Chromatography* **2006,** *20* (8), 718-728.

[15] Jitsukawa, K.; Katoh, A.; Funato, K.; Ohata, N.; Funahashi, Y.; Ozawa, T.; Masuda, H. Kinetic Resolution of rac-Phenylalanine by Stereoselective Complexation to a Chiral Cobalt Complex through π−π Stacking Interaction. *Inorganic Chemistry* **2003,** *42* (20), 6163-6165.

[16] Wang, J.; Yang, H.; Yu, J.; Chen, X.; Jiao, F. Macrocyclic β-cyclodextrin derivative-based aqueous-two phase systems: Phase behaviors and applications in enantioseparation. *Chemical Engineering Science* **2016,** *143*, 1-11.

[17] Chen, X.; Wang, J.; Jiao, F. Efficient enantioseparation of phenylsuccinic acid enantiomers by aqueous two-phase system-based biphasic recognition chiral extraction: Phase behaviors and distribution experiments. *Process Biochemistry* **2015,** *50* (9), 1468-1478.

[18] Tan, Z.; Li, F.; Zhao, C.; Teng, Y.; Liu, Y. Chiral separation of mandelic acid enantiomers using an aqueous two-phase system based on a thermo-sensitive polymer and dextran. *Separation and Purification Technology* **2017,** *172*, 382-387.

[19] Tan, L.; Long, Y.; Jiao, F.; Chen, X. Enantioselective extraction of mandelic acid enantiomers by aqueous two-phase systems of polyethylene glycol and ammonium sulfate containing β-cyclodextrin as chiral selector. *Journal of the Iranian Chemical Society* **2011,** *8* (4), 889-896.

[20] Meng, H.; Yan, T.; Jiao, F.; Wang, S. Enantioseparation of Phenylsuccinic Acid Enantiomers by Solvent Sublation with Collaborative Selectors. *Journal of Solution Chemistry* **2017,** *46* (12), 2159-2170.

[21] Wang, Z.; Hou, Z.; Yao, S.; Lin, M.; Song, H. A new and recyclable system based on tropin ionic liquids for resolution of several racemic amino acids. *Analytica Chimica Acta* **2017,** *960*, 81-89.

[22] Wang, J.; Chen, X.; Jiao, F. Enantioseparation of phenylsuccinic acid enantiomers based on aqueous two-phase system with ethanol/ammonium sulfate: phase diagrams optimization and partitioning experiments. *Journal of Inclusion Phenomena and Macrocyclic Chemistry* **2015,** *81* (3), 475-484.

[23] Xing, J.-M.; Li, F.-F. Chiral separation of mandelic acid by temperature-induced aqueous two-phase system. *Journal of Chemical Technology and Biotechnology* **2012,** *87* (3), 346-350.

[24] Tang, F.; Zhang, Q.; Ren, D.; Nie, Z.; Liu, Q.; Yao, S. Functional amino acid ionic liquids as solvent and selector in chiral extraction. *Journal of Chromatography A* **2010,** *1217* (28), 4669-4674.

[25] Soares, R. R. G.; Azevedo, A. M.; Van Alstine, J. M.; Aires-Barros, M. R. Partitioning in aqueous two-phase systems: Analysis of strengths, weaknesses, opportunities and threats. *Biotechnology Journal* **2015,** *10* (8), 1158–1169.

[26] Iqbal, M.; Tao, Y.; Xie, S.; Zhu, Y.; Chen, D.; Wang, X.; Huang, L.; Peng, D.; Sattar, A.; Shabbir, M. A. B., et al. Aqueous two-phase system (ATPS): an overview and advances in its applications. *Biological Procedures Online* **2016,** *18*, 18.

[27] Li, F.-F.; Tan, Z.-J.; Guo, Z.-F. Enantioseparation of mandelic acid and α-cyclohexylmandelic acid using an alcohol/salt-based aqueous two-phase system. *Chemical Papers* **2014,** *68* (11), 1539-1545.

[28] Payagala, T.; Armstrong, D. W. Chiral ionic liquids: A compendium of syntheses and applications (2005–2012). *Chirality* **2012,** *24* (1), 17-53.

[29] Blaser, H.-U. Chirality and its implications for the pharmaceutical industry. *Rendiconti Lincei* **2013,** *24* (3), 213-216.

3.1.2. Aqueous biphasic systems using chiral ionic liquids bearing chiral anions for enantioseparations

This section is based on e Silva, F. A.; Sintra, T. E.; Rocha, S. N.; Monteiro, C.; Ventura, S. P. M.; Coutinho, J. A. P. Aqueous biphasic systems composed of ionic liquids bearing chiral anions for enantioseparations. *in preparation*.

Contributions: J.A.P.C conceived and directed this work. Francisca A. e Silva, T.E.S., S.N.R. and C.M. acquired the experimental data. This chapter is the second part of a work involving synthesis and characterization of ILs, which was responsibility of T.E.S.[1] Francisca A. e Silva was responsible for ABS phase diagrams determination and further application. Francisca A. e Silva, T.E.S., S.P.M.V. and J.A.P.C. interpreted the experimental data. Francisca A. e Silva, T.E.S. and J.A.P.C. are the responsible for the manuscript preparation with contributions from the remaining authors.

Abstract

In this work, a study in the field of CILs-based ABS for enantioseparations is reported. It firstly addresses the use of amino acids as chiral anions in the synthesis of ILs to be further applied in the formulation of ABS. Secondly, two different types of ABS were developed, namely CIL + salt and CIL + polymer, by the determination and characterization of their phase diagrams. These allowed inferring on the role of CIL anion, salt and polymer in the two-phase formation. The application of such CIL-based ABS in the enantioseparation of racemic basic drugs is suggested, for which future work will be required.

Introduction

Amino acids have been studied as ions of ILs due to their aptitude to function as cations[2, 3] or anions,[4, 5] their natural origin, ready availability, low toxicity, high biodegradability, good biocompatibility, and enantiopurity (if CILs are envisaged). [6, 7] As recently reviewed,[7] ILs composed of amino acids have attracted considerable interest. From biomass processing to CO_2 capture, asymmetric synthesis and extraction and

separation of valuable biomolecules, amino acid-based ILs were shown to be highly performant solvents.[7, 8]

Previously, CILs bearing chiral cations, some of them derived from proline and valine, to form enantioselective ABS, were investigated by our group.[9] The range of CIL-based ABS is enlarged in this work in two directions: (i) instead of chiral cations, which have been the major focus of literature,[9, 10] amino acids will function as chiral anions in tetrabutylammonium and cholinium-based ILs, suiting the enantioseparation of positively charged drugs; and (ii) instead of salts as the phase former pair (i.e., IL-salt-based ABS),[9-11] polymers are also used (i.e., IL-polymer-based ABS), rendering a distinct chemical environment for enantioseparations. For that purpose, the ternary phase diagrams of ABS composed of CILs and salts or polymers were determined and characterized, allowing to understand the role played by the amino acid anion on the phase separation.

Experimental section

Materials

In this work, the synthesis of two families of CILs, namely those belonging to the tetrabutylammonium and cholinium, comprising six amino acids derived anions was carried: tetrabutylammonium L-phenylalaninate, $[N_{4444}][L\text{-Phe}]$; tetrabutylammonium D-phenylalaninate, $[N_{4444}][D\text{-Phe}]$; tetrabutylammonium L-valinate, $[N_{4444}][L\text{-Val}]$; tetrabutylammonium L-alaninate $[N_{4444}][L\text{-Ala}]$; tetrabutylammonium L-prolinate, $[N_{4444}][L\text{-Pro}]$; di(tetrabutylammonium) L-glutamate, $[N_{4444}]_2[L\text{-Glu}]$; cholinium L-phenylalaninate, $[Ch][L\text{-Phe}]$; cholinium, $[Ch][D\text{-Phe}]$; and dicholinium L-glutamate, $[Ch]_2[L\text{-Glu}]$. For the synthesis, the reagents used were the tetrabutylammonium hydroxide, $[N_{4444}]OH$ (40 wt % in water), cholinium hydroxide, [Ch]OH (45 wt % in methanol), D-phenylalanine, D-Phe (purity = 98%) and L-phenylalanine, L-Phe (purity = 99%) obtained from Sigma-Aldrich; L-proline, L-Pro (purity = 99%), L-glutamic acid, L-Glu (purity = 99%), L-valine, L-Val (purity = 99%) and L-alanine, L-Ala (purity = 99%) from Acros Organics, Riedel-de-Haën, Fluka and BDH, respectively; methanol (HPLC grade) and acetonitrile (purity = 99.9%) purchased at VWR. The water used was double distilled, passed by a reverse osmosis system and further treated with a Milli-Q plus 185 water

purification apparatus. The salts used in ABS were: sodium sulfate, Na_2SO_4 (purity = 99.99%); potassium carbonate, K_2CO_3 (purity = 99%); potassium phosphate monobasic, KH_2PO_4 (purity = 99.5%); sodium succinate dibasic hexahydrate, $Na_2C_4H_4O_4 \cdot 6H_2O$ (purity = 99.0%); potassium acetate, KCH_3CO_2 (purity = 99%) from Sigma-Aldrich; sodium carbonate, Na_2CO_3 (purity = 99%) from Vencilab; potassium phosphate dibasic, K_2HPO_4 (purity > 98%) from JMVP; potassium phosphate tribasic, K_3PO_4 (purity > 98%) from Acros Organics; potassium citrate tribasic monohydrate, $K_3C_6H_5O_7 \cdot H_2O$ (purity ≥ 99% GPR RECTAPUR) from VWR; potassium sodium tartrate tetrahydrate, $KNaC_4H_4O_6 \cdot 4H_2O$ (purity = 99%) from Scharlau; and potassium chloride, KCl (purity > 99%), from Pronalab. The polymers/copolymers used in ABS were polyethylene glycol of 400, 600 and 1000, $g.mol^{-1}$ of molecular weight (abbreviated as PEG 400, PEG 600 and PEG 1000 respectively), polypropylene glycol of 400 $g.mol^{-1}$ of molecular weight (abbreviated as PPG 400) and poly(ethylene glycol)-block-poly(propylene glycol)-block-poly(ethylene glycol), with an average molecular weight of 1900 g mol^{-1} and a EO/PO ratio of 50/50 (commercially known as Pluronic® L-35, PL35). The abbreviation and chemical structures of all CILs and polymers are depicted in Figure 3.13.

Synthesis of the CILs based on amino acids

CILs were synthesized through neutralization of $[N_{4444}]OH$ or [Ch]OH with the respective amino acid, following well-established protocols[12, 13] that were previously validated in our laboratory.[1]

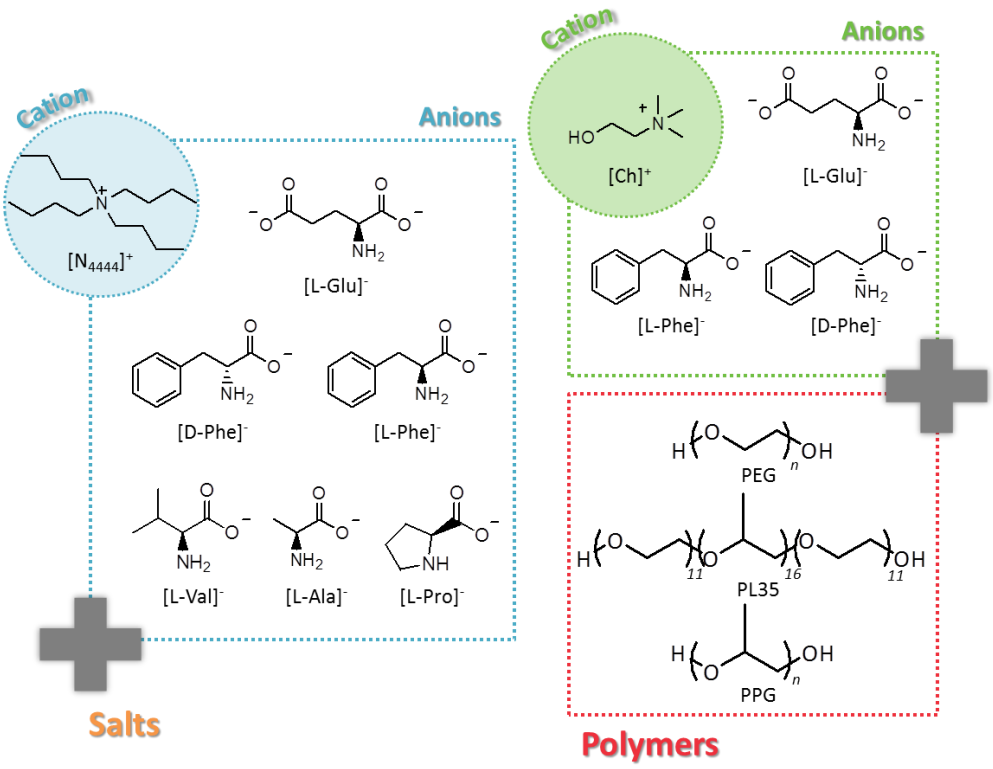

Figure 3.13. Chemical structures and abbreviations of the CILs and polymers investigated.

Determination of the phase diagrams and tie-lines

The ternary phase diagrams of the ABS composed of CILs and salts or polymers were determined by the cloud point titration method at 25 (± 1) °C. The alternate dropwise addition of aqueous solutions of salts (at circa 20 – 50 wt%) or [Ch]-based CILs (at circa 70 wt%) – cloudy solution – and water – clear solution – was done to initial aqueous solutions of [N_{4444}]-based CILs (at circa 50 – 60 wt%) or polymer (at circa 70 – 90 wt%), under constant agitation. The systems' compositions were determined by weight quantification of all components within $\pm 10^{-4}$ g and discounting complexed water in hydrated salts. The experimental phase diagrams were fitted using Equation 3.4.[14]

$$[\mathrm{Y}] = A\mathrm{e}^{[(B[\mathrm{X}])^{0.5}-(C[\mathrm{X}]^3)]} \qquad (\textbf{\textit{Equation 3.4}})$$

where [Y] and [X] are the [N_{4444}]-based CIL and salt weight fraction percentages (CIL + salt ABS) or the polymer and [Ch]-based CIL (CIL + polymer ABS), respectively. *A*, *B* and *C* are the fitting parameters. The tie-lines were determined by a gravimetric method proposed by Merchuk et al.,[14] where biphasic ternary mixtures were prepared by weighing CIL +

salt + water within ± 10^{-4} g, vigorously stirred and left to equilibrate at 25 (± 1) °C for at least 12 h. For CIL + polymer ABS, TLs will be further determined to complete the ABS characterization. After separating and weighing the two phases, the lever-arm rule was applied by the relationship between the top phase and the overall system weight. The top phase is [N_{4444}]-based CIL-enriched in CIL + salt ABS. More details on the tie-lines determination are reported elsewhere.[15] The pH of the phases was measured using a Mettler Toledo S47 SevenMulti^{TM} dual meter pH equipment (± 0.02).

Results and Discussion

Since this study aims at designing enantioselective ABS for the separation of chiral drugs, information on the ternary phase diagrams is paramount. Two distinct types of ABS were developed, namely CIL + salt and CIL + polymer. This allows showcasing the versatility on the implementation of CILs in ABS, at the same time that enlarges the range of CIL-based systems available up to date.

[N_{4444}]-based CILs were paired with salts to form ABS, due to their hydrophobicity that it is useful to screen a wide range of salts and thus of distinct salting-out effects (Figure E1 in Appendix E).[15] Even though [Ch]-based ILs can form ABS with salts of strong salting-out aptitude,[16, 17] these work better in the preparation of ABS with more hydrophobic phase forming agents, such as polymers (Figure E2 in Appendix E), due to their higher polarity when compared to their [N_{4444}] congeners.[18-20] Using [Ch]-based ILs it is possible to move from CIL + salt to CIL + polymer ABS.

Ternary phase diagrams of CIL + salt ABS

The development of CIL + salt ABS was initially based on the use of CILs in combination with Na_2SO_4, a salt of moderate salting-out aptitude.[21] By fixing the $[N_{4444}]^+$ cation, the ability of diverse amino acid derived anions (viz. $[L\text{-}Glu]^-$, $[L\text{-}Phe]^-$, $[D\text{-}Phe]^-$, $[L\text{-}Val]^-$, $[L\text{-}Pro]^-$ and $[L\text{-}Ala]^-$) to induce phase separation was addressed. Using [N_{4444}][Phe] (to cover two enantiomeric forms of the same anion) and $[N_{4444}]_2$[L-Glu] (the most performant CIL at inducing phase separation), a screening of salts covering the Hofmeister series[21] (viz. K_3PO_4, $K_3C_6H_5O_7$, K_2HPO_4, Na_2CO_3, K_2CO_3, Na_2SO_4, $KNaC_4H_4O_6$, $Na_2C_4H_4O_4$, KH_2PO_4, KCH_3CO_2 and KCl) was carried – all tested combinations are indicated

in Figure E1 in Appendix E. The ternary phase diagrams are depicted in Figures 3.14 and 3.15, in molality units (mol.kg^{-1}, moles of salt or CIL per kg of CIL+ water or salt+ water - A) and in weight fraction percentage (wt% - B): the former allows a better comparison of ILs and salts' effect on phase separation so that differences resulting from the distinct molecular weights of the CILs or salts are neglected; the latter is of relevance for the development of enantioseparation processes. Detailed experimental data (ternary phase diagrams weight fraction compositions, Equation 3.4 regression parameters and TL information) are provided in Tables E1 – E23 in Appendix E).

Figure 3.14A shows the CILs' aptitude to be salted-out by Na_2SO_4 forming ABS, with the biphasic region decreasing in the order (at [CIL] = [salt]): $[N_{4444}]_2$[L-Glu] > $[N_{4444}]$[D-Phe] ≈ $[N_{4444}]$[L-Phe] > $[N_{4444}]$[L-Pro] ≈ $[N_{4444}]$[L-Val] > $[N_{4444}]$[L-Ala]. Such a trend translates the distinct hydrophobicities of each amino acid as further corroborated by their octanol-water partition coefficients logarithmic function ($\log K_{o/w}$), agreeing with previous studies:[15, 22] [L/D-Phe]$^-$ ($\log K_{o/w}$ = -1.18) > [L-Val]$^-$ ($\log K_{o/w}$ = -1.95) ≈ [L-Pro]$^-$ ($\log K_{o/w}$ = -2.57) > [L-Ala]$^-$ ($\log K_{o/w}$ = -2.84).[23] $[N_{4444}]_2$[L-Glu], bearing the most hydrophilic anion ($\log K_{o/w}$ = -3.24),[23] is however the most effective CIL, representing an exception to this tendency. It should be underlined that under the pH of these ABS (i.e., from 10.4 to 11.5, cf. Table E23 in Appendix E), the studied amino acids are mostly presented in their anionic form. All ion speciation profiles are provided in Appendix E (Figures E3 – E7).[23] In particular, [L-Glu] has an extra acidic group and it is mainly present as a divalent anion. So, the unexpected enhanced aptitude of $[N_{4444}]_2$[L-Glu] to form ABS seems to be a result of the presence of two hydrophobic $[N_{4444}]^+$ cations. Nonetheless, L-Pro is present in its zwitterionic form in a more significant concentration (40.45 % at pH ≈ 11.5, cf. Figure E6 in Appendix E) when compared to the remaining amino acids (lower than 10 %). As recently discussed, zwiterions have lower solubility in water when compared to their ionic counterparts, and this may justify the similar aptitude of $[N_{4444}]$[L-Pro], which has a lower $\log K_{o/w,}$ and $[N_{4444}]$[L-Val] to form ABS.[23] Moreover, the role of optical isomerism ([L-Phe]$^-$ *versus* D-Phe]$^-$) on ABS formation was shown to be insignificant, in good agreement with findings for structural isomers.[24, 25]

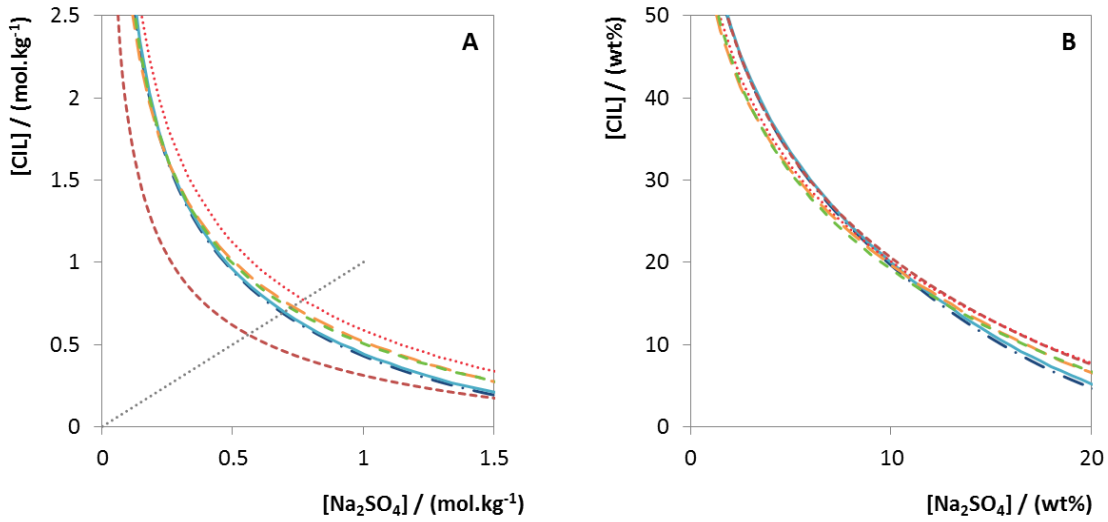

Figure 3.14. Binodal curves of ABS composed of CILs and Na_2SO_4 in molality (A) and weight fraction (B) units: $[N_{4444}]_2$[L-Glu] (dark red dashed line), $[N_{4444}]$[D-Phe] (dark blue dashed-dotted line), $[N_{4444}]$[L-Phe] (blue solid line), $[N_{4444}]$[L-Pro] (green dashed line), $[N_{4444}]$[L-Val] (orange dashed line) and $[N_{4444}]$[L-Ala] (pink dotted line). The dotted grey line represents [CIL] = [salt] and is a guide to the eye.

Not all salts tested, in particular those categorized as weak salting-out agents by the Hofmeister series,[26] were prone to induce two-phase separation in the presence of CILs aqueous solutions (Figure E1 shows all CILs-salts pairs tested as a function of their ability or inability). The aptitude of those able to salt-out CILs in aqueous media is pictured in Figure 3.15, and organized according to the type of salt and CIL considered. Figure 3.15A shows that the salts ability to promote liquid-liquid demixing is generally independent from both the isomerism ($[\text{L-Phe}]^-$ *versus* $[\text{D-Phe}]^-$) and structure ($[\text{Phe}]^-$ *versus* $[\text{Glu}]^{2-}$) of the CIL studied (at [CIL] = [salt]): $Na_2SO_4 \approx Na_2CO_3 > KNaC_4H_4O_6$, $K_3PO_4 > K_2HPO_4 > K_2CO_3 > K_3C_6H_5O_7 > KNaC_4H_4O_6$ and $K_2CO_3 > K_3C_6H_5O_7 \approx KNaC_4H_4O_6$ as well as $Na_2CO_3 > K_2CO_3$ are the rankings observed. This scenario is generally consistent with observations made for IL + salt[21] and polymer + salt ABS.[18, 27] It is well-established that the ability of a salt to induce ABS formation complies with the Hofmeister series and follows the Gibbs free energy of hydration of the salt ions. Stronger salting-out agents

(those of higher valence) have higher affinity to water molecules, thus performing better at expelling the CIL to a second aqueous phase.[21]

$C_6H_5O_7^{3-}$ (the ion present in solution under the pH of these ABS, circa 10.3 – 10.7, cf. Figure E8 in Appendix E), however, as a triple charged ion, was expected to follow PO_4^{3-} in the rankings described above. Some deviations to the Hofmeister series can occur, as cautioned by Kurnia et al.[28] Even though the hydration aptitude of each ion in the system plays a central role in IL-based ABS formation, the interactions between the salts ions and the ions speciation in aqueous solution need to be considered,[28] particularly if polyvalent ions are used. Some salts are composed of ions with a higher aptitude for ion pairing, reducing the number of "free ions" to participate in hydration complexes and hence, in a decrease of the ability to form ABS.[28] Yet, amino acid-based IL may also yield a distinct molecular scenario than that afforded by more conventional ILs (e.g., $[C_4C_1im][CF_3SO_3]$).[21, 28]

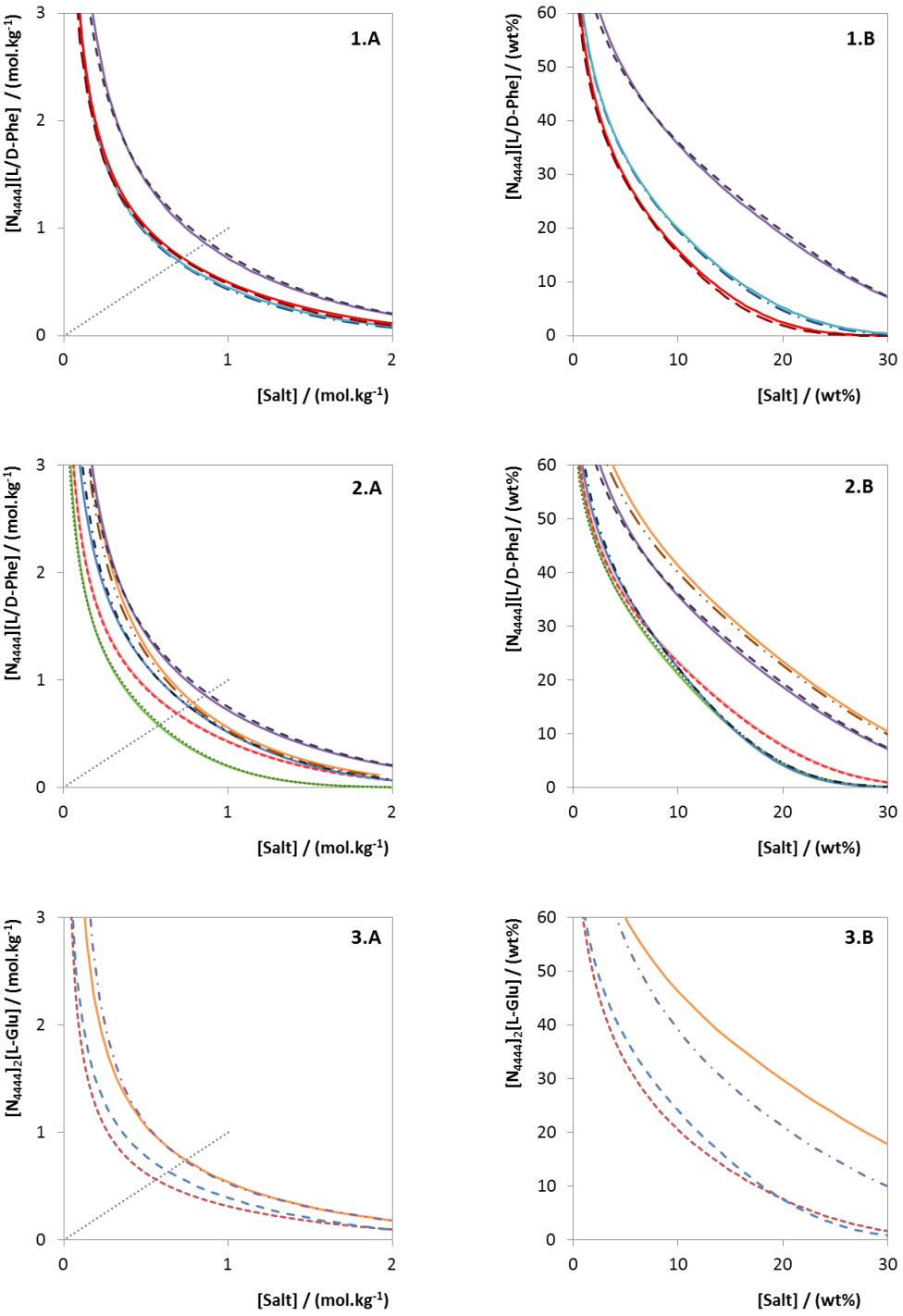

Figure 3.15. Binodal curves of ABS composed of [N_{4444}][L-Phe] (solid lines) or [N_{4444}][D-Phe] (dashed/dotted lines) and sodium salts (1) or potassium salts (2) and [N_{4444}][L-Glu] and salts (3) in molality (A) and weight fraction (B) units: Na_2SO_4 (blue lines), Na_2CO_3 (red lines), $KNaC_4H_4O_6$ (purple lines), K_3PO_4 (green lines), K_2HPO_4 (pink lines), K_2CO_3 (grey lines), $K_3C_6H_5O_7$ (orange lines). The dotted grey line represents [CIL] = [salt] and is a guide to the eye.

Ternary phase diagrams of CIL + polymer ABS

In order to develop CIL + polymers ABS, [Ch]-based CILs were paired with three polymers of distinct hydrophobicity (viz. PEG, PL35 and PPG) – all tested pairs are presented in Figure E2 in Appendix E. Beyond studying the role of the polymer structure on the two-phase formation, the impact of the chiral amino acid anions (viz. [L-Glu], [L-Phe] and [D-Phe]) was also addressed. Using polymers instead of salts to form ABS, it is possible to reduce the salting-out effect and to extend the hydrophobic-hydrophilic range.[29] The ternary phase diagrams are depicted in Figure 3.16. Like aforementioned, the ternary phase diagrams are depicted in Figures 3.16, in molality units (mol.kg^{-1}, moles of polymer or CIL per kg of CIL+ water or polymer + water - A) and in weight fraction percentage (wt% - B). Again, Appendix E contains all experimental data related (Tables E24 – E29).

Figure 3.16A provides information on the distinct aptitude of three CILs to induce ABS formation with PPG, as translated by decreasing extension of the biphasic regions as follows (at [CIL] = [PPG400]): $[Ch]_2$[L-Glu] > [Ch][L-Phe] ≈ [Ch][D-Phe]. The remarkable aptitude of ILs to induce ABS formation with polymers is generally attributed to those presenting lower (more negative) log$K_{o/w}$ and higher polar surface area of the anions.[18, 30-32] In other words, the hydration aptitude and/or affinity for water seem to govern the phase separation phenomenon, meaning that [Ch]-based ILs function as salting-out agents. The findings gathered in this work are in close agreement as described below.

Log$K_{o/w}$: [L-Glu] (-3.24) < [L-Phe] (-1.18) ≈ [D-Phe] (-1.18)[23]

Anion polar surface: [L-Glu] (100.62 Å^2) > [L-Phe] (63.32 Å^2) ≈ [D-Phe] (63.32 Å^2)[23]

Again, isomeric CILs yielded similar biphasic areas, showing an equal aptitude to form ABS. $[Ch]_2$[L-Glu] was the only CIL able to form ABS with polymers other than PPG400 (the most hydrophobic polymer studied, thus easier to be salted-out, cf. Figure E2 in Appendix E) due to the features highlighted above. While $[Ch]_2$[L-Glu] was able to salt-out PEG1000 to form ABS, no two-phase formation occurred for PEGs of lower molecular weights. Higher molecular weights of PEG are more favourable for ABS formation due to their higher hydrophobicity, being thus more easily salted-out.[32] The aptitude of $[Ch]_2$[L-Glu] to salt-out three distinct polymer/copolymers can be ranked as

follows (at [CIL] = [polymer]): PL35 > PPG 400 > PEG 1000. Such a trend is a result of the PL35 molecular weight (1900 mol.kg^{-1}), as previously shown by others.[33] Instead, the ability of PPG400 to perform ABS in the presence of all CILs' studied complies with the trend retrived in Figure 3.16. (2.B), i.e., PPG 400 > PL35 > PEG 1000. More hydrophobic polymers (i.e., PPG due to the presence of an extra methyl group in the PPG monomer compared to PEG) are more prone to form ABS, while PL35 is a copolymer of both PPG and PEG at 50/50 presenting an intermediate nature.

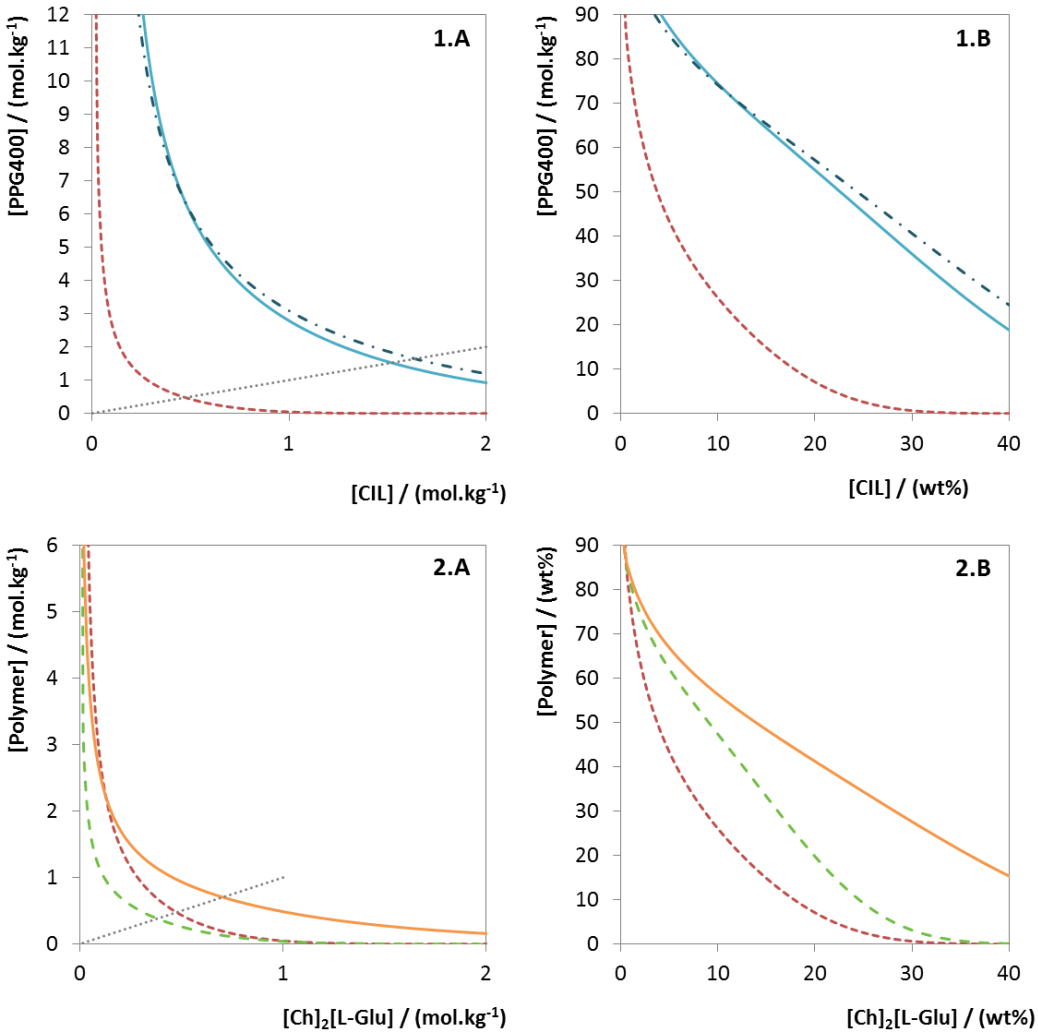

Figure 3.16. Binodal curves of ABS composed of $[Ch]_2$[L-Glu] (red dashed line), [Ch][L-Phe] (blue solid line) and [Ch][D-Phe] (blue dashed dotted line) with PPG400 (1) and $[Ch]_2$[L-Glu] with PL35 (green dashed line), PPG 400 (red dashed line) and PEG1000 (orange solid line) (2) in molality (A) and weight fraction (B) units. The dotted grey line represents [CIL] = [polymer] and is a guide to the eye.

Conclusions

This work focuses on the search for alternative enantioseparation approaches by the creation of CILs-based ABS. Instead of using chiral cations and salts as phase former pairs, as previously proposed by us[9] and others,[10, 11] it is here proposed the use of chiral anions and polymers. As a first approach, the use of [N_{4444}]-based CILs derived from amino acids was investigated in the formation of ABS in combination with salts covering the Hofmeister series (CIL + salt ABS). In this case, the ABS formation was dominated by the hydrophobic character of the CIL and the salting-out aptitude of the salt. As a second approach, and resorting to [Ch]-based CILs (more hydrophilic than their [N_{4444}] counterparts), the development of CIL + polymer ABS was performed. The molecular scenario dictating the ABS formation was instead ruled by the salting-out aptitude of the CIL and by the hydrophobicity of the polymers.

With the systems here reported, it may be possible to design specific enantioseparations by the cautious choice of the CIL properties (by changing the amino acids functional groups or chirality) and the salting-out or pH afforded by the salt. In addition to the chiral resolution of acidic drugs,[9] this new set of ABS will impact on the enantioseparation of specific drugs, showcasing the broad applicability of such a technology. Moreover, CIL + salt *versus* CIL + polymers will render distinct chemical environments for enantioseparations, allowing a more judicious balance of the interactions leading to better enantioselectivies.

References

[1] Sintra, T. E. Synthesis of more benign ionic liquids for specific applications. PhD Thesis, University of Aveiro, 2017.

[2] Li, H.; Yang, S. Catalytic Transformation of Fructose and Sucrose to HMF with Proline-Derived Ionic Liquids under Mild Conditions. *International Journal of Chemical Engineering* **2014,** *2014*, 7.

[3] Roshan, K. R.; Jose, T.; Kim, D.; Cherian, K. A.; Park, D. W. Microwave-assisted one pot-synthesis of amino acid ionic liquids in water: simple catalysts for styrene carbonate

synthesis under atmospheric pressure of CO2. *Catalysis Science & Technology* **2014,** *4* (4), 963-970.

[4] Fukumoto, K.; Yoshizawa, M.; Ohno, H. Room Temperature Ionic Liquids from 20 Natural Amino Acids. *Journal of the American Chemical Society* **2005,** *127* (8), 2398-2399.

[5] Moriel, P.; García-Suárez, E. J.; Martínez, M.; García, A. B.; Montes-Morán, M. A.; Calvino-Casilda, V.; Bañares, M. A. Synthesis, characterization, and catalytic activity of ionic liquids based on biosources. *Tetrahedron Letters* **2010,** *51* (37), 4877-4881.

[6] Hulsbosch, J.; De Vos, D. E.; Binnemans, K.; Ameloot, R. Biobased Ionic Liquids: Solvents for a Green Processing Industry? *ACS Sustainable Chemistry & Engineering* **2016,** *4* (6), 2917-2931.

[7] Kirchhecker, S.; Esposito, D. Amino acid based ionic liquids: A green and sustainable perspective. *Current Opinion in Green and Sustainable Chemistry* **2016,** *2*, 28-33.

[8] Ventura, S. P. M.; Silva, F. A. e.; Quental, M. V.; Mondal, D.; Freire, M. G.; Coutinho, J. A. P. Ionic liquid-mediated extraction and purification of bioactive compounds: Past, Present and Future Trends. *Chemical Reviews* **2017,** *117* (10), 6984–7052.

[9] e Silva, F. A.; Kholany, M.; Sintra, T. E.; Caban, M.; Stepnowski, P.; Ventura, S. P. M.; Coutinho, J. A. P. Aqueous biphasic systems using chiral ionic liquids for the enantioseparation of mandelic acid enantiomers. *Solvent Extraction and Ion Exchange* **2018,** *36* (5), accepted.

[10] Wu, D.; Zhou, Y.; Cai, P.; Shen, S.; Pan, Y. Specific cooperative effect for the enantiomeric separation of amino acids using aqueous two-phase systems with task-specific ionic liquids. *Journal of Chromatography A* **2015,** *1395*, 65-72.

[11] Wu, H.; Yao, S.; Qian, G.; Yao, T.; Song, H. A resolution approach of racemic phenylalanine with aqueous two-phase systems of chiral tropine ionic liquids. *Journal of Chromatography A* **2015,** *1418*, 150-157.

[12] Allen, C. R.; Richard, P. L.; Ward, A. J.; van de Water, L. G. A.; Masters, A. F.; Maschmeyer, T. Facile synthesis of ionic liquids possessing chiral carboxylates. *Tetrahedron Letters* **2006,** *47* (41), 7367-7370.

[13] De Santis, S.; Masci, G.; Casciotta, F.; Caminiti, R.; Scarpellini, E.; Campetella, M.; Gontrani, L. Cholinium-amino acid based ionic liquids: a new method of synthesis and physico-chemical characterization. *Physical Chemistry Chemical Physics* **2015,** *17* (32), 20687-20698.

[14] Merchuk, J. C.; Andrews, B. A.; Asenjo, J. A. Aqueous two-phase systems for protein separation: Studies on phase inversion. *Journal of Chromatography B: Biomedical Sciences and Applications* **1998,** *711* (1), 285-293.

[15] Freire, M. G.; Claudio, A. F. M.; Araujo, J. M. M.; Coutinho, J. A. P.; Marrucho, I. M.; Lopes, J. N. C.; Rebelo, L. P. N. Aqueous biphasic systems: a boost brought about by using ionic liquids. *Chemical Society Reviews* **2012,** *41* (14), 4966-4995.

[16] Shahriari, S.; Tome, L. C.; Araujo, J. M. M.; Rebelo, L. P. N.; Coutinho, J. A. P.; Marrucho, I. M.; Freire, M. G. Aqueous biphasic systems: a benign route using cholinium-based ionic liquids. *RSC Advances* **2013,** *3* (6), 1835-1843.

[17] Wang, R.; Chang, Y.; Tan, Z.; Li, F. Phase behavior of aqueous biphasic systems composed of novel choline amino acid ionic liquids and salts. *Journal of Molecular Liquids* **2016,** *222*, 836-844.

[18] e Silva, F. A.; Carmo, R. M. C.; Fernandes, A. P. M.; Kholany, M.; Coutinho, J. A. P.; Ventura, S. P. M. Using Ionic Liquids To Tune the Performance of Aqueous Biphasic Systems Based on Pluronic L-35 for the Purification of Naringin and Rutin. *ACS Sustainable Chemistry & Engineering* **2017,** *5* (8), 6409-6419.

[19] Song, C. P.; Ramanan, R. N.; Vijayaraghavan, R.; MacFarlane, D. R.; Chan, E.-S.; Ooi, C.-W. Green, Aqueous Two-Phase Systems Based on Cholinium Aminoate Ionic Liquids with Tunable Hydrophobicity and Charge Density. *ACS Sustainable Chemistry & Engineering* **2015,** *3* (12), 3291-3298.

[20] Taha, M.; Almeida, M. R.; e Silva F., A.; Domingues, P.; Ventura, S. P. M.; Coutinho, J. A. P.; Freire, M. G. Novel Biocompatible and Self-buffering Ionic Liquids for Biopharmaceutical Applications. *Chemistry – A European Journal* **2015,** *21* (12), 4781-4788.

[21] Shahriari, S.; Neves, C. M. S. S.; Freire, M. G.; Coutinho, J. A. P. Role of the Hofmeister Series in the Formation of Ionic-Liquid-Based Aqueous Biphasic Systems. *The Journal of Physical Chemistry B* **2012,** *116* (24), 7252-7258.

[22] Taha, M.; e Silva, F. A.; Quental, M. V.; Ventura, S. P. M.; Freire, M. G.; Coutinho, J. A. P. Good's buffers as a basis for developing self-buffering and biocompatible ionic liquids for biological research. *Green Chemistry* **2014,** *16* (6), 3149-3159.

[23] Chemspider - The free chemical database at http://www.chemspider.com (accessed June 22, 2018).

[24] Marques, C. F. C.; Mourão, T.; Neves, C. M. S. S.; Lima, A. S.; Boal-Palheiros, I.; Coutinho, J. A. P.; Freire, M. G. Aqueous biphasic systems composed of ionic liquids and sodium carbonate as enhanced routes for the extraction of tetracycline. *Biotechnology Progress* **2013,** *29* (3), 645-654.

[25] Ventura, S. P. M.; Sousa, S. G.; Serafim, L. S.; Lima, Á. S.; Freire, M. G.; Coutinho, J. A. P. Ionic Liquid Based Aqueous Biphasic Systems with Controlled pH: The Ionic Liquid Cation Effect. *Journal of Chemical & Engineering Data* **2011,** *56* (11), 4253-4260.

[26] Hofmeister, F. Zur Lehre von der Wirkung der Salze. *Archiv für experimentelle Pathologie und Pharmakologie* **1888,** *24* (4), 247-260.

[27] Hey, M. J.; Jackson, D. P.; Yan, H. The salting-out effect and phase separation in aqueous solutions of electrolytes and poly(ethylene glycol). *Polymer* **2005,** *46* (8), 2567-2572.

[28] Kurnia, K. A.; Freire, M. G.; Coutinho, J. A. P. Effect of Polyvalent Ions in the Formation of Ionic-Liquid-Based Aqueous Biphasic Systems. *The Journal of Physical Chemistry B* **2014,** *118* (1), 297-308.

[29] Pereira, J. F. B.; Rebelo, L. P. N.; Rogers, R. D.; Coutinho, J. A. P.; Freire, M. G. Combining ionic liquids and polyethylene glycols to boost the hydrophobic-hydrophilic range of aqueous biphasic systems. *Physical Chemistry Chemical Physics* **2013,** *15* (45), 19580-19583.

[30] Mondal, D.; Sharma, M.; Quental, M. V.; Tavares, A. P. M.; Prasad, K.; Freire, M. G. Suitability of bio-based ionic liquids for the extraction and purification of IgG antibodies. *Green Chemistry* **2016,** *18* (22), 6071-6081.

[31] Ramalho, C. C.; Neves, C. M. S. S.; Quental, M. V.; Coutinho, J. A. P.; Freire, M. G. Separation of immunoglobulin G using aqueous biphasic systems composed of cholinium-based ionic liquids and poly(propylene glycol). *Journal of Chemical Technology & Biotechnology* **2018,** *93* (7), 1931-1939.

[32] Pereira, J. F. B.; Kurnia, K. A.; Cojocaru, O. A.; Gurau, G.; Rebelo, L. P. N.; Rogers, R. D.; Freire, M. G.; Coutinho, J. A. P. Molecular interactions in aqueous biphasic systems composed of polyethylene glycol and crystalline vs. liquid cholinium-based salts. *Physical Chemistry Chemical Physics* **2014,** *16* (12), 5723-5731.

[33] Liu, X.; Li, Z.; Prei, Y.; Wang, H.; Wang, J. (Liquid+liquid) equilibria for (cholinium-based ionic liquids+polymers) aqueous two-phase systems. *Journal of Chemical Thermodynamics* **2012**, *60*, 1-8.

3.2. Chiral eutectic solvents as alternative solvents for the separation of chiral compounds

DES are neoteric solvents generated from blending two (or more) solid compounds, i.e., a hydrogen bond acceptor (HBA) and a hydrogen bond donor (HBD), with melting temperatures well below those of the starting materials.[1, 2] As soon as the research community became cognizant of DES physical and chemical properties, several works were launched shedding light on the molecular level mechanisms governing their formation and on their role as alternative chemicals in several applications.[1]

By adequate choice of the starting materials, DES may be characterized by their low volatility, low flammability, broad liquidus temperature range and high solvency power.[3] Moreover, and analogously to ILs, DES are recognized as "designer solvents" due to the plethora of starting materials and stoichiometric ratios that can be used for their preparation.[4, 5] In combination with halide salts, i.e., HBA, carboxylic acids,[6-9] alcohols and polyols,[4, 9-13] amino acids[14] and carbohydrates[9, 15, 16] are amongst the most popular HBD. DES are not only highly performant candidates as alternative solvents, but also economically viable and easy to prepare since they mostly use cheap and naturally occurring starting materials, dismissing reaction and purification steps.[3] Under this scenario, it is not surprising that DES may find application in several areas.[1, 3] A generous amount of reviews on the topic were recently published, highlighting the outstanding potential of DES in chemistry,[17, 18] chemical engineering,[5, 19] materials science,[20, 21] biotechnology and bioengineering.[22, 23] Some sound examples encompass the use of DES as either solvent or catalyst in (bio)catalysis,[18, 23] metals' processing,[24, 25] extraction and separation of natural products,[26, 27] storage of nucleic acids,[28] proteins,[29] cells, tissues and organs,[30] and as therapeutic agents.[31-33]

Due to the chiral nature that many DES constituents present, these can be envisaged as highly performant chiral chemicals to be applied when chiral applications are intended. The use of chiral compounds to prepare DES is manifested in literature, as outlined in Figure 3.17. As implied by the "designer solvent" character of DES, the possibility of creating chiral DES is broad: one or two chiral compounds can be used in

eutectics formulation and using distinct molar ratios. Sugars are amongst the natural chiral structures most used in the preparation of DES: monosaccharides (e.g., glucose, fructose, mannose and xylose),[9, 34-39] disaccharides (e.g., maltose, sucrose, trehalose and lactose),[9, 34, 36, 37] trisaccharides (e.g., raffinose)[9] or even polyols (e.g., xylitol, adonitol and sorbitol)[9, 11] can be combined with each other[9, 36, 38] or with other types of molecules (e.g., urea, [Ch]-based salts, betaine and organic acids). [9, 34-37, 39] Another class of biomolecules widely used to form DES are the amino acids (e.g., proline, alanine and histidine).[9, 35-37, 40] These are combined with sugars[9] and organic acids, some of them chiral (e.g., lactic acid, malic acid), others achiral (e.g., citric acid, acetic acid and propionic acid).[9, 35, 36] Beyond their ability to create "double chiral" DES with either sugars[9, 36, 39] or amino acids,[9, 35, 37, 40] some chiral organic acids (e.g., mandelic acid, lactic acid, tartaric acid and malic acid)[9, 11, 35, 36, 38, 40-42] can also be paired with urea,[35, 38] [Ch]Cl[9, 11, 35, 36, 40, 42] and betaine[9, 35, 40, 41] in the formulation of chiral DES. In the framework of therapeutic DES, other chiral structures emerge in DES preparation, namely active pharmaceutical ingredients (API) (e.g., ibuprofen and D-isosorbide)[11, 31, 33, 43] along with [Ch]Cl,[11] lidocaine[33, 43] and menthol.[31] The later, belonging to the terpenes class, opens another opportunity for hydrophobic chiral DES preparation when conjugated with camphor (also a chiral terpenoid),[44] acetylsalicylic acid[45] and other carboxylic acids.[45-47]

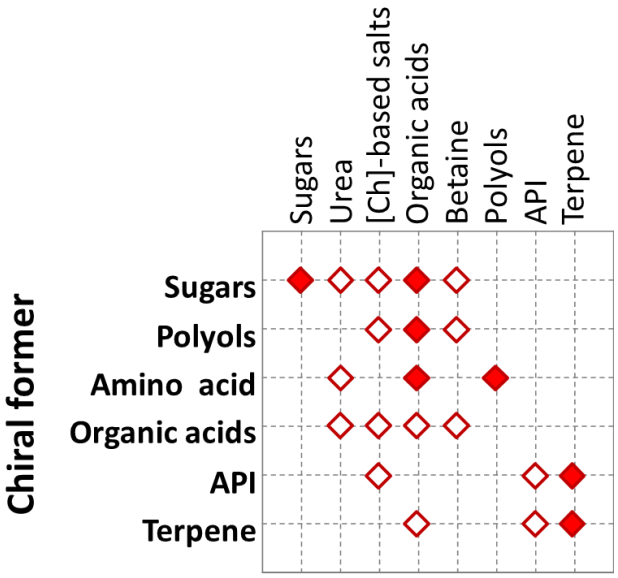

Figure 3.17. Chiral DES reported in literature as a function of HBD-HBA combinations: one chiral component (open diamonds), two chiral components (closed diamonds).

Yet, and in spite of the plethora of chiral DES hitherto proposed, the understanding of the chirality role upon DES formation is lagging. Moreover and given the

wide applicability of DES,[1, 3] chiral applications remain restricted to organo or biotransformations.

Role of chirality on DES formation

Only one work aimed at studying the role of the chirality in DES formation is currently available.[48] The chiral DES investigated were composed of the two enantiomers of camphorsulfonic acid (HBD) and the two enantiomers of *N,N,N*-trimethyl-(1-phenylethyl)ammonium methanesulfonate (HBA). A depression of the melting temperature (T_m = 17 to 21 ^{o}C) occurred when mixing these compounds together compared to those of the starting materials ($T_{m,\ HBA}$ = 166 – 168 ^{o}C and $T_{m,\ HBD}$ = 198 ^{o}C). Regardless of the HBD:HBA molar ratios, very small changes in the melting points were observed.[48] NMR and DFT studies were carried to provide insight on the chirality role upon DES structural conformation. The major differences afforded by different enantiomeric combinations were identified at the level of hydrogen bond and electrostatic interactions sites.[48] DFT additionally showed that the interactions between camphorsulfonic acid and methanesulfonate lead to the formation of a supramolecular-anion able to interact differently with the two enantiomers of the HBA ammonium core. Even though being the most complete systematic study in the field and providing important insight on the chiral DES formation,[48] the eutectic profiles were only determined for two of the possible chiral combinations and for a narrow range of HBD:HBA molar ratios. Remarkably, it was possible to correlate the distinct interactions occurring within different chiral DES with the yields of a Michael-type Friedel-Crafts probe reaction.[48] Such finding reinforces the need for understanding the chirality role upon DES formation to better design any desired chiral application. In fact, several works related to DES in chiral applications have been hitherto reported. The main body is dedicated to the use of DES either as solvents or co-solvents, in some cases also as catalysts, in organo- or bio-catalyzed reactions.

Application of DES in enantioselective (bio)transformations

Using DES as reaction media came up as a very promising application within the Green Chemistry field, especially if organocatalyzed reactions are envisaged. Cross-aldol

reactions,[39, 49, 50] Michael type additions, [48, 51-53] α-amination of 1,3-dicarbonyl compounds,[54] epoxidation of soybean oil,[55] Betti reactions,[56] Schiff bases synthesis,[57] reduction of epoxides and carbonyl compounds[58] and taste enhancers synthesis[59] lay among related successful examples. Indeed, a wide range of diverse organotransformations was carried resorting to DES, underlining the flexible implementation of these liquids in organocatalyzed reactions. Likely, cross-aldol reactions and Michael type additions are the most exploited in literature. L-Proline-catalyzed cross-aldol reactions have been conducted in DES formed through combination of [Ch]Cl as HBA with multiple HBD, some of them chiral, (e.g., urea, organic acids, polyols and sugars) and D-glucose with malic acid.[39] Such approach allowed not only using a bio-renewable catalyst but also to avoid the use of organic solvents in the entire process (recycling and reuse included, as showcased below). Among all DES screened, [Ch]Cl:glycerol was the [Ch]Cl-based DES affording the best compromise between conversion and enantiomeric excess, whereas D-glucose:malic acid was by far the most effective DES. In a similar line of research, using instead L-isoleucine as catalyst, DES were found to be highly performant solvents to conduct cross-aldol reactions, with maximum enantiomeric excesses of 99 % comparable to organic solvents.[49] In both works, it was possible to recycle and reuse both the DES and the catalyst, which reinforces the sustainable character of these approaches.[39, 49] To be highlighted is the DES capacity at rendering suitable reaction media for distinct catalysts.[39, 49] The possibility of performing a L-proline-catalyzed reaction in continuous mode was also shown, contributing to the intensification of organocatalyzed reactions in DES.[50] Michael additions were also studied, with DES being used as solvents, co-solvents or even as catalysts. The DES studied entail those composed of [Ch]Cl plus polyols, urea, carboxylic acids, sugars, ethylene glycol;[51-53] ammonium and phosphonium salts (triphenylmethylphosphonium bromide and tetrabutylammonium bromide) plus glycerol;[53] and camphorsulfonic acid plus *N,N,N*-trimethyl-(1-phenylethyl)ammonium methanesulfonate.[48] A complete screening of [Ch]Cl-based DES as reaction medium for the organocatalyzed enantioselective Michael additions of 1,3-dicarbonyl compounds or aldehydes to β-nytrostyrenes was recently done by Ñiguez et al.[52] and Massolo et al.[51] With DES providing better reaction outcomes than toluene

(with higher yields and enantiomeric excesses), the authors were able to deliver greener protocols for Michael additions.[51, 52] Additionally, the recyclability and reuse of the organocatalyst was addressed using organic solvents as extractive solvents for unreacted materials and/or final product, allowing thus to separate the DES-organocatalyst system.[51, 52] Finally, to infer about the scalability and applicability range of DES as reaction medium, gram-scale experiments[52] and other types of organocatalyzed stereoselective transformations[51] were investigated with success. Furthermore, Flores-Ferrándiz and Chinchilla expanded the DES applied to mixtures not based on [Ch]Cl.[53] The use of triphenylmethylphosphonium bromide and tetrabutylammonium bromide instead of [Ch]Cl allowed them to significantly improve the enantioselectivity of the organocatalyzed conjugate addition of aldehydes to maleimides, keeping the possibility of recycling and reusing the DES-organocatalyst system.[53] In spite of DES being implemented as organic solvents substitutes, most catalytic systems hitherto reported resort to organic solvents (e.g., hexane, ethyl acetate, ethereal solvents) in the recycle stage of these approaches, what may restrict the processes sustainability.[49-53] A more sustainable recycling route was proposed by Martinez et al.[39] by recycling the DES-catalyst system utilizing water as solvent. Although providing an useful insight on the application of DES in stereoselective transformations, such works have neglected the role that DES chirality plays on the reactions targeted.[51-53] Recently, Palomba et al. proposed the use of DES formed by chiral components.[48] The authors have not only developed a successful enantioselective transformation with DES acting as reaction media and catalysts, but have also provided insight on the role of DES' chirality in the reaction outcome. In fact, the use of DES in Michael-type Friedel-Crafts reaction of indole to chalcone lead to similar yields and enantiomeric excesses to those rendered by acetonitrile, providing a greener yet efficient option.[48] By playing with the enantiomeric structure of these DES, using the two enantiomers of camphorsulfonic acid (HBD) combined with the two enantiomers of *N,N,N*-trimethyl-(1-phenylethyl)ammonium methanesulfonate, the authors proved the tunable nature of the reaction considering both the conversion yield and enantiomeric excess. The authors attributed this phenomenon to the diastereoisomerical differences of the eutectic liquids formed and

further demonstrated their hypothesis by spectroscopic and computational studies.[48] Taking into account all the works discussed above, a cautious selection of the HBD and HBA forming the DES dictates the efficiency of any reaction developed using DES. The type of reactions envisaged, operational conditions adopted and final product quality hugely impacts on the solvent choice. If several reactions were effectively undertaken using specific DES, others faced practical limitations that led to failure. Although not centered in enantioselective reactions, Ilgen and König provided an important perspective on how a DES can fail at rendering a suitable media for organic transformations.[60] The lack of thermal and chemical stability, high viscosity and high costs of L-carnitine-urea-based DES limits its broad application as solvent in organic reactions, when compared with the highly efficient sugar-based DES.[60]

Enantioselective biotransformations in DES have been widely studied, with an additional challenge related to biocompatibility when compared to organocatalyzed reactions.[18, 23, 61] DES as co-solvents, usually in water or buffers, coupled to microbial and plant cells,[62-68] enzymes[69-74] and nucleic acids[75, 76] as the biocatalysts are the covered systems. Analogously to what was observed in organocatalyzed reactions, DES formed by [Ch]Cl are ubiquitous among reports.[62-76] Hydrolase-catalyzed biotransformations are likely the most common case-study. Back in 2007, Gorke et al.[77] provided a comprehensive study on the topic. The lipase-catalyzed (free and immobilized) transesterification of ethyl valerate with 1-butanol, the hydrolase-catalyzed hydrolysis of styrene oxide and the esterase-catalyzed hydrolysis of *p*-nitrophenyl acetate were studied, indicating the possibility of different hydrolases to retain their activity in presence of DES.[77] This work highlighted the biocompatible nature of DES, thus opening the path to investigate enantioselective biotransformations. An epoxide hydrolase from *Streptomyces griseus* was overexpressed in *Escherichia coli* and the whole cells were implemented as biocatalysts in the kinetic resolution of racemic phenyl glycidyl ether into *R*-phenyl glycidyl ether.[62] After selecting the optimal reaction conditions (pH, temperature and cell/substrate ratio), the authors have assessed the role of organic solvents and DES as co-solvents, since these may increase the solubility of epoxides in the reaction medium (phosphate buffer).[62] DES ([Ch]Cl:Urea, [Ch]Cl:ethylene glycol and

[Ch]Cl:glycerol) were considerably less efficient than the best organic solvent identified, dimethylformamide, in both conversion yields and enantioselectivity.[62] Contrarily, instead of using epoxide hydrolases from potato and mung bean to catalyze the asymmetric hydrolysis of styrene derived epoxides in the same kind of DES-buffer reaction media, Lindeberg et al.[69] and Peng et al.[70] were able to enhance regioselectivity in the reaction, thus rendering a final product of higher quality. However, the authors struggled with the impact of DES structure on the enzyme activity, with urea and carboxylic acids having deleterious effects.[69, 70] The hydrolysis of the aromatic ester (±)-1-phenylethyl acetate by carrot roots was also successfully carried out in the presence of several [Ch]Cl-based DES.[67] When compared to water, DES aqueous solutions yielded similar conversions and higher enantiomeric excesses.[67] Still, the stability of these enzymes in the presence of DES remains the major challenge and it has been usually solved by working with diluted DES aqueous solutions rather than with pure DES or highly concentrated DES aqueous solutions.[67, 69, 70] Additionally, immobilization is envisaged as a suitable option, as recently proposed by Cao et al.[71] for soybean epoxide hydrolases. With the hydrolysis of the *R*-1,2-epoxyoctane to produce *R*-1,2-octanediol being investigated, yields and enantiomeric excesses were improved in DES-buffer, using the immobilized enzyme (*versus* only buffer and free enzyme) at the same time that the authors have assured enzymatic stability.[71] Beyond asymmetric hydrolysis,[62, 67, 69-71] asymmetric oxidations[64] and reductions,[63, 65-68] Henry reactions,[72] Michael additions,[75, 76] C-C bond formation[73] and kinetic resolutions through transesterification[74] were studied. Regarding the available body of literature, DES are flexible within asymmetric biotransformations since these can serve distinct reactions and diverse types of biocatalysts.

Scopes and Objectives

The role of DES in asymmetric (bio)transformations has been largely scrutinized[18, 23, 61] and so has been their capability to extract and separate an enormous variety of products from different sources.[19, 78, 79] This outstanding solvency power can be allied to the improved enantioselectivities that DES may provide in (bio)transformations, being surprising that their use as chiral extractive solvents remains neglected. A single work

integrates DES as extractive agents with kinetic resolution of alcohols [(*R,S)*-1-phenylethanol].[80] DES composed of [Ch]Cl:Glycerol were merely used to promote the separation between the two products of the reaction, an alcohol and an ester.[80]

In this context, it is here foreseen that DES may afford suitable chiral solvents for enantioseparations. This chapter delivers an initial fundamental study aimed to deepen knowledge on the role of chirality in DES formation. It is firstly intended to fulfill the existent gap[48] on the characterization of their solid-liquid phase diagrams and on the comprehension of interactions occurring in the liquid phase, by playing with all possible HBD and HBA enantiomers combinations (***section 3.2.1.***). At the end, useful knowledge for future application may be gathered.

References

[1] Zhang, Q.; De Oliveira Vigier, K.; Royer, S.; Jerome, F. Deep eutectic solvents: syntheses, properties and applications. *Chemical Society Reviews* **2012,** *41* (21), 7108-7146.

[2] Abbott, A. P.; Capper, G.; Davies, D. L.; Rasheed, R. K.; Tambyrajah, V. Novel solvent properties of choline chloride/urea mixtures. *Chemical Communications* **2003,** *0* (1), 70-71.

[3] Smith, E. L.; Abbott, A. P.; Ryder, K. S. Deep Eutectic Solvents (DESs) and Their Applications. *Chemical Reviews* **2014,** *114* (21), 11060-11082.

[4] Farias, F. O.; Passos, H.; Sanglard, M. G.; Igarashi-Mafra, L.; Coutinho, J. A. P.; Mafra, M. R. Designer solvent ability of alcohols in aqueous biphasic systems composed of deep eutectic solvents and potassium phosphate. *Separation and Purification Technology* **2018,** *200*, 84-93.

[5] Wazeer, I.; Hayyan, M.; Hadj-Kali Mohamed, K. Deep eutectic solvents: designer fluids for chemical processes. *Journal of Chemical Technology & Biotechnology* **2017,** *93* (4), 945-958.

[6] Pontes, P. V. A.; Crespo, E. A.; Martins, M. A. R.; Silva, L. P.; Neves, C. M. S. S.; Maximo, G. J.; Hubinger, M. D.; Batista, E. A. C.; Pinho, S. P.; Coutinho, J. A. P., et al. Measurement and PC-SAFT modeling of solid-liquid equilibrium of deep eutectic solvents

of quaternary ammonium chlorides and carboxylic acids. *Fluid Phase Equilibria* **2017,** *448*, 69-80.

[7] Li, J.-J.; Xiao, H.; Tang, X.-D.; Zhou, M. Green Carboxylic Acid-Based Deep Eutectic Solvents as Solvents for Extractive Desulfurization. *Energy & Fuels* **2016,** *30* (7), 5411-5418.

[8] Abbott, A. P.; Boothby, D.; Capper, G.; Davies, D. L.; Rasheed, R. K. Deep Eutectic Solvents Formed between Choline Chloride and Carboxylic Acids: Versatile Alternatives to Ionic Liquids. *Journal of the American Chemical Society* **2004,** *126* (29), 9142-9147.

[9] Dai, Y.; van Spronsen, J.; Witkamp, G.-J.; Verpoorte, R.; Choi, Y. H. Natural deep eutectic solvents as new potential media for green technology. *Analytica Chimica Acta* **2013,** *766*, 61-68.

[10] Lin, Z. S.; Huang, Y. Tetraalkylammonium salt/alcohol mixtures as deep eutectic solvents for syntheses of high-silica zeolites. *Microporous and Mesoporous Materials* **2016,** *224*, 75-83.

[11] Maugeri, Z.; Dominguez de Maria, P. Novel choline-chloride-based deep-eutectic-solvents with renewable hydrogen bond donors: levulinic acid and sugar-based polyols. *RSC Advances* **2012,** *2* (2), 421-425.

[12] Zhao, H.; Baker, G. A.; Holmes, S. Protease activation in glycerol-based deep eutectic solvents. *Journal of Molecular Catalysis B: Enzymatic* **2011,** *72* (3), 163-167.

[13] Zahrina, I.; Mulia, K.; Yanuar, A.; Nasikin, M. Molecular interactions in the betaine monohydrate-polyol deep eutectic solvents: Experimental and computational studies. *Journal of Molecular Structure* **2018,** *1158*, 133-138.

[14] Chemat, F.; Anjum, H.; Shariff, A. M.; Kumar, P.; Murugesan, T. Thermal and physical properties of (Choline chloride+urea+l-arginine) deep eutectic solvents. *Journal of Molecular Liquids* **2016,** *218*, 301-308.

[15] Hayyan, A.; Mjalli, F. S.; AlNashef, I. M.; Al-Wahaibi, T.; Al-Wahaibi, Y. M.; Hashim, M. A. Fruit sugar-based deep eutectic solvents and their physical properties. *Thermochimica Acta* **2012,** *541*, 70-75.

[16] Florindo, C.; Oliveira, M. M.; Branco, L. C.; Marrucho, I. M. Carbohydrates-based deep eutectic solvents: Thermophysical properties and rice straw dissolution. *Journal of Molecular Liquids* **2017,** *247*, 441-447.

[17] Shishov, A.; Bulatov, A.; Locatelli, M.; Carradori, S.; Andruch, V. Application of deep eutectic solvents in analytical chemistry. A review. *Microchemical Journal* **2017,** *135*, 33-38.

[18] Alonso Diego, A.; Baeza, A.; Chinchilla, R.; Guillena, G.; Pastor Isidro, M.; Ramón Diego, J. Deep Eutectic Solvents: The Organic Reaction Medium of the Century. *European Journal of Organic Chemistry* **2016,** *2016* (4), 612-632.

[19] Zainal-Abidin, M. H.; Hayyan, M.; Hayyan, A.; Jayakumar, N. S. New horizons in the extraction of bioactive compounds using deep eutectic solvents: A review. *Analytica Chimica Acta* **2017,** *979*, 1-23.

[20] Tomé, L. I. N.; Baião, V.; da Silva, W.; Brett, C. M. A. Deep eutectic solvents for the production and application of new materials. *Applied Materials Today* **2018,** *10*, 30-50.

[21] Abo-Hamad, A.; Hayyan, M.; AlSaadi, M. A.; Hashim, M. A. Potential applications of deep eutectic solvents in nanotechnology. *Chemical Engineering Journal* **2015,** *273*, 551-567.

[22] Mbous, Y. P.; Hayyan, M.; Hayyan, A.; Wong, W. F.; Hashim, M. A.; Looi, C. Y. Applications of deep eutectic solvents in biotechnology and bioengineering—Promises and challenges. *Biotechnology Advances* **2017,** *35* (2), 105-134.

[23] Domínguez de María, P.; Maugeri, Z. Ionic liquids in biotransformations: from proof-of-concept to emerging deep-eutectic-solvents. *Current Opinion in Chemical Biology* **2011,** *15* (2), 220-225.

[24] Riano, S.; Petranikova, M.; Onghena, B.; Vander Hoogerstraete, T.; Banerjee, D.; Foreman, M. R. S.; Ekberg, C.; Binnemans, K. Separation of rare earths and other valuable metals from deep-eutectic solvents: a new alternative for the recycling of used NdFeB magnets. *RSC Advances* **2017,** *7* (51), 32100-32113.

[25] Abbott, A. P.; Capper, G.; Davies, D. L.; Rasheed, R. K.; Shikotra, P. Selective Extraction of Metals from Mixed Oxide Matrixes Using Choline-Based Ionic Liquids. *Inorganic Chemistry* **2005,** *44* (19), 6497-6499.

[26] Dai, Y.; van Spronsen, J.; Witkamp, G.-J.; Verpoorte, R.; Choi, Y. H. Ionic Liquids and Deep Eutectic Solvents in Natural Products Research: Mixtures of Solids as Extraction Solvents. *Journal of Natural Products* **2013,** *76* (11), 2162-2173.

[27] Jeong, K. M.; Ko, J.; Zhao, J.; Jin, Y.; Yoo, D. E.; Han, S. Y.; Lee, J. Multi-functioning deep eutectic solvents as extraction and storage media for bioactive natural products that are readily applicable to cosmetic products. *Journal of Cleaner Production* **2017,** *151*, 87-95.

[28] Zhao, H. DNA stability in ionic liquids and deep eutectic solvents. *Journal of Chemical Technology & Biotechnology* **2014,** *90* (1), 19-25.

[29] Lee, M. S.; Lee, K.; Nam, M. W.; Jeong, K. M.; Lee, J. E.; Kim, N. W.; Yin, Y.; Lim, S. Y.; Yoo, D. E.; Lee, J., et al. Natural deep eutectic solvents as a storage medium for human interferon-α2: a green and improved strategy for room-temperature biologics. *Journal of Industrial and Engineering Chemistry* **2018**, 10.1016/j.jiec.2018.05.005.

[30] Gertrudes, A.; Craveiro, R.; Eltayari, Z.; Reis, R. L.; Paiva, A.; Duarte, A. R. C. How Do Animals Survive Extreme Temperature Amplitudes? The Role of Natural Deep Eutectic Solvents. *ACS Sustainable Chemistry & Engineering* **2017,** *5* (11), 9542-9553.

[31] Aroso, I. M.; Craveiro, R.; Rocha, Â.; Dionísio, M.; Barreiros, S.; Reis, R. L.; Paiva, A.; Duarte, A. R. C. Design of controlled release systems for THEDES—Therapeutic deep eutectic solvents, using supercritical fluid technology. *International Journal of Pharmaceutics* **2015,** *492* (1), 73-79.

[32] Duarte, A. R. C.; Ferreira, A. S. D.; Barreiros, S.; Cabrita, E.; Reis, R. L.; Paiva, A. A comparison between pure active pharmaceutical ingredients and therapeutic deep eutectic solvents: Solubility and permeability studies. *European Journal of Pharmaceutics and Biopharmaceutics* **2017,** *114*, 296-304.

[33] Berton, P.; Di Bona, K. R.; Yancey, D.; Rizvi, S. A. A.; Gray, M.; Gurau, G.; Shamshina, J. L.; Rasco, J. F.; Rogers, R. D. Transdermal Bioavailability in Rats of Lidocaine in the Forms of Ionic Liquids, Salts, and Deep Eutectic. *ACS Medicinal Chemistry Letters* **2017,** *8* (5), 498-503.

[34] Ilgen, F.; Ott, D.; Kralisch, D.; Reil, C.; Palmberger, A.; Konig, B. Conversion of carbohydrates into 5-hydroxymethylfurfural in highly concentrated low melting mixtures. *Green Chemistry* **2009,** *11* (12), 1948-1954.

[35] Soares, B.; Tavares, D. J. P.; Amaral, J. L.; Silvestre, A. J. D.; Freire, C. S. R.; Coutinho, J. A. P. Enhanced Solubility of Lignin Monomeric Model Compounds and Technical Lignins in Aqueous Solutions of Deep Eutectic Solvents. *ACS Sustainable Chemistry & Engineering* **2017,** *5* (5), 4056-4065.

[36] Choi, Y. H.; van Spronsen, J.; Dai, Y.; Verberne, M.; Hollmann, F.; Arends, I. W. C. E.; Witkamp, G.-J.; Verpoorte, R. Are Natural Deep Eutectic Solvents the Missing Link in Understanding Cellular Metabolism and Physiology? *Plant Physiology* **2011,** *156* (4), 1701.

[37] Duan, L.; Dou, L.-L.; Guo, L.; Li, P.; Liu, E. H. Comprehensive Evaluation of Deep Eutectic Solvents in Extraction of Bioactive Natural Products. *ACS Sustainable Chemistry & Engineering* **2016,** *4* (4), 2405-2411.

[38] Faggian, M.; Sut, S.; Perissutti, B.; Baldan, V.; Grabnar, I.; Dall'Acqua, S. Natural Deep Eutectic Solvents (NADES) as a Tool for Bioavailability Improvement: Pharmacokinetics of Rutin Dissolved in Proline/Glycine after Oral Administration in Rats: Possible Application in Nutraceuticals. *Molecules* **2016,** *21* (11), 1531.

[39] Martinez, R.; Berbegal, L.; Guillena, G.; Ramon, D. J. Bio-renewable enantioselective aldol reaction in natural deep eutectic solvents. *Green Chemistry* **2016,** *18* (6), 1724-1730.

[40] Francisco, M.; van den Bruinhorst, A.; Kroon, M. C. New natural and renewable low transition temperature mixtures (LTTMs): screening as solvents for lignocellulosic biomass processing. *Green Chemistry* **2012,** *14* (8), 2153-2157.

[41] Cardellini, F.; Tiecco, M.; Germani, R.; Cardinali, G.; Corte, L.; Roscini, L.; Spreti, N. Novel zwitterionic deep eutectic solvents from trimethylglycine and carboxylic acids: characterization of their properties and their toxicity. *RSC Advances* **2014,** *4* (99), 55990-56002.

[42] Wang, P.; Ma, F.-P.; Zhang, Z.-H. l-(+)-Tartaric acid and choline chloride based deep eutectic solvent: An efficient and reusable medium for synthesis of N-substituted pyrroles via Clauson-Kaas reaction. *Journal of Molecular Liquids* **2014,** *198*, 259-262.

[43] Wang, H.; Gurau, G.; Shamshina, J.; Cojocaru, O. A.; Janikowski, J.; MacFarlane, D. R.; Davis, J. H.; Rogers, R. D. Simultaneous membrane transport of two active pharmaceutical ingredients by charge assisted hydrogen bond complex formation. *Chemical Science* **2014,** *5* (9), 3449-3456.

[44] Phaechamud, T.; Tuntarawongsa, S.; Charoensuksai, P. Evaporation Behavior and Characterization of Eutectic Solvent and Ibuprofen Eutectic Solution. *AAPS PharmSciTech* **2016,** *17* (5), 1213-1220.

[45] Aroso, I. M.; Silva, J. C.; Mano, F.; Ferreira, A. S. D.; Dionísio, M.; Sá-Nogueira, I.; Barreiros, S.; Reis, R. L.; Paiva, A.; Duarte, A. R. C. Dissolution enhancement of active pharmaceutical ingredients by therapeutic deep eutectic systems. *European Journal of Pharmaceutics and Biopharmaceutics* **2016,** *98*, 57-66.

[46] Florindo, C.; Branco, L. C.; Marrucho, I. M. Development of hydrophobic deep eutectic solvents for extraction of pesticides from aqueous environments. *Fluid Phase Equilibria* **2017,** *448*, 135-142.

[47] Martins, M. A. R.; Crespo, E. A.; Pontes, P. V. A.; Silva, L. P.; Bülow, M.; Maximo, G. J.; Batista, E. A. C.; Held, C.; Pinho, S. P.; Coutinho, J. A. P. Tunable Hydrophobic Eutectic Solvents Based on Terpenes and Monocarboxylic Acids. *ACS Sustainable Chemistry & Engineering* **2018**, 10.1021/acssuschemeng.8b01203.

[48] Palomba, T.; Ciancaleoni, G.; Del Giacco, T.; Germani, R.; Ianni, F.; Tiecco, M. Deep Eutectic Solvents formed by chiral components as chiral reaction media and studies of their structural properties. *Journal of Molecular Liquids* **2018,** *262*, 285-294.

[49] Fanjul-Mosteirín, N.; Concellón, C.; del Amo, V. L-Isoleucine in a choline chloride/ethylene glycol deep eutectic solvent: a reusable reaction kit for the asymmetric cross-aldol carboligation. *Organic Letters* **2016,** *18* (17), 4266-4269.

[50] Brenna, D.; Massolo, E.; Puglisi, A.; Rossi, S.; Celentano, G.; Benaglia, M.; Capriati, V. Towards the development of continuous, organocatalytic, and stereoselective reactions in deep eutectic solvents. *Beilstein journal of organic chemistry* **2016,** *12*, 2620-2626.

[51] Massolo, E.; Palmieri, S.; Benaglia, M.; Capriati, V.; Perna, F. M. Stereoselective organocatalysed reactions in deep eutectic solvents: highly tunable and biorenewable reaction media for sustainable organic synthesis. *Green Chemistry* **2016,** *18* (3), 792-797.

[52] Ñíguez, D. R.; Guillena, G.; Alonso, D. A. Chiral 2-Aminobenzimidazoles in deep eutectic mixtures: recyclable organocatalysts for the enantioselective Michael addition of 1, 3-dicarbonyl compounds to β-nitroalkenes. *ACS Sustainable Chemistry & Engineering* **2017,** *5* (11), 10649-10656.

[53] Flores-Ferrándiz, J.; Chinchilla, R. Organocatalytic enantioselective conjugate addition of aldehydes to maleimides in deep eutectic solvents. *Tetrahedron: Asymmetry* **2017,** *28* (2), 302-306.

[54] Ñíguez, D. R.; Khazaeli, P.; Alonso, D. A.; Guillena, G. Deep Eutectic Mixtures as Reaction Media for the Enantioselective Organocatalyzed α-Amination of 1,3-Dicarbonyl Compounds. *Catalysts* **2018,** *8* (5), 217.

[55] Wang, J.; Liu, Y.; Zhou, Z.; Fu, Y.; Chang, J. Epoxidation of Soybean Oil Catalyzed by Deep Eutectic Solvents Based on the Choline Chloride–Carboxylic Acid Bifunctional Catalytic System. *Industrial & Engineering Chemistry Research* **2017,** *56* (29), 8224-8234.

[56] Azizi, N.; Edrisi, M. Multicomponent reaction in deep eutectic solvent for synthesis of substituted 1-aminoalkyl-2-naphthols. *Research on Chemical Intermediates* **2017,** *43* (1), 379-385.

[57] Molnar, M.; Komar, M.; Brahmbhatt, H.; Babić, J.; Jokić, S.; Rastija, V. Deep Eutectic Solvents as Convenient Media for Synthesis of Novel Coumarinyl Schiff Bases and Their QSAR Studies. *Molecules* **2017,** *22* (9), 1482.

[58] Azizi, N.; Batebi, E.; Bagherpour, S.; Ghafuri, H. Natural deep eutectic salt promoted regioselective reduction of epoxides and carbonyl compounds. *RSC Advances* **2012,** *2* (6), 2289-2293.

[59] Kranz, M.; Hofmann, T. Food-Grade Synthesis of Maillard-Type Taste Enhancers Using Natural Deep Eutectic Solvents (NADES). *Molecules* **2018,** *23* (2), 261.

[60] Ilgen, F.; Konig, B. Organic reactions in low melting mixtures based on carbohydrates and l-carnitine-a comparison. *Green Chemistry* **2009,** *11* (6), 848-854.

[61] Xu, P.; Zheng, G.-W.; Zong, M.-H.; Li, N.; Lou, W.-Y. Recent progress on deep eutectic solvents in biocatalysis. *Bioresources and Bioprocessing* **2017,** *4* (1), 34.

[62] Saini, P.; Kumar, N.; Wani, S. I.; Sharma, S.; Chimni, S. S.; Sareen, D. Bioresolution of racemic phenyl glycidyl ether by a putative recombinant epoxide hydrolase from Streptomyces griseus NBRC 13350. *World Journal of Microbiology and Biotechnology* **2017,** *33* (5), 82.

[63] Xu, P.; Du, P.-X.; Zong, M.-H.; Li, N.; Lou, W.-Y. Combination of deep eutectic solvent and ionic liquid to improve biocatalytic reduction of 2-octanone with Acetobacter pasteurianus GIM1.158 cell. *Scientific Reports* **2016,** *6*, 26158.

[64] Wei, P.; Liang, J.; Cheng, J.; Zong, M.-H.; Lou, W.-Y. Markedly improving asymmetric oxidation of 1-(4-methoxyphenyl) ethanol with Acetobacter sp. CCTCC M209061 cells by adding deep eutectic solvent in a two-phase system. *Microbial Cell Factories* **2016,** *15*, 5.

[65] Xu, P.; Xu, Y.; Li, X.-F.; Zhao, B.-Y.; Zong, M.-H.; Lou, W.-Y. Enhancing Asymmetric Reduction of 3-Chloropropiophenone with Immobilized Acetobacter sp. CCTCC M209061 Cells by Using Deep Eutectic Solvents as Cosolvents. *ACS Sustainable Chemistry & Engineering* **2015,** *3* (4), 718-724.

[66] Müller, C. R.; Lavandera, I.; Gotor-Fernández, V.; Domínguez de María, P. Performance of Recombinant-Whole-Cell-Catalyzed Reductions in Deep-Eutectic-Solvent–Aqueous-Media Mixtures. *ChemCatChem* **2015,** *7* (17), 2654-2659.

[67] Panić, M.; Elenkov, M. M.; Roje, M.; Bubalo, M. C.; Redovniković, I. R. Plant-mediated stereoselective biotransformations in natural deep eutectic solvents. *Process Biochemistry* **2018,** *66*, 133-139.

[68] Vitale, P.; Abbinante, V. M.; Perna Filippo, M.; Salomone, A.; Cardellicchio, C.; Capriati, V. Unveiling the Hidden Performance of Whole Cells in the Asymmetric Bioreduction of Aryl-containing Ketones in Aqueous Deep Eutectic Solvents. *Advanced Synthesis & Catalysis* **2016,** *359* (6), 1049-1057.

[69] Lindberg, D.; de la Fuente Revenga, M.; Widersten, M. Deep eutectic solvents (DESs) are viable cosolvents for enzyme-catalyzed epoxide hydrolysis. *Journal of Biotechnology* **2010,** *147* (3), 169-171.

[70] Peng, F.; Zhao, Y.; Li, F.-Z.; Zong, M.-H.; Lou, W.-Y. The effect of deep eutectic solvents on the asymmetric hydrolysis of styrene oxide by mung bean epoxide hydrolases. *Bioresources and Bioprocessing* **2018,** *5* (1), 5.

[71] Cao, S.-L.; Yue, D.-M.; Li, X.-H.; Smith, T. J.; Li, N.; Zong, M.-H.; Wu, H.; Ma, Y.-Z.; Lou, W.-Y. Novel Nano-/Micro-Biocatalyst: Soybean Epoxide Hydrolase Immobilized on UiO-66-NH2 MOF for Efficient Biosynthesis of Enantiopure (R)-1, 2-Octanediol in Deep Eutectic Solvents. *ACS Sustainable Chemistry & Engineering* **2016,** *4* (6), 3586-3595.

[72] Tian, X.; Zhang, S.; Zheng, L. Enzyme-catalyzed henry reaction in choline chloride-based deep eutectic solvents. *Journal of Microbiology and Biotechnology* **2016,** *26* (1), 80-88.

[73] Maugeri, Z.; Domínguez de María, P. Benzaldehyde lyase (BAL)-catalyzed enantioselective CC bond formation in deep-eutectic-solvents–buffer mixtures. *Journal of Molecular Catalysis B: Enzymatic* **2014,** *107*, 120-123.

[74] Petrenz, A.; María, P. D. d.; Ramanathan, A.; Hanefeld, U.; Ansorge-Schumacher, M. B.; Kara, S. Medium and reaction engineering for the establishment of a chemo-enzymatic dynamic kinetic resolution of rac-benzoin in batch and continuous mode. *Journal of Molecular Catalysis B: Enzymatic* **2015,** *114*, 42-49.

[75] Zhao, H.; Shen, K. G-quadruplex DNA-based asymmetric catalysis of michael addition: Effects of sonication, ligands, and co-solvents. *Biotechnology Progress* **2016,** *32* (4), 891-898.

[76] Zhao, H.; Shen, K. DNA-based asymmetric catalysis: role of ionic solvents and glymes. *RSC Advances* **2014,** *4* (96), 54051-54059.

[77] Gorke, J. T.; Srienc, F.; Kazlauskas, R. J. Hydrolase-catalyzed biotransformations in deep eutectic solvents. *Chemical Communications* **2008,** *0* (10), 1235-1237.

[78] Ruesgas-Ramón, M.; Figueroa-Espinoza, M. C.; Durand, E. Application of Deep Eutectic Solvents (DES) for Phenolic Compounds Extraction: Overview, Challenges, and Opportunities. *Journal of Agricultural and Food Chemistry* **2017,** *65* (18), 3591-3601.

[79] Tang, B.; Zhang, H.; Row, K. H. Application of deep eutectic solvents in the extraction and separation of target compounds from various samples. *Journal of Separation Science* **2015,** *38* (6), 1053-1064.

[80] Maugeri, Z.; Leitner, W.; Domínguez de María, P. Practical separation of alcohol–ester mixtures using Deep-Eutectic-Solvents. *Tetrahedron Letters* **2012,** *53* (51), 6968-6971.

3.2.1. Does chirality play a role on deep eutectic solvents formation?

This section is based on e Silva, F. A.; Kelley, S. P.; Silva, L. P.; Berton, P.; Ventura, S. P. M.; Coutinho, J. A. P.; Rogers, R. D. Does chirality play a role on deep eutectic solvents formation?. *in preparation*.

Contributions: S.P.K., J.A.P.C. and R.D.R. conceived and directed this work. Francisca A. e Silva, S.P.K. and L.P.S. acquired the experimental data. In particular, Francisca A. e Silva acquired all experimental data using DSC, TGA and FTIR. Francisca A. e Silva, S.P.K., P.B., S.P.M.V., J.A.P.C. and R.D.R. interpreted the experimental data. Francisca A. e Silva, S.P.K., J.A.P.C. and R.D.R. are the responsible for the manuscript preparation with contributions from the remaining authors.

Abstract

In this work, the opportunity of using the chirality that most traditional DES constituents present to create versatile and efficient solvents for enantioseparations is identified. For that, the role of chirality in the formation of DES was studied in a fundamental approach by measuring the solid-liquid phase diagrams of all enantiomeric combinations of proline:malic acid mixtures. After characterizing the eutectic point and realizing that distinct enantomeric combinations lead to distinct eutectic temperatures, the molecular scenario behind DES formation was unveiled. Infra-red (IR) spectroscopy and powder X-ray diffraction (PXRD) were used to study the molecular interactions participating in the formation of chiral DES. Although deprotonation-protonation was found to be at the basis of proline:malic acid DES formation, the different interactions established between distinct enantiomeric pairs remain unknown.

Introduction

The nature of DES is not yet fully understood, albeit considerable efforts have been made to unveil the molecular scenario underlying DES formation. Some notions on the molecular interactions occurring in DES are currently available, especially in DES formed by [Ch]Cl, the hydrogen bond network, resulting from intermolecular interactions,

was identified as playing the major role.[1, 2] Even though DES formation is believed to be mainly driven by hydrogen bond networks, other interactions occurring in the liquid phase (viz. *"HBA-HBD"*, *"HBA-HBA"* and *"HBD-HBD"*) cannot be neglected, as recently reported.[3-5]

It is well-established that chemical interactions, such as the hydrogen bond network, are affected by the stereochemistry.[6-10] In [Ch]Cl-based DES, distinct structural isomers of dihydroxybenzene were shown to yield distinct melting points, that correlate well with their water solubilities,[11] considering the DES formation dominated by hydrogen bonding (inferred by IR and NMR analysis).[11] Based on this hypothesis, and in line with the seminal work from Palomba et al.[12] (discussed before), it is believed that chirality may play a role in DES formation and that such knowledge may contribute to more performant chiral applications.

Proline and malic acid are two common components used for DES formulation, either as a HBA:HBD pair or combined with other chemicals.[13-18] Mixed up together,[13-15] proline:malic acid form an eutectic mixture, whose formation is governed by intermolecular hydrogen bonding (inferred by MD simulations) although acid-acid hydrogen bonds may also take place.[13] Due to the considerable literature data available on proline:malic acid DES (centred on its application as "green" – not chiral – solvent[14, 15] rather than on their physical-chemical characterization[13]), its natural origin and the commercial availability of all enantiomers, these were selected on the preparation of a model DES in the current study. Here we examined the four possible combinations of each enantiomer of both compounds across a series of mole fractions. The melting points were determined by two methods (visual detection and differential scanning calorimetry, DSC), allowing to fully characterize the solid-liquid phase diagram. As an attempt to understand the interactions governing chiral DES formation and to explain the differences in the melting points depression, Fourier Transform Infrared Spectroscopy (FTIR) and Powder X-Ray Diffraction (PXRD) analysis were carried.

Experimental section

Materials

All chiral components used in DES preparation, D-Proline, D-Pro (99 wt% purity), L-Proline, L-Pro (99 wt%purity), D-Malic acid, D-MalA (≥ 98 wt% purity) and L-Malic acid, L-MalA (99 wt% purity) were purchased at Alfa Aesar. Their chemical structures are shown in Figure 3.18.

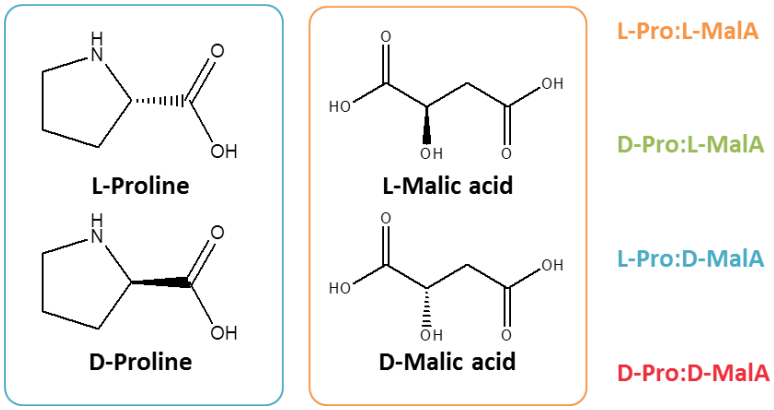

Figure 3.18. Chemical structure and abbreviation of DES chiral formers studied.

Thermogravimetric analysis (TGA)

The TGA thermograms were collected using a TA Instruments TGA5500. All analyses were performed for the L-enantiomers of the pure compounds and a representative binary mixture, and were conducted under nitrogen atmosphere. Samples (circa 8 – 15 mg) were heated to 700 °C, using a constant heating ramp of 5 °C.min^{-1} with a 30 min isotherm at 75 °C to remove excess volatiles or solvents traces. Decomposition temperatures ($T_{5\%dec}$) were taken as the onset to 5 wt% mass loss (within ±0.1 °C).

Solid-liquid equilibria

The solid-liquid phase diagrams were determined according to two distinct methods as follows.

Visual method.[19] The binary mixtures are prepared by weighing (within ± 0.002 g), inside a dry-argon glove-box, the desired amounts of each pure compound to obtain molar ratios covering the entire composition range. The vials with the mixtures were heated under stirring until complete melting and then solidified. Given the paste-like aspect of such mixtures, a visual method where the mixtures were gradually heated in an

oil bath until complete melting was employed. The temperature was controlled with a PT100 probe with a precision of ±0.1 ^{o}C, which was prior calibrated against a calibrated platinum resistance thermometer, SPRT100 (Fluke-Hart Scientific 1529 Chub-E4), traceable to the National Institute of Standards and Technology (NIST), with an uncertainty less than 2×10^{-2} ^{o}C.

Differential scanning calorimetry (DSC). The mixtures were prepared by weighing (within ± 0.002 g) the correct amounts of each pure compound covering the entire composition range, followed by homogenization to mix the two components. A TA Instruments DSC2500 calorimeter was utilized under a nitrogen stream. Both pure and binary mixture samples (circa 2 – 10 mg) were placed in hermetically sealed aluminium pans. Samples were first heated up to 120 ^{o}C (circa 60 ^{o}C below the lowest $T_{5\%dec}$) and then cooled down to -90 ^{o}C, for three consecutive cycles, at a ramp rate of 5 ^{o}C.min^{-1}. Isotherms of 5 min and 10 min followed each heating and cooling ramp, respectively, to guarantee equilibration of the temperature in the cell. For pure enantiomers of malic acid, the same procedure was implemented, whereas proline was heated up to 150 ^{o}C. Melting temperatures were taken as the onset for pure compounds and as the maximum temperatures of the melting peak for binary mixtures.

Fourier Transform Infrared Spectroscopy (FT-IR)

Binary mixtures (weighed and homogenized) were placed at 120 ^{o}C (upper limit on DSC analysis) for at least 1 hour. The corresponding spectra were obtained from 400 to 4000 cm^{-1} using a Bruker Alpha FT-IR (Bruker Optics Ltd., Milton, On, Canada) by direct measurement via attenuated total reflection (ATR) of the neat samples on a diamond crystal.

Powder X-Ray Diffraction (PXRD)

Binary mixtures (weighed and homogenized) were placed at 120 ^{o}C (upper limit on DSC analysis) for at least 1 hour. After cooling down, the samples were smeared onto the silicon wafer of a proprietary low-background sample holder. Data on PXRD Powder X-ray

diffraction (PXRD) was recorded with a Bruker D8 Advance equipped with a Lynxeye linear position sensitive detector Bruker AXS, using Ni-filtered Cu-Kα radiation.

Results and Discussion

Effect of chirality on solid-liquid equilibria

The role of chirality on DES formation was initially studied by determining the solid-liquid diagrams of proline:malic acid DES. All enantiomer combinations, viz. L-Pro:L-MalA, L-Pro:D-MalA, D-Pro:L-MalA and D-Pro:D-MalA, were investigated. For that purpose two methods were employed, namely a visual method and DSC. Prior DSC studies, the decomposition temperatures (i.e., $T_{5\%dec}$) of L-proline and L-malic acid were determined (and further assumed to be similar to that of the D-enantiomers). $T_{5\%dec}$ values of 220.7 and 183.1 ^{o}C for L-proline and L-malic acid, respectively, were obtained (the corresponding thermograms are depicted in Figure F1 of Appendix F). This step allowed setting the upper temperature limit on DSC, no greater than 60 ^{o}C below $T_{5\%dec}$ of L-malic acid, where no contamination of the DSC cell due to DES formers degradation is assured. To guarantee that proline and malic acid mixtures do not have an effect onthe thermal stability, a representative binary mixture at x_{MalA} = 0.1 was subjected to TGA, yielding a $T_{5\%dec}$ similar to that of pure L-malic acid (185.7 ^{o}C *versus* 183.1 ^{o}C, cf. Figure F2 of Appendix F).

It should be noted that proline is reported to decompose before melting at circa 221 ^{o}C,[20] so no melting point is observed in DSC thermograms (DSC data in Figure F3 of Appendix F). L-malic acid and D-malic acid displayed similar melting points ($T_{m,\text{L-MalA}}$ = 100.8 ^{o}C and $T_{m,\text{D-MalA}}$ = 103.7 ^{o}C) (DSC data in Figure F3 of Appendix F). This body of data is consistent with the results gathered by the visual method ($T_{m,\text{L-Pro}}$ = 220.3 ^{o}C, $T_{m,\text{D-Pro}}$ = 220.3 ^{o}C, $T_{m,\text{L-MalA}}$ = 106.0 ^{o}C and $T_{m,\text{D-MalA}}$ = 103.0 ^{o}C). The solid-liquid phase diagrams are shown in Figure 3.19, with data obtained with the two methodologies adopted plotted together (detailed data on T_m is given in Table F1 of Appendix F). It should be highlighted that some inconsistency on the data collected is observed. This problem is due to the melting of the component with lower melting temperature that is the only one being measured by DSC. Likely, this is due to the DSC upper limit temperature set, particularly

for x_{MalA} < 0.5 or even a consequence of the sample preparation. Indeed, the sample preparation was previously shown to impact on DES properties[13, 21] and new measurements should be carried. Also, DSC did not allow the study of the entire range of molar fractions, as a consequence of the upper temperature limited set for the analysis (as explained above). A good agreement was found for both methods in T_m of binary mixtures of higher malic acid contents. DSC thermograms of binary mixtures covering all possible enantiomeric combinations in the entire composition range are provided in Appendix F, Figure F4.

The systems reported in Figure 3.19 are characterized by the presence of a single eutectic point and display significant melting point depressions. These allow obtaining liquid mixtures at operationally convenient temperatures, albeit within a composition range limited to high acid molar fractions. The eutectic composition was consistently identified at around 0.6 of malic acid molar fraction for all systems (Figure 3.19). Distinct melting point depressions arising from combining distinct enantiomers were identified, with the eutectic temperatures (T_{Eut}) differing significantly. A maximum temperature difference of 27 ^{o}C was observed between L-Pro:L-MalA (the lowest T_{Eut}) and L-Pro:D-MalA (the highest T_{Eut}). The eutectic temperatures can be ranked as follows: L-Pro:L-MalA < D-Pro:L-MalA < D-Pro:D-MalA < L-Pro:D-MalA. Proline:malic acid DES formation is a result of intermolecular hydrogen bonds activated by the presence of proline breaking acid-acid interactions.[13] So, the higher the ability to form interspecies hydrogen bonds, the lower the eutectic points. Here, the chirality of the acid is dictating the order described above ($T_{Eut,L\text{-}MalA\text{-}based\ DES}$ < $T_{Eut,D\text{-}MalA\text{-}based\ DES}$), with L- and D-proline being more prone to interact with L- and D-malic acid, respectively. Comparatively, eutectics formed by components of opposite chirality (D-Pro:L-MalA and L-Pro:D-MalA) present higher melting temperatures. This is consistent with the fact that structural isomers acting as HBD with [Ch]Cl afford eutectics with different melting temperatures.[11] Opposing to enantiomers, however, structural isomers possess significantly distinct physico-chemical properties, which helps to understand the different phase behaviours. Enantiomers, although sharing the same physico-chemical properties (except for their specific rotation) under achiral environment, can interact distinctly with chiral entities – this being the most

likely foundation for chiral DES formation.[22] Using DFT and NMR spectroscopy, it was also recently concluded that in DES composed of chiral constituents, hydrogen bonds were the main responsible for diastereoisomerical differences in liquids.[12] In particular, and in agreement with our findings, it was demonstrated that HBA and HBD with the same chirality interact more specifically.[12]

Molecular scenario behind chiral DES formation

To gather information on the interactions leading to the formation of chiral proline:malic acid DES, FT-IR and PXRD experiments were carried. IR has been widely used on the study of DES nature.[11, 23] Samples covering the whole composition range were analysed. By comparison of the IR spectra at distinct compositions of Pro:MA (cf. Figure 3.20), it is possible to observe that the C=O stretching mode for malic acid (≈1710 – 1690 cm^{-1})[24] changes its position and profile but does not disappear in the entire composition range. Proline is a zwitterion, as indicated by the bands present at ≈ 1611 cm^{-1} ($-COO^-$) and ≈ 1550 cm^{-1} ($=NH_2^+$).[25] The CO asymmetric stretch for proline in the range of ≈ 1611 cm^{-1} shifts to higher energy, indicating proline protonation. So, it can be argued that the DES formation occurs by the deprotonation of malic acid (in only one –COOH group), protonating proline. Despite the differences observed in the melting points depression may be a result of distinct interspecies interactions, their deepest comprehension remains a challenge (Figure 3.21).

By PXRD analysis of solidified binary mixtures, it was observed that within the molar ratio $0.5 < x_{MalA} < 0.9$, proline was undetectable. The difractograms are depicted in Figures F5 – F8 of Appendix F. A new peak emerges that does not match either of the enantiomer starting materials, which suggests the existence of a new compound after melting-solidifying (salt?, co-crystal?), that requires further investigation.

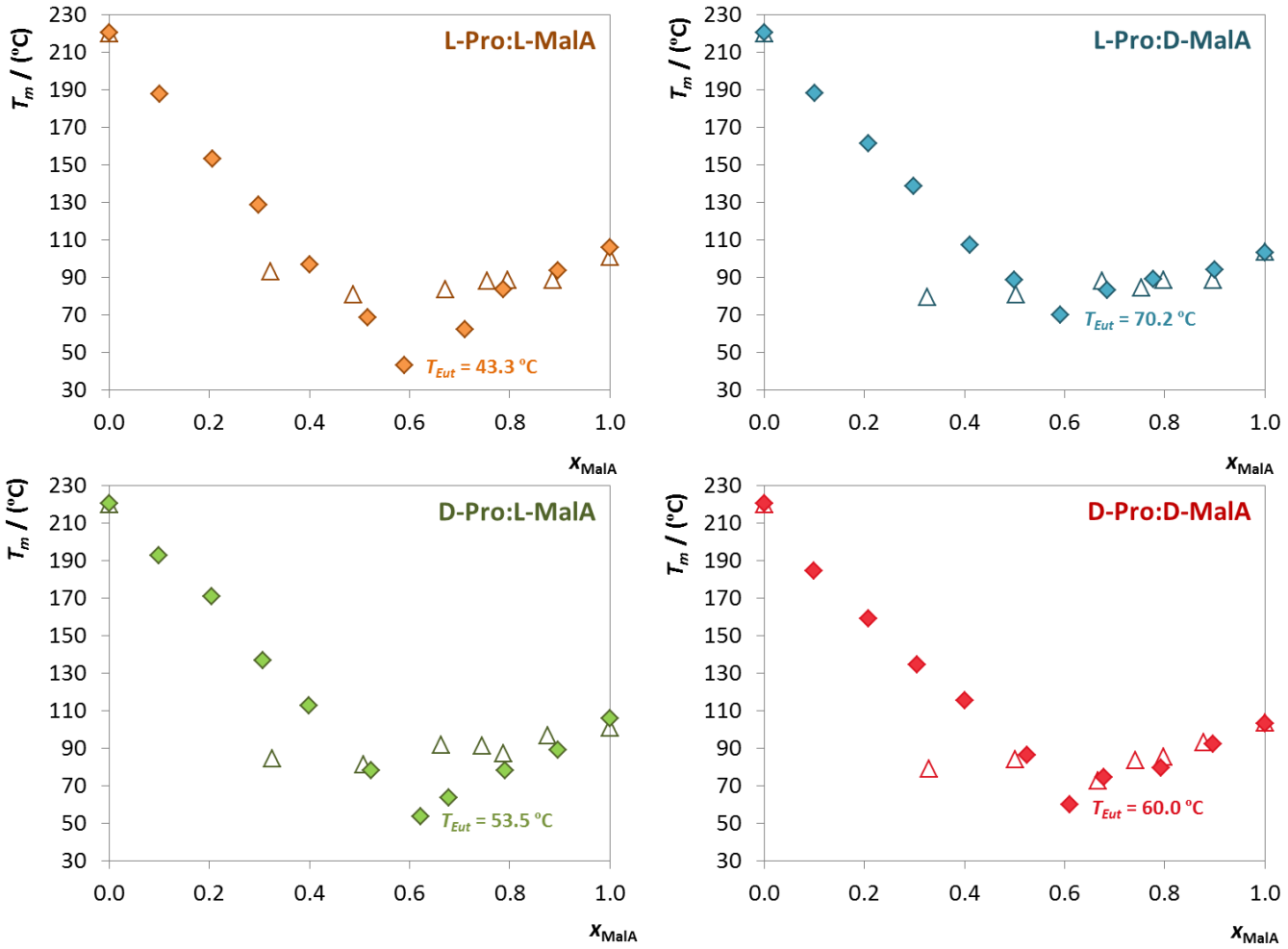

Figure 3.19. Solid-liquid phase diagrams of chiral DES formed by proline:malic acid as a function of enantiomers combination: (◆) visual method; (△) DSC.

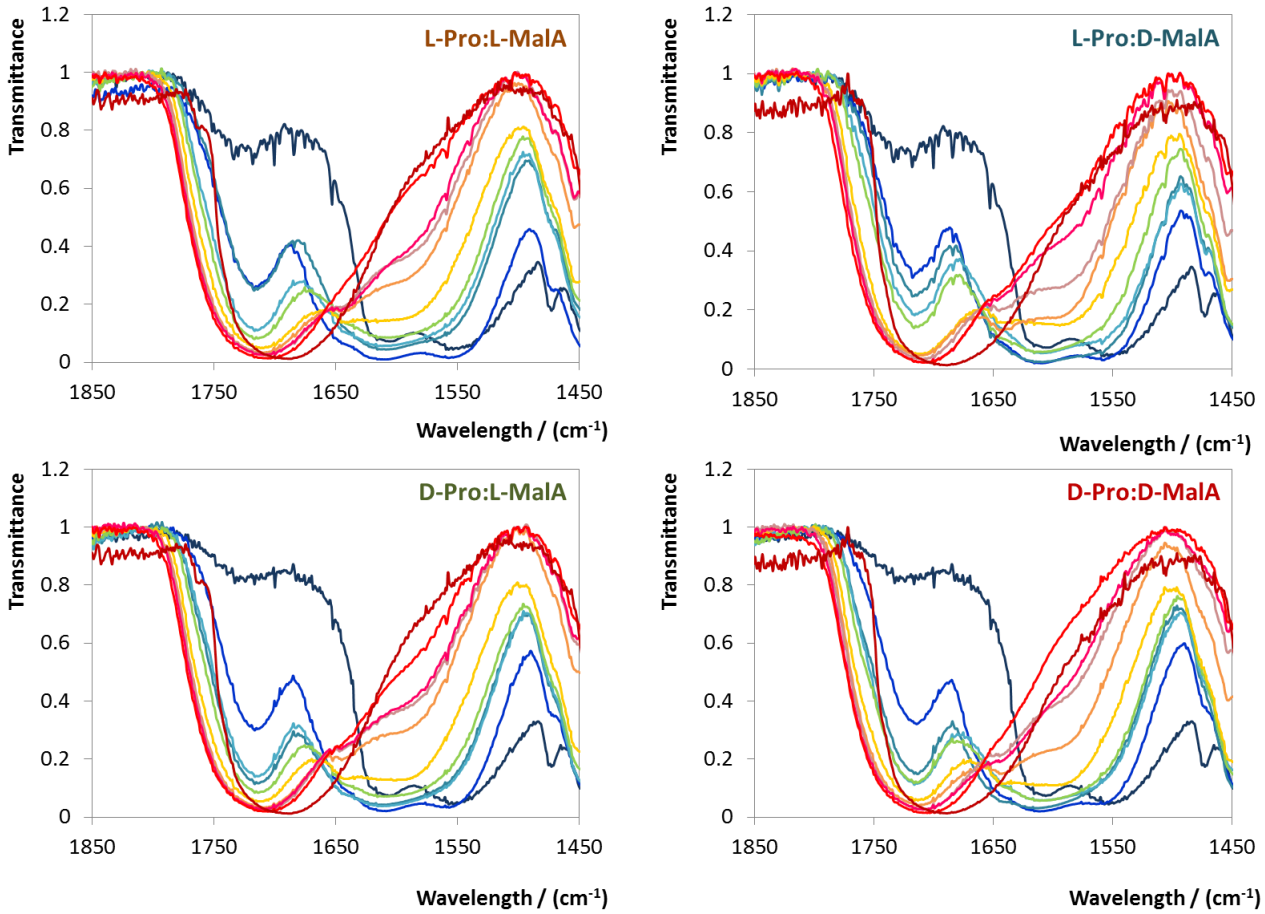

Figure 3.20. IR spectra of proline:malic acid binary mixtures as a function of the enantiomeric combinations studied: (■) x_{MalA} = 0, (■) x_{MalA} = 0.1, (■) x_{MalA} = 0.2, (■) x_{MalA} = 0.25, (■) x_{MalA} = 0.33, (■) x_{MalA} = 0.5, (■) x_{MalA} = 0.67, (■) x_{MalA} = 0.75, (■) x_{MalA} = 0.8, (■) x_{MalA} = 0.9 and (■) x_{MalA} = 1.

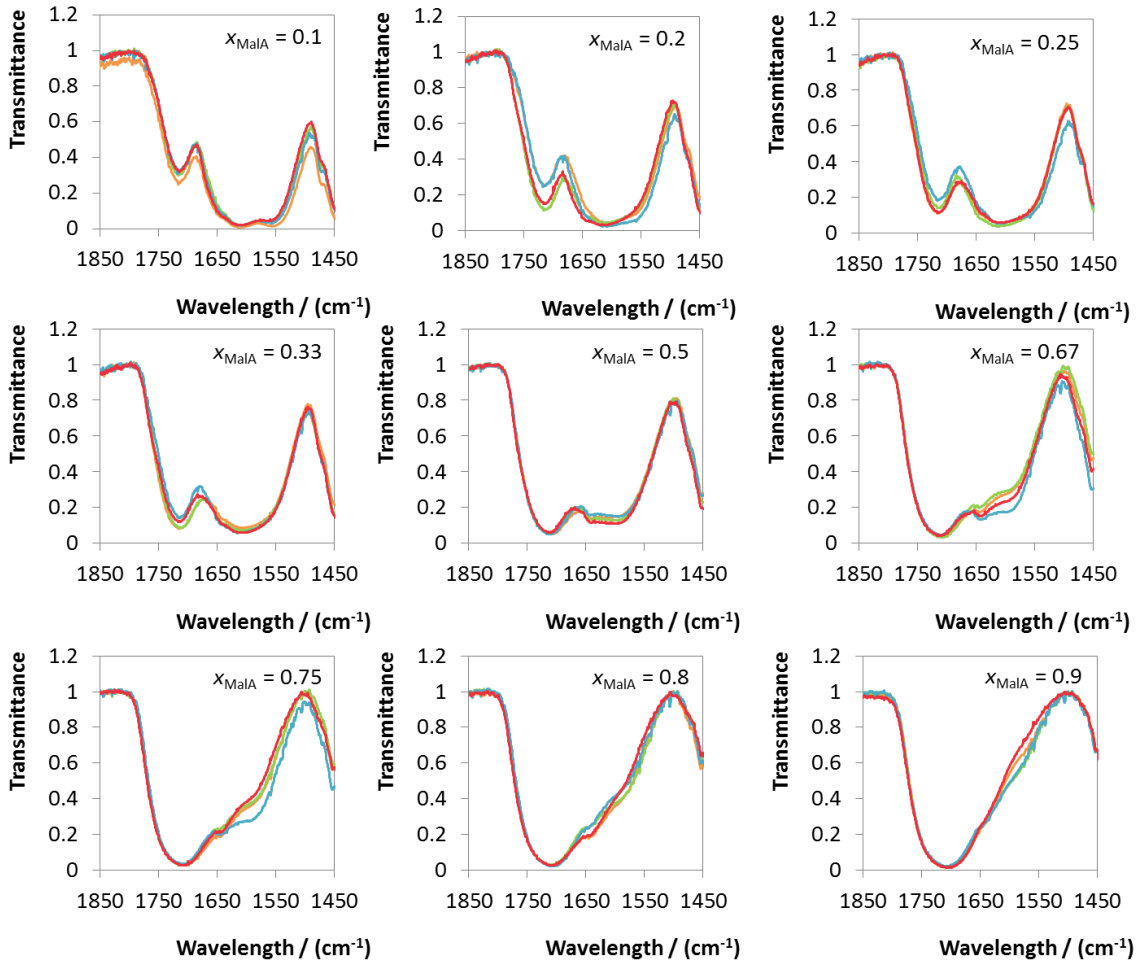

Figure 3.21. IR spectra of proline:malic acid binary mixtures covering the possible enantiomers combinations in the whole composition range under study: (■) L-Pro:L-MalA, (■) L-Pro:D-MalA, (■) D-Pro:L-MalA and (■) D-Pro:D-MalA.

Conclusions

A preliminary study on how chirality impacts on DES formation was here performed. The solid-liquid phase diagrams for chiral DES formed by proline and malic acid were characterized for all enantiomeric combinations available (viz. L-Pro:L-MalA, L-Pro:D-MalA, D-Pro:L-MalA and D-Pro:D-MalA). The results showed the possibility of having liquid mixtures at relatively suitable temperatures (from the operational point of view), ranging from 43.3 and 70.2 °C if considering the eutectic composition (x_{MalA} ≈ 0.6). Moreover, distinct enantiomers combinations led to different levels of melting temperature depressions, these more significant if pairs bearing the same chirality were used. This is particularly relevant if application as chiral solvents, as outlined before, is

anticipated. To provide additional insights on the molecular interactions affecting the DES formation, in particular chiral DES, IR and PXRD studies were also conducted. Proline:malic acid DES has on its genesis the deprotonation of the acid (in only one –COOH group), protonating the amino acid zwitterion. Useful knowledge was obtained, yet the chirality-related molecular scenario underlying the proline:malic acid DES remains unclear. NMR and DFT simulations have been used elsewhere[12] to this purpose. More recently, van den Bruinhorst et al.[13] reported proline:malic acid as having a low chemical stability (it undergoes esterification upon preparation) and highly viscous DES. Even though the current study is of more fundamental basis and proline:malic acid DES only served as a model, the use of chiral DES as solvents in enantioseparations is the ultimate goal. Under this scenario, the search for chiral chemicals affording highly chemically stable, watery and room temperature DES is urgent (e.g., chiral ammonium-based salts, sugars and terpenes).[12, 26-28] Once such a task is accomplished, it will be possible to play with the "double chirality" phenomenon to create versatile, yet more efficient solvents for chiral separations.

References

[1] Zhekenov, T.; Toksanbayev, N.; Kazakbayeva, Z.; Shah, D.; Mjalli, F. S. Formation of type III Deep Eutectic Solvents and effect of water on their intermolecular interactions. *Fluid Phase Equilibria* **2017,** *441*, 43-48.

[2] Florindo, C.; McIntosh, A. J. S.; Welton, T.; Branco, L. C.; Marrucho, I. M. A closer look into deep eutectic solvents: exploring intermolecular interactions using solvatochromic probes. *Physical Chemistry Chemical Physics* **2018,** *20* (1), 206-213.

[3] Araujo, C. F.; Coutinho, J. A. P.; Nolasco, M. M.; Parker, S. F.; Ribeiro-Claro, P. J. A.; Rudic, S.; Soares, B. I. G.; Vaz, P. D. Inelastic neutron scattering study of reline: shedding light on the hydrogen bonding network of deep eutectic solvents. *Physical Chemistry Chemical Physics* **2017,** *19* (27), 17998-18009.

[4] Martins, M. A. R.; Pinho, S. P.; Coutinho, J. A. P. Insights into the Nature of Eutectic and Deep Eutectic Mixtures. *Journal of Solution Chemistry* **2018**.

[5] Hammond, O. S.; Bowron, D. T.; Jackson, A. J.; Arnold, T.; Sanchez-Fernandez, A.; Tsapatsaris, N.; Garcia Sakai, V.; Edler, K. J. Resilience of Malic Acid Natural Deep Eutectic

Solvent Nanostructure to Solidification and Hydration. *The Journal of Physical Chemistry B* **2017,** *121* (31), 7473-7483.

[6] Belo, E. A.; Pereira, J. E. M.; Freire, P. T. C.; Argyriou, D. N.; Eckert, J.; Bordallo, H. N. Hydrogen bonds in crystalline d-alanine: diffraction and spectroscopic evidence for differences between enantiomers. *IUCrJ* **2018,** *5* (1), 6-12.

[7] Suezawa, H.; Ishihara, S.; Umezawa, Y.; Tsuboyama, S.; Nishio, M. The Aromatic CH/π Hydrogen Bond as an Important Factor in Determining the Relative Stability of Diastereomeric Salts Relevant to Enantiomeric Resolution − A Crystallographic Database Study. *European Journal of Organic Chemistry* **2004,** *2004* (23), 4816-4822.

[8] Katrusiak, A. Stereochemistry and transformations of NH---N hydrogen bonds Part I. Structural preferences for the hydrogen site. *Journal of Molecular Structure* **1999,** *474* (1), 125-133.

[9] Ahmed, M.; Jelsch, C.; Guillot, B.; Lecomte, C.; Domagała, S. Relationship between Stereochemistry and Charge Density in Hydrogen Bonds with Oxygen Acceptors. *Crystal Growth & Design* **2013,** *13* (1), 315-325.

[10] Katrusiak, A. Stereochemistry and transformation of -OH…O= hydrogen bonds Part I. Polymorphism and phase transition of 1,3-cyclohexanedione crystals. *Journal of Molecular Structure* **1992,** *269* (3), 329-354.

[11] Abbott, A. P.; Ahmed, E. I.; Prasad, K.; Qader, I. B.; Ryder, K. S. Liquid pharmaceuticals formulation by eutectic formation. *Fluid Phase Equilibria* **2017,** *448*, 2-8.

[12] Palomba, T.; Ciancaleoni, G.; Del Giacco, T.; Germani, R.; Ianni, F.; Tiecco, M. Deep Eutectic Solvents formed by chiral components as chiral reaction media and studies of their structural properties. *Journal of Molecular Liquids* **2018,** *262*, 285-294.

[13] van den Bruinhorst, A.; Spyriouni, T.; Hill, J.-R.; Kroon, M. C. Experimental and Molecular Modeling Evaluation of the Physicochemical Properties of Proline-Based Deep Eutectic Solvents. *The Journal of Physical Chemistry B* **2018,** *122* (1), 369-379.

[14] Dai, Y.; van Spronsen, J.; Witkamp, G.-J.; Verpoorte, R.; Choi, Y. H. Natural deep eutectic solvents as new potential media for green technology. *Analytica Chimica Acta* **2013,** *766*, 61-68.

[15] Francisco, M.; van den Bruinhorst, A.; Kroon, M. C. New natural and renewable low transition temperature mixtures (LTTMs): screening as solvents for lignocellulosic biomass processing. *Green Chemistry* **2012,** *14* (8), 2153-2157.

[16] Soares, B.; Tavares, D. J. P.; Amaral, J. L.; Silvestre, A. J. D.; Freire, C. S. R.; Coutinho, J. A. P. Enhanced Solubility of Lignin Monomeric Model Compounds and Technical Lignins in Aqueous Solutions of Deep Eutectic Solvents. *ACS Sustainable Chemistry & Engineering* **2017,** *5* (5), 4056-4065.

[17] Choi, Y. H.; van Spronsen, J.; Dai, Y.; Verberne, M.; Hollmann, F.; Arends, I. W. C. E.; Witkamp, G.-J.; Verpoorte, R. Are Natural Deep Eutectic Solvents the Missing Link in Understanding Cellular Metabolism and Physiology? *Plant Physiology* **2011,** *156* (4), 1701.

[18] Duan, L.; Dou, L.-L.; Guo, L.; Li, P.; Liu, E. H. Comprehensive Evaluation of Deep Eutectic Solvents in Extraction of Bioactive Natural Products. *ACS Sustainable Chemistry & Engineering* **2016,** *4* (4), 2405-2411.

[19] Pontes, P. V. A.; Crespo, E. A.; Martins, M. A. R.; Silva, L. P.; Neves, C. M. S. S.; Maximo, G. J.; Hubinger, M. D.; Batista, E. A. C.; Pinho, S. P.; Coutinho, J. A. P., et al. Measurement and PC-SAFT modeling of solid-liquid equilibrium of deep eutectic solvents of quaternary ammonium chlorides and carboxylic acids. *Fluid Phase Equilibria* **2017,** *448*, 69-80.

[20] Drugbank. https://www.drugbank.ca/drugs/DB00172 (accessed on June 17th, 2018).

[21] Florindo, C.; Oliveira, F. S.; Rebelo, L. P. N.; Fernandes, A. M.; Marrucho, I. M. Insights into the Synthesis and Properties of Deep Eutectic Solvents Based on Cholinium Chloride and Carboxylic Acids. *ACS Sustainable Chemistry and Engineering* **2014**, *2* (10), 2416−2425.

[22] Davankov, V. A. The nature of chiral recognition: Is it a three-point interaction? *Chirality* **1997,** *9* (2), 99-102.

[23] Bica, K.; Shamshina, J.; Hough, W. L.; MacFarlane, D. R.; Rogers, R. D. Liquid forms of pharmaceutical co-crystals: exploring the boundaries of salt formation. *Chemical Communications* **2011,** *47* (8), 2267-2269.

[24] Max, J.-J.; Chapados, C. Infrared Spectroscopy of Aqueous Carboxylic Acids: Malic Acid. *The Journal of Physical Chemistry A* **2002,** *106* (27), 6452-6461.

[25] Mary, Y. S.; Ushakumari, L.; Harikumar, B.; Varghese, H. T.; Panicker, C. Y. FT-IR, FT-raman and SERS spectra of L-proline. *Journal of the Iranian Chemical Society* **2009,** *6* (1), 138-144.

[26] Silva, L. P.; Fernández, L.; Conceição, J. H. F.; Martins, M. A. R.; Sosa, A.; Ortega, J.; Pinho, S. P.; Coutinho, J. A. P. Design and characterization of sugar-based deep eutectic solvents using COSMO-RS. *ACS Sustainable Chemistry & Engineering* **2018**, 10.1021/acssuschemeng.8b02042.

[27] Martins, M. A. R.; Crespo, E. A.; Pontes, P. V. A.; Silva, L. P.; Bülow, M.; Maximo, G. J.; Batista, E. A. C.; Held, C.; Pinho, S. P.; Coutinho, J. A. P. Tunable Hydrophobic Eutectic Solvents Based on Terpenes and Monocarboxylic Acids. *ACS Sustainable Chemistry & Engineering* **2018**, 10.1021/acssuschemeng.8b01203.

[28] Aroso, I. M.; Craveiro, R.; Rocha, Â.; Dionísio, M.; Barreiros, S.; Reis, R. L.; Paiva, A.; Duarte, A. R. C. Design of controlled release systems for THEDES—Therapeutic deep eutectic solvents, using supercritical fluid technology. *International Journal of Pharmaceutics* **2015,** *492* (1), 73-79.

CHAPTER 4

Concluding remarks and future perspectives

4. Concluding remarks and future perspectives

The current thesis was focused on the development of novel and more sustainable extraction and separation platforms for drugs. Two major challenges related to pharmaceutical industry and their products were addressed, so far with important insights gathered on how to design greener and more efficient extraction and separation strategies.

Regarding the valorization of pharmaceutical wastes (Chapter 2), the use of ILs' aqueous solutions for the extraction of drugs (***section 2.2.1.***) and their purification resorting to ILs-based ABS and TPP (***section 2.2.2*** and ***2.2.3***) was explored as an alternative to incineration. The proper adjustment of the solvents involved was shown to dictate the extractive and purification performance of the processes. Most works developed in this thesis, although focused on model compounds deal with real matrices (i.e., pills). Finally, the isolation of target drugs was successfully achieved by playing with the solvent/anti-solvent combinations. These two latter aspects are important stepping-stones to disclose the real viability of the extraction and purification platforms created.

During this thesis, a considerable array of model compounds of relatively low commercial value was covered, forcing further steps towards more valuable drugs. The creation of an integrated process applicable to highly valuable drugs would catch more interest on this valorization approach. Even though using real matrices as drugs' sources, these were limited to pills, other types of formulations (e.g., topical, injectable liquids, oral liquids) should be addressed to emphasize the broad applicability of ILs. Moreover, in some formulations more than one active principle of interest is present and to exploit the outstanding selectivity of IL-based ABS, and in particular IL-based TPP[1] (single-step extraction and purification), would be beneficial. The addition of anti-solvents was the approach adopted for the isolation of the target pharmaceuticals. Instead, approaches solely based on cooling-heating cycles should also be studied in future for the sake of operational simplicity.[2, 3] Additionally, the recycling and reuse tasks should be carefully addressed. Still, and given the enhanced polymorphic design in IL media[4, 5] (overviewed in Chapter 2, ***section 2.1***), the polymorphic forms and crystals' properties of the drugs isolated should be also addressed in future.

In what concerns the resolution of racemic drugs (Chapter 3), the work here developed has significantly contributed to improve the CIL-based ABS database, by employing CILs with chirality at the cation (***section 3.1.1.***) or the anion (***section 3.1.2.***) in combination with either salts or polymers. The results indicate that the CIL, salt and polymer employed significantly impact on the ABS phase diagrams as well as on the enantioseparation ability of the system (e.g., for mandelic acid using CIL with chiral cations + salt, cf. ***section 3.1.1.***). However, and although a wide range of operational conditions was optimized, only modest enantiomeric excesses were accomplished along this work. Nevertheless, the use of polymers can be seen also as a promising alternative to the salts studied. Given the promising results reported in literature for biphasic recognition systems, the development and application of ABS with chirality in both phases (i.e., composed of two chiral phase formers) could be the solution to the poor enantioselectivities exhibited. Another bottleneck of the CIL-based ABS reported along this work is the strong alkaline environment. Assuming that electrostatic interactions can be involved in the enantiomeric recognition mechanism, it seems of utmost importance the manipulation of the speciation of the phase formers but also the enantiomers. Additionally, crystallization from CILs[6] may also yield enantiopure drugs and this route should be followed in the future.

In this work, DES were also suggested as potential chiral solvents for the enantioseparation of racemic drugs (***section 3.2.1.***). Proline:malic acid (and all four enantiomer combinations – L:L, L:D, D:L and D:D) were chosen as a case study to understand the chirality role on DES formation. After determining the solid-liquid phase diagrams and assessing the molecular interactions leading to the eutectic formation, one major conclusion arises, i.e. distinct enantiomeric combinations yield distinct eutectic temperatures. In this context, the use of other techniques to infer on the molecular interactions (e.g., NMR and DFT)[7] and the application of crystallization in DES media (the intended application) are some of the important tasks to be performed in the future. The industrial relevance of the processes developed during this thesis is also an important issue to take into account in the near future. The scale-up (e.g.,[8]) and operation in continuous flow (e.g.,[9, 10]) for the wastes valorization and chiral resolution approaches

should be conducted. Furthermore, the processes' life cycle assessment or environmental analysis (e.g.,[9, 11]) should be matter of future study as well as their economic analyses (e.g.,[12, 13]) involving the chemicals, equipments and the cost and purity level needed for the drugs' recovered/separated.

References

[1] Ventura, S. P. M.; Silva, F. A. e.; Quental, M. V.; Mondal, D.; Freire, M. G.; Coutinho, J. A. P. Ionic liquid-mediated extraction and purification of bioactive compounds: Past, Present and Future Trends. *Chemical Reviews* **2017,** *117* (10), 6984–7052.

[2] Weber, C. C.; Kulkarni, S. A.; Kunov-Kruse, A. J.; Rogers, R. D.; Myerson, A. S. The Use of Cooling Crystallization in an Ionic Liquid System for the Purification of Pharmaceuticals. *Crystal Growth & Design* **2015,** *15* (10), 4946-4951.

[3] Smith, K. B.; Bridson, R. H.; Leeke, G. A. Crystallisation control of paracetamol from ionic liquids. *CrystEngComm* **2014,** *16* (47), 10797-10803.

[4] Martins, I. C. B.; Gomes, J. R. B.; Duarte, M. T.; Mafra, L. Understanding Polymorphic Control of Pharmaceuticals Using Imidazolium-Based Ionic Liquid Mixtures as Crystallization Directing Agents. *Crystal Growth & Design* **2017,** *17* (2), 428-432.

[5] An, J.-H.; Kim, J.-M.; Chang, S.-M.; Kim, W.-S. Application of Ionic Liquid to Polymorphic Design of Pharmaceutical Ingredients. *Crystal Growth & Design* **2010,** *10* (7), 3044-3050.

[6] Reichert, W. M.; Holbrey, J. D.; Vigour, K. B.; Morgan, T. D.; Broker, G. A.; Rogers, R. D. Approaches to crystallization from ionic liquids: complex solvents-complex results, or, a strategy for controlled formation of new supramolecular architectures? *Chemical Communications* **2006,** *46* (0), 4767-4779.

[7] Palomba, T.; Ciancaleoni, G.; Del Giacco, T.; Germani, R.; Ianni, F.; Tiecco, M. Deep Eutectic Solvents formed by chiral components as chiral reaction media and studies of their structural properties. *Journal of Molecular Liquids* **2018,** *262*, 285-294.

[8] Builder, S. E.; Ogez, J. R.; Olson, C. V.; Reifsnyder, D. Purification of insulin-like growth factor. **1995**, U.S. Patent No. 5,446,024.

[9] Santos, J. H. P. M.; Almeida, M. R.; Martins, C. I. R.; Dias, A. C. R. V.; Freire, M. G.; Coutinho, J. A. P.; Ventura, S. P. M. Separation of phenolic compounds by centrifugal partition chromatography. *Green Chemistry* **2018,** *20* (8), 1906-1916.

[10] Soares, R. R. G.; Silva, D. F. C.; Fernandes, P.; Azevedo, A. M.; Chu, V.; Conde, J. P.; Aires-Barros, M. R. Miniaturization of aqueous two-phase extraction for biological applications: From micro-tubes to microchannels. *Biotechnology Journal* **2016,** *11* (12), 1498-1512.

[11] Amado Alviz, P. L.; Alvarez, A. J. Comparative life cycle assessment of the use of an ionic liquid ([Bmim]Br) versus a volatile organic solvent in the production of acetylsalicylic acid. *Journal of Cleaner Production* **2017,** *168*, 1614-1624.

[12] Torres-Acosta, M. A.; Pereira, J. F. B.; Freire, M. G.; Aguilar-Yáñez, J. M.; Coutinho, J. A. P.; Titchener-Hooker, N. J.; Rito-Palomares, M. Economic evaluation of the primary recovery of tetracycline with traditional and novel aqueous two-phase systems. *Separation and Purification Technology* **2018,** *203*, 178-184.

[13] Chen, L.; Sharifzadeh, M.; Mac Dowell, N.; Welton, T.; Shah, N.; Hallett, J. P. Inexpensive ionic liquids: [HSO4]--based solvent production at bulk scale. *Green Chemistry* **2014,** *16* (6), 3098-3106.

List of publications

List of publications

1. e Silva, F. A.; Kholany, M.; Sintra, T. E.; Caban, M.; Stepnowski, P.; Ventura, S. P. M.; Coutinho, J. A. P. Aqueous biphasic systems using chiral ionic liquids for the enantioseparation of mandelic acid enantiomers. *Solvent Extraction and Ion Exchange* **2018**, *36*, accepted.
2. e Silva, F. A.; Caban, M.; Kholany, M.; Stepnowski, P.; Coutinho, J. A. P.; Ventura, S.P.M. Recovery of non-steroidal anti-inflammatory drugs from wastes using ionic liquid-based three-phase partitioning systems. *ACS Sustainable Chemistry and Engineering* **2018**, *6*, 4574–4585.
3. e Silva, F. A.; Pereira, J. F. B.; Kurnia, K. A.; Ventura, S. P. M.; Silva, A. M. S.; Rogers, R. D.; Coutinho, J. A. P.; Freire, M. G. Temperature Dependency of Aqueous Biphasic Systems: an Alternative Approach for Exploring the Differences Between Coulombic-Dominated Salts and Ionic Liquids. *Chemical Communications* **2017**, *53*, 7298-7301.
4. e Silva, F. A.; Carmo, R. M. C.; Fernandes, A. P. M.; Kholany, M.; Coutinho, J. A. P.; Ventura, S. P. M. Using Ionic Liquids to Tune the Performance of Aqueous Biphasic Systems Based on Pluronic L-35 for the Purification of Naringin and Rutin. *ACS Sustainable Chemistry and Engineering* **2017**, *5*, 6409-6419.
5. Taha, M.; Quental, M. V.; e Silva, F. A.; Capela, E.; Freire, M. G.; Ventura, S. P. M.; Coutinho, J. A. P. Good's Buffer Ionic Liquids as Relevant Phase-Forming Components of Self-Buffered Aqueous Biphasic Systems. *Journal of Chemical Technology and Biotechnology* **2017**, *92*, 2287–2299.
6. Ventura, S. P. M.; e Silva, F. A.; Quental, M. V.; Mondal, D.; Freire, M. G.; Coutinho, J. A. P. Ionic-Liquid-Mediated Extraction and Separation Processes for Bioactive Compounds: Past, Present, and Future Trends. *Chemical Reviews* **2017**, *117* (10), 6984–7052.
7. e Silva, F. A.; Caban, M.; Stepnowski, P.; Coutinho, J. A. P.; Ventura, S.P.M. Recovery of ibuprofen from pharmaceutical wastes using ionic liquids. *Green Chemistry* **2016**, *18*, 3749-3757.

8. Zawadzki, M.; e Silva, F.A.; Domańska, U.; Coutinho, J. A. P.; Ventura, S. P. M. Recovery of an antidepressant from pharmaceutical wastes using ionic liquid-based aqueous biphasic systems. *Green Chemistry* **2016**, *18*, 3527-3536. (Front Cover article)
9. Lee, S. Y.; Vicente, F. A.; e Silva, F. A.; Sintra, T. E.; Taha, M.; Khoiroh, I; Coutinho, J. A. P.; Show, P. L.; Ventura, S. P. M. Evaluating Self-buffering Ionic Liquids for Biotechnological Applications. *ACS Sustainable Chemistry and Engineering* **2016**, *3*, 3420-3428.
10. Santos, J. I.; Gonçalves, A. M. M.; Pereira, J. L.; Figueiredo, B. F. H. T.; e Silva, F. A.; Coutinho, J. A. P.; Ventura, S. P. M.; Gonçalves, F. Environmental safety of cholinium-based ionic liquids: assessing structure-ecotoxicity relationships. *Green Chemistry* **2015**, *17*, 4657-4668.
11. Santos, J. H. P. M.; e Silva, F. A.; Coutinho, J. A. P.; Ventura, S. P. M.; Pessoa-Jr, A. Ionic liquids as a novel class of electrolytes in polymeric aqueous biphasic systems. *Process Biochemistry* **2015**, *50*, 661–668.
12. Taha, M.; Almeida, M. R.; e Silva, F. A.; Domingues, P.; Ventura, S. P. M.; Coutinho, J. A. P.; Freire, M. G. Novel biocompatible and self-buffering ionic liquids for biopharmaceutical applications. *Chemistry A European Journal* **2015**, *21*, 4781–4788.
13. Santos, J. H.; de Souza, R. L.; e Silva, F. A.; Soares, C. M. F.; Lima, Á. S; Ventura, S. P. M. and Coutinho, J. A. P. Ionic liquid-based aqueous biphasic systems as a versatile tool for the recovery of antioxidant compounds. *Biotechnology Progress* **2014**, 31, 70-77.
14. Vicente, F. A.; Malpiedi, L. P.; e Silva, F. A.; Pessoa Jr, A.; Coutinho J. A. P.; Ventura S. P. M. Design of novel aqueous micellar two-phase systems using ionic liquids as co-surfactants for the selective extraction of (bio)molecules. Separation and Purification Technology **2014**, *135*, 259-267.
15. Campanari, S.; e Silva, F. A.; Bertin, L.; Villano, M.; Majone, M. Effect of the organic loading rate on the production of polyhydroxyalkanoates in a multi-stage process aimed at the valorization of olive oil mill wastewater. *International Journal of Biological Macromolecules* **2014**, *71*, 34-41.
16. e Silva, F. A.; Siopa, F.; Figueiredo, B. F. H. T.; Gonçalves, A. M. M.; Pereira, J. L.; Gonçalves, F.; Coutinho, J. A. P.; Afonso, C. A. M. and Ventura, S. P. M. Sustainable

design for environment-friendly mono and dicationic cholinium-based ionic liquids. *Ecotoxicology and Environmental Safety* **2014**, *108*, 302–310.

17. Taha, M.; e Silva, F. A.; Quental, M. V.; Ventura, S. P. M.; Freire, M. G. and Coutinho, J. A. P. Good's buffers as a basis for developing self-buffering and biocompatible ionic liquids for biological research. *Green Chemistry* **2014**, *16*, 3149-3159.
18. Ventura, S. P. M.; e Silva, F. A.; Gonçalves, A. M. M.; Pereira, J. L.; Gonçalves, F.;. Coutinho, J. A. P. Ecotoxicity analysis of cholinium-based ionic liquids to Vibrio fischeri marine bacteria *Ecotoxicology and Environmental Safety* **2014**, *102*, 48–54.
19. e Silva, F. A.; Sintra, T. E.; Ventura, S. P. M.; Coutinho, J. A. P. Recovery of paracetamol from pharmaceutical wastes. *Separation and Purification Technology* **2014**, *122*, 315–322.
20. Freitas, S. V. D.; e Silva, F. A.; Pastoriza-Gallego, M. J.; Piñeiro, M. M.; Lima, A. S.; Coutinho, J. A. P. Measurement and prediction of densities of vegetable oils at pressures up to 45 MPa. *Journal of Chemical Engineering Data* **2013**, *58*, 3046-3053.
21. Pereira, J. F. B.; Ventura, S. P. M.; e Silva, F. A.; Shahriari, S.; Freire, M. G.; Coutinho, J. A. P. Aqueous biphasic systems composed of ionic liquids and polymers: a platform for the purification of biomolecules. *Separation and Purification Technology* **2013**, *113*, 83-89.

Appendix

Appendix A

2.1.1. Recovery of ibuprofen from pharmaceutical wastes using ionic liquids

e Silva, F. A.; Caban, M.; Stepnowski, P.; Coutinho, J. A. P.; Ventura, S.P.M. Recovery of ibuprofen from pharmaceutical wastes using ionic liquids. *Green Chemistry* **2016**, *18* (13), 3749-3757.

Table A1. Detailed extraction efficiency of ibuprofen data acquired during the initial screening aimed at finding the optimal IL.

IL	**100 × mass fraction composition (wt%)**			EE_{IBU} **± σ/ (%)**
	IL	**Citrate buffer salt**	**H_2O**	
[BzCh]Cl	45	0	55	11.58 ± 0.63
	45	5	50	93.73 ± 1.62
$[C_4C_1im]Cl$	45	0	55	17.94 ± 1.20
	45	5	50	90.41 ± 0.50
$[N_{4444}]Cl$	45	0	55	93.53 ± 0.62
	45	5	50	97.92 ± 2.65

Table A2. Detailed extraction efficiency of ibuprofen data acquired during the optimization studies using the system based in different concentrations of $[N_{4444}]Cl$ and citrate buffer salt.

100 × mass fraction composition (wt%)			EE_{IBU} ± σ/ (%)
$[N_{4444}]Cl$	**Citrate buffer salt**	**H_2O**	
0	0	100	1.69 ± 0.03
15	0	85	2.40 ± 0.02
25	0	75	7.20 ± 0.19
35	0	65	61.12 ± 0.57
45	0	55	93.53 ± 0.62
50	0	50	91.78 ± 3.82
55	0	45	98.49 ± 0.40
0	5	95	16.59 ± 0.57
0	15	85	4.70 ± 0.29
0	25	75	2.51 ± 0.04
0	35	65	0.69 ± 0.11
15	5	80	13.66 ± 0.80
25	5	70	47.55 ± 0.76
35	5	60	88.80 ± 0.45
45	5	50	97.92 ± 2.65
25	10	65	79.52 ± 1.60
10	25	65	12.95 ± 0.76
15	15	70	19.34 ± 1.01
5	15	80	3.53 ± 0.10

Table A3. Experimental data of recovery efficiency of ibuprofen acquired during the ibuprofen recovery step through precipitation with an anti-solvent.

extract : anti-solvent	RE_{IBU} ± σ /(%)	
	45 wt% $[N_{4444}]Cl$ + 5 wt% citrate buffer + 50 wt% H_2O	**45 wt% $[N_{4444}]Cl$ + 55 wt% H_2O**
Anti-solvent: 25 wt% of KCl aqueous solution		
1:1	13.53 ± 0.86	60.94 ± 2.41
1:2	58.40 ± 2.57	85.79 ± 0.29
1:3	75.08 ± 0.53	94.04 ± 0.49
1:4	84.53 ± 1.26	96.00 ± 0.15
1:5	87.97 ± 1.00	97.07 ± 0.14
Anti-solvent: H_2O		
1:1	22.37 ± 2.46	86.11 ± 0.72
1:2	33.71 ± 2.32	90.45 ± 0.13
1:3	34.71 ± 4.00	91.60 ± 0.19
1:4	28.31 ± 0.45	89.17 ± 0.30
1:5	26.72 ± 5.45	88.09 ± 0.17

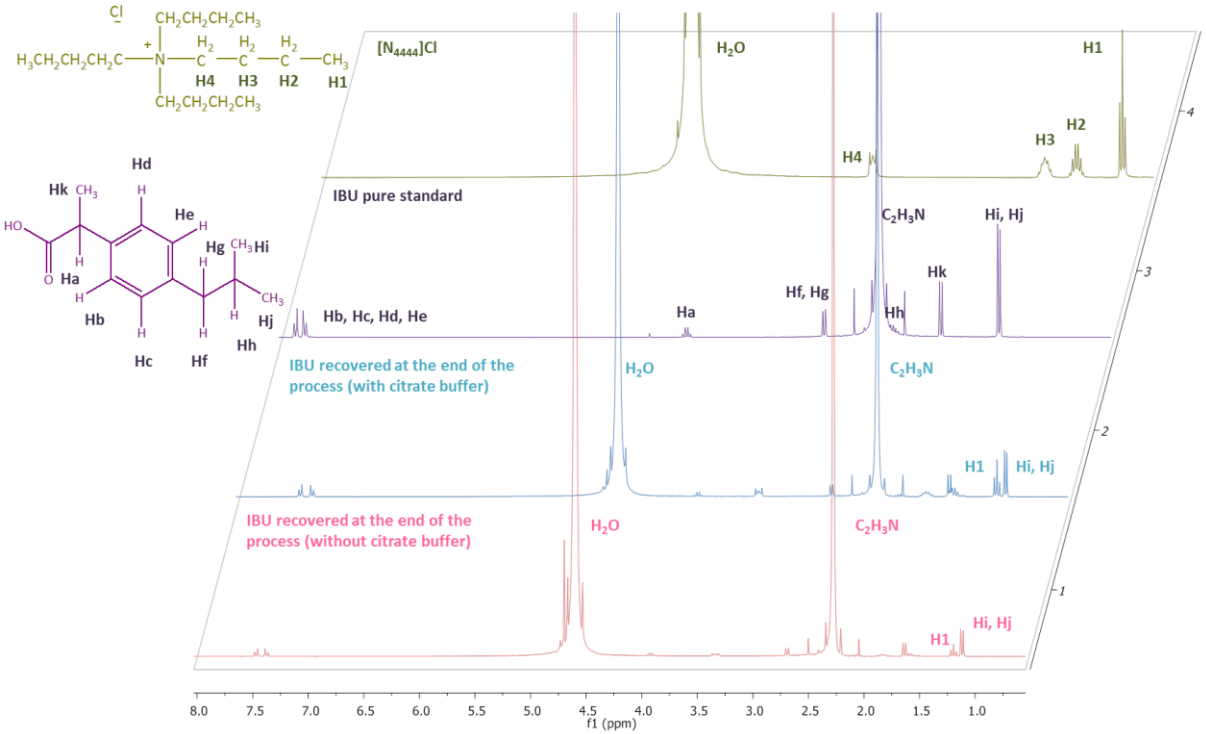

Figure A1. ^{1}H NMR spectra for ibuprofen recovered from the 45 wt% of $[N_{4444}]Cl$ aqueous solution after the addition of water in a ratio of 1:3 in a 50:50 H_2O:C_2H_3N mixture (1), 45 wt% $[N_{4444}]Cl$ + 5 wt% citrate buffer aqueous solution after the addition of KCl aqueous solution in a ratio of 1:4 in a 50:50 H_2O:C_2H_3N mixture (2), ibuprofen pure standard from Sigma in C_2H_3N (3) and $[N_{4444}]Cl$ in H_2O (4). A Bruker Avance 300 spectrometer operating at 300.13 MHz was used, utilizing appropriate tubes containing closed reference capillaries with D_2O and TSP as the internal reference. Ibuprofen and $[N_{4444}]Cl$ atom labelling is also provided.

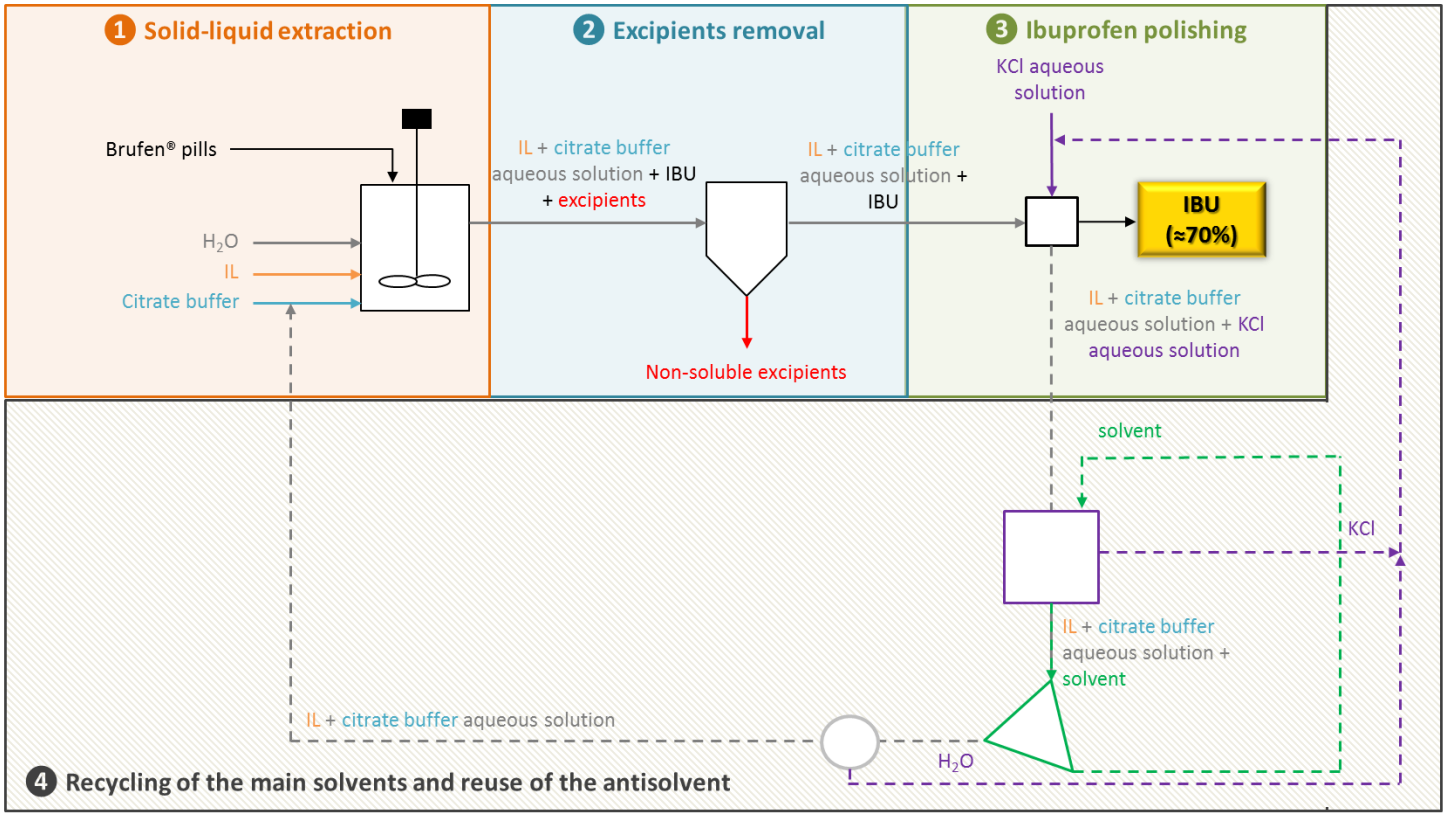

Figure A2. Schematic representation of the integrated process of extraction, purification, ibuprofen recovery and recycling of the main solvents based on the use of $[N_{4444}]Cl$ + citrate buffer aqueous solution and KCl as the solvent and anti-solvent, respectively. The purple square represents the removal of KCl in solution, the green square consists on the separation of the solvent used in the KCl removal and the grey circle is the evaporation of the extra amount of water added together with KCl as anti-solvent.

Appendix B

2.1.2. Recovery of an antidepressant from pharmaceutical wastes using ionic liquid-based aqueous biphasic systems

Zawadzki, M.; e Silva, F.A.; Domańska, U.; Coutinho, J. A. P.; Ventura, S. P. M. Recovery of an antidepressant from pharmaceutical wastes using ionic liquid-based aqueous biphasic systems. *Green Chemistry* **2016**, *18* (12), 3527-3536.

$$[IL] = A \cdot \exp\left(B \cdot [Salt]^{0.5} - C \cdot [Salt]^{3}\right) \quad (\textbf{\textit{Equation B1}})$$

$$[IL]_{Salt} = A \cdot \exp\left(B \cdot [Salt]_{Salt}^{\ 0.5} - C \cdot [Salt]_{Salt}^{\ 3}\right) \quad (\textbf{\textit{Equation B2}})$$

$$[IL]_{IL} = A \cdot \exp\left(B \cdot [Salt]_{IL}^{\ 0.5} - C \cdot [Salt]_{IL}^{\ 3}\right) \quad (\textbf{\textit{Equation B3}})$$

$$[IL]_{IL} = \frac{[IL]_M}{\alpha} - \frac{1-\alpha}{\alpha} \cdot [IL]_{Salt} \quad (\textbf{\textit{Equation B4}})$$

$$[Salt]_{IL} = \frac{[Salt]_M}{\alpha} - \frac{1-\alpha}{\alpha} \cdot [Salt]_{Salt} \quad (\textbf{\textit{Equation B5}})$$

$$TLL = \sqrt{\left([IL]_{IL} - [IL]_{Salt}\right)^2 + \left([Salt]_{IL} - [Salt]_{Salt}\right)^2} \quad (\textbf{\textit{Equation B6}})$$

where *A*, *B*, and *C* are the constants obtained through the regression of experimental data, while [IL] and [Salt] are, respectively, IL and salt weight percentage compositions. α is the ratio between the mass of the top phase and the overall system and subscripts *IL*, *Salt* and *M* correspond to IL-rich (top), salt-rich (bottom) and mixture point, respectively.

Table B1. Validation parameters for the HPLC method developed.

	Concentration regime	
	High	**Low**
Number of standards	10	7
Quantification range (ppm)	2 - 25	0.15- 3.5
Correlation coefficient	0.9992	0.9996
RSD (%)	1.8	6
Limit of Detection *(taken as a + 3Sa)*	0.6	0.05
Limit of Quantification *(taken as 3 times LOD)*	1.9	0.15
Intraday standard deviation (%)	1.7 - 4.8	
Interday standard deviation (%)	2.1 - 9.3	

Table B2. Weight fraction data for systems composed of $[N_{4444}]Br$ + K_2HPO_4 + water at 298 (± 1) K and atmospheric pressure.

$100w_{[N_{4444}]Br}$	$100w_{H_2O}$	$100w_{K_2HPO_4}$	$100w_{[N_{4444}]Br}$	$100w_{H_2O}$	$100w_{K_2HPO_4}$
57.27	40.88	1.859	15.96	72.14	11.91
44.16	53.95	1.886	15.80	72.23	11.97
40.64	56.22	3.142	15.57	72.29	12.14
37.88	58.81	3.308	15.41	72.39	12.20
37.08	59.36	3.562	15.28	72.47	12.25
34.89	60.66	4.447	15.08	72.52	12.40
33.01	62.39	4.592	14.96	72.58	12.46
32.37	62.79	4.838	14.81	72.68	12.51
31.04	63.66	5.300	14.63	72.71	12.67
30.11	64.44	5.455	14.50	72.79	12.71
29.64	64.67	5.682	14.19	72.93	12.89
29.14	64.98	5.881	14.00	72.97	13.02
27.96	65.67	6.371	13.82	73.02	13.15
27.04	66.29	6.666	13.61	73.16	13.23
26.47	66.75	6.785	13.46	73.21	13.34
26.09	66.97	6.940	13.25	73.22	13.53
25.73	67.17	7.100	13.14	73.29	13.57
25.41	67.35	7.237	12.99	73.38	13.63
25.06	67.53	7.405	12.85	73.41	13.74
24.68	67.78	7.547	12.69	73.46	13.85
24.33	67.97	7.705	12.59	73.54	13.87
24.08	68.06	7.852	12.35	73.62	14.03
23.81	68.20	7.996	11.60	73.86	14.54
23.47	68.42	8.114	10.99	74.04	14.96
23.24	68.55	8.215	10.22	74.32	15.46

22.92	68.75	8.329	9.597	74.50	15.90
22.60	68.96	8.441	8.925	74.65	16.43
22.19	69.06	8.754	8.334	74.77	16.89
21.87	69.24	8.890	7.557	74.90	17.54
21.58	69.41	9.012	6.845	74.94	18.21
21.12	69.66	9.215	6.281	74.98	18.74
20.64	69.92	9.439	5.695	74.94	19.37
20.38	70.08	9.534	5.334	74.67	20.00
20.14	70.22	9.639	5.118	74.80	20.08
19.77	70.33	9.895	4.411	74.63	20.96
19.56	70.46	9.981	4.381	74.66	20.96
19.19	70.59	10.22	3.854	74.42	21.72
18.94	70.75	10.31	3.709	74.24	22.05
18.65	70.93	10.43	3.185	73.91	22.90
18.45	71.05	10.51	2.728	73.52	23.75
18.09	71.16	10.75	2.354	73.15	24.50
17.88	71.28	10.83	1.960	72.59	25.45
17.57	71.38	11.05	1.601	71.89	26.51
17.37	71.50	11.13	1.284	71.32	27.40
17.17	71.65	11.19	0.955	70.19	28.85
16.90	71.73	11.36	0.660	68.86	30.48
16.67	71.82	11.51	0.426	67.29	32.29
16.48	71.95	11.57	0.277	65.77	33.96
16.22	72.04	11.75			

Table B3. Weight fraction data for systems composed of $[N_{4444}]Br$ + K_3PO_4 + water at 298 (± 1) K and atmospheric pressure.

$100w_{[N_{4444}]Br}$	$100w_{H_2O}$	$100w_{K_3PO_4}$	$100w_{[N_{4444}]Br}$	$100w_{H_2O}$	$100w_{K_3PO_4}$
34.40	61.45	4.149	9.801	75.35	14.85
33.28	62.20	4.525	9.058	75.60	15.34
32.39	62.91	4.706	8.278	75.83	15.89
31.51	63.41	5.074	7.557	75.39	17.05
30.51	64.02	5.470	7.428	76.01	16.56
29.22	64.95	5.832	6.707	76.15	17.14
28.32	65.61	6.070	6.532	76.13	17.34
27.01	66.41	6.574	5.899	76.21	17.89
25.75	67.20	7.055	5.465	75.94	18.60
24.09	68.21	7.703	5.236	76.23	18.54
22.67	69.04	8.285	4.699	75.85	19.45
21.79	69.51	8.696	3.903	75.79	20.30
20.38	70.35	9.279	3.052	75.33	21.62
19.11	71.07	9.818	2.525	74.99	22.48
17.91	71.69	10.40	1.958	74.47	23.57
16.81	72.29	10.90	1.508	73.80	24.69
15.81	72.75	11.44	1.134	73.02	25.85
14.98	73.15	11.87	0.8591	72.19	26.95
14.14	73.57	12.29	0.6813	71.48	27.84
13.29	73.95	12.76	0.5457	70.81	28.65
12.45	74.32	13.23	0.3715	69.64	29.99
11.57	74.71	13.73	0.3140	69.15	30.54
10.62	75.02	14.37			

Table B4. Weight fraction data for the systems composed of $[N_{4444}]Cl$ + K_2HPO_4 + water at 298 (± 1) K and atmospheric pressure.

$100w_{[N_{4444}]Cl}$	$100w_{H_2O}$	$100w_{K_2HPO_4}$	$100w_{[N_{4444}]Cl}$	$100w_{H_2O}$	$100w_{K_2HPO_4}$
55.68	43.53	0.7904	13.79	71.68	14.52
42.79	55.31	1.894	12.42	71.88	15.71
40.77	57.02	2.201	11.22	72.02	16.76
39.12	58.23	2.644	10.03	72.15	17.82
37.40	59.77	2.821	8.915	72.21	18.88
35.34	61.10	3.565	8.450	71.86	19.69
33.80	62.23	3.966	7.867	72.20	19.93
32.46	63.20	4.342	7.014	72.16	20.82
30.94	64.21	4.852	6.840	72.06	21.10
29.62	65.07	5.306	6.349	72.10	21.55
27.46	66.37	6.171	5.523	71.87	22.60
26.15	67.20	6.654	4.674	71.62	23.71
24.24	68.01	7.752	3.814	71.25	24.93
22.91	68.77	8.322	3.299	71.05	25.66
21.48	69.34	9.181	2.741	70.67	26.59
20.27	69.87	9.860	2.165	70.11	27.72
18.77	70.38	10.84	1.508	69.18	29.32
17.25	70.85	11.91	1.083	68.27	30.65
15.88	71.23	12.89	0.7603	67.28	31.96
14.98	71.45	13.57	0.5341	66.27	33.20

Table B5. Parameters of Merchuk equation for the different IL + salt + H_2O systems determined in this work.

IL	Salt	*A*	*B*	$C \cdot 10^4$
$[N_{4444}]Br$	**K_2HPO_4**	94.4 ± 4.7	-0.473 ± 0.022	0.93 ± 0.14
	K_3PO_4	86.2 ± 3.1	-0.440 ± 0.015	1.384 ± 0.072
$[N_{4444}]Cl$	**K_2HPO_4**	77.0 ± 1.9	-0.410 ± 0.012	0.585 ± 0.61

Table B6. Compositions (weight fraction) for the IL + phosphate-based salts + H_2O ternary systems at 298 (± 1) K and corresponding values of TLL at 298 (±1) K and atmospheric pressure. [a]values retrieved from Sintra, T. E. et al. *Journal of Chemical Thermodynamics* **2014,** *77*, 206-213.

IL	Salt	$[IL]_{IL}$ / (wt%)	$[Salt]_{IL}$ / (wt%)	$[IL]_{M}$ / (wt%)	$[Salt]_{M}$ / (wt%)	$[IL]_{Salt}$ / (wt%)	$[Salt]_{Salt}$ / (wt%)	TLL
$[P_{4444}]Br$	K_2HPO_4/KH_2PO_4	66.80	0.84	29.92	15.06	0.85	26.27	70.69
$[N_{4444}]Br$	K_2HPO_4/KH_2PO_4	53.09	1.45	29.99	15.39	0.78	33.01	61.10[a]
$[N_{4444}]Cl$	K_2HPO_4/KH_2PO_4	39.02	2.50	27.52	13.86	0.13	40.89	54.64
$[N_{4444}]Br$	K_2HPO_4	60.61	0.58	30.01	15.03	0.57	28.94	66.41
$[N_{4444}]Br$	K_3PO_4	65.20	0.63	29.99	15.04	0.72	27.02	69.66
$[N_{4444}]Cl$	K_3PO_4	53.95	0.70	29.88	15.13	0.22	32.91	62.65
$[P_{i(444)1}][Tos]$	K_2HPO_4/KH_2PO_4	61.91	3.77	30.06	15.00	0.92	25.27	64.67
$[P_{4441}][C_1SO_4]$	K_2HPO_4/KH_2PO_4	51.77	1.60	29.54	14.79	1.25	31.57	58.74
$[N_{4444}]Cl$	K_2HPO_4	49.53	1.01	30.02	15.04	0.31	36.40	60.63

Table B7. Weight fraction and extraction efficiency data obtained during the assessment of the maximum concentration of amitriptyline hydrochloride able to be processed by IL-based ABS (considering the ternary system composed of $[N_{4444}]Br$ + K_3PO_4 + H_2O): mass of amitriptyline initially added in the ABS (m_{Ami}^{ABS}), concentration of amitriptyline IL-rich phase (C_{Ami}^{IL}), concentration of amitriptyline in salt-rich phase (C_{Ami}^{Salt}), extraction efficiencies (EE_{Ami}) and logarithmic partition coefficients ($\log K_{Ami}$) with corresponding standard deviations (σ).

$[N_{4444}]Br]_M$ / (wt%)	$[K_3PO_4]_M$ / (wt%)	$[water]_M$ / (wt%)	m_{Ami}^{ABS} / (mg)	C_{Ami}^{IL} / ($mg.g^{-1}$)	C_{Ami}^{Salt} / ($\mu g.g^{-1}$)	$EE_{Ami} \pm \sigma$ / (%)	$\log K_{Ami} \pm \sigma$
10.01	24.78	65.21	2.53	3.2	0.52	89.3 ± 0.6	>2.5
9.97	24.78	65.25	5.12	6.0	0.31	83 ± 2	>2.5
10.02	24.76	65.22	10.2	12.1	0.37	84 ± 2	>2.5
10.00	24.76	65.24	13.8	16.3	0.70	87.0 ± 0.5	>2.5
10.13	24.86	65.01	29.9	37.4	1.52	88.5 ± 0.7	>2.5
10.13	24.98	64.89	49.8	67.9	3.18	97 ± 3	>2.5
10.16	25.21	64.63	75.4	93.5	2.04	90 ± 3	>2.5
10.24	25.22	64.54	100.6	88.2	3.46	66 ± 1	>2.5

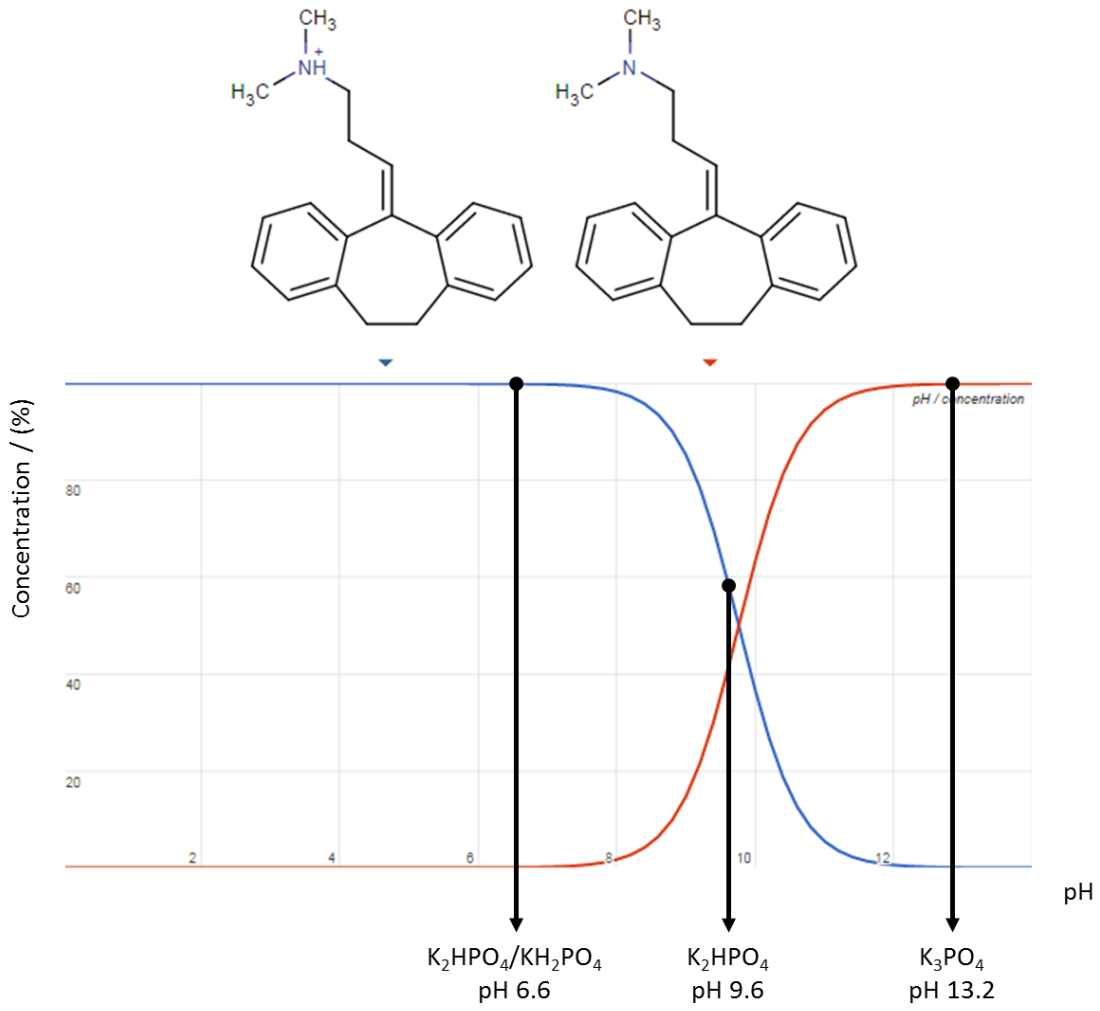

Figure B1. Speciation curves of amitriptyline hydrochloride for the different values of pH investigated in this work (adapted from Chemspider - The free chemical database at http://www.chemspider.com (accessed Nov 24, 2015).

Appendix C

2.1.3. Recovery of non-steroidal anti-inflammatory drugs from wastes using ionic liquid-based three-phase partitioning systems

e Silva, F. A.; Caban, M.; Kholany, M.; Stepnowski, P.; Coutinho, J. A. P.; Ventura, S.P.M. Recovery of non-steroidal anti-inflammatory drugs from wastes using ionic liquid-based three-phase partitioning systems. *ACS Sustainable Chemistry and Engineering* **2018**, *6* (4), 4574–4585.

Table C1. General information of the pills used as real matrices in this study; identification and content of the NSAIDs , name of the medicine, list of excipients and MA holder [information available on the website of the Portuguese National Authority of Medicines and Health Products (INFARMED, I.P.) - www.infarmed.pt].

API	***Medicine name* (NSAIDs content)**	**Excipients**	**MA holder**
NAP	*Naproxeno Generis* (naproxen 250 mg)	Magnesium stearate, microcrystalline cellulose, colloidal silica, povidone	Generis Farmacêutica, Amadora, Portugal
KET	*Profenid Retard* (ketoprofen 200 mg)	Tablet core: calcium hydrogen phosphate dihydrate, hydroxyethyl cellulose, magnesium stearate Coating: cellulose acetate phthalate, ethyl phthalate	Sanofi Aventis, Porto Salvo, Portugal
IBU	*Brufen* (ibuprofen 200 mg)	Microcrystalline cellulose, crosslinked sodium carboxymethylcellulose, lactose monohydrate, colloidal silica dioxide, sodium lauryl sulfate, magnesium stearate, hypromellose (hydroxypropyl methylcellulose) 2910, hypromellose 2910, talc and titanium dioxide	Abbott Laboratórios, Amadora, Portugal

Table C2. Validation parameters for the HPLC-DAD analytical method.

	Ibuprofen	Naproxen	Ketoprofen
Retention Time (min)	16.48[a]	12.73	12.27
Concentration range (µg.mL^{-1}) Minimum of 6 concentrations	10 – 750[a] *0.50 - 50*	10 - 750 *0.05 - 50*	10 - 750 *0.10 – 50*
Injection volume (µL)	10[a] *25*	10 *25*	10 *25*
Wavelength (nm)	230[a] *230*	270 *245*	270 *245*
R^2	0.9999[a] *1.0000*	1.0000 *1.0000*	1.0000 *1.0000*
Linearity range (µg.mL^{-1})	10-750[a] *0.5-50.00*	10-750 *0.05-50.00*	10-750 *0.10-50.00*
LOQ	10[a] *0.50*	10 *0.05*	10 *0.10*
LOD	1[a] *0.20*	1 *0.02*	1 *0.05*
Accuracy intra-day (%)	83.1-101.0[a] *92.9-101.6*	80.5-104.9 *98.2-112.6*	83.0-99.5 *89.2 - 100.5*
Accuracy inter-day (%)	88.7-109.7[a]	87.2-109.3	81.9-114.3
Precision intra-day (RSD, %)	0.15-3.00[a] *0.70-4.00*	0.04-1.73 *0.20-1.90*	0.02-0.50 *0.10-2.00*
Precision inter-day, (%)	0.01-1.93[a]	0.00-0.64	0.00-0.14

[a] Values taken from e Silva, F. A. et al. *Green Chemistry* **2016***, 18* (13), 3749-3757.

Table C3. Tie-lines (TLs) and corresponding values of tie-line lengths (TLLs) information for the IL-based ABS at 25 (±1) ^{o}C utilized in the NSAIDs extraction.

ABS	**$[IL]_T$ [a]**	**$[salt]_T$ [b]**	**$[water]_T$ [c]**	**$[IL]_M$ [d]**	**$[salt]_M$ [e]**	**$[IL]_B$ [f]**	**$[salt]_B$ [g]**	**$[water]_B$ [h]**	**TLL**
$[N_{4444}]Cl$ + citrate buffer (pH 7)	68.44	1.74	29.82	29.76	30.11	0.65	51.46	47.89	84.07
[BzCh]Cl + citrate buffer (pH 7)	58.34	7.72	33.94	34.88	30.05	8.95	54.73	36.32	68.18
$[C_4C_1im]Cl$ + citrate buffer (pH 7)	51.05	8.13	40.82	29.93	29.93	7.82	52.75	39.43	62.13
	55.21	6.01	38.78	33.02	28.12	7.23	53.81	38.96	67.73
	55.62	5.82	38.55	35.25	26.64	5.72	56.82	37.46	71.35
$[C_4C_1im]Cl$ + citrate buffer (pH 8)	52.27	7.91	39.81	29.95	30.04	7.10	52.69	40.22	63.60
$[C_4C_1im]Cl$ + potassium citrate tribasic (pH ≈9)	52.95	7.17	39.88	30.10	29.94	6.25	53.72	40.03	65.94

[a] Weight fraction composition (in wt%) of IL in the top phase. | [b] Weight fraction composition (in wt%) of salt in the top phase. | [c] Weight fraction composition (in wt%) of water in the top phase. | [d] Weight fraction composition (in wt%) of IL in the biphasic mixture. | [e] Weight fraction composition (in wt%) of salt in the biphasic mixture. | [f] Weight fraction composition (in wt%) of IL in the bottom phase. | [g] Weight fraction composition (in wt%) of salt in the bottom phase. | [h] Weight fraction composition (in wt%) of water in the bottom phase.

Table C4. Extraction efficiencies (EE_{NSAID}, %) and recovery toward the top phase (R_T, %) plus the corresponding standard deviations (σ) of the three target NSAIDs obtained using the ABS composed of 30 wt% of $[C_4C_1im]Cl$ + 30 wt% of potassium citrate buffer (pH 7), and with distinct NSAIDs contents (in mg NSAID *per* g ABS).

NSAID content / (mg NSAID *per* g ABS)	1	2	4
Ibuprofen			
$\boldsymbol{EE_{NSAID} \pm \sigma}$**, %**	87 ± 1	87.9 ± 0.7	98 ± 3
$\boldsymbol{R_T \pm \sigma}$**, %**	98.2 ± 0.1	98.77 ± 0.04	99.2 ± 0.3
Naproxen			
$\boldsymbol{EE_{NSAID} \pm \sigma}$**, %**	90 ± 3	98 ± 2	93 ± 7
$\boldsymbol{R_T \pm \sigma}$**, %**	98.2 ± 0.1	98.54 ± 0.01	98.7 ± 0.7
Ketoprofen			
$\boldsymbol{EE_{NSAID} \pm \sigma}$**, %**	94 ± 4	91.9 ± 0.1	99 ± 3
$\boldsymbol{R_T \pm \sigma}$**, %**	98.7 ± 0.1	98.9 ± 0.1	99.1 ± 0.5

Table C5. Extraction efficiencies (EE_{NSAID}, %) and recovery toward the top phase (R_T, %) plus the corresponding standard deviations (σ) of the three target NSAIDs obtained using distinct IL-based ABS.

IL	$[C_4C_1im]Cl$	$[N_{4444}]Cl$	[BzCh]Cl
Ibuprofen			
$\boldsymbol{EE_{NSAID} \pm \sigma}$**, %**	98 ± 3	89 ± 8	90 ± 7
$\boldsymbol{R_T \pm \sigma}$**, %**	99.2 ± 0.3	100	100
Naproxen			
$\boldsymbol{EE_{NSAID} \pm \sigma}$**, %**	93 ± 7	85 ± 6	87 ± 8
$\boldsymbol{R_T \pm \sigma}$**, %**	98.7 ± 0.7	100	99.8 ± 0.01
Ketoprofen			
$\boldsymbol{EE_{NSAID} \pm \sigma}$**, %**	99 ± 3	90 ± 10	100
$\boldsymbol{R_T \pm \sigma}$**, %**	99.1 ± 0.5	100	99.60 ± 0.02

Table C6. Extraction efficiencies (EE_{NSAID}, %) and recovery toward the top phase (R_T, %) plus the corresponding standard deviations (σ) of the three target NSAIDs obtained using the ABS composed of 30 wt% of $[C_4C_1im]Cl$ + 30 wt% of potassium citrate buffer at distinct temperatures (±1 °C) and pH 7.

Temperature (°C)	15	25	35	45
Ibuprofen				
EE_{NSAID} **± σ, %**	90 ± 2	98 ± 3	92 ± 2	91.3 ± 0.5
R_T **± σ, %**	97.8 ± 0.5	99.2 ± 0.3	99.2 ±0.1	99.33 ±0.04
Naproxen				
EE_{NSAID} **± σ, %**	91 ± 2	93 ± 7	92.5 ± 0.4	96 ± 2
R_T **± σ, %**	97.4 ± 0.9	98.7 ± 0.7	99.1 ± 0.1	99.21 ± 0.05
Ketoprofen				
EE_{NSAID} **± σ, %**	95 ± 2	99 ± 3	95 ± 1	100
R_T **± σ, %**	97.7 ± 0.7	99.1 ± 0.5	99.3 ± 0.1	99.4 ± 0.1

Table C7. Extraction efficiencies (EE_{NSAID}, %) and recovery toward the top phase (R_T, %) plus the corresponding standard deviations (σ) of the three target NSAIDs obtained using ABS composed of 30 wt% of $[C_4C_1im]Cl$ + 30 wt% of potassium citrate buffer or potassium citrate tribasic, at distinct pH values.

pH	7	8	≈9
Ibuprofen			
EE_{NSAID} **± σ, %**	98 ± 3	94 ± 5	85 ± 4
R_T **± σ, %**	99.2 ± 0.3	99.0 ± 0.2	99.1 ± 0.2
Naproxen			
EE_{NSAID} **± σ, %**	93 ± 7	91.7 ± 0.8	86.5 ± 0.6
R_T **± σ, %**	98.7 ± 0.7	98.8 ± 0.3	99.0 ± 0.2
Ketoprofen			
EE_{NSAID} **± σ, %**	99 ± 3	95 ± 4	89.1 ± 0.8
R_T **± σ, %**	99.1 ± 0.5	99.1 ± 0.2	99.1 ± 0.3

Table C8. Extraction efficiencies (EE_{NSAID}, %) and recovery toward the top phase (R_T, %) plus the corresponding standard deviations (σ) of the three target NSAIDs obtained using the ABS composed of $[C_4C_1im]Cl$ + potassium citrate buffer (pH 7) at variable mixture compositions (in wt%)/TLLs.

$([IL]_M, [Salt]_M)$ / (wt%) ***TLL***	(30, 30) *62.13*	(33, 28) *67.73*	(35, 26.5) *71.35*
Ibuprofen			
EE_{NSAID} ± σ, %	98 ± 3	86 ± 4	80 ± 3
R_T ± σ, %	99.2 ± 0.3	98 ± 1	99.4 ± 0.2
Naproxen			
EE_{NSAID} ± σ, %	93 ± 7	87 ± 3	83 ± 3
R_T ± σ, %	98.7 ± 0.7	98 ± 1	99.4 ± 0.2
Ketoprofen			
EE_{NSAID} ± σ, %	99 ± 3	93 ± 1	85 ± 3
R_T ± σ, %	99.1 ± 0.5	99.0 ± 0.8	99.4 ± 0.2

Table C9. Comparison between the proposed stability study protocol and the original OECD 111e one.

Parameter	OECD 111e	Present protocol
Purpose	Estimating hydrolysis as abiotic degradation path in environment.	Determining ILs' influence on the stability of drugs in extraction processes.
Test substance application	Compounds with good solubility in water are required.	Compounds with good solubility in water are not mandatory. It will depend upon compounds' solubility in IL enriched matrix.
Concentration of tested compound	10^{-2} to 10^{-3} M for environmental conditions (≤10^{-6} M).	Not confined. Similar concentrations to those instilled by the extraction process are preferable.
Temperature	50 °C	Temperature at which the IL-based ABS was conducted. Other temperatures may be included if a temperature effect study is targeted.
Time of incubation	5 days (preliminary test)	5 days
Sample pH	4, 7 and 9	pH at which the IL-based ABS was conducted. Other pH values may be included if a pH effect study is targeted.
Buffer solution	CLARK and LUBS, Citrate buffers of KOLTHOFF and VLEESCHHOUWER, Borate and phosphate mixtures of SÖRENSEN	Buffer (or salt) used as phase-forming agent in the ABS. Also samples without salt addition may be included to control salt effect on analyte stability.
Sub-samples taking time	t_0 and after 5 days.	St_0 (control) and after 5 days (St_{25} and St_{50}).

Table C10. Extraction efficiencies (EE_{NSAID}, %) and recovery toward the top phase (R_T, %) plus the corresponding standard deviations (σ) of the three target NSAIDs obtained using the IL-TPP investigated.

	$[C_4C_1im]Cl$	$[N_{4444}]Cl$	[BzCh]Cl
Ibuprofen			
EE_{NSAID} ± σ, %	92 ± 5	90 ± 5	86 ± 6
R_T ± σ, %	97.8 ± 0.7	100	99.8 ± 0.1
Naproxen			
EE_{NSAID} ± σ, %	87 ± 5	90 ± 3	85 ± 4
R_T ± σ, %	97.8 ± 0.3	100	99.65 ± 0.03
Ketoprofen			
EE_{NSAID} ± σ, %	100	84 ± 8	87 ± 4
R_T ± σ, %	98.1 ± 0.3	100	98 ± 1

Table C11. Isolation efficiencies (IE_{NSAID}, %) plus the corresponding standard deviations (σ) of the three target NSAIDs obtained using the distinct approaches based on the precipitation with an anti-solvent.

Ratio of top phase and anti-solvent volume	**IE_{IBU} ± σ, %**	**IE_{NAP} ± σ, %**	**IE_{KET} ± σ, %**
Citric acid aqueous solution at 25 wt%			
1:4	78 ± 2	79 ± 3	-
Aluminium sulphate aqueous solution at 15 wt%			
1:4	-	-	76 ± 2
1:6	-	-	80.9 ± 0.7
1:8	-	-	83 ± 4
1:10	-	-	87.1 ± 0.2
1:12	-	-	87.9 ± 0.3

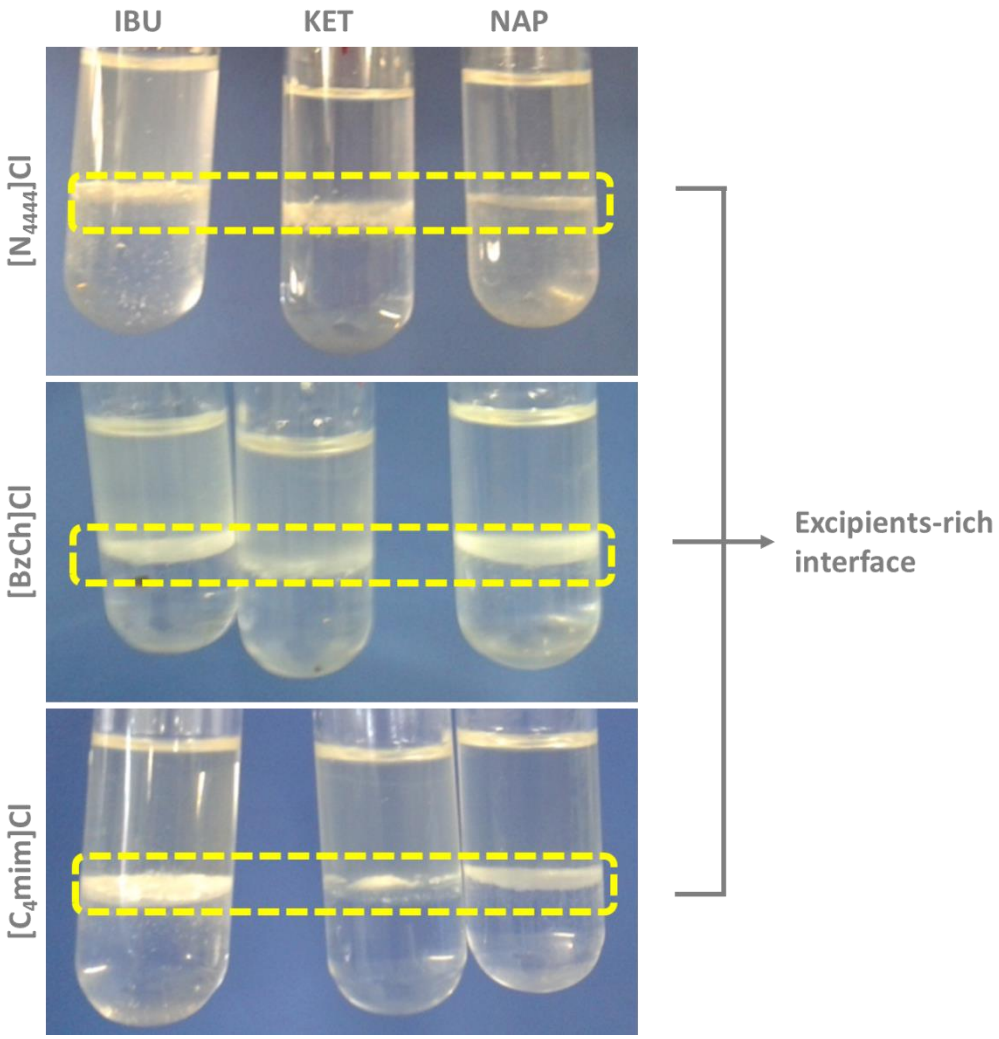

Figure C1. Visual appearance of IL-based TPP developed in the present study for the recovery of active ingredients, namely ibuprofen (IBU), ketoprofen (KET) and naproxen (NAP) from solid state pills.

Appendix D

3.1.1. Aqueous biphasic systems using chiral ionic liquids bearing chiral cations for the enantioseparation of mandelic acid enantiomers

e Silva, F. A.; Kholany, M.; Sintra, T. E.; Caban, M.; Stepnowski, P.; Ventura, S. P. M.; Coutinho, J. A. P. Aqueous biphasic systems using chiral ionic liquids for the enantioseparation of mandelic acid enantiomers. *Solvent Extraction and Ion Exchange* **2018**, *36* (5), accepted.

Table D1. Brief characterization of the CILs used: melting temperature (T_m), decomposition temperature and specific rotation (values retrieved from Sintra, T. E. Synthesis of more benign ionic liquids for specific applications. PhD Thesis, University of Aveiro, 2017).

CILs	T_m **/ (°C)**	T_d **/ (°C)**	$[\alpha]_D^{25}$ **(± 0.1)**
$[C_1Qui][C_1SO_4]$	191.10	240.93	-124.0
$[C_1C_1C_1Val]I$	222.10	230.84	8.9
$[C_1C_1C_1Val][C_1SO_4]$	48.61	212.50	15.1
$[C_1C_1C_1Pro]I$	103.85	217.94	-18.7
$[C_2C_2C_2Pro]Br$	102.85	177.92	-28.6
$[C_1C_1C_1Pro][C_1SO_4]$	-42.77	275.04	-9.5

Table D2. Overall set of conditions evaluated and approximate mixture compositions used in the enantioseparation of mandelic acid studies with CIL-based ABS.

CIL	**Salt**	**([CIL]$_M$, [Salt]$_M$) / (wt%, wt%)**	**([*R*-MA]$_M$, [*S*-MA]$_M$) / (wt%, wt%)**	***T*** **(± 1) / °C**
CIL structure				
$[C_1Qui][C_1SO_4]$	K_3PO_4	(2.5, 18)	(0.8, 0.8)	25
$[C_1C_1C_1Pro]I$	K_3PO_4	(14, 32)	(0.8, 0.8)	25
$[C_2C_2C_2Pro]Br$	K_3PO_4	(10, 35)	(0.8, 0.8)	25
$[C_1C_1C_1Val]I$	K_3PO_4	(10, 35)	(0.8, 0.8)	25
$[C_1C_1C_1Val]$ $[C_1SO_4]$	K_3PO_4	(10, 25)	(0.8, 0.8)	25
TLL				
$[C_1Qui][C_1SO_4]$	K_3PO_4	(3, 15); (2.5, 18); (4, 20)	(0.8, 0.8)	25
$[C_2C_2C_2Pro]Br$	K_3PO_4	(10, 30); (10, 35); (10, 40)	(0.8, 0.8)	25
Mixture points along the same TL - Phases weight ratio				
$[C_2C_2C_2Pro]Br$	K_3PO_4	(30, 16); (20, 25); (10, 35); (5, 40)	(0.8, 0.8)	25
$[C_2C_2C_2Pro]Br$	K_2HPO_4	(20, 25); (15, 30); (10; 35); (5, 40)	(0.8, 0.8)	25
Temperature				
$[C_1Qui][C_1SO_4]$	K_3PO_4	(2.5, 18)	(0.8, 0.8)	15, 25, 35, 45
$[C_2C_2C_2Pro]Br$	K_3PO_4	(10, 35)	(0.8, 0.8)	15, 25, 35, 45
MA content				
$[C_1Qui][C_1SO_4]$	K_3PO_4	(2.5, 18)	(0.17, 0.17); (0.8, 0.8); (1.7; 1.7)	25
$[C_2C_2C_2Pro]Br$	K_3PO_4	(10, 35)	(0.17, 0.17); (0.8, 0.8); (1.7; 1.7)	25
Salt				
$[C_2C_2C_2Pro]Br$	K_3PO_4	(10, 35)	(0.8, 0.8)	25
$[C_2C_2C_2Pro]Br$	K_2HPO_4	(10, 35)	(0.8, 0.8)	25
$[C_2C_2C_2Pro]Br$	K_2CO_3	(10, 35)	(0.8, 0.8)	25

Table D3. Weight fraction data experimentally obtained for the ternary system composed of $[C_1Qui][C_1SO_4]$ + K_3PO_4 + water at 25 (± 1) °C.

$100w_{K_3PO_4}$	$100w_{CIL}$	$100w_{K_3PO_4}$	$100w_{CIL}$	$100w_{K_3PO_4}$	$100w_{CIL}$	$100w_{K_3PO_4}$	$100w_{CIL}$
13.48	3.48	15.65	1.81	17.31	1.04	18.24	0.70
12.99	3.35	15.49	1.79	17.10	1.03	18.06	0.69
13.63	3.27	15.67	1.78	17.34	1.02	18.35	0.68
13.18	3.17	15.43	1.75	17.17	1.01	18.11	0.67
13.81	3.09	15.82	1.73	17.43	0.99	18.36	0.67
13.44	3.01	15.66	1.71	17.26	0.98	18.21	0.66
13.97	2.95	15.91	1.69	17.43	0.98	18.44	0.66
13.78	2.91	15.60	1.66	17.26	0.97	18.26	0.65
14.00	2.89	16.06	1.63	17.51	0.96	18.51	0.64
13.91	2.87	15.85	1.61	17.35	0.95	18.28	0.63
14.21	2.83	16.08	1.59	17.58	0.94	18.61	0.62
13.88	2.77	15.92	1.58	17.39	0.93	18.24	0.61
14.25	2.73	16.14	1.56	17.59	0.92	18.70	0.60
14.14	2.71	15.94	1.55	17.40	0.91	18.26	0.59
14.31	2.69	16.24	1.53	17.65	0.90	18.95	0.57
14.13	2.65	16.00	1.51	17.45	0.89	18.45	0.55
14.41	2.63	16.30	1.49	17.68	0.88		
14.20	2.59	16.03	1.46	17.53	0.88		
14.65	2.54	16.41	1.44	17.76	0.87		
14.38	2.50	16.21	1.42	17.58	0.86		
14.59	2.48	16.46	1.41	17.78	0.85		
14.41	2.44	16.31	1.40	17.62	0.84		
14.78	2.41	16.55	1.38	17.82	0.84		
14.50	2.37	16.25	1.36	17.68	0.83		
14.82	2.34	16.60	1.34	17.88	0.82		
14.64	2.31	16.27	1.31	17.74	0.81		
14.85	2.29	16.62	1.29	17.94	0.81		
14.65	2.26	16.41	1.28	17.80	0.80		
15.06	2.23	16.80	1.26	17.95	0.80		
14.76	2.18	16.47	1.23	17.80	0.79		
15.15	2.15	16.80	1.21	18.05	0.78		
14.77	2.09	16.60	1.20	17.90	0.77		
15.23	2.06	16.84	1.19	18.08	0.77		
15.04	2.03	16.57	1.17	17.90	0.76		
15.32	2.01	16.92	1.15	18.20	0.75		
15.14	1.99	16.77	1.14	17.97	0.74		
15.41	1.97	17.00	1.13	18.18	0.74		
15.14	1.93	16.82	1.12	17.99	0.73		
15.51	1.91	17.16	1.10	18.11	0.72		
15.26	1.87	16.82	1.08	17.98	0.72		
15.61	1.85	17.24	1.06	18.13	0.71		
15.44	1.83	17.04	1.05	17.99	0.71		

Table D4. Weight fraction data experimentally obtained for the ternary system composed of $[C_1C_1C_1Val][C_1SO_4]$ + K_3PO_4 + water at 25 (± 1) °C.

$100w_{K_3PO_4}$	$100w_{CIL}$	$100w_{K_3PO_4}$	$100w_{CIL}$
10.26	38.11	21.14	11.52
9.33	34.64	20.68	11.27
11.55	32.15	21.33	10.90
11.05	30.74	21.08	10.77
13.09	28.58	21.52	10.53
12.70	27.72	21.02	10.29
13.37	27.04	21.89	9.82
13.15	26.59	21.57	9.67
13.91	25.83	22.16	9.37
13.66	25.37	21.83	9.22
14.55	24.52	22.67	8.80
14.24	24.00	22.31	8.66
15.46	22.87	22.87	8.39
15.30	22.62	22.59	8.28
15.83	22.13	23.10	8.04
15.63	21.84	22.77	7.93
16.33	21.21	23.52	7.59
16.06	20.86	22.64	7.30
16.58	20.42	24.26	6.63
16.11	19.85	23.87	6.52
17.25	18.91	24.42	6.30
16.90	18.52	22.36	5.76
17.72	17.87	26.18	4.52
17.54	17.68	23.19	4.01
17.91	17.39		
17.71	17.20		
18.19	16.83		
17.95	16.62		
18.51	16.20		
18.12	15.86		
18.98	15.24		
18.60	14.93		
19.28	14.45		
18.91	14.17		
19.73	13.62		
19.44	13.42		
20.20	12.93		
19.92	12.75		
20.66	12.28		
20.27	12.05		

Table D5. Weight fraction data experimentally obtained for the ternary system composed of $[C_1C_1C_1Val]I$ + K_3PO_4 + water at 25 (± 1) °C.

$100w_{K_3PO_4}$	$100w_{CIL}$	$100w_{K_3PO_4}$	$100w_{CIL}$
4.39	45.35	16.28	14.24
4.28	44.15	16.09	14.08
5.03	43.22	16.39	13.91
4.88	41.99	16.07	13.64
6.08	40.56	16.87	13.18
5.80	38.69	16.57	12.95
6.69	37.68	17.18	12.61
6.42	36.15	17.05	12.52
7.70	34.78	17.42	12.32
7.45	33.67	17.11	12.10
8.74	32.34	17.82	11.72
8.40	31.09	17.58	11.56
9.16	30.34	18.13	11.28
8.97	29.70	17.91	11.14
10.16	28.57	18.44	10.88
9.79	27.55	18.36	10.84
10.57	26.84	19.44	10.30
10.24	25.99	19.06	10.10
11.19	25.17	19.88	9.71
10.86	24.43	19.55	9.54
11.97	23.51	20.37	9.16
11.65	22.88	19.80	8.90
12.35	22.33	20.89	8.43
11.98	21.66	20.51	8.27
12.95	20.91		
12.59	20.34		
13.63	19.57		
13.23	18.99		
14.14	18.34		
13.83	17.94		
14.63	17.39		
14.47	17.20		
14.89	16.92		
14.50	16.48		
15.41	15.90		
15.20	15.68		
15.69	15.37		
15.39	15.07		
16.05	14.67		
15.85	14.50		

Table D6. Weight fraction data experimentally obtained for the ternary system composed of $[C_1C_1C_1Pro]I$ + K_3PO_4 + water at 25 (± 1) °C.

$100w_{K_3PO_4}$	$100w_{CIL}$
1.38	67.36
1.16	56.68
4.68	51.59
4.78	52.68
5.84	51.11
5.54	48.49
6.56	47.08
6.35	45.61
7.03	44.70
6.83	43.44
7.47	42.62
7.29	41.63
8.84	39.69
8.58	38.51
10.77	35.85
10.53	35.04
32.98	8.74
32.79	8.69
33.39	8.01
33.21	7.96
34.06	7.03
33.79	6.97
35.50	5.18
35.05	5.11

Table D7. Weight fraction data experimentally obtained for the ternary system composed of $[C_2C_2C_2Pro]Br$ + K_3PO_4 + water at 25 (± 1) °C.

$100w_{K_3PO_4}$	$100w_{CIL}$	$100w_{K_3PO_4}$	$100w_{CIL}$	$100w_{K_3PO_4}$	$100w_{CIL}$
1.69	45.76	22.24	14.27	25.99	8.49
3.28	43.84	22.70	13.89	26.42	8.22
3.16	42.18	22.59	13.82	26.17	8.15
3.85	41.38	22.90	13.56	26.73	7.80
3.73	40.04	22.79	13.49	26.48	7.73
4.60	39.07	23.12	13.22	27.00	7.42
4.54	38.56	23.00	13.16	26.76	7.35
5.08	37.96	23.31	12.91	27.36	7.01
4.93	36.88	23.19	12.84	27.06	6.93
6.03	35.71	23.48	12.61	27.69	6.58
5.87	34.76	23.37	12.55	27.39	6.51
6.83	33.78	23.67	12.32	28.12	6.12
6.66	32.95	23.55	12.26	27.79	6.05
7.68	31.92	23.81	12.06	28.82	5.52
7.60	31.59	23.70	12.01	28.43	5.44
8.03	31.17	23.98	11.80		
7.94	30.82	23.87	11.74		
8.78	30.00	24.11	11.56		
8.67	29.60	24.01	11.51		
9.47	28.83	24.34	11.27		
9.35	28.50	24.23	11.22		
10.12	27.77	24.45	11.06		
10.01	27.45	24.35	11.02		
11.07	26.47	24.57	10.86		
10.95	26.19	24.48	10.81		
11.94	25.29	24.71	10.65		
11.82	25.04	24.61	10.61		
15.99	21.27	24.83	10.45		
15.84	21.08	24.75	10.41		
16.71	20.30	25.03	10.21		
16.58	20.14	24.84	10.13		
19.82	17.30	25.25	9.85		
19.70	17.20	25.06	9.78		
21.01	16.07	25.51	9.48		
20.87	15.97	25.34	9.41		
21.62	15.33	25.72	9.16		
21.50	15.24	25.55	9.09		
22.12	14.71	25.92	8.85		
22.01	14.63	25.75	8.79		
22.36	14.34	26.15	8.54		

Table D8. Weight fraction data experimentally obtained for the ternary system composed of $[C_2C_2C_2Pro]Br$ + K_2HPO_4 + water at 25 (± 1) °C.

$100w_{K_2HPO_4}$	$100w_{CIL}$	$100w_{K_2HPO_4}$	$100w_{CIL}$	$100w_{K_2HPO_4}$	$100w_{CIL}$	$100w_{K_2HPO_4}$	$100w_{CIL}$
3.40	44.79	14.10	20.62	20.08	12.28	24.22	7.93
3.25	42.85	13.98	20.44	19.98	12.22	24.05	7.87
3.70	42.33	14.62	19.93	20.22	12.08	24.53	7.63
3.59	41.11	14.50	19.77	20.13	12.03	24.37	7.58
5.13	39.36	14.94	19.43	20.40	11.87	24.76	7.39
4.82	36.96	14.82	19.27	20.35	11.84	24.60	7.34
6.34	35.36	15.42	18.82	20.46	11.77	25.08	7.11
6.22	34.69	15.30	18.67	20.37	11.72	24.84	7.04
6.93	33.96	15.81	18.28	20.73	11.50	25.42	6.77
6.82	33.40	15.69	18.15	20.63	11.45	25.25	6.73
7.45	32.76	15.94	17.96	20.86	11.31	25.82	6.46
7.22	31.76	15.81	17.81	20.78	11.26	25.58	6.40
8.19	30.81	16.36	17.40	21.03	11.12	26.32	6.06
8.11	30.53	16.11	17.14	20.92	11.06	26.05	6.00
8.43	30.22	16.85	16.60	21.22	10.89		
8.33	29.86	16.72	16.48	21.12	10.84		
8.87	29.35	17.18	16.15	21.42	10.67		
8.76	28.98	17.05	16.03	21.33	10.63		
9.33	28.45	17.50	15.72	21.59	10.48		
9.23	28.17	17.37	15.60	21.50	10.43		
9.91	27.55	17.91	15.23	21.82	10.25		
9.81	27.27	17.79	15.13	21.73	10.21		
10.27	26.85	18.11	14.91	21.87	10.13		
10.15	26.55	18.00	14.82	21.78	10.09		
10.77	25.99	18.33	14.60	22.06	9.93		
10.66	25.72	18.20	14.50	21.98	9.89		
11.20	25.25	18.51	14.29	22.20	9.77		
11.09	24.99	18.41	14.22	22.11	9.73		
11.76	24.41	18.75	14.00	22.40	9.58		
11.64	24.16	18.56	13.85	22.32	9.54		
12.04	23.82	19.07	13.52	22.54	9.42		
11.92	23.58	18.98	13.46	22.46	9.39		
12.55	23.04	19.25	13.29	22.70	9.26		
12.45	22.84	19.16	13.23	22.61	9.22		
13.04	22.35	19.52	13.00	22.84	9.11		
12.93	22.15	19.41	12.93	22.75	9.07		
13.48	21.70	19.64	12.79	23.51	8.67		
13.35	21.49	19.55	12.73	23.25	8.57		
13.75	21.17	19.86	12.54	23.88	8.24		
13.64	20.99	19.77	12.48	23.71	8.18		

Table D9. Weight fraction data experimentally obtained for the ternary system composed of $[C_2C_2C_2Pro]Br$ + K_2CO_3 + water at 25 (± 1) °C.

$100w_{K_2CO_3}$	$100w_{CIL}$	$100w_{K_2CO_3}$	$100w_{CIL}$	$100w_{K_2CO_3}$	$100w_{CIL}$	$100w_{K_2CO_3}$	$100w_{CIL}$
2.71	52.51	21.03	20.81	29.06	10.34	31.89	5.25
2.65	51.39	21.92	20.18	28.82	10.25	32.81	4.99
5.70	48.10	21.71	19.99	29.18	10.08	31.76	4.83
5.42	45.70	22.30	19.58	28.90	9.98		
6.26	44.85	22.08	19.39	29.30	9.80		
6.15	44.06	22.65	19.00	29.04	9.71		
8.69	41.52	22.45	18.83	29.41	9.54		
8.16	38.95	23.06	18.42	29.17	9.46		
9.46	37.75	22.82	18.22	29.61	9.26		
9.34	37.26	23.53	17.76	29.24	9.15		
10.33	36.35	23.33	17.61	29.81	8.90		
10.19	35.83	24.55	16.81	29.51	8.81		
11.47	34.68	24.16	16.54	29.91	8.64		
11.30	34.16	24.92	16.06	29.58	8.55		
12.56	33.06	24.73	15.94	30.06	8.35		
12.37	32.54	25.36	15.54	29.69	8.25		
13.35	31.70	25.17	15.42	30.32	8.00		
13.17	31.29	27.58	13.94	29.91	7.89		
13.73	30.82	27.38	13.84	30.58	7.63		
13.54	30.40	27.83	13.57	30.16	7.52		
14.57	29.54	27.36	13.34	30.80	7.28		
14.37	29.13	28.03	12.95	30.32	7.17		
15.37	28.32	27.73	12.81	30.97	6.94		
15.15	27.92	28.40	12.43	30.56	6.85		
16.12	27.14	28.01	12.26	31.28	6.60		
15.95	26.85	28.38	12.05	30.88	6.51		
18.78	24.64	28.10	11.93	31.48	6.31		
18.43	24.18	28.62	11.65	31.13	6.24		
19.16	23.62	28.25	11.50	31.73	6.04		
18.97	23.38	28.63	11.30	31.34	5.97		
19.69	22.85	28.28	11.16	31.92	5.79		
19.48	22.60	28.71	10.95	31.58	5.73		
20.78	21.65	28.46	10.85	32.12	5.56		
20.56	21.42	28.96	10.61	31.75	5.50		
21.19	20.97	28.70	10.51	32.34	5.32		

Table D10. Merchuk equation parameters (*A*, *B* and *C*) with the respective standard deviations (σ) for the ternary systems composed of CILs + salt + water at 25 (± 1) °C.

ABS	$A \pm \sigma$	$B \pm \sigma$	$C \pm \sigma$
$[C_1Qui][C_1SO_4] + K_3PO_4$	100.00 ± 0.17	-0.74 ± 0.01	$2.99\times10^{-4} \pm 1.06\times10^{-5}$
$[C_1C_1C_1Val][C_1SO_4] + K_3PO_4$	76.10 ± 23.54	-0.21 ± 0.10	$1.04\times10^{-4} \pm 1.53\times10^{-5}$
$[C_1C_1C_1Val]I + K_3PO_4$	103.38 ± 7.64	-0.39 ± 0.03	$9.36\times10^{-5} \pm 1.17\times10^{-5}$
$[C_1C_1C_1Pro]I + K_3PO_4$	82.01 ± 8.27	-0.23 ± 0.04	$2.86\times10^{-5} \pm 8.25\times10^{-6}$
$[C_2C_2C_2Pro]Br + K_3PO_4$	63.96 ± 2.71	-0.24 ± 0.02	$4.02\times10^{-5} \pm 3.47\times10^{-6}$
$[C_2C_2C_2Pro]Br + K_2HPO_4$	77.05 ± 1.46	-0.31 ± 0.01	$5.40\times10^{-5} \pm 1.84\times10^{-6}$
$[C_2C_2C_2Pro]Br + K_2CO_3$	72.40 ± 3.34	-0.20 ± 0.02	$3.75\times10^{-5} \pm 2.25\times10^{-6}$

Table D11. Weight fraction composition (wt%) of both CIL-rich and salt-rich phases of biphasic ternary systems composed of CILs and salts at 25 (± 1) °C, along with the respective values of tie-line length (TLL).

ABS	100 × weight fraction composition / (wt%)						TLL
	$[CIL]_{CIL}$ / (wt%)	$[Salt]_{CIL}$ / (wt%)	$[CIL]_{M}$ / (wt%)	$[Salt]_{M}$ / (wt%)	$[CIL]_{Salt}$ / (wt%)	$[Salt]_{Salt}$(wt%)	
$[C_1Qui][C_1SO_4]$ + K_3PO_4	29.39	2.75	3.09	14.73	1.96	15.25	30.14
	40.22	1.53	2.37	17.71	0.65	18.45	43.04
	63.12	0.39	3.75	20.77	0.13	22.01	66.60
$[C_1C_1C_1Val][C_1SO_4]$ + K_3PO_4	49.12	4.04	10.02	24.92	1.72	29.35	53.73
$[C_1C_1C_1Val]I$ + K_3PO_4	50.98	3.23	9.98	34.49	0.01	42.09	64.10
$[C_1C_1C_1Pro]I$ + K_3PO_4	48.11	5.30	13.97	31.82	2.86	40.46	57.31
$[C_2C_2C_2Pro]Br$ + K_3PO_4	43.13	2.68	10.21	29.86	2.10	36.56	53.21
	49.25	1.18	9.92	34.37	0.66	42.19	63.59
	58.44	0.14	9.69	39.85	0.16	47.60	75.16
$[C_2C_2C_2Pro]Br$ + K_2HPO_4	55.38	1.11	9.89	34.97	0.17	42.20	68.81
$[C_2C_2C_2Pro]Br$ + K_2CO_3	44.95	5.60	9.87	34.43	1.42	41.37	56.34

Table D12. Extraction efficiencies of mandelic acid enantiomers ($EE_{R\text{-MA}}$ and $EE_{S\text{-MA}}$, %) and enantiomeric excesses (*e.e.*, %) plus the corresponding standard deviations (σ) obtained using ABS composed of CIL and salts.

ABS	**$[CIL]_M \pm \sigma$**	**$[Salt]_M \pm \sigma$**	**$EE_{R\text{-MA}} \pm \sigma$**	**$EE_{S\text{-MA}} \pm \sigma$**	***e.e.* / (%)**
CIL structure					
$[C_1Qui][C_1SO_4] + K_3PO_4$	2.43 ± 0.04	17.91 ± 0.16	23.32 ± 3.73	23.91 ± 4.30	1.61 ± 0.92
$[C_1C_1C_1Val][C_1SO_4] + K_3PO_4$	10.06 ± 0.34	24.89 ± 0.05	25.12 ± 1.37	34.86 ± 0.22	15.53 ± 1.11
$[C_1C_1C_1Val]I + K_3PO_4$	9.83 ± 0.11	33.84 ± 0.92	61.87 ± 7.77	68.77 ± 9.23	9.29 ± 1.15
$[C_1C_1C_1Pro]I + K_3PO_4$	13.66 ± 0.44	31.46 ± 0.52	49.81 ± 2.99	65.90 ± 1.47	14.03 ± 0.93
$[C_2C_2C_2Pro]Br + K_3PO_4$	9.94 ± 0.07	34.67 ± 0.20	44.62 ± 2.50	61.58 ± 3.96	17.37 ± 1.92
TLL					
$[C_1Qui][C_1SO_4] + K_3PO_4$	2.96 ± 0.11	15.17 ± 0.47	24.93 ± 4.53	25.90 ± 5.36	2.06 ± 1.49
$[C_1Qui][C_1SO_4] + K_3PO_4$	2.43 ± 0.04	17.91 ± 0.16	23.32 ± 3.73	23.91 ± 4.30	1.61 ± 0.92
$[C_1Qui][C_1SO_4] + K_3PO_4$	3.95 ± 0.28	20.76 ± 0.00	33.21 ± 0.70	34.48 ± 0.45	1.87 ± 1.14
$[C_2C_2C_2Pro]Br + K_3PO_4$	10.14 ± 0.14	29.56 ± 0.26	25.01 ± 1.50	31.13 ± 2.80	9.67 ± 2.79
$[C_2C_2C_2Pro]Br + K_3PO_4$	9.94 ± 0.07	34.67 ± 0.20	44.62 ± 2.50	61.58 ± 3.96	17.37 ± 1.92
$[C_2C_2C_2Pro]Br + K_3PO_4$	9.81 ± 0.18	39.73 ± 0.22	53.71 ± 5.56	55.46 ± 5.09	1.10 ± 3.41
Mixture points along the same TL - Phases weight ratio					
$[C_2C_2C_2Pro]Br + K_3PO_4$	30.18 ± 0.13	15.94 ± 0.15	87.17 ± 7.70	86.63 ± 8.15	-0.55 ± 0.19
$[C_2C_2C_2Pro]Br + K_3PO_4$	19.78 ± 0.22	24.84 ± 0.35	94.51 ± 5.94	92.81 ± 5.79	-1.98 ± 1.34
$[C_2C_2C_2Pro]Br + K_3PO_4$	9.94 ± 0.07	34.67 ± 0.20	44.62 ± 2.50	61.58 ± 3.96	17.37 ± 1.92
$[C_2C_2C_2Pro]Br + K_3PO_4$	5.08 ± 0.13	40.18 ± 0.21	37.32 ± 2.74	48.10 ± 2.62	12.33 ± 0.51
$[C_2C_2C_2Pro]Br + K_2HPO_4$	19.69 ± 0.13	25.27 ± 0.26	81.43 ± 1.25	81.55 ± 0.19	-1.48 ± 0.10
$[C_2C_2C_2Pro]Br + K_2HPO_4$	14.93 ± 0.15	29.99 ± 0.22	90.05 ± 5.13	85.76 ± 4.14	-2.37 ± 0.84
$[C_2C_2C_2Pro]Br + K_2HPO_4$	9.82 ± 0.14	35.02 ± 0.06	81.90 ± 5.59	81.63 ± 5.08	0.82 ± 0.18

$[C_2C_2C_2Pro]Br + K_2HPO_4$	5.12 ± 0.04	39.77 ± 0.35	85.66 ± 2.71	84.04 ± 4.34	-1.00 ± 0.57
Temperature					
$[C_1Qui][C_1SO_4] + K_3PO_4$ (15 °C)	2.52 ± 0.10	17.82 ± 0.01	13.44 ± 0.39	15.54 ± 0.39	7.88 ± 0.70
$[C_1Qui][C_1SO_4] + K_3PO_4$ (25 °C)	2.43 ± 0.04	17.91 ± 0.16	23.32 ± 3.73	23.91 ± 4.30	1.61 ± 0.92
$[C_1Qui][C_1SO_4] + K_3PO_4$ (35 °C)	2.52 ± 0.01	18.08 ± 0.62	28.46 ± 4.81	28.65 ± 5.14	0.70 ± 0.22
$[C_1Qui][C_1SO_4] + K_3PO_4$ (45 °C)	2.40 ± 0.02	17.74 ± 0.06	59.03 ± 2.12	59.13 ± 3.96	-1.81 ± 1.44
$[C_2C_2C_2Pro]Br + K_3PO_4$ (15 °C)	9.82 ± 0.36	34.19 ± 0.42	45.48 ± 2.34	59.05 ± 5.19	12.48 ± 1.70
$[C_2C_2C_2Pro]Br + K_3PO_4$ (25 °C)	9.94 ± 0.07	34.67 ± 0.20	44.62 ± 2.50	61.58 ± 3.96	17.37 ± 1.92
$[C_2C_2C_2Pro]Br + K_3PO_4$ (35 °C)	9.99 ± 0.18	34.48 ± 0.16	46.45 ± 0.63	59.44 ± 0.89	11.54 ± 2.19
$[C_2C_2C_2Pro]Br + K_3PO_4$ (45 °C)	9.94 ± 0.20	34.71 ± 0.20	39.21 ± 4.48	50.03 ± 5.42	12.26 ± 3.73
MA content					
$[C_1Qui][C_1SO_4] + K_3PO_4$ (0.17 wt%)	2.49 ± 0.02	18.09 ± 0.27	31.30 ± 2.96	31.10 ± 1.84	-1.61 ± 1.95
$[C_1Qui][C_1SO_4] + K_3PO_4$ (0.8 wt%)	2.43 ± 0.04	17.91 ± 0.16	23.32 ± 3.73	23.91 ± 4.30	1.61 ± 0.92
$[C_1Qui][C_1SO_4] + K_3PO_4$ (1.7 wt%)	2.51 ± 0.02	17.78 ± 0.19	13.48 ± 3.78	15.25 ± 4.41	6.04 ± 1.35
$[C_2C_2C_2Pro]Br + K_3PO_4$ (0.17 wt%)	9.88 ± 0.15	34.51 ± 0.23	79.16 ± 1.94	76.29 ± 2.66	-4.91 ± 1.34
$[C_2C_2C_2Pro]Br + K_3PO_4$ (0.8 wt%)	9.94 ± 0.07	34.67 ± 0.20	44.62 ± 2.50	61.58 ± 3.96	17.37 ± 1.92
$[C_2C_2C_2Pro]Br + K_3PO_4$ (1.7 wt%)	9.83 ± 0.15	34.60 ± 0.41	42.66 ± 3.33	38.19 ± 3.27	-6.40 ± 2.92
Salt					
$[C_2C_2C_2Pro]Br + K_3PO_4$	9.94 ± 0.07	34.67 ± 0.20	44.62 ± 2.50	61.58 ± 3.96	17.37 ± 1.92
$[C_2C_2C_2Pro]Br + K_2HPO_4$	9.82 ± 0.14	35.02 ± 0.06	81.90 ± 5.59	81.63 ± 5.08	0.82 ± 0.18
$[C_2C_2C_2Pro]Br + K_2CO_3$	10.06 ± 0.14	35.16 ± 0.10	55.13 ± 0.03	62.61 ± 2.31	5.79 ± 0.12

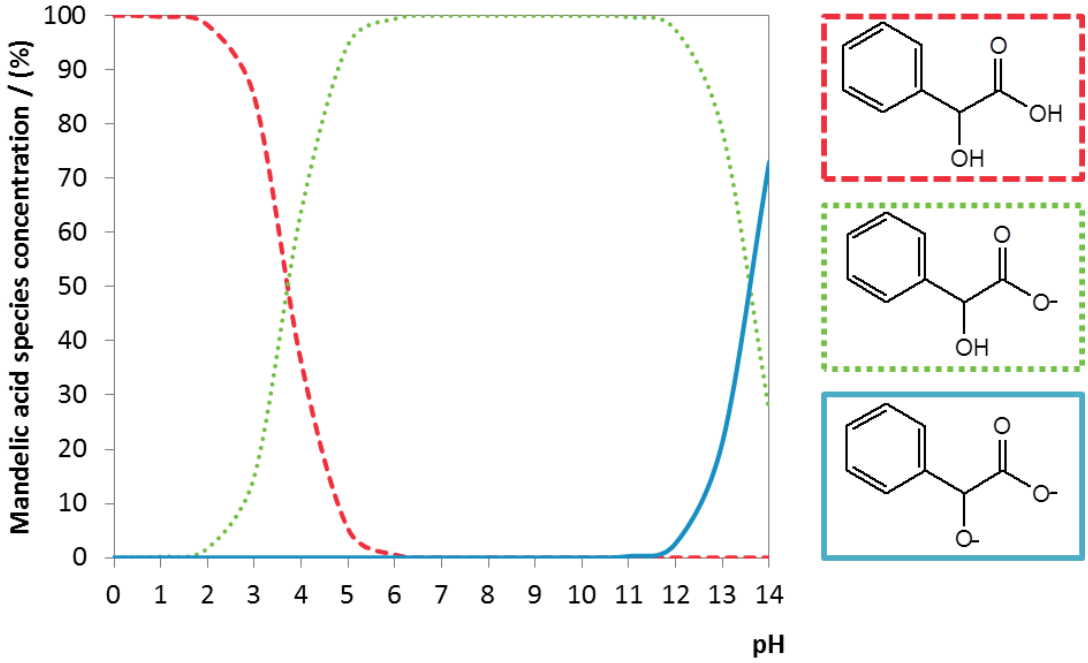

Figure D1. Speciation profile of mandelic acid as a function of the pH (content adapted from the chemical free database Chemspider – www.chemspider.com, accessed Feb 10, 2018).

Appendix E

3.1.2. Aqueous biphasic systems using chiral ionic liquids bearing chiral anions for enantioseparations

e Silva, F. A.; Sintra, T. E.; Rocha, S. N.; Monteiro, C.; Ventura, S. P. M.; Coutinho, J. A. P. Aqueous biphasic systems composed of ionic liquids bearing chiral anions for enantioseparations. *in preparation*.

Table E1. Weight fraction data experimentally obtained for the ternary system composed of $[N_{4444}]_2$[L-Glu] + Na_2SO_4 + water at 25 (± 1) °C.

$100w_{Na_2SO_4}$	$100w_{CIL}$	$100w_{Na_2SO_4}$	$100w_{CIL}$	$100w_{Na_2SO_4}$	$100w_{CIL}$
4.73	35.00	8.11	25.13	11.36	18.78
4.63	34.24	7.98	24.74	11.13	18.40
5.16	33.05	8.13	24.68	11.98	17.79
5.10	32.65	8.09	24.57	11.74	17.43
5.63	31.47	8.51	23.69	12.62	16.82
5.58	31.14	8.82	23.55	12.36	16.48
6.30	29.59	8.40	23.38	13.28	15.99
6.23	29.27	8.61	22.99	12.97	15.62
6.82	28.21	9.23	22.75	14.06	14.75
6.83	27.99	9.10	22.42	13.75	14.43
6.80	27.87	9.73	21.77	14.92	13.72
6.67	27.59	9.57	21.42	14.50	13.34
7.21	26.99	10.23	20.76	15.91	12.26
7.14	26.73	10.07	20.43	15.50	11.94
7.68	26.07	10.75	19.79		
7.45	25.30	10.58	19.46		

Table E2. Weight fraction data experimentally obtained for the ternary system composed of $[N_{4444}]$[L-Phe] + Na_2SO_4 + water at 25 (± 1) °C.

$100w_{Na_2SO_4}$	$100w_{CIL}$	$100w_{Na_2SO_4}$	$100w_{CIL}$	$100w_{Na_2SO_4}$	$100w_{CIL}$
3.34	41.38	7.32	26.35	10.70	18.72
3.23	40.04	7.24	26.04	10.60	18.55
3.69	38.93	7.36	25.75	11.60	17.13
3.63	38.27	7.24	25.31	11.36	16.78
3.95	37.52	7.94	24.57	11.93	16.57
3.86	36.71	7.98	24.51	11.84	16.44
4.46	35.33	7.83	24.23	12.97	14.67
4.40	34.78	7.86	24.14	12.71	14.38
4.96	33.52	8.82	22.48	14.08	12.79
4.89	33.04	8.69	22.17	13.76	12.50
5.43	31.85	9.39	21.34	15.11	11.11
5.32	31.24	9.27	21.07	14.81	10.89
6.07	29.65	10.20	19.72	16.06	9.62
5.97	29.18	10.03	19.40	15.75	9.44

Table E3. Weight fraction data experimentally obtained for the ternary system composed of $[N_{4444}]$[D-Phe] + Na_2SO_4 + water at 25 (± 1) °C.

$100w_{Na_2SO_4}$	$100w_{CIL}$	$100w_{Na_2SO_4}$	$100w_{CIL}$	$100w_{Na_2SO_4}$	$100w_{CIL}$
2.76	43.92	6.35	28.48	9.72	20.41
2.71	43.12	6.26	28.06	9.59	20.15
3.05	42.28	6.68	27.96	10.28	19.29
2.99	41.53	6.66	27.90	10.15	19.04
3.28	40.82	6.85	27.51	10.87	18.22
3.23	40.11	6.82	27.40	10.71	17.95
3.69	39.01	7.15	26.73	11.50	17.08
3.61	38.21	7.02	26.58	11.34	16.83
4.10	37.09	7.08	26.48	12.16	15.95
4.04	36.56	6.95	26.34	11.97	15.69
4.40	35.73	7.59	25.10	12.91	14.57
4.34	35.22	7.51	24.85	12.72	14.35
4.80	34.21	7.96	24.70	13.65	13.42
4.76	33.97	7.93	24.63	13.41	13.18
5.06	33.31	8.10	23.91	14.56	11.88
4.98	32.79	8.41	23.67	14.29	11.66
5.57	31.51	8.01	23.64	15.63	9.98
5.50	31.12	8.32	23.44	15.33	9.79
6.02	30.00	8.59	22.72	16.67	8.48
5.95	29.64	8.52	22.52	16.28	8.28
6.44	28.62	9.17	21.50		
6.41	28.51	9.05	21.22		

Table E4. Weight fraction data experimentally obtained for the ternary system composed of $[N_{4444}][L\text{-}Ala] + Na_2SO_4$ + water at 25 (± 1) °C.

$100w_{Na_2SO_4}$	$100w_{CIL}$	$100w_{Na_2SO_4}$	$100w_{CIL}$	$100w_{Na_2SO_4}$	$100w_{CIL}$
2.49	43.57	5.12	31.64	11.07	18.71
2.42	42.29	5.06	31.22	10.90	18.43
2.99	40.92	5.67	29.94	11.69	17.70
2.89	39.55	5.57	29.45	11.52	17.44
3.38	38.41	6.63	27.27	12.45	16.65
3.31	37.68	6.55	26.94	12.20	16.31
3.83	36.52	9.92	20.55	13.10	15.75
3.76	35.94	9.79	20.26	12.89	15.49
4.21	34.96	10.36	19.90	13.71	14.87
4.15	34.51	10.23	19.64	13.51	14.66
4.79	33.10	10.56	19.41	14.39	13.91
4.71	32.53	10.54	19.38	14.16	13.69

Table E5. Weight fraction data experimentally obtained for the ternary system composed of $[N_{4444}][L\text{-}Val] + Na_2SO_4$ + water at 25 (± 1) °C.

$100w_{Na_2SO_4}$	$100w_{CIL}$	$100w_{Na_2SO_4}$	$100w_{CIL}$	$100w_{Na_2SO_4}$	$100w_{CIL}$
2.15	44.63	7.34	24.10	11.13	17.85
2.09	43.31	7.96	23.62	11.00	17.63
2.31	42.79	7.86	23.31	11.60	17.11
2.24	41.58	8.41	22.75	11.45	16.89
2.92	39.99	8.30	22.45	12.18	16.11
2.76	37.82	8.91	21.71	12.01	15.88
3.87	35.39	8.80	21.44	12.70	15.35
3.79	34.66	9.31	20.96	12.52	15.12
4.46	33.24	9.21	20.73	13.34	14.45
4.33	32.30	9.81	20.01	13.11	14.20
5.41	30.07	9.68	19.75	13.88	13.81
5.29	29.41	10.24	19.32	13.65	13.58
7.02	25.96	10.10	19.06	15.25	11.94
6.91	25.56	10.74	18.43	14.72	11.52
7.50	24.60	10.60	18.19		

Table E6. Weight fraction data experimentally obtained for the ternary system composed of $[N_{4444}][L\text{-}Pro] + Na_2SO_4$ + water at 25 (± 1) °C.

$100w_{Na_2SO_4}$	$100w_{CIL}$	$100w_{Na_2SO_4}$	$100w_{CIL}$	$100w_{Na_2SO_4}$	$100w_{CIL}$
2.58	42.83	6.85	25.55	11.62	17.14
2.47	40.92	6.93	25.27	11.47	16.91
3.34	38.87	7.73	24.17	11.92	16.62
3.21	37.36	7.61	23.81	11.85	16.52
3.79	36.07	8.10	23.35	12.52	15.79
3.68	35.00	8.04	23.17	12.32	15.54
4.55	33.12	8.99	21.57	12.88	15.25
4.40	32.09	8.79	21.11	12.77	15.12
5.33	30.17	9.61	20.40	13.34	14.51
5.25	29.74	9.46	20.09	13.21	14.37
6.09	28.05	10.12	19.60	14.15	13.42
6.15	28.00	9.97	19.31	13.86	13.15
6.01	27.71	10.86	18.37	14.97	12.24
5.98	27.22	10.66	18.02	14.70	12.01
6.94	25.87	11.10	17.96		
7.05	25.71	11.04	17.86		

Table E7. Weight fraction data experimentally obtained for the ternary system composed of $[N_{4444}]_2[L\text{-}Glu] + K_3C_6H_5O_7$ + water at 25 (± 1) °C.

$100w_{Salt}$	$100w_{CIL}$	$100w_{Salt}$	$100w_{CIL}$	$100w_{Salt}$	$100w_{CIL}$
9.00	49.50	16.88	34.69	28.60	19.68
8.84	48.61	16.58	34.09	28.41	19.54
9.61	47.70	18.41	32.20	30.55	17.57
9.42	46.74	18.27	31.96	30.36	17.46
10.50	45.48	19.29	30.92	32.52	15.51
10.35	44.84	19.04	30.51	32.32	15.41
12.18	42.75	21.61	27.94	34.71	13.29
11.92	41.86	21.33	27.58	34.55	13.23
13.48	40.13	23.82	25.16	36.48	11.54
13.25	39.44	23.57	24.89	36.32	11.49
15.08	37.46	26.13	22.45	38.88	9.28
14.83	36.85	25.88	22.23	38.75	9.25

Table E8. Weight fraction data experimentally obtained for the ternary system composed of $[N_{4444}]_2$[L-Glu] + $KNaC_4H_4O_6$ + water at 25 (± 1) °C.

$100w_{Salt}$	$100w_{CIL}$	$100w_{Salt}$	$100w_{CIL}$	$100w_{Salt}$	$100w_{CIL}$
7.17	47.75	11.03	37.07	15.10	28.88
7.04	46.85	10.89	36.61	14.99	28.67
8.74	44.00	11.64	35.47	17.27	25.42
8.38	42.17	11.46	34.93	17.09	25.16
10.32	39.09	13.04	32.59		
10.15	38.43	12.86	32.13		

Table E9. Weight fraction data experimentally obtained for the ternary system composed of $[N_{4444}]_2$[L-Glu] + K_2CO_3 + water at 25 (± 1) °C.

$100w_{Salt}$	$100w_{CIL}$	$100w_{Salt}$	$100w_{CIL}$	$100w_{Salt}$	$100w_{CIL}$	$100w_{Salt}$	$100w_{CIL}$
1.29	56.61	7.18	30.52	12.59	18.92	16.60	12.19
1.26	55.14	7.42	30.20	12.48	18.76	16.88	11.93
2.32	53.10	7.31	29.73	13.05	18.15	16.80	11.87
2.22	50.69	7.92	28.93	12.94	17.99	17.15	11.55
2.88	49.48	7.82	28.56	13.48	17.42	17.06	11.49
2.75	47.35	8.37	27.85	13.37	17.28	17.33	11.24
3.32	46.38	8.26	27.49	13.92	16.72	17.24	11.18
3.19	44.55	8.72	26.91	13.81	16.58	17.58	10.89
3.62	43.82	8.62	26.58	14.30	16.08	17.49	10.83
3.55	42.97	9.15	25.92	14.20	15.97	17.79	10.57
4.32	41.73	9.04	25.61	14.65	15.52	17.70	10.52
4.16	40.19	9.56	24.97	14.55	15.42	17.95	10.30
5.00	38.89	9.44	24.68	14.98	14.99	17.86	10.25
4.81	37.44	10.03	23.97	14.87	14.88	18.16	10.00
5.66	36.19	9.92	23.70	15.30	14.46	18.07	9.95
5.58	35.69	10.43	23.10	15.20	14.36	18.36	9.70
5.92	35.18	10.32	22.86	15.56	14.01	18.28	9.66
5.83	34.65	11.07	21.99	15.47	13.93	18.53	9.45
6.22	34.10	10.93	21.71	15.85	13.56	18.45	9.41
6.13	33.59	11.26	21.34	15.75	13.48	18.71	9.20
6.50	33.06	11.15	21.12	16.17	13.08	18.63	9.16
6.40	32.55	11.77	20.43	16.07	13.00	18.86	8.97
6.98	31.76	11.66	20.23	16.41	12.69	18.78	8.93
6.89	31.36	12.22	19.61	16.31	12.62		
7.26	30.85	12.12	19.44	16.69	12.26		

Table E10. Weight fraction data experimentally obtained for the ternary system composed of $[N_{4444}]$[L-Phe] + Na_2CO_3 + water at 25 (± 1) °C.

$100w_{Salt}$	$100w_{CIL}$	$100w_{Salt}$	$100w_{CIL}$	$100w_{Salt}$	$100w_{CIL}$
1.82	46.20	6.66	24.04	10.44	15.39
1.79	45.27	6.60	23.84	10.31	15.20
2.33	44.21	6.87	23.49	10.78	14.72
2.21	41.91	6.78	23.18	10.67	14.57
2.75	40.90	7.28	22.54	11.02	14.21
2.66	39.58	7.22	22.35	10.94	14.12
3.17	38.68	7.43	22.09	11.17	13.89
3.05	37.26	7.35	21.85	11.07	13.77
3.52	36.45	7.74	21.37	11.41	13.43
3.43	35.50	7.65	21.13	11.33	13.34
3.83	34.83	8.06	20.64	11.54	13.13
3.70	33.61	7.99	20.47	11.44	13.02
4.04	33.07	8.17	20.26	11.73	12.74
3.99	32.62	8.09	20.05	11.65	12.65
4.34	32.08	8.42	19.65	11.92	12.39
4.28	31.63	8.35	19.47	11.84	12.31
4.62	31.11	8.71	19.04	12.11	12.05
4.52	30.43	8.62	18.86	12.04	11.98
4.89	29.89	8.92	18.51	12.23	11.81
4.81	29.44	8.85	18.35	12.16	11.74
5.14	28.97	9.16	17.98	12.39	11.52
5.07	28.56	9.14	17.93	12.34	11.48
5.34	28.16	9.29	17.76	12.50	11.34
5.29	27.87	9.22	17.61	12.43	11.27
5.60	27.42	9.52	17.27	12.67	11.06
5.52	27.03	9.45	17.14	12.59	10.99
5.84	26.58	9.75	16.81	12.76	10.84
5.73	26.09	9.68	16.68	12.68	10.77
6.29	25.34	9.97	16.36	12.85	10.62
6.22	25.06	9.88	16.22	12.78	10.57
6.47	24.71	10.14	15.93		
6.39	24.39	10.06	15.80		

Table E11. Weight fraction data experimentally obtained for the ternary system composed of $[N_{4444}][D\text{-Phe}]$ + Na_2CO_3 + water at 25 (± 1) °C.

$100w_{Salt}$	$100w_{CIL}$	$100w_{Salt}$	$100w_{CIL}$	$100w_{Salt}$	$100w_{CIL}$
2.16	44.61	6.60	23.66	12.56	10.92
2.06	42.46	7.08	22.82	12.48	10.86
2.54	41.34	6.99	22.53	12.87	10.32
2.43	39.65	7.65	21.42	12.83	10.29
2.82	38.79	7.56	21.16	13.22	9.76
2.76	37.96	8.35	19.84	13.17	9.73
3.24	36.91	8.27	19.64	13.52	9.25
3.12	35.51	8.77	18.82	13.45	9.20
3.97	33.76	8.67	18.60	13.83	8.68
3.90	33.12	9.33	17.54	13.76	8.64
4.30	32.30	9.24	17.36	14.22	8.02
4.22	31.68	9.93	16.27	14.18	7.99
4.56	31.02	9.83	16.11	14.42	7.68
4.48	30.53	10.46	15.14	14.35	7.64
4.81	29.90	10.37	15.00	14.73	7.16
4.73	29.40	10.99	14.06	14.66	7.13
5.39	28.14	10.90	13.95	15.03	6.66
5.30	27.67	11.40	13.21	14.95	6.62
5.59	27.14	11.32	13.12	15.56	5.88
5.50	26.68	11.87	12.32	15.50	5.86
6.06	25.67	11.78	12.23	16.35	4.82
5.97	25.26	12.16	11.69	16.24	4.79
6.69	23.99	12.07	11.61		

Table E12. Weight fraction data experimentally obtained for the ternary system composed of $[N_{4444}]$[L-Phe] + K_2CO_3 + water at 25 (± 1) °C.

$100w_{Salt}$	$100w_{CIL}$	$100w_{Salt}$	$100w_{CIL}$	$100w_{Salt}$	$100w_{CIL}$
3.48	44.04	11.82	18.01	15.51	10.60
3.34	42.35	12.14	17.69	15.42	10.54
4.05	41.23	12.01	17.50	15.63	10.39
3.88	39.57	12.38	17.14	15.53	10.32
4.60	38.48	12.27	16.98	15.76	10.16
4.51	37.74	12.65	16.62	15.69	10.12
5.14	36.81	12.52	16.45	15.84	10.01
5.02	36.01	12.95	16.05	15.77	9.96
5.56	35.23	12.83	15.91	15.86	9.90
5.45	34.52	13.18	15.59	15.82	9.87
5.86	33.95	13.05	15.44	15.98	9.76
5.66	32.79	13.46	15.06	15.89	9.70
6.38	31.81	13.36	14.94	16.08	9.57
6.27	31.24	13.82	14.53	15.99	9.52
6.84	30.50	13.60	14.29	16.15	9.41
6.71	29.93	13.85	14.08	16.07	9.36
7.33	29.14	13.75	13.97	16.20	9.28
7.22	28.72	13.97	13.78	16.11	9.23
8.00	27.73	13.87	13.68	16.29	9.11
7.88	27.32	14.13	13.46	16.20	9.06
8.17	26.96	14.02	13.36	16.36	8.95
8.05	26.56	14.33	13.10	16.28	8.91
8.60	25.89	14.21	12.99	16.44	8.81
8.47	25.49	14.48	12.77	16.36	8.76
9.55	24.21	14.37	12.67	16.54	8.64
9.29	23.56	14.58	12.51	16.46	8.60
9.78	23.00	14.48	12.43	16.64	8.49
9.68	22.75	14.73	12.23	16.57	8.45
10.23	22.12	14.63	12.14	16.68	8.37
10.11	21.86	14.85	11.97	16.60	8.33
10.57	21.35	14.75	11.88	16.76	8.24
10.44	21.07	14.99	11.70	16.68	8.20
10.96	20.51	14.89	11.62	16.91	8.06
10.84	20.28	15.10	11.47	16.83	8.02
11.26	19.83	15.00	11.39	16.95	7.94
11.14	19.61	15.23	11.22	16.87	7.91
11.45	19.27	15.14	11.16	17.08	7.78
11.34	19.08	15.30	11.03	16.95	7.72
11.76	18.66	15.21	10.96	17.32	7.49
11.64	18.47	15.40	10.82	17.11	7.40
11.94	18.18	15.30	10.75		

Table E13. Weight fraction data experimentally obtained for the ternary system composed of $[N_{4444}]$[D-Phe] + K_2CO_3 + water at 25 (± 1) °C.

$100w_{Salt}$	$100w_{CIL}$	$100w_{Salt}$	$100w_{CIL}$	$100w_{Salt}$	$100w_{CIL}$	$100w_{Salt}$	$100w_{CIL}$
3.52	44.05	10.14	22.18	14.08	13.87	16.22	9.75
3.43	42.82	10.02	21.91	13.98	13.77	16.14	9.70
3.81	42.21	10.37	21.53	14.24	13.54	16.33	9.56
3.71	41.15	10.23	21.26	14.14	13.45	16.28	9.53
4.40	40.07	10.83	20.62	14.42	13.22	16.35	9.48
4.30	39.17	10.70	20.36	14.31	13.12	16.26	9.43
4.58	38.75	11.17	19.87	14.66	12.83	16.46	9.29
4.48	37.88	11.10	19.76	14.57	12.75	16.36	9.23
4.97	37.16	11.17	19.69	14.69	12.65	16.52	9.13
4.85	36.29	11.05	19.48	14.60	12.58	16.44	9.09
5.71	35.05	11.54	18.98	14.84	12.38	16.60	8.98
5.60	34.34	11.49	18.90	14.74	12.30	16.52	8.93
6.10	33.63	11.70	18.68	14.96	12.12	16.72	8.80
5.98	32.97	11.58	18.48	14.85	12.03	16.62	8.75
6.24	32.61	11.94	18.13	15.13	11.81	16.76	8.66
6.15	32.11	11.85	17.99	15.03	11.74	16.67	8.62
6.71	31.36	12.10	17.74	15.25	11.56	16.90	8.47
6.58	30.78	12.07	17.70	15.18	11.51	16.82	8.43
7.22	29.94	12.21	17.56	15.35	11.37	16.94	8.35
7.10	29.45	12.10	17.41	15.25	11.29	16.86	8.31
7.46	28.99	12.52	17.00	15.48	11.12	17.04	8.19
7.34	28.52	12.40	16.84	15.40	11.06	16.96	8.15
7.75	28.01	12.76	16.49	15.52	10.96	17.10	8.06
7.61	27.51	12.62	16.31	15.51	10.96	17.02	8.02
8.37	26.58	13.02	15.94	15.57	10.91	17.18	7.93
8.23	26.16	12.90	15.80	15.47	10.84	17.11	7.90
8.83	25.45	13.26	15.47	15.69	10.68	17.27	7.80
8.71	25.11	13.15	15.34	15.60	10.61	17.20	7.77
9.26	24.47	13.51	15.01	15.87	10.42	17.32	7.70
9.14	24.16	13.41	14.90	15.76	10.35	17.24	7.66
9.49	23.75	13.61	14.72	16.00	10.18	17.39	7.57
9.37	23.45	13.48	14.58	15.90	10.12	17.33	7.54
9.88	22.88	13.85	14.25	16.08	9.99	17.46	7.47
9.76	22.60	13.76	14.15	15.98	9.92		

Table E14. Weight fraction data experimentally obtained for the ternary system composed of $[N_{4444}]$[L-Phe] + K_2HPO_4 + water at 25 (± 1) °C.

$100w_{Salt}$	$100w_{CIL}$	$100w_{Salt}$	$100w_{CIL}$	$100w_{Salt}$	$100w_{CIL}$	$100w_{Salt}$	$100w_{CIL}$
3.48	42.17	10.30	22.65	16.51	12.59	19.81	7.96
3.32	40.22	10.18	22.38	16.40	12.51	19.73	7.92
3.93	39.33	10.93	21.57	16.90	12.07	20.01	7.72
3.83	38.40	10.83	21.37	16.79	11.99	19.93	7.69
4.71	37.16	11.36	20.80	17.04	11.78	20.20	7.49
4.52	35.63	11.24	20.56	16.93	11.71	20.13	7.46
5.45	34.37	11.79	19.98	17.28	11.42	20.40	7.27
5.35	33.74	11.66	19.76	17.16	11.34	20.32	7.24
5.76	33.21	12.43	18.97	17.50	11.06	20.54	7.09
5.65	32.57	12.32	18.79	17.40	10.99	20.45	7.06
6.14	31.93	12.84	18.26	17.88	10.60	20.73	6.87
6.03	31.32	12.71	18.07	17.78	10.54	20.64	6.85
6.49	30.74	13.32	17.46	18.09	10.28	21.06	6.57
6.42	30.41	13.20	17.30	17.99	10.22	20.92	6.53
7.21	29.42	13.82	16.70	18.35	9.93	21.22	6.33
7.08	28.89	13.69	16.54	18.25	9.88	21.10	6.29
7.49	28.39	14.33	15.91	18.50	9.68	21.55	6.00
7.37	27.92	14.19	15.76	18.41	9.63	21.41	5.96
8.00	27.16	14.74	15.24	18.76	9.36	21.70	5.78
7.95	26.99	14.62	15.12	18.65	9.31	21.56	5.74
8.55	26.29	15.12	14.66	19.00	9.04	21.96	5.49
8.45	25.99	14.98	14.52	18.89	8.99	21.83	5.46
8.69	25.71	15.54	14.01	19.21	8.74	22.26	5.20
8.57	25.36	15.43	13.90	19.11	8.70	22.11	5.17
9.31	24.52	15.95	13.44	19.50	8.41	22.46	4.96
9.21	24.24	15.84	13.34	19.39	8.37	22.32	4.93
9.76	23.62	16.25	12.98	19.66	8.17		
9.65	23.36	16.15	12.90	19.56	8.13		

Table E15. Weight fraction data experimentally obtained for the ternary system composed of $[N_{4444}][D\text{-Phe}] + K_2HPO_4$ + water at 25 (± 1) °C.

$100w_{Salt}$	$100w_{CIL}$	$100w_{Salt}$	$100w_{CIL}$	$100w_{Salt}$	$100w_{CIL}$	$100w_{Salt}$	$100w_{CIL}$
2.80	44.41	10.55	22.23	17.32	11.44	20.33	7.35
2.72	43.16	10.41	21.93	17.25	11.40	20.25	7.32
3.62	41.75	11.34	20.91	17.55	11.14	20.51	7.13
3.43	39.55	11.29	20.82	17.42	11.05	20.42	7.09
4.18	38.45	11.56	20.52	17.91	10.64	20.68	6.91
4.08	37.51	11.41	20.26	17.78	10.56	20.59	6.88
4.67	36.66	12.17	19.45	18.23	10.18	20.87	6.67
4.55	35.73	12.03	19.23	18.12	10.12	20.78	6.64
5.21	34.83	12.75	18.48	18.47	9.83	21.08	6.43
5.10	34.14	12.60	18.26	18.35	9.77	20.99	6.41
5.68	33.35	13.41	17.42	18.73	9.46	21.22	6.24
5.57	32.69	13.26	17.22	18.61	9.40	21.13	6.22
6.41	31.58	14.02	16.45	18.98	9.10	21.60	5.90
6.28	30.96	13.86	16.26	18.91	9.07	21.44	5.86
6.78	30.31	14.59	15.54	19.12	8.91	21.87	5.58
6.65	29.74	14.43	15.38	19.01	8.86	21.78	5.55
7.62	28.52	15.28	14.55	19.35	8.60	22.02	5.40
7.50	28.06	15.13	14.40	19.21	8.54	21.93	5.38
7.93	27.53	15.73	13.83	19.67	8.19	22.19	5.21
7.80	27.06	15.59	13.71	19.58	8.16	22.08	5.19
8.58	26.13	16.14	13.19	19.82	7.97	22.51	4.91
8.45	25.73	15.99	13.07	19.72	7.93	22.37	4.88
9.15	24.90	16.65	12.47	20.07	7.67	23.27	4.33
9.00	24.50	16.52	12.37	19.99	7.64	22.98	4.28
10.05	23.29	16.98	11.96	20.21	7.48	23.54	3.95
9.90	22.96	16.84	11.87	20.18	7.46	23.34	3.92

Table E16. Weight fraction data experimentally obtained for the ternary system composed of $[N_{4444}][L\text{-Phe}] + K_3PO_4$ + water at 25 (± 1) °C.

$100w_{Salt}$	$100w_{CIL}$	$100w_{Salt}$	$100w_{CIL}$	$100w_{Salt}$	$100w_{CIL}$	$100w_{Salt}$	$100w_{CIL}$
2.54	44.91	9.63	21.40	14.60	12.40	16.85	8.29
2.39	42.34	10.17	20.83	14.38	12.21	17.02	8.18
3.74	40.27	10.04	20.55	15.05	11.68	16.95	8.14
3.55	38.21	10.67	19.90	14.84	11.51	17.23	7.96
4.28	37.14	10.53	19.63	15.33	11.14	17.08	7.89
4.20	36.38	11.01	19.14	15.22	11.06	17.33	7.74
4.86	35.44	10.87	18.91	15.47	10.87	17.25	7.70
4.75	34.61	11.38	18.41	15.36	10.80	17.42	7.60
5.21	33.98	11.27	18.22	15.59	10.63	17.34	7.56
5.10	33.27	11.75	17.75	15.50	10.57	17.68	7.36
5.58	32.62	11.62	17.55	15.72	10.41	17.52	7.30
5.46	31.93	12.24	16.96	15.61	10.34	17.68	7.20
5.77	31.52	12.11	16.79	15.91	10.12	17.49	7.12
5.67	30.94	12.41	16.51	15.80	10.05	17.94	6.87
6.25	30.20	12.26	16.32	16.11	9.84	17.79	6.81
6.16	29.76	12.71	15.92	16.00	9.77	18.08	6.64
6.54	29.28	12.59	15.77	16.25	9.59	17.95	6.59
6.41	28.68	13.05	15.34	16.10	9.50	18.16	6.48
7.31	27.59	12.92	15.19	16.34	9.33	18.02	6.42
7.18	27.10	13.36	14.80	16.25	9.28	18.36	6.24
7.56	26.64	13.22	14.64	16.42	9.17	18.22	6.20
7.46	26.29	13.58	14.33	16.33	9.12	18.42	6.09
8.03	25.62	13.45	14.20	16.54	8.98	18.30	6.05
7.90	25.20	13.82	13.88	16.45	8.93	18.66	5.87
8.62	24.39	13.71	13.77	16.66	8.79	18.50	5.82
8.49	24.02	13.98	13.54	16.57	8.75	18.72	5.71
9.12	23.32	13.87	13.43	16.74	8.64	18.60	5.67
8.99	22.98	14.29	13.07	16.66	8.60	18.85	5.54
9.33	22.61	14.17	12.96	16.81	8.50	18.71	5.50
9.20	22.29	14.47	12.72	16.73	8.46	18.94	5.39
9.76	21.69	14.34	12.61	16.93	8.33	18.81	5.35

Table E17. Weight fraction data experimentally obtained for the ternary system composed of $[N_{4444}][D\text{-Phe}] + K_3PO_4$ + water at 25 (± 1) °C.

$100w_{Salt}$	$100w_{CIL}$	$100w_{Salt}$	$100w_{CIL}$	$100w_{Salt}$	$100w_{CIL}$	$100w_{Salt}$	$100w_{CIL}$
1.75	46.78	10.00	21.20	15.47	11.24	17.54	7.57
1.70	45.54	10.44	20.75	15.36	11.16	17.71	7.47
2.45	44.34	10.31	20.50	15.60	10.98	17.63	7.44
2.39	43.30	10.75	20.04	15.51	10.92	17.80	7.34
3.08	42.23	10.62	19.80	15.74	10.75	17.71	7.31
3.01	41.24	11.23	19.19	15.67	10.70	17.85	7.23
3.54	40.44	11.09	18.96	15.83	10.58	17.77	7.20
3.47	39.57	11.48	18.57	15.73	10.52	18.14	6.99
4.09	38.65	11.36	18.38	15.99	10.33	17.93	6.90
3.96	37.44	11.97	17.79	15.89	10.27	18.16	6.78
4.28	36.98	11.84	17.60	16.09	10.12	18.09	6.75
4.20	36.25	12.19	17.26	16.00	10.06	18.24	6.66
4.87	35.32	12.05	17.06	16.23	9.90	18.17	6.64
4.77	34.59	12.53	16.61	16.14	9.85	18.37	6.53
5.31	33.86	12.40	16.44	16.32	9.72	18.29	6.50
5.21	33.21	12.88	15.99	16.23	9.67	18.45	6.41
5.69	32.58	12.71	15.78	16.45	9.51	18.38	6.39
5.59	32.03	13.15	15.39	16.36	9.46	18.48	6.34
6.06	31.42	13.02	15.24	16.57	9.32	18.42	6.31
5.97	30.94	13.56	14.76	16.48	9.26	18.56	6.24
6.43	30.35	13.43	14.62	16.68	9.12	18.48	6.21
6.32	29.81	13.70	14.39	16.60	9.08	18.62	6.14
6.76	29.25	13.58	14.26	16.82	8.94	18.55	6.12
6.65	28.78	13.95	13.95	16.72	8.88	18.67	6.06
7.29	28.01	13.81	13.81	16.93	8.75	18.61	6.03
7.17	27.57	14.19	13.50	16.84	8.70	18.71	5.98
7.85	26.76	14.07	13.38	17.01	8.59	18.65	5.96
7.74	26.40	14.48	13.04	16.92	8.55	18.80	5.88
8.09	26.00	14.36	12.93	17.07	8.46	18.73	5.86
8.00	25.70	14.61	12.73	16.98	8.42	18.82	5.82
8.34	25.30	14.53	12.67	17.25	8.25	18.73	5.79
8.21	24.91	14.78	12.48	17.10	8.17	18.97	5.67
8.75	24.30	14.68	12.39	17.36	8.01	18.91	5.65
8.63	23.98	14.91	12.20	17.28	7.97	19.07	5.57
9.30	23.24	14.80	12.11	17.51	7.83	18.97	5.54
9.17	22.92	15.16	11.82	17.43	7.79	19.17	5.44
9.75	22.28	15.05	11.74	17.54	7.73	19.06	5.41
9.63	21.99	15.28	11.56	17.46	7.69	20.07	4.92
10.13	21.46	15.16	11.47	17.61	7.60	19.51	4.79

Table E18. Weight fraction data experimentally obtained for the ternary system composed of $[N_{4444}]$[L-Phe] + $K_3C_6H_5O_7$ + water at 25 (± 1) °C.

$100w_{Salt}$	$100w_{CIL}$	$100w_{Salt}$	$100w_{CIL}$	$100w_{Salt}$	$100w_{CIL}$
5.99	51.96	14.37	32.89	21.56	21.47
5.88	51.03	14.19	32.47	21.40	21.31
6.52	50.39	15.15	31.73	21.96	20.97
6.42	49.61	14.99	31.38	21.84	20.85
7.09	48.95	15.56	30.95	22.11	20.69
6.99	48.30	15.44	30.71	21.98	20.56
7.63	47.69	15.80	30.44	22.32	20.36
7.51	46.98	15.61	30.06	22.11	20.17
8.36	46.17	16.32	29.54	22.61	19.87
8.24	45.50	16.13	29.18	22.50	19.78
8.83	44.94	16.82	28.67	22.73	19.65
8.71	44.30	16.66	28.40	22.59	19.53
9.28	43.77	17.23	28.00	22.96	19.32
9.13	43.08	17.13	27.83	22.78	19.17
9.76	42.51	17.75	27.39	23.29	18.88
9.62	41.90	17.49	26.98	23.22	18.83
10.18	41.40	18.36	26.38	23.37	18.74
10.03	40.77	18.22	26.19	23.25	18.65
10.76	40.13	18.52	25.98	23.53	18.49
10.70	39.93	18.36	25.75	23.43	18.41
11.20	39.50	18.91	25.38	23.82	18.19
10.99	38.75	18.69	25.09	23.69	18.09
11.67	38.17	19.37	24.64	23.89	17.98
11.52	37.69	19.20	24.42	23.74	17.87
12.23	37.10	19.74	24.06	24.06	17.69
12.07	36.63	19.58	23.85	23.96	17.62
12.57	36.22	20.05	23.55	24.26	17.46
12.43	35.82	19.88	23.35	24.09	17.33
12.93	35.42	20.57	22.91	24.57	17.07
12.81	35.10	20.37	22.67	24.51	17.02
13.53	34.52	21.04	22.25	24.69	16.93
13.38	34.15	20.90	22.12	24.63	16.89
14.13	33.56	21.13	21.97	24.77	16.82
13.98	33.19	20.98	21.82	24.71	16.78

Table E19. Weight fraction data experimentally obtained for the ternary system composed of $[N_{4444}][D\text{-Phe}]$ + $K_3C_6H_5O_7$ + water at 25 (± 1) °C.

$100w_{Salt}$	$100w_{CIL}$	$100w_{Salt}$	$100w_{CIL}$	$100w_{Salt}$	$100w_{CIL}$
3.80	57.21	11.03	37.43	17.26	27.07
3.73	56.10	12.08	36.57	17.08	26.79
4.54	55.24	11.90	36.03	17.67	26.39
4.47	54.40	12.32	35.69	17.50	26.13
5.56	53.27	12.16	35.22	18.26	25.62
5.38	51.56	12.85	34.66	18.08	25.37
5.98	50.96	12.72	34.30	18.61	25.02
5.88	50.14	13.21	33.92	18.45	24.80
6.60	49.43	13.04	33.48	19.12	24.37
6.39	47.90	13.87	32.84	18.95	24.16
7.13	47.20	13.76	32.57	19.45	23.83
7.05	46.71	14.21	32.23	19.25	23.59
7.80	46.00	14.04	31.86	19.89	23.19
7.63	44.96	14.59	31.45	19.73	23.00
8.44	44.21	14.43	31.11	20.15	22.74
8.31	43.54	15.13	30.59	19.99	22.56
8.87	43.04	15.00	30.33	20.60	22.18
8.72	42.30	15.41	30.03	20.42	21.99
9.53	41.57	15.23	29.69	20.78	21.77
9.42	41.07	15.90	29.21	20.64	21.62
9.75	40.78	15.75	28.95	21.41	21.15
9.66	40.42	16.49	28.42	21.28	21.02
10.51	39.69	16.34	28.17	21.50	20.90
10.39	39.23	16.74	27.89	21.34	20.74
10.89	38.80	16.64	27.72	22.04	20.34
10.76	38.35	16.94	27.51	21.89	20.19
11.20	37.99	16.85	27.36		

Table E20. Weight fraction data experimentally obtained for the ternary system composed of $[N_{4444}][L\text{-Phe}]$ + $KNaC_4H_4O_6$ + water at 25 (± 1) °C.

$100w_{Salt}$	$100w_{CIL}$	$100w_{Salt}$	$100w_{CIL}$	$100w_{Salt}$	$100w_{CIL}$
10.32	36.79	17.68	22.96	23.72	14.43
10.10	36.00	17.42	22.62	23.55	14.32
10.63	35.35	18.96	21.07	24.52	13.47
10.43	34.69	18.73	20.81	24.36	13.38
12.18	32.63	20.13	19.43	24.95	12.87
11.94	31.97	19.92	19.22	24.63	12.71
12.69	31.11	21.11	18.09	25.46	12.02
12.45	30.54	20.88	17.89	25.30	11.95
14.21	28.60	22.13	16.72	25.97	11.39
13.97	28.13	22.01	16.63	25.88	11.35
15.11	26.90	22.43	16.24	26.34	10.99
14.89	26.50	22.22	16.08	26.18	10.92
16.42	24.89	23.18	15.21	26.72	10.49
16.17	24.51	22.99	15.08	26.58	10.43

Table E21. Weight fraction data experimentally obtained for the ternary system composed of $[N_{4444}][D\text{-Phe}]$ + $KNaC_4H_4O_6$ + water at 25 (± 1) °C.

$100w_{Salt}$	$100w_{CIL}$	$100w_{Salt}$	$100w_{CIL}$	$100w_{Salt}$	$100w_{CIL}$
10.07	37.38	19.99	19.59	26.22	11.41
9.71	36.02	19.80	19.41	26.09	11.36
11.14	34.31	21.05	18.20	26.61	10.94
10.93	33.67	20.77	17.97	26.45	10.87
12.67	31.65	22.41	16.43	26.90	10.51
12.45	31.10	22.24	16.30	26.78	10.46
13.59	29.80	23.09	15.52	27.35	10.01
13.47	29.53	22.97	15.45	27.22	9.96
14.46	28.42	23.60	14.88	27.71	9.58
14.25	28.00	23.41	14.76	27.50	9.51
15.18	26.97	24.20	14.06	28.15	9.01
14.99	26.63	24.02	13.95	28.02	8.97
16.23	25.31	24.84	13.22	28.42	8.67
15.98	24.92	24.67	13.13	28.35	8.65
17.58	23.26	25.33	12.57	28.67	8.41
17.22	22.79	25.17	12.49	28.55	8.38
19.17	20.83	25.82	11.94	28.99	8.05
18.96	20.60	25.67	11.87	28.86	8.02

Table E22. Merchuk equation parameters (*A*, *B* and *C*) with the respective standard deviations (σ) for the ternary systems composed of CILs + salt + water at 25 (± 1) °C.

ABS	$A \pm \sigma$	$B \pm \sigma$	$(C \pm \sigma) \times 10^5$
$[N_{4444}]_2$[L-Glu] + Na_2SO_4	93.15 ± 6.50	-0.46 ± 0.03	5.62 ± 1.75
$[N_{4444}]$[L-Phe] + Na_2SO_4	92.30 ± 4.30	-0.45 ± 0.02	10.64 ± 1.8
$[N_{4444}]$[D-Phe] + Na_2SO_4	91.78 ± 2.34	-0.45 ± 0.01	11.85 ± 1.10
$[N_{4444}]$[L-Ala] + Na_2SO_4	85.39 ± 3.56	-0.44 ± 0.02	5.39 ± 2.05
$[N_{4444}]$[L-Val] + Na_2SO_4	80.51 ± 2.93	-0.42 ± 0.02	7.85 ± 2.06
$[N_{4444}]$[L-Pro] + Na_2SO_4	85.00 ± 3.88	-0.45 ± 0.02	6.12 ± 2.00
$[N_{4444}]_2$[L-Glu] + K_2CO_3	90.36 ± 2.15	-0.39 ± 0.01	9.39 ± 0.72
$[N_{4444}]_2$[L-Glu] + $K_3C_6H_5O_7$	108.89 ± 5.03	-0.27 ± 0.01	1.31 ± 0.12
$[N_{4444}]_2$[L-Glu] + $KNaC_4H_4O_6$	124.88 ± 26.64	-0.36 ± 0.08	2.03 ± 2.69
$[N_{4444}]$[L-Phe] + Na_2CO_3	89.51 ± 2.30	-0.49 ± 0.01	17.16 ± 1.80
$[N_{4444}]$[D-Phe] + Na_2CO_3	84.46 ± 2.71	-0.47 ± 0.02	20.97 ± 1.62
$[N_{4444}]$[L-Phe] + K_2CO_3	84.34 ± 2.79	-0.37 ± 0.01	17.11 ± 0.74
$[N_{4444}]$[D-Phe] + K_2CO_3	89.98 ± 2.23	-0.39 ± 0.01	15.26 ± 0.55
$[N_{4444}]$[L-Phe] + K_2HPO_4	80.00 ± 2.00	-0.36 ± 0.01	8.79 ± 0.36
$[N_{4444}]$[D-Phe] + K_2HPO_4	79.38 ± 1.84	-0.36 ± 0.01	9.01 ± 0.36
$[N_{4444}]$[L-Phe] + K_3PO_4	78.09 ± 2.18	-0.37 ± 0.01	15.20 ± 0.62
$[N_{4444}]$[D-Phe] + K_3PO_4	74.41 ± 1.23	-0.34 ± 0.01	15.68 ± 0.42
$[N_{4444}]$[L-Phe] + $K_3C_6H_5O_7$	104.51 ± 2.46	-0.28 ± 0.01	2.74 ± 0.15
$[N_{4444}]$[D-Phe] + $K_3C_6H_5O_7$	99.01 ± 2.47	-0.28 ± 0.01	2.90 ± 0.28
$[N_{4444}]$[L-Phe] + $KNaC_4H_4O_6$	98.51 ± 10.85	-0.31 ± 0.03	3.39 ± 0.42
$[N_{4444}]$[D-Phe] + $KNaC_4H_4O_6$	90.80 ± 7.80	-0.28 ± 0.03	3.65 ± 0.28

Table E23. Weight fraction composition (wt%) and pH of both CIL-rich and salt-rich phases of biphasic ternary systems composed of CILs and salts at 25 (± 1) °C, along with the respective values of tie-line length (TLL).

ABS	100 × weight fraction composition / (wt%)								
	pH_{CIL}	$[Salt]_{CIL}$ / (wt%)	$[CIL]_{CIL}$ / (wt%)	$[Salt]_{M}$ / (wt%)	$[CIL]_{M}$ / (wt%)	$[Salt]_{Salt}$ / (wt%)	$[CIL]_{Salt}$ / (wt%)	pH_{Salt}	TLL
$[N_{4444}]_2$[L-Glu] + Na_2SO_4	10.99	5.75	30.85	10.02	25.00	25.68	3.56	10.58	33.80
	11.10	3.50	39.56	9.99	29.98	28.91	2.06	10.78	45.30
$[N_{4444}]$[L-Phe] + Na_2SO_4	10.47	4.37	35.36	10.14	24.96	22.01	3.52	9.91	36.40
	10.42	2.91	42.39	9.98	29.97	26.31	1.29	9.96	47.29
$[N_{4444}]$[D-Phe] + Na_2SO_4	10.43	4.68	34.26	9.99	24.96	22.71	2.68	9.93	36.36
	10.42	2.90	42.52	9.98	30.10	26.59	0.97	9.85	47.83
$[N_{4444}]$[L-Ala] + Na_2SO_4	11.41	4.72	32.70	10.03	24.98	23.90	4.78	10.92	33.88
	11.20	3.20	38.86	9.98	30.05	32.23	1.16	10.78	47.58
$[N_{4444}]$[L-Val] + Na_2SO_4	10.95	4.47	32.60	10.00	24.97	26.59	2.06	10.45	37.71
	10.85	2.55	40.84	9.98	30.09	30.14	0.91	9.95	48.53
$[N_{4444}]$[L-Pro] + Na_2SO_4	11.53	4.51	32.68	9.97	24.97	25.24	3.36	11.12	35.91
	11.52	2.55	41.55	9.96	29.97	27.72	2.19	11.08	46.72
$[N_{4444}]_2$[L-Glu] + K_2CO_3		2.84	46.95	15.01	24.99	28.05	1.47		52.00
		6.62	32.43	9.96	26.94	24.14	3.60		33.73
$[N_{4444}]_2$[L-Glu] + $K_3C_6H_5O_7$		6.26	55.73	21.18	39.96	57.92	1.13		75.17
		9.37	47.65	16.40	39.98	50.14	3.18		60.33
$[N_{4444}]_2$[L-Glu] + $KNaC_4H_4O_6$		5.20	54.68	24.13	35.02	57.70	0.16		75.69
		4.95	55.78	20.77	39.90	60.41	0.09		78.60
$[N_{4444}]$[L-Phe] + Na_2CO_3	12.14	1.46	49.42	10.00	24.98	16.91	5.20	11.64	46.84

	12.01	3.45	35.76	10.00	20.00	15.41	6.96	11.59	31.18
$[N_{4444}][D\text{-Phe}] + Na_2CO_3$	12.02	1.06	52.32	10.00	24.99	16.56	4.91	11.51	49.88
	11.97	3.00	37.54	10.06	20.03	15.79	5.83	11.55	34.19
$[N_{4444}][L\text{-Phe}] + K_2CO_3$	12.42	5.85	33.61	10.01	24.98	20.08	4.09	12.09	32.77
	12.36	3.25	43.33	10.00	30.01	24.70	1.04	12.05	47.42
$[N_{4444}][D\text{-Phe}] + K_2CO_3$	12.34	6.34	32.21	9.99	24.92	20.36	4.22	12.11	31.30
	12.38	3.20	44.37	10.03	30.01	23.40	1.91	12.10	47.02
$[N_{4444}][L\text{-Phe}] + K_2HPO_4$	10.44	6.87	29.89	10.10	24.95	23.64	4.25	11.10	30.63
	10.51	3.67	39.61	10.01	30.05	29.12	1.28	11.11	46.01
$[N_{4444}][D\text{-Phe}] + K_2HPO_4$	10.42	7.01	29.64	10.01	25.02	23.49	4.31	10.77	30.22
	10.43	3.74	39.33	9.99	30.01	29.28	1.18	10.9	45.91
$[N_{4444}][L\text{-Phe}] + K_3PO_4$	12.53	5.87	31.24	9.99	25.09	26.27	0.76	12.72	36.68
	12.41	2.88	41.84	10.05	29.95	27.86	0.42	12.74	48.37
$[N_{4444}][D\text{-Phe}] + K_3PO_4$	12.48	5.60	32.36	10.02	24.97	24.01	1.60	13.05	35.85
	12.40	2.71	42.36	10.21	29.97	28.11	0.38	12.84	49.08
$[N_{4444}][L\text{-Phe}] + K_3C_6H_5O_7$	10.67	14.04	33.36	19.87	24.82	28.71	11.89	10.44	26.01
	10.66	7.18	48.26	19.97	30.04	38.38	3.81	10.32	54.31
$[N_{4444}][D\text{-Phe}] + K_3C_6H_5O_7$	10.62	12.34	35.43	20.02	24.94	33.17	6.97	10.55	35.27
	10.61	6.74	47.81	19.92	29.95	40.04	2.67	10.42	56.09
$[N_{4444}][L\text{-Phe}] + KNaC_4H_4O_6$	10.63	8.91	38.70	19.73	24.54	36.02	3.23	10.30	44.65
	10.52	5.48	47.97	19.85	29.83	42.73	0.95	10.18	59.99
$[N_{4444}][D\text{-Phe}] + KNaC_4H_4O_6$	10.48	15.12	26.96	18.14	22.68	26.26	11.17	10.29	19.32
	10.58	5.25	47.55	19.77	29.74	43.41	0.73	10.17	60.41

Table E24. Weight fraction data experimentally obtained for the ternary system composed of [Ch][D-Phe] + PPG400 + water at 25 (± 1) °C.

$100w_{CIL}$	$100w_{PPG}$	$100w_{CIL}$	$100w_{PPG}$	$100w_{CIL}$	$100w_{PPG}$
6.33	81.48	23.03	52.42	32.60	36.35
6.26	80.59	22.78	51.86	32.34	36.06
8.53	77.72	24.72	49.73	33.91	34.55
8.44	76.96	24.50	49.28	33.68	34.32
10.42	74.48	25.78	47.89	34.47	33.57
10.32	73.79	25.56	47.48	34.26	33.36
12.03	71.67	26.81	46.13	34.92	32.74
11.85	70.56	26.55	45.68	34.74	32.56
13.72	68.28	27.96	44.19	35.54	31.81
13.58	67.58	27.75	43.85	35.32	31.61
15.47	65.32	29.06	42.48	36.13	30.88
15.29	64.57	28.87	42.21	35.91	30.68
17.58	61.86	29.73	41.33	36.83	29.85
17.36	61.12	29.49	41.00	36.60	29.67
19.08	59.12	30.41	40.07	37.50	28.87
18.90	58.57	30.19	39.77	37.26	28.69
20.64	56.57	31.33	38.63	38.08	27.97
20.45	56.06	31.11	38.37	37.88	27.82
21.56	54.80	31.82	37.66		
21.36	54.28	31.57	37.36		

Table E25. Weight fraction data experimentally obtained for the ternary system composed of [Ch][L-Phe] + PPG400 + water at 25 (± 1) °C.

$100w_{CIL}$	$100w_{PPG}$	$100w_{CIL}$	$100w_{PPG}$	$100w_{CIL}$	$100w_{PPG}$
6.31	82.74	19.45	55.52	27.00	41.53
6.23	81.65	20.54	54.32	26.79	41.21
7.99	79.39	20.32	53.74	28.28	39.80
7.86	78.06	21.38	52.59	27.86	39.21
11.55	73.42	21.11	51.92	28.87	38.27
11.40	72.48	22.01	50.97	28.65	37.98
12.95	70.56	21.79	50.44	29.58	37.13
12.78	69.65	23.02	49.15	29.14	36.57
15.45	66.40	22.80	48.68	30.76	35.12
15.05	64.70	23.61	47.84	30.33	34.63
15.77	63.85	23.38	47.39	31.91	33.24
15.48	62.67	24.40	46.35	31.71	33.03
17.52	60.33	24.20	45.97	32.73	32.14
17.31	59.60	25.13	45.03	32.36	31.77
18.57	58.18	24.92	44.66	34.38	30.06
18.36	57.50	25.99	43.60	34.03	29.75
19.64	56.08	25.58	42.91		

Table E26. Weight fraction data experimentally obtained for the ternary system composed of $[Ch]_2$[L-Glu] + PPG400 + water at 25 (± 1) °C.

$100w_{CIL}$	$100w_{PPG}$	$100w_{CIL}$	$100w_{PPG}$	$100w_{CIL}$	$100w_{PPG}$	$100w_{CIL}$	$100w_{PPG}$
1.06	88.12	6.82	35.54	10.14	24.59	12.72	18.98
0.82	68.11	7.07	35.40	10.01	24.27	13.22	18.82
1.71	67.23	6.94	34.73	10.36	24.13	12.99	18.49
1.59	62.17	7.38	34.49	10.21	23.79	13.46	18.33
2.40	61.43	7.19	33.61	10.54	23.66	13.26	18.05
2.29	58.48	7.65	33.37	10.47	23.50	13.74	17.90
3.15	57.73	7.49	32.68	10.80	23.38	13.55	17.65
2.96	54.08	7.92	32.46	10.65	23.05	14.03	17.50
3.61	53.55	7.79	31.95	10.94	22.94	13.83	17.25
3.48	51.69	8.18	31.76	10.86	22.77	14.24	17.13
4.11	51.21	8.04	31.20	11.19	22.65	14.03	16.88
3.95	49.23	8.29	31.07	11.04	22.36	14.54	16.72
4.41	48.89	8.19	30.68	11.28	22.27	14.34	16.49
4.30	47.67	8.48	30.53	11.21	22.13	14.71	16.38
4.99	47.16	8.32	29.96	11.50	22.02	14.51	16.16
4.79	45.25	8.70	29.77	11.38	21.79	14.95	16.03
5.40	44.83	8.55	29.25	11.62	21.70	14.75	15.82
5.21	43.24	8.95	29.06	11.47	21.43	15.14	15.70
5.61	42.97	8.79	28.55	11.97	21.25	15.01	15.57
5.49	42.06	9.14	28.39	11.77	20.90	15.45	15.45
6.00	41.73	8.77	27.23	12.06	20.79	15.25	15.24
5.82	40.43	9.18	27.04	11.91	20.54	15.60	15.15
6.04	40.29	8.95	26.36	12.38	20.37	15.39	14.94
5.97	39.84	9.35	26.19	12.19	20.07	15.78	14.84
6.46	39.53	9.22	25.82	12.45	19.98	15.58	14.65
6.26	38.27	9.58	25.67	12.34	19.80	16.01	14.54
6.74	37.98	9.43	25.29	12.61	19.71	15.81	14.36
6.53	36.81	9.74	25.16	12.46	19.47	16.19	14.26
7.01	36.53	9.60	24.81	12.94	19.31	16.05	14.14

Table E27. Weight fraction data experimentally obtained for the ternary system composed of $[Ch]_2$[L-Glu] + PL35 + water at 25 (± 1) °C.

$100w_{CIL}$	$100w_{PL35}$	$100w_{CIL}$	$100w_{PL35}$	$100w_{CIL}$	$100w_{PL35}$
5.77	64.33	10.07	45.58	13.90	36.53
5.39	60.10	10.75	45.05	13.79	36.23
6.71	58.88	10.56	44.25	14.27	35.92
6.48	56.86	11.52	43.54	14.16	35.63
7.24	56.18	11.30	42.73	14.58	35.36
7.15	55.49	11.89	42.30	14.34	34.78
7.68	55.02	11.67	41.52	14.77	34.51
7.48	53.62	12.16	41.17	14.67	34.29
8.16	53.04	11.96	40.50	15.09	34.03
8.07	52.47	12.52	40.11	14.88	33.56
8.83	51.83	12.43	39.82	15.36	33.26
8.64	50.73	12.95	39.47	15.14	32.80
9.43	50.07	12.74	38.84	15.70	32.47
9.15	48.56	13.36	38.42	15.49	32.03
9.81	48.04	13.15	37.82	15.96	31.76
9.60	47.04	13.63	37.50	15.74	31.31
10.27	46.52	13.39	36.86		

Table E28. Weight fraction data experimentally obtained for the ternary system composed of $[Ch]_2$[L-Glu] + PEG1000 + water at 25 (± 1) °C.

$100w_{CIL}$	$100w_{PEG}$	$100w_{CIL}$	$100w_{PEG}$	$100w_{CIL}$	$100w_{PEG}$
2.72	76.66	16.30	46.87	29.49	28.47
2.56	72.30	16.15	46.43	29.31	28.30
3.63	71.16	17.27	45.46	30.23	27.66
3.56	69.79	17.09	45.00	30.08	27.51
4.52	68.77	18.35	43.93	30.39	27.29
4.45	67.58	18.17	43.52	30.20	27.12
5.45	66.54	19.32	42.56	30.81	26.71
5.36	65.51	19.13	42.15	30.64	26.56
6.18	64.68	19.73	41.65	31.47	26.00
6.10	63.86	19.39	40.93	31.25	25.82
7.18	62.78	21.80	38.99	32.13	25.24
7.06	61.76	21.44	38.35	31.94	25.09
7.92	60.92	23.22	36.94	32.40	24.78
7.83	60.16	23.02	36.62	32.23	24.65
8.71	59.30	23.90	35.93	32.78	24.29
8.62	58.66	23.49	35.31	32.58	24.15
9.58	57.74	25.54	33.76	33.35	23.65
9.46	57.02	25.28	33.42	32.98	23.39
10.90	55.66	26.61	32.43	33.89	22.81
10.78	55.04	26.38	32.15	33.71	22.68
11.69	54.19	27.34	31.44	34.51	22.18
11.53	53.44	27.13	31.20	34.32	22.06
13.19	51.91	27.92	30.62	34.68	21.84
13.02	51.23	27.70	30.39	34.49	21.72
13.79	50.54	28.48	29.83	35.24	21.26
13.62	49.91	28.29	29.64	35.07	21.15
15.75	48.02	28.99	29.14		
15.58	47.50	28.80	28.96		

Table E29. Merchuk equation parameters (*A*, *B* and *C*) with the respective standard deviations (σ) for the ternary systems composed of CILs + polymers + water at 25 (± 1) °C.

ABS	$A \pm \sigma$	$B \pm \sigma$	$(C \pm \sigma) \times 10^5$
$[Ch]_2$[L-Glu] + PPG400	121.15 ± 5.99	-0.45 ± 0.02	10.09 ± 2.54
[Ch][L-Phe] + PPG400	124.30 ± 5.26	-0.16 ± 0.01	1.39 ± 0.13
[Ch][D-Phe] + PPG400	117.62 ± 2.30	-0.14 ± 0.01	1.04 ± 0.04
$[Ch]_2$[L-Glu] + PL35	100.66 ± 2.16	-0.21 ± 0.01	8.53 ± 0.86
$[Ch]_2$[L-Glu] + PEG1000	98.99 ± 1.34	-0.17 ± 0.01	1.19 ± 0.06

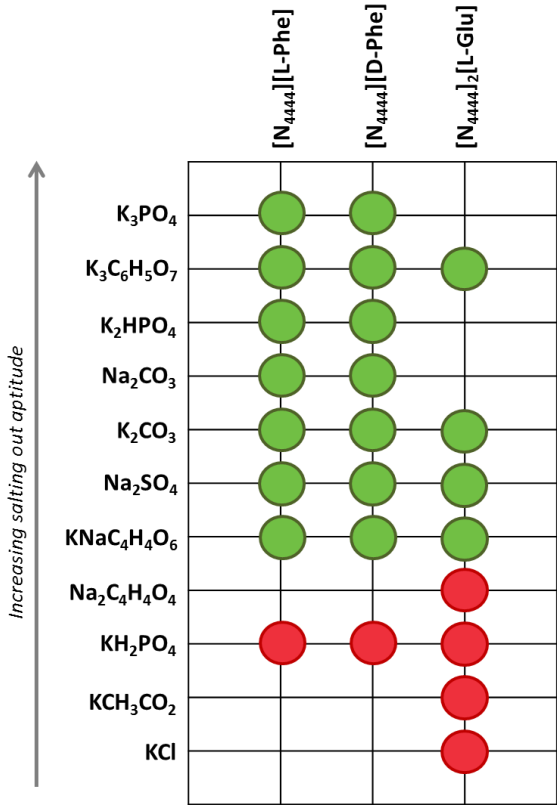

Figure E1. Indicative matrix of the salt/CILs combinations tested in the formation of ABS and main results obtained as a function of the salt salting-out ability: able to form ABS (green circles), not able to form ABS (red circles) and not tested (not assigned).

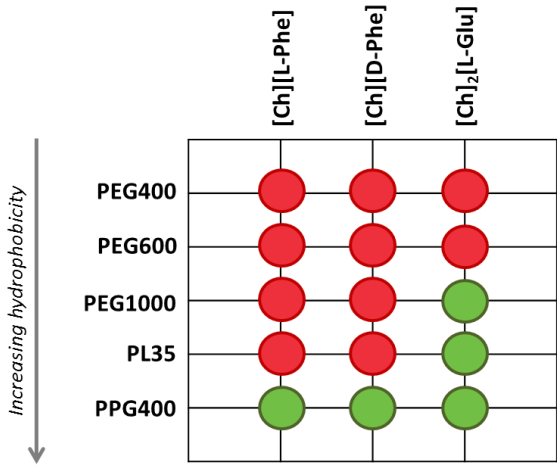

Figure E2. Indicative matrix of the polymers/CILs combinations tested in the formation of ABS and main results obtained as a function of the polymer hydrophobicity: able to form ABS (green circles) and not able to form ABS (red circles).

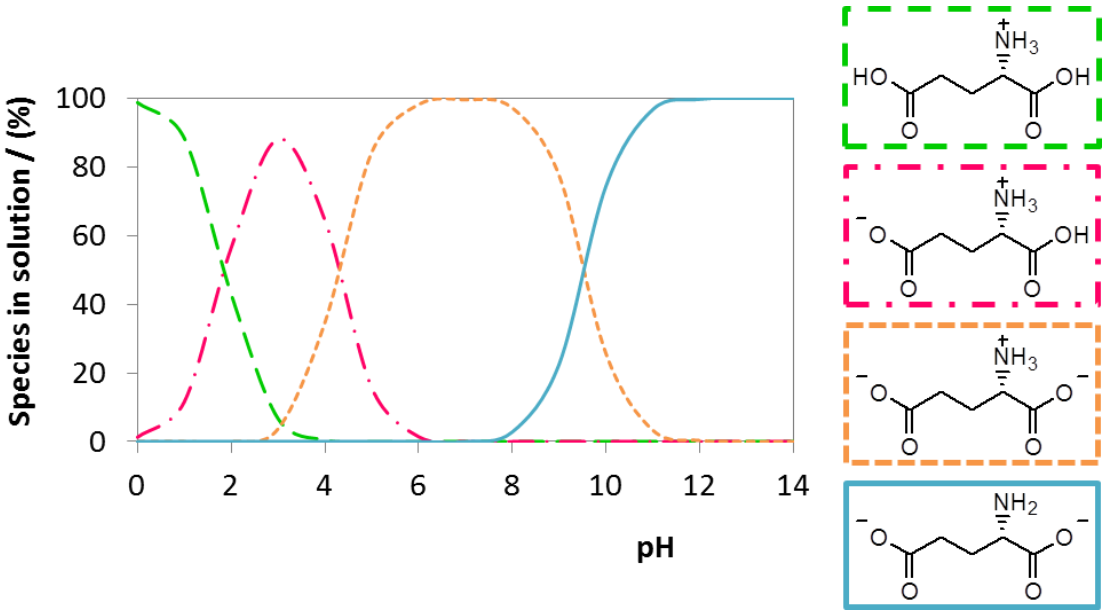

Figure E3. Ion speciation profile of L-glutamic acid as a function of pH [adapted from Chemspider - The free chemical database at http://www.chemspider.com (accessed June 22, 2018)].

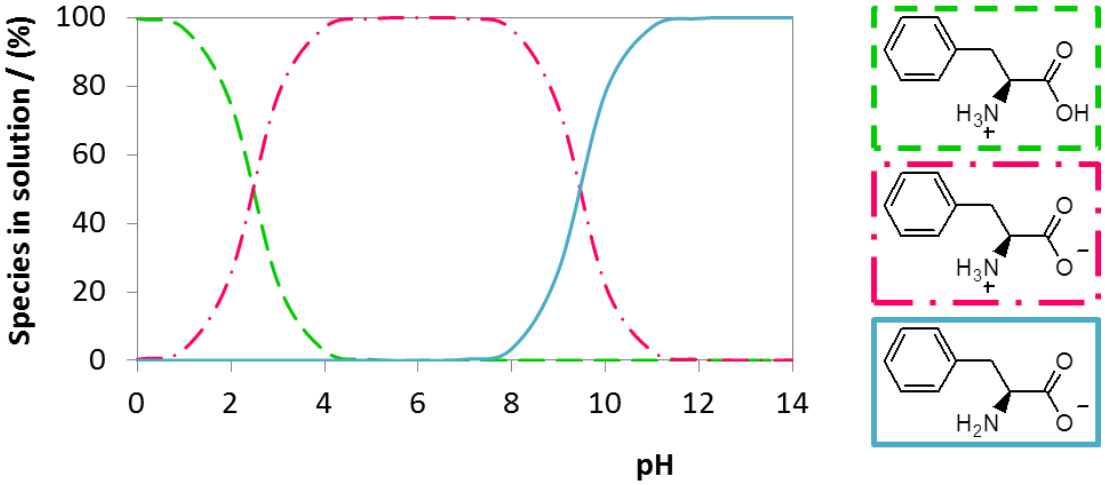

Figure E4. Ion speciation profile of L/D-phenylalanine as a function of pH [adapted from Chemspider - The free chemical database at http://www.chemspider.com (accessed June 22, 2018)].

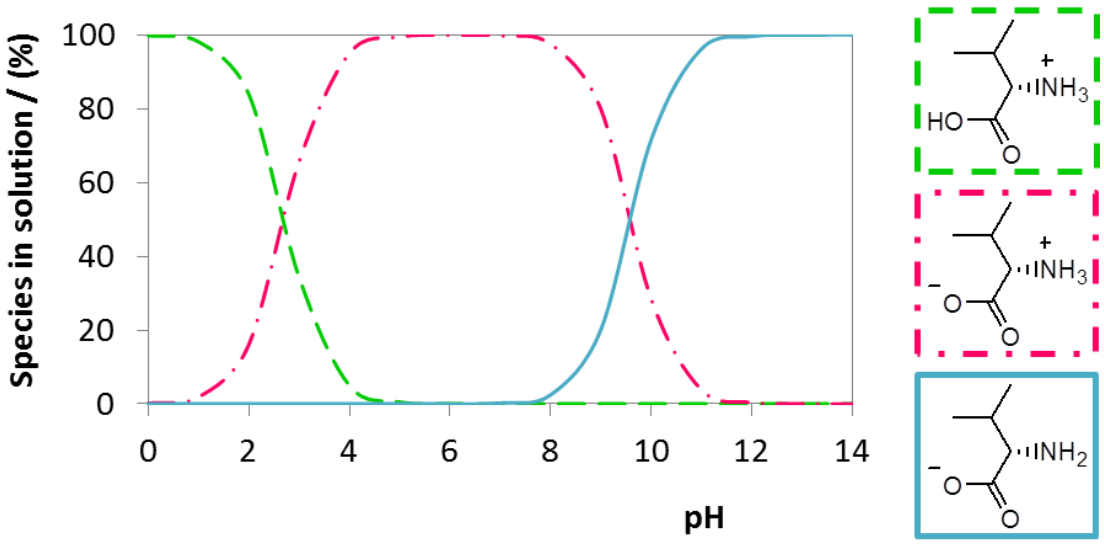

Figure E5. Ion speciation profile of L-valine as a function of pH [adapted from Chemspider - The free chemical database at http://www.chemspider.com (accessed June 22, 2018)].

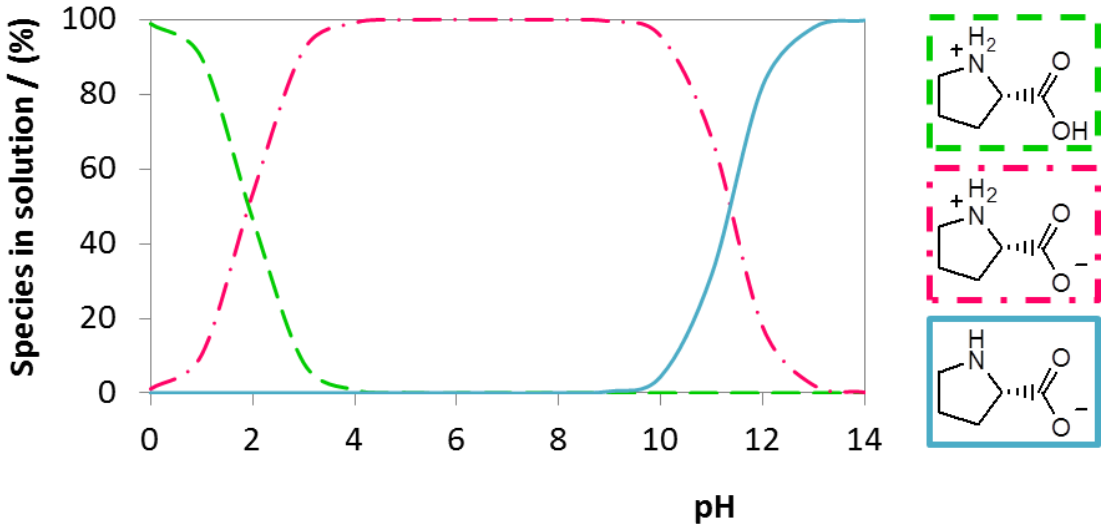

Figure E6. Ion speciation profile of L-proline as a function of pH [adapted from Chemspider - The free chemical database at http://www.chemspider.com (accessed June 22, 2018)].

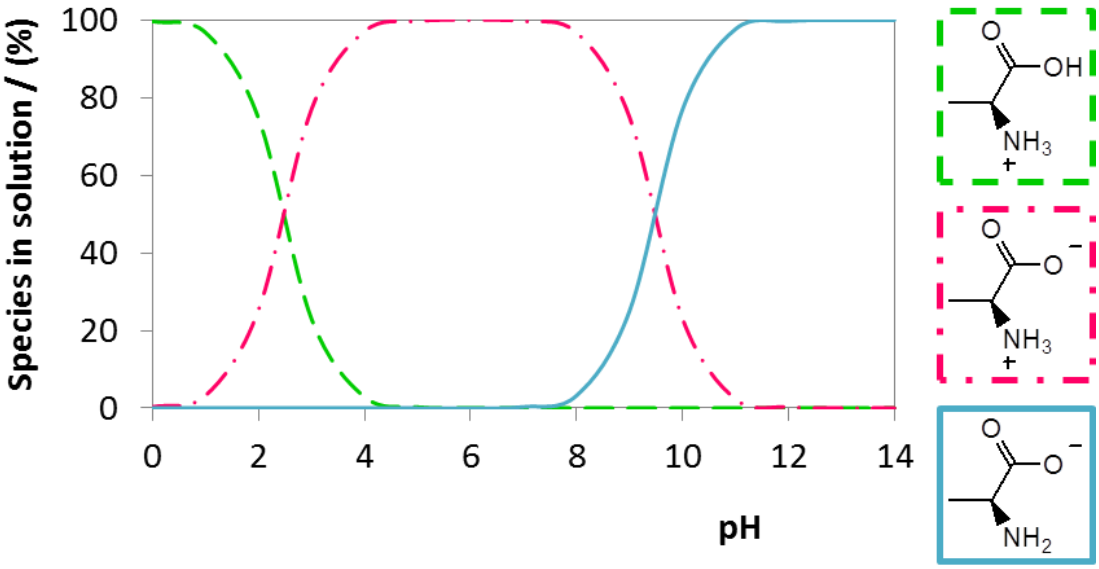

Figure E7. Ion speciation profile of L-alanine as a function of pH [adapted from Chemspider - The free chemical database at http://www.chemspider.com (accessed June 22, 2018)].

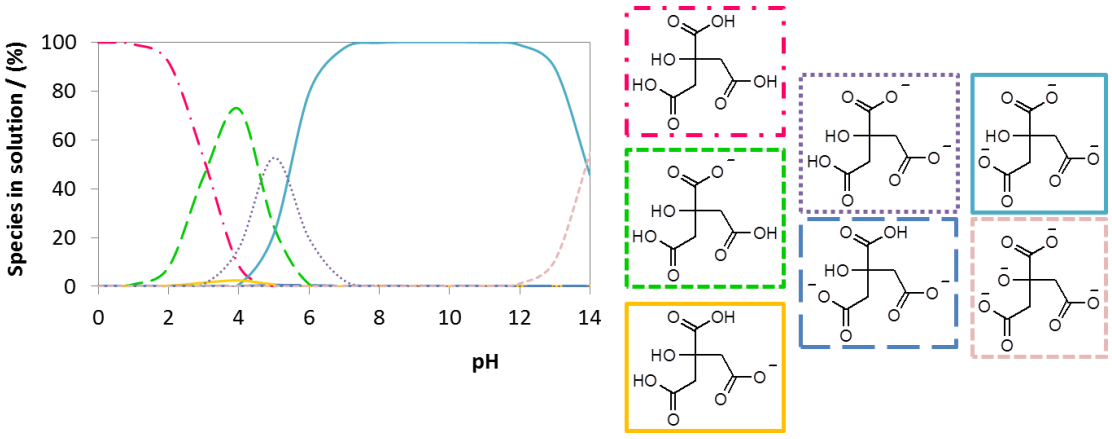

Figure E8. Ion speciation profile of citrate as a function of pH [adapted from Chemspider - The free chemical database at http://www.chemspider.com (accessed June 22, 2018)].

Appendix F

3.2.1. Does chirality play a role on deep eutectic solvents formation?

---

e Silva, F. A.; Kelley, S. P.; Silva, L. P.; Berton, P.; Ventura, S. P. M.; Coutinho, J. A. P.; Rogers, R. D. Does chirality play a role on deep eutectic solvents formation?. *in preparation*.

Table F1. Experimental solid-liquid equilibria data of proline:malic acid systems as a function of enantiomers combinations. (black, visual method; underlined, DSC; italic bold, eutectic point)

x_{MalA}	T_m / (°C)	x_{MalA}	T_m / (°C)	x_{MalA}	T_m / (°C)	x_{MalA}	T_m / (°C)
L-Pro:L-MalA		*L-Pro:D-MalA*		*D-Pro:D-MalA*		*D-Pro:L-MalA*	
0.00	220.3	0.00	220.3	0.00	220.3	0.00	220.3
0.10	187.8	0.10	187.9	0.10	184.5	0.10	192.5
0.21	153.3	0.21	161.4	0.21	159.0	0.21	170.8
0.30	128.8	0.30	138.6	0.31	134.3	0.31	136.5
0.32	93.2	0.33	79.7	0.33	79.2	0.33	84.7
0.40	97.0	0.41	107.1	0.40	115.4	0.40	112.7
0.49	80.9	0.50	80.7	0.50	84.0	0.51	81.4
0.52	68.5	0.50	88.4	0.52	86.3	0.52	78.1
0.59	***43.3***	***0.59***	***70.2***	***0.61***	***60.0***	***0.62***	***53.5***
0.67	83.8	0.67	87.9	0.67	72.7	0.66	91.6
0.71	62.4	0.68	83.0	0.68	74.3	0.68	63.7
0.76	88.2	0.75	84.6	0.74	83.8	0.74	91.2
0.79	83.6	0.78	89.2	0.79	79.7	0.79	78.2
0.80	88.7	0.80	88.6	0.80	85.6	0.79	87.3
0.89	88.6	0.90	88.5	0.88	93.0	0.88	96.7
0.90	93.8	0.90	94.2	0.90	92.2	0.90	89.1
1.00	106.0	1.00	103.0	1.00	103.0	1.00	106.0
1.00	100.8	1.00	103.7	1.00	103.7	1.00	100.8

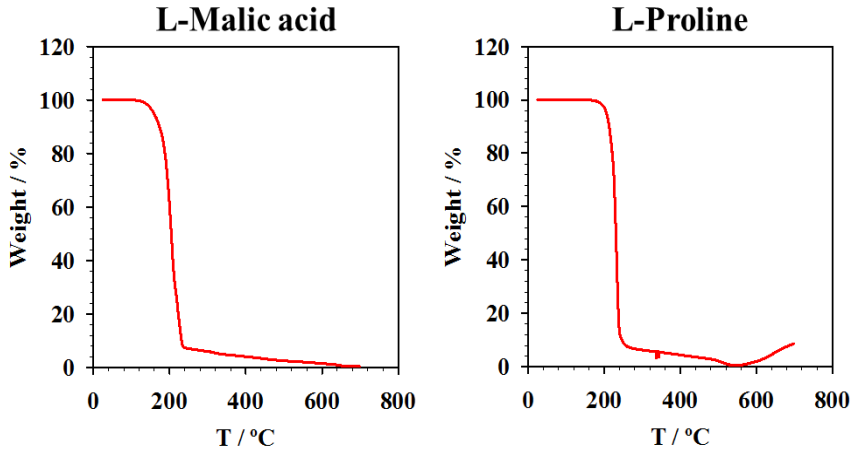

Figure F1. TGA thermograms of L-proline and L-malic acid pure compounds.

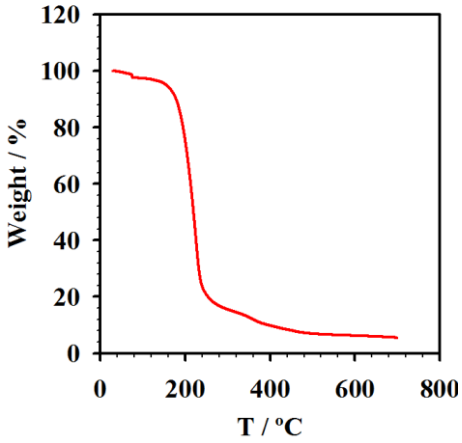

Figure F2. TGA thermograms of a representative mixture of L-proline:L-malic acid, x_{MalA} = 0.1.

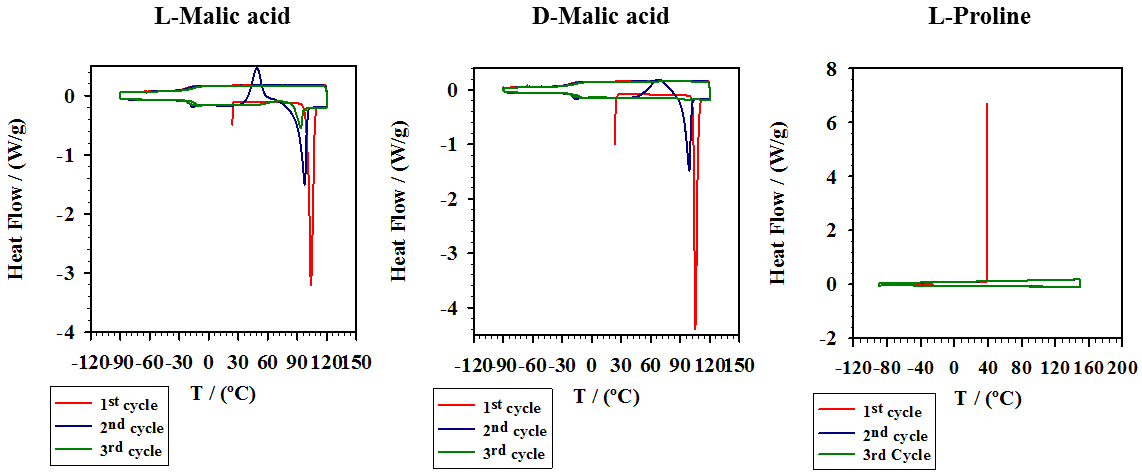

Figure F3. DSC thermograms of pure malic acid enantiomers and L-proline.

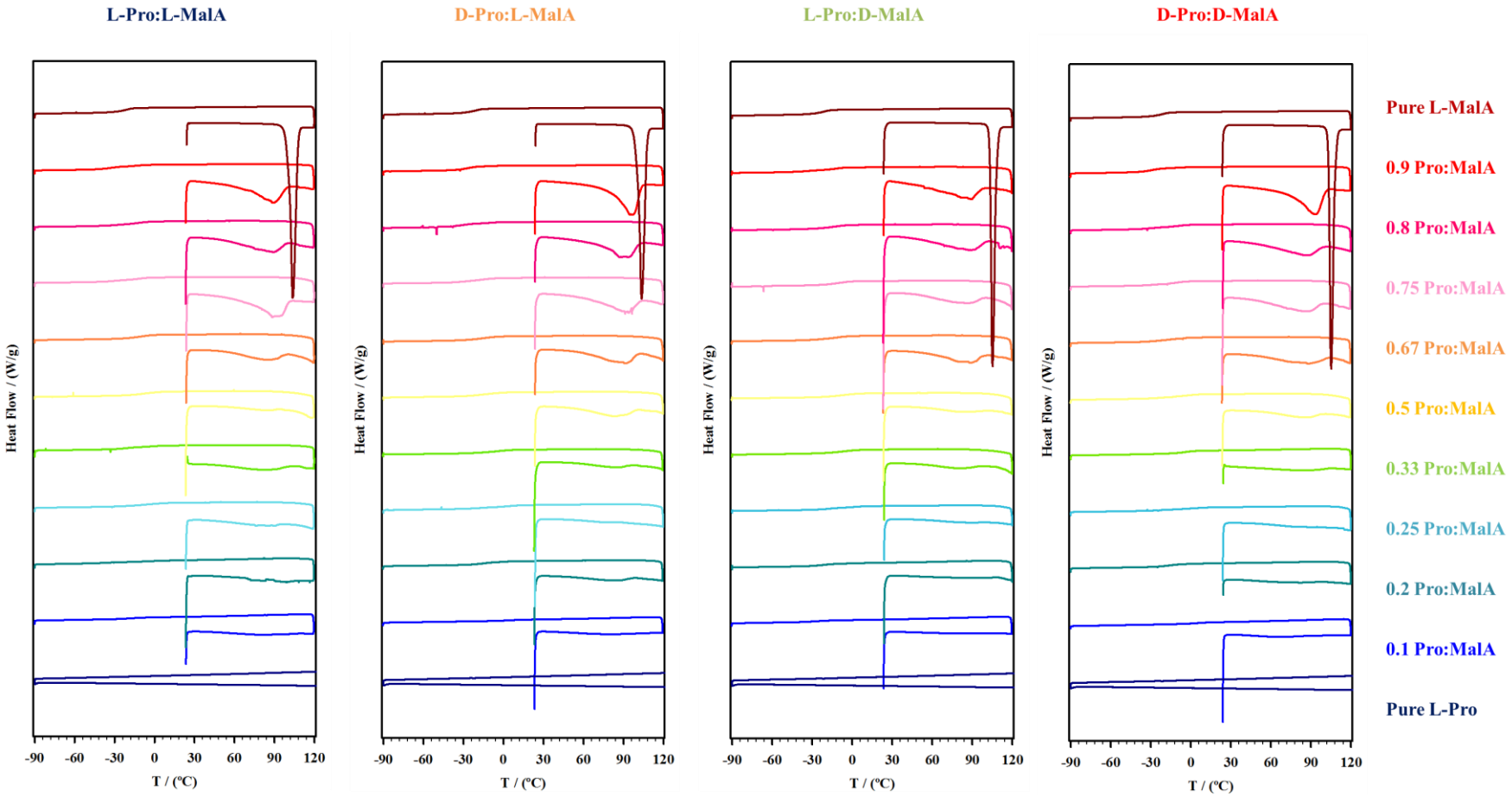

Figure F4. DSC thermograms of proline:malic acid binary mixtures covering the possible enantiomer combinations in the whole composition range (x_{MalA}) over the first cycle.

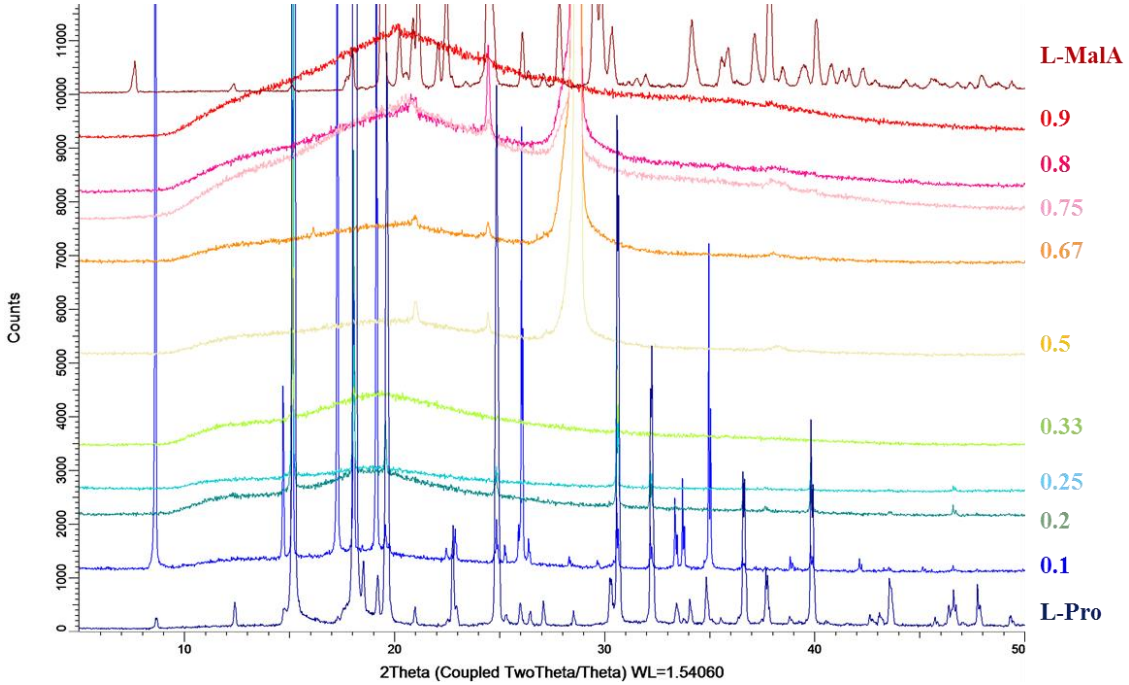

Figure F5. PXRD patterns of L-proline:L-malic acid binary mixtures and respective pure components.

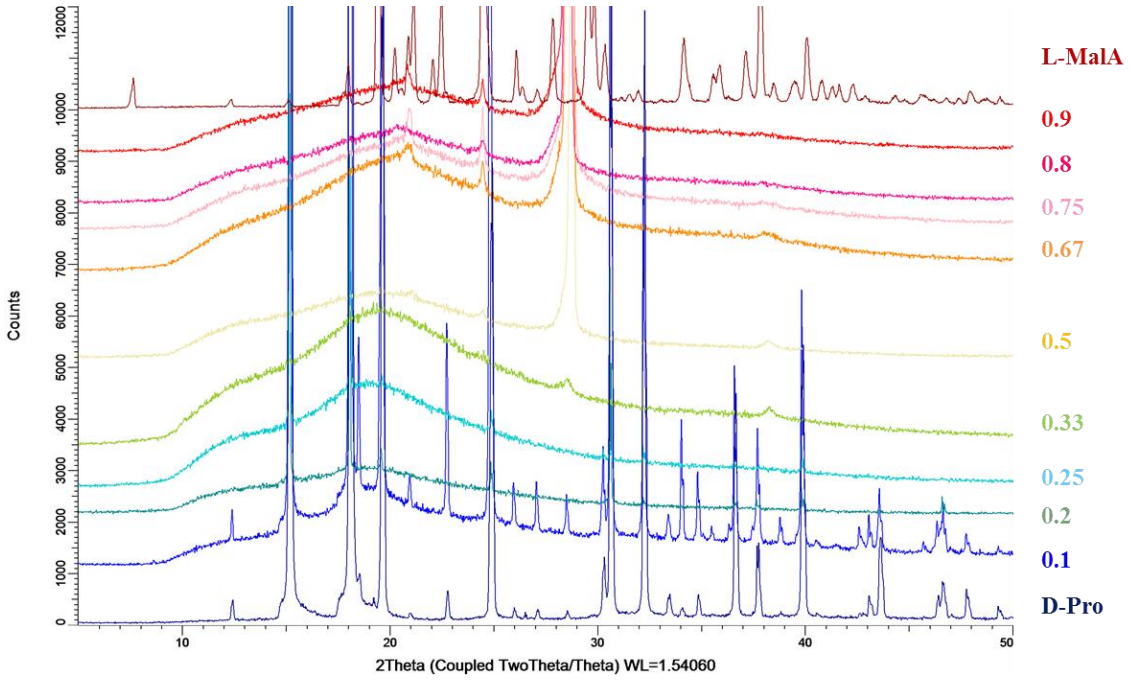

Figure F6. PXRD patterns of D-proline:L-malic acid binary mixtures and respective pure components.

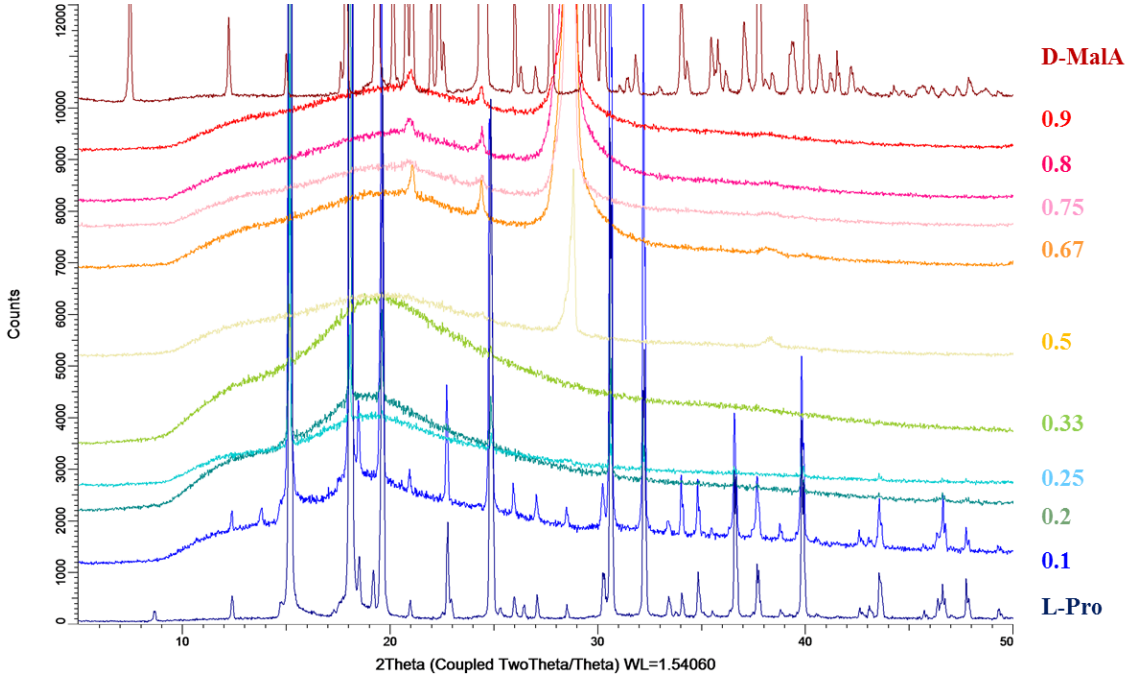

Figure F7. PXRD patterns of L-proline:D-malic acid binary mixtures and respective pure components.

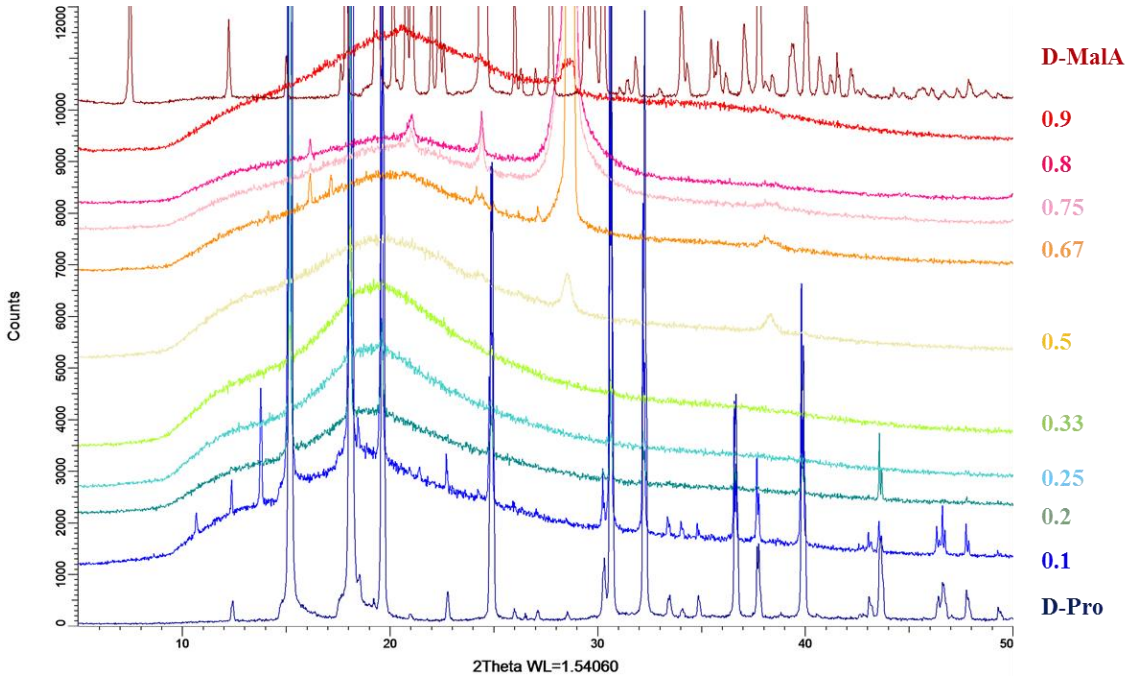

Figure F8. PXRD patterns of D-proline:D-malic acid binary mixtures and respective pure components.